UNIVERSITY OF BIRMINGHAM

THE COMBUSTION AND EMISSIONS PERFORMANCE OF FUEL BLENDS IN MODERN COMBUSTION SYSTEMS

By

Dale Michael Turner

A thesis submitted to

The University of Birmingham

For the degree of

DOCTOR OF PHILOSOPHY

The University of Birmingham

School of Engineering

November 2010

Abstract

The combustion and emissions performance of fuel blends in modern combustion systems has been investigated with the intention of reducing emissions, improving efficiency and assessing the suitability of future automotive fuels. The combustion systems used in this study include Homogeneous Charge Compression Ignition (HCCI) and Direct Injection Spark Ignition (DISI).

By adding a small quantity (10%) of diesel to gasoline, the HCCI combustion of this 'Dieseline' mixture shows a 4% increase in the maximum and a 16% reduction in the minimum loads (IMEP) achievable. The NO_X emissions are reduced, with greater than 30% savings seen for high engine loads. The addition of bio-fuels (ethanol and 2,5 di-methylfuran) to gasoline in HCCI combustion resulted in reduced ignitability giving rise to a 0.25 bar IMEP reduction of the maximum load. A 70% increase in NO_X emissions is seen at an engine load of 3.5 bar IMEP.

The addition of ethanol and to a lesser extent 2,5 di-methylfuran (DMF) to gasoline in DISI combustion shows increased combustion efficiency. The NO_X emissions are reduced with ethanol, but are increased with the addition of DMF. At wide open throttle the bio-fuels show up to a 3 percentage point increase in efficiency through the use of more favourable spark timings brought about by the increased octane ratings and enthalpies of vaporisation.

The PM emissions from DISI combustion can be reduced by up to 58% (mass) with the addition of ethanol. The soluble organic fraction forms a significant part of the total PM, particularly for the higher ethanol blends at wide open throttle. The addition of DMF however increases the total PM by up to 70% (mass) through the incomplete combustion of the ring structure.

Acknowledgements

I would like to thank Professor Hongming Xu and Professor Mirosław L. Wyszyński for their help and guidance during my PhD course, it was greatly appreciated. The help from Dr Athanasios Tsolakis was also greatly appreciated.

I would like to thank Peter Thornton, Carl Hingley and Lee Gauntlett for their technical support given during upgrading and maintaining the test rig.

Thanks go to Jaguar Land Rover for their support and help with the supply of hardware during the upgrading of the test rig. In particular the input from Dr Jun Qiao and Dr Rob Stevens was invaluable.

The support from Shell Global Solutions UK in supplying the hydrocarbon and ethanol fuels used in this study is appreciated.

I would like to thank Dr Pawel Luszcz for his help with the data acquisition and engine control software.

Table of Contents

List of Figures

List of Tables

List of Abbreviations

$AFR_{Stoich.}$	Stoichiometric Air to Fuel Ratio
CAD	Crank Angle Degrees
CAI	Controlled Auto-Ignition
CI	Compression Ignition
CLD	Chemiluminescent Detector
CO	Carbon Monoxide
CO_2	Carbon Dioxide
COV	Coefficient of Variation
CPC	Condensing Particle Counter
D_{50}	Diameter at which only 50% of particles pass
DI	Direct Injection
DISI	Direct Injection Spark Ignition
DMA	Differential Mobility Analyser
DMF	2,5 Di-methylfuran
DMFx	x% by volume DMF in DMF/Gasoline Blend
Dx	x% by mass Diesel in Diesel/Gasoline Blend
DOC	Diesel Oxidation Catalyst
D_P	Particle Diameter
EGR	Exhaust Gas Recirculation
ER	Exhaust Residuals
EoI	End of Injection
EV	Exhaust Valve
EVC	Exhaust Valve Closing
Ex	x% by volume Bio-Ethanol in Ethanol/Gasoline Blend
FBP	Final Boiling Point
FID	Flame Ionisation Detector
FSN	Filter Smoke Number

FTIR	Fourier Transform Infrared Detector
γ	Polytropic Exponent of Compression/Expansion
GE	Gas Exchange
HC	Hydrocarbons
HCCI	Homogeneous Charge Compression Ignition
HRR	Heat Release Rate
IBP	Initial Boiling Point
IMEP	Indicated Mean Effective Pressure
IV	Intake Valve
IVO	Intake Valve Opening
IVC	Intake Valve Closing
K-L	Knock Limited
λ	Relative Air-Fuel Ratio
LCV	Lower Calorific Value
LTC	Low Temperature Combustion
$\dot{m}_{air}$	Mass Flow of Air
$\dot{m}_{fuel}$	Mass Flow of Fuel
MBT	Minimum advance for Best Torque
MFB	Mass Fraction Burned
MON	Motor Octane Number
NDIR	Non-Dispersive Infrared Detector
NO	Nitric Oxide
NO_X	Oxides of Nitrogen
$\eta_{combustion}$	Combustion Efficiency
NVO	Negative Valve Overlap
TDC	Top Dead Centre
$°aTDC_{COMB}$	Crank angle degrees after Top Dead Centre of Combustion
$°bTDC_{COMB}$	Crank angle degrees before Top Dead Centre of Combustion
$°aTDC_{GE}$	Crank angle degrees after Top Dead Centre of Gas Exchange
$°bTDC_{GE}$	Crank angle degrees before Top Dead Centre of Gas Exchange

PAH	Polycyclic Aromatic Hydrocarbons
PFI	Port Fuel Injection
φ	Fuel-Air Equivalence Ratio
p	Pressure
PM	Particulate Matter
PRF	Primary Reference Fuel
Q	Heat Flow
Q_{LHVco}	Lower Heating Value of Carbon Monoxide
$Q_{LHVfuel}$	Lower Heating Value of the Fuel
RON	Research Octane Number
RPM	Engine speed, Revolutions per Minute
RPR	Rate of Pressure Rise
SCR	Selective Catalytic Reduction
SI	Spark Ignition
SMPS	Scanning Mobility Particle Sizer
SoC	Start of Combustion
SOF	Soluble Organic Fraction
SoI	Start of Injection
ST	Spark Timing
θ	Crank Angle
ULG95	Standard Unleaded Gasoline (95 Research Octane Number)
ULSD	Ultra Low Sulphur Diesel
V	Volume
VCT	Variable Cam Timing
VOC	Volatile Organic Compounds
WOT	Wide Open Throttle
x_{CO}	Mass Fraction of Carbon Monoxide
x_{HC}	Mass Fraction of Hydrocarbons

List of Publications

Conference Papers

1 An Experimental Study of Dieseline Combustion in a Direct Injection Engine
D. Turner, G. Tian, H.M. Xu, M. L Wyszynski, E. Theodoridis. SAE Paper 2009-01-1101. (2009).

Invited Presentations

1 Combustion and Emissions of Dieseline in a Direct Injection HCCI Engine
H.M. Xu, D. Turner, P. Luszcz, M.L. Wyszynski. Intentional Energy Agency HCCI Task Leader Meetings, Capri, Italy, 15 September, 2008.

2 Combustion of Dieseline in HCCI Engines
H.M. Xu, D. Turner, P. Luszcz, M.L. Wyszynski. Institute of Physics, Combustion Physics Group Meeting, Alternative Fuels and Combustion Strategies for Internal Combustion Engines, Cambridge, 18 September, 2008.

CHAPTER 1

1 Introduction

With the ever increasing concerns regarding atmospheric CO_2 levels and global climate change the need for fuel efficient vehicles has never been so great. This has led to the development and evolution of existing combustion systems such as using direct fuel injection in spark ignition engines. A new combustion system has also received much attention because of its ability to reduce fuel consumption, this being homogeneous charge compression ignition (HCCI) combustion. There is also increased pressure to reduce the emissions (NO_X, HC, CO, PM etc.) from internal combustion engines. This though is where compromises have to be made; fuel efficient combustion modes such as HCCI or stratified spark ignition tend to have increased emissions of HC, CO and PM. Likewise the after treatment devices required for these lean-burn technologies often incur a fuel consumption penalty. This is why oxygenated bio-fuels are considered attractive as they are renewable, can produce less regulated emissions and reduce the net CO_2 emissions.

1.1 Background – Modern Combustion Systems

With the need to reduce global CO_2 emissions comes the need to reduce vehicular fuel consumption. One proposed method for this is homogeneous charge compression ignition (HCCI) combustion. This is where the combustion of a homogeneous mixture is ignited by the temperature rise caused by compressing the mixture. The benefits of this include high efficiency brought about by near zero pumping losses and near zero NO_X and particulate matter emissions

from the combustion of lean homogenous mixtures. This technology however has significant problems, these mainly being there is no direct control over the start of combustion and the low temperature combustion can cause increased HC and CO emissions.

The load produced is controlled by the amount of fuel combusted, with the combustion initiation being governed by the temperature, pressure and fuel species histories of the in-cylinder charge. The methods put forward for the control of HCCI load and combustion include intake air heating, variable compression ratio, dual fuel, spark assistance and the addition of hydrogen. However the two control methods chosen by the author for this study are internal trapping of exhaust residuals and the use of direct fuel injection. This is because it is felt that these two methods are the most practical and can be varied on a cycle-by-cycle basis, with the hardware required already being fitted to many modern spark ignition engines.

No matter what control method is chosen the practical speed-load window achievable for HCCI combustion is limited and generally restricted to medium speeds and loads. This is partially due to the control methods employed and partially by the fuels used. The two most common automotive fuels are diesel and gasoline, which over time have been developed for compression ignition and spark ignition combustion respectively. This means that these fuels perform very well in their respective combustion modes but are less well suited to HCCI combustion, necessitating the need for research into the fuel properties required for HCCI combustion.

Another method proposed for reduced fuel consumption is stratified spark ignition combustion. This is where a combustible mixture ($\lambda \approx 1$) is created in the region of the spark plug electrodes, whilst the remainder of the cylinder is filled with fresh air. This allows for a more open throttle position to be used and hence reduced pumping losses. The fuel stratification is generated by injecting the fuel directly into the cylinder and using specially shaped pistons, in-cylinder motion or fuel injection spray patterns to transport the fuel to the region of the spark plug electrodes.

By injecting the fuel directly into the cylinder the time available for mixture preparation is reduced, especially for late injection timings required to produce stratified mixtures. This can result in increases of HC, CO and PM emissions caused by under mixed (rich) and overly mixed (lean) regions within the combustion chamber. At wide open throttle conditions however the injection of the fuel directly into the cylinder can increase the volumetric efficiency through charge cooling, but can cause cold start problems.

1.2 Research Outline

The research presented in this thesis was conducted at the University of Birmingham with help and support from Jaguar Land Rover and Shell Global Solutions UK. The research conducted was to investigate the effects on combustion and emissions of mixtures of both conventional and bio-derived fuels in modern combustion systems.

The research is split into two parts, HCCI combustion and direct injection spark ignition combustion. The aspects of HCCI combustion investigated include the beneficial aspects of adding diesel to standard gasoline with the intended outcome of an increased operating window with reduced emissions and increased efficiency. The combustion and emissions performance of a novel bio-fuel, 2,5 di-methylfuran, blended with gasoline is investigated and compared to the equivalent ethanol/gasoline blend. The HCCI combustion and load is controlled by the use of internal exhaust gas recirculation and direct fuel injection.

The direct injection spark ignition part of the study assesses the performance of ethanol/gasoline blends at part load and wide open throttle conditions which is also used as a reference for blends of 2,5 di-methylfuran and gasoline. The particulate matter emissions are measured for all fuel blends with the solid carbon particles being measured for the ethanol blends to assess the quantities of solid carbon and soluble organic fraction.

All of the investigations in this study were conducted on a prototype research single cylinder direct injection spark ignition engine, representative of a multi-cylinder (V8) engine that is currently in production. For HCCI operation special low lift, short duration camshafts were fitted along with a variable cam timing system (VCT) that was developed in-house.

1.3 Objectives and Approaches

The main objectives of this study are to investigate the combustion and emissions performance in modern combustion systems. The individual investigations include:

- The beneficial effects of adding diesel to gasoline in HCCI combustion
- The effects of ethanol/gasoline and DMF/gasoline fuel blends on HCCI combustion
- The effects of ethanol and DMF fuel blends on SI combustion at part load
- The effects of ethanol and DMF fuel blends on SI combustion at wide open throttle
- The effect of oxygenated fuels on PM emissions from spark ignition combustion
- The effect of split injection on PM emissions from spark ignition combustion at WOT
- Using a thermo-denuder to assess the ratio of SOF and solid carbon in spark ignition PM

1.4 Thesis Outline

This thesis is divided into eight chapters that cover different aspects of using fuel blends in modern combustion systems. A brief description of the contents of the following chapters is given bellow.

Chapter 2 – Literature Review

The literature is reviewed and the significant points are presented ahead of the author presenting and discussing his own findings. Particular attention is applied to HCCI control methods, the use of bio/oxygenated fuels in HCCI combustion, aspects of gasoline direct injection and the use of bio/oxygenated fuels in spark ignition combustion.

Chapter 3 – Experimental Setup and Techniques

The engine and measurement equipment used for this study are described in detail including their setup and operation. Details are given of the key calculations used in this study.

Chapter 4 – The Effect of Conventional and Bio-Fuel Blends on Gasoline HCCI Combustion and Emissions Performance

Diesel is blended with gasoline in an attempt to increase the load range achievable by HCCI combustion compared to standard gasoline. Load control is achieved by varying the level of trapped exhaust residuals and start of fuel injection timings. A novel bio-derived fuel is blended with gasoline to investigate its effect on HCCI combustion and emissions performance.

Chapter 5 – The Effect of Bio-Fuels on Direct Injection Spark Ignition (DISI) Combustion – Part Load

Ethanol and 2,5 di-methylfuran are blended with gasoline to assess their impacts on combustion, emissions and engine efficiency, at a part load condition of 3.4 bar IMEP at 1500 RPM. A split injection strategy is investigated for the ethanol blends.

Chapter 6 – The Effect of Bio-Fuels on Direct Injection Spark Ignition (DISI) Combustion – Full Load

The impact of blending ethanol and 2,5 di-methylfuran with gasoline on combustion, emissions and engine efficiency are investigated at a wide open throttle condition at 1500 RPM.

Chapter 7 – The Effect of Bio-Fuels on Direct Injection Spark Ignition (DISI) Particulate Matter Emissions

The particulate matter emissions from direct injection spark ignition combustion of bio-fuel/gasoline blends are investigated at both part and full load. A thermo-denuder is used to assess the relative proportions of solid carbon and the soluble organic fraction in the total particulate matter emitted.

Chapter 8 – Conclusions

The conclusions made in the previous chapters are summarised, with recommendations for future study also being given.

CHAPTER 2

2 Literature Review

The review of the literature for this study is divided into two parts, to reflect the nature of this study. The first part gives a review of the relevant aspects of HCCI combustion, while the second part reviews the aspects of spark ignition combustion that are relevant to this study.

2.1 HCCI Combustion

Homogeneous Charge Compression Ignition (HCCI) combustion, which is similar to and sometimes referred to as Controlled Auto-Ignition (CAI), is regarded by many as a solution to the requirement for ever cleaner and more fuel efficient internal combustion engines. This is because HCCI operation has near-diesel-like fuel economy, without the problems of NO_X and soot emissions [Stanglmaier and Roberts (1999), Epping et al (2002) and Johansson et al (2009)] associated with diesel engines. This high fuel efficiency results from the fact that the engines are operated un-throttled, which results in reduced pumping losses compared to standard spark ignition operation. The low soot and NO_X emissions result from the combustion of a homogeneously mixed lean mixture (soot abatement), which also results in low combustion temperatures (NO_X abatement) [Peng et al (2003)].

At present the load-speed range achievable with HCCI combustion is too narrow for pure HCCI engines to be a reality [Hyvönen et al (2003a and 2003b) and Cairns and Blaxill (2005)]. Currently the technology is only suitable for medium speeds and loads, and thus conventional spark ignition or compression ignition (Diesel) combustion has to be used for high and low speed and load conditions. However the current evolution of the spark ignition engine allows for the relatively simple implementation of HCCI as a 'bolt-on' combustion mode for reduced emissions and improved efficiency. This is because modern SI engines are employing direct fuel injection [Baumgarten et al (2001), Han et al (2007) and Sandford et al (2009)] and variable valve timing and lift systems [Crawford et al (2002), Turner et al (2006) and Stansfield et al (2007)] along with increased compression ratio. The first two methods are considered to be particularly effective for controlling HCCI combustion and load.

2.1.1 Combustion and Load Control Methods

With HCCI combustion generally there is no direct trigger for or control over the initiation of combustion, unlike for example spark ignition operation where combustion is initiated with a spark discharge. For HCCI combustion a homogeneous mixture is compressed and combustion is initiated when a certain condition has been reached, as described by the Arrhenius formula [Sazhina et al (1999)]. This 'critical' condition is a function of the time-histories of the in-cylinder pressure, temperature and concentration of the individual fuel and pre-combustion species. The lack of in-cycle control is a contributing factor to HCCI combustion having a limited speed and load window.

There have been many methods put forward for the control of HCCI combustion and load. The use of variable compression ratio has been suggested [Haraldsson et al (2002), Chen and Mitsuru (2003) and Gérard et al (2008)], but the mechanical system required for this is complex and likely to be too expensive for automobile engines. Intake air heating has successfully been used as a control method [Aroonsrisopon (2001 and 2002) and Wang et al (2009)]. A significant drawback to this is that the thermal inertia of the inducted air is too great for cycle-cycle control to be achieved. This is further compounded if the exhaust stream is to be used as the heat source, so no fuel penalty is encountered. The addition of hydrogen has been shown to improve the combustion properties of certain fuels [Shudo (2002), Yap et al (2005) and Ng and Thomson (2005)]. This however adds complexity and cost to the complete engine and fuel system, whether the hydrogen is generated on-board through fuel reforming or generated externally and stored in a tank.

Spark assisted HCCI, where a spark discharge is used to initiate the combustion of a homogeneous mixture, has been shown to improve the stability of HCCI combustion, Bunting (2004). Persson et al (2005) has proposed this as a possible method for 'balancing' the combustion in the individual cylinders of a multi-cylinder engine. Spark assistance has been suggested Wagner et al (2006) as a method for improving the transition from SI combustion to HCCI combustion. Although this is simple to implement on a spark ignition based HCCI engine this control method is not used in this study.

The trapping of exhaust residuals and the use of direct fuel injection are discussed in more detail in relation to combustion and load control because the author feels these are the most practical

control methods for HCCI combustion. These technologies are also already in production, fitted to modern spark ignition engines.

2.1.1.1 Trapping of Exhaust Gas Residuals

The trapping of exhaust residuals in the cylinder, whether delivered by an external EGR loop or internally retained with modified valve events has been shown to be a suitable method for HCCI combustion or load control. The modelling studies by Zhao et al (2001) and Chen and Milovanovic (2002) both show that trapping hot exhaust gas in the cylinder significantly affects the combustion timing and duration/heat release rates, caused by two competing factors. The first factor is the thermal effect of the hot residuals. This is where the hot exhaust gas increases the temperature of the trapped charge to that required to initiate combustion. As the quantity of (constant temperature) exhaust residuals is increased the start of combustion is advanced and the combustion duration is reduced.

The second factor is the chemical effects of the exhaust residuals. The four main components of the exhaust gas are CO_2, H_2O, O_2 and N_2 arranged in order of decreasing molar heat capacity. The heat capacity of N_2 is slightly lower than that of air, with CO_2 having a significantly higher heat capacity. Both CO_2 and H_2O, because of the increased heat capacity, retarded ignition and increased combustion duration. Oxygen in the trapped exhaust gas has very little effect on the heat release rate, but shows a slight advance in ignition timing. The N_2 species in the exhaust stream has very little effect on combustion timing, but considerably reduces the rate of heat release through the increase in dilution of the trapped charge.

This means that when the two effects of the trapped exhaust residuals are combined the rate of ignition advance, relative to EGR rate, reduces as the EGR rate increases. The combustion duration has a 'horseshoe' distribution relative to EGR rate. For low EGR rates an increase in EGR reduces the combustion duration through the thermal effect. As the EGR rate is increased further the combustion duration plateaus and then increases, as the chemical effects become more significant. This will be further compounded by the fact that in a real engine as the EGR rate increases the exhaust temperature reduces, because of the reduced load. This means that as the EGR rate is increased the relative heating effect is reduced and the chemical effects become dominant.

With the current trends in spark ignition engine development the simplest way to trap exhaust residuals in the cylinder is to use modified valve timings and lifts, as used in the studies by He at al (2005) and Ibara et al (2006). The amount of residuals trapped is governed by the valve timings used. The studies by Milovanovic et al (2004a) and Cao et al (2005a) show that the exhaust valve closing has the greatest effect on the amount of trapped residuals. The timing of the intake valve opening has little effect on the combustion parameters, but does affect the pumping losses and the release of the in-cylinder contents into the intake manifold. If the intake valve is opened too early then the pressure in the cylinder is higher than that in the intake port and some of the cylinder contents flow back into the intake port and runner. If the valve opening is delayed too much then the in-cylinder pressure will drop below that in the intake port, which has the effect of increasing the pumping losses. The exhaust valve opening and intake valve closing are shown to have very little effect on the combustion performance. However overly late intake valve closing should be avoided as this reduces the effective (trapped) compression ratio

and lowers the in-cylinder temperature at TDC, though this could possibly be used as a control method for avoiding overly advanced combustion.

2.1.1.2 Direct Fuel Injection

The use of direct fuel injection as a method for controlling HCCI combustion has been shown to be effective. The simplest implementation of direct injection is the use of a 'liquid sparkplug'. This is where the combustion of a homogeneous air-fuel mixture is initiated by the combustion of a small quantity of diesel injected near TDC. This technique is normally used to improve the combustion performance of high octane fuels such as gasoline [Yoshida et al (1998) and Jiang (2005)] and ethanol [He et al (2004)].

Direct injection can also be used to generate a homogeneous or near homogeneous charge in the cylinder if the injection takes place at a suitable time before TDC_{COMB}. The timing of the injection can be used as a means of combustion and load control. The work by Kong et al (2002) showed that by changing the start of injection timing the intake temperature required for optimum combustion phasing could by reduced by as much as 20°C depending on the load/equivalence ratio. Jang et al (2008) showed that for an equivalence ratio of 0.3 the indicated load (IMEP) produced could be controlled from 2.2 – 3.8 bar by varying the start of injection timing from 20°bTDC_{COMB} to 350°bTDC_{COMB}. This change in load is brought about by the change in injection timing causing the combustion timing and duration to change, which in turn alters the balance of positive and negative work produced by the engine.

Yamaoka et al (2004) suggests that the change in combustion timing is caused by the changes in mixture distribution caused by the change in injection timing. The mixture is likely to become more inhomogeneous as the start of injection is retarded, with rich spots advancing combustion and the overly lean regions slowing down the rate of heat release. Cao et al (2005b) also cites the change in in-cylinder temperature with changing injection timing as a reason for the change in ignition timing. It is shown that with the start of injection set at IVC the in-cylinder temperature 20 CAD before TDC_{COMB} is over 20 K lower than that for the start of injection occurring at TDC_{GE}. This temperature reduction gives rise to a relative delay of 6 CAD for the 10% mass fraction burned timing.

The start of injection timing affects more than just combustion phasing. If the injection occurs during the negative overlap period the pumping losses are going to increase, as seen in the study by Cao et al (2005b). This is caused by the evaporating fuel lowering the in-cylinder temperature and therefore pressure during the expansion of the compressed exhaust residuals. This lower pressure means less work is recovered during the expansion and hence higher pumping losses. The injection timing also has an effect on the levels of emissions produced; advanced combustion is likely to produce increased NO_X whilst reducing the HC levels through increased in-cylinder temperatures. If retarded injection timings are used the air-fuel mixture is likely to be more stratified. The rich zones will increase the NO_X levels through increased local temperature and soot emissions through the lack of available oxygen for the complete oxidation of carbon. The lean regions will increase the HC emissions through reduced local temperatures and reaction quenching.

If some or all of the fuel is injected before the recompression TDC the elevated temperatures and pressure during recompression can partially 'crack'/reform the fuel to produce radicals which advance the timing of the main combustion. This technique is normally associated with a split-injection strategy where only a small proportion of the fuel is injected prior to recompression, with the remainder of the fuel being injected during the induction stroke. Guohong et al (2006) reported both an advance in combustion phasing and improved combustion stability through internal reformation of the early injected fuel. Waldman et al (2007) reported that by advancing the injection of the fuel in the recompression stroke the main combustion is advanced by up to 8 CAD. Both Koopmans et al (2003) and Urushihara et al (2003) report that during the recompression period the chemical reactions associated with the injected fuel are not just limited to cracking and reforming but combustion is also observed. Koopmans et al reports that the amount of oxygen available during the recompression period governs the amount of combustion seen. The combustion in the recompression period raises the in-cylinder temperature which can advance the phasing of the main combustion, but Urushihara reports that if all of the fuel is injected during recompression (compared to only partial fuel reformation) the lean limit is reduced and the fuel consumption increased.

Direct injection strategy can be used to control HCCI combustion and load. However the combustion phasing is relatively insensitive to small changes in injection timing because of the relatively long 'delay' between start of injection and start of combustion. Conventional compression ignition and spark ignition combustion are far more sensitive to injection and spark timing respectively.

2.1.2 Emissions

It is generally reported that HCCI combustion can achieve a substantial reduction in NO_X emissions compared to both conventional compression ignition and spark ignition combustion, however generally considerable carbon monoxide and hydrocarbon emissions are produced. This emissions characteristic is related to the low in-cylinder temperature typical of HCCI combustion, especially for low load operation. With HCCI combustion there appears to be a 'trade-off' between NO_X and HC/CO emissions, with Bression et al (2008) presenting work on attempts made to reduce this trade-off.

The studies by Sjöberg and Dec (2003) using port injected gasoline, iso-octane and two PRF blends and Li et al (2007) using port injected n-heptane show that as the combustion phasing is retarded the emissions of unburned hydrocarbons and carbon monoxide increase. In these studies the combustion phasing was retarded by using leaner mixtures (reduced fuelling rate), reduced compression ratio and by the use of EGR. The study by Sjöberg et al (2002) that uses direct injection of a gasoline blend that contains $5\%_{Vol.}$ ethanol reports that leaner mixtures result in reduced combustion efficiency, whilst the careful selection of injection timing is required. For an equivalence ratio of 0.29, if the injection timing was advanced or retarded from the optimum position the NO_X and CO emissions increased. The NO_X increase was caused by the presence of rich 'hot spots' and the increase in CO was caused by reaction quenching in the overly lean regions. It is also shown that increasing the level of air swirl can greatly reduce the HC and CO emissions, by improved mixing, when homogeneous injection timings are used.

However for leaner mixtures (φ=0.20) the HC and CO emissions can be improved by using a late (stratified) injection timing with only a minor increase in NO_X emissions.

The modelling study by Easley et al (2001) using a single zone model shows that the NO_X emissions for equivalence ratios equal to or greater than 0.20 are predominantly NO with very little conversion to NO_2. With the use of a multi-zone model it is shown that the NO_X emissions originate in the core of the combustion chamber, where the temperature is the greatest. It is said that the hydrocarbon emissions originate from the boundary layer and crevice volumes, while the CO emissions are caused by the partial oxidation of the hydrocarbons as they are released from the boundary layer and crevice volumes during the expansion stroke.

The modelling study by Aceves et al (2004) shows how the distribution of un-reacted fuel, intermediate hydrocarbon species and CO changes with respect to fuel-air equivalence ratio (φ). For the richest mixture (φ=0.26) the hydrocarbon and CO emissions originate from the boundary layer and crevice volumes due to the low temperatures in these regions caused by heat transfer to the combustion chamber walls. As the mixture is leaned to a value of φ=0.16 the low temperature boundary layer expands inwards increasing the HC and CO emissions. When the equivalence ratio is 0.10 even the centre of the combustion chamber is too cold for complete combustion and most of the fuels carbon atoms are partially oxidised to CO. As the mixture is further leaned to φ=0.04 the in-cylinder temperatures are very low, resulting in only the centre core of the combustion chamber oxidising the fuel to CO and causing a wide boundary layer predominantly containing un-reacted and partially oxidised fuel, this causes the CO emissions to decrease while the HC emissions increase for extremely lean mixtures.

As reported above if prohibitively high emissions levels from HCCI combustion are to be avoided the mixture of air, fuel and recycled exhaust gas needs to be well mixed to reduce NO_X levels, with the combustion temperature being suitably high enough to allow the complete oxidation of the fuel into carbon dioxide rather than carbon monoxide and partially oxidised hydrocarbons.

2.1.3 Fuels

HCCI combustion has been demonstrated to operate on a wide range of fuels, both gaseous and liquid. The gaseous fuels include natural gas [Fiveland (2001), Stanglmaier (2001) and Jun (2003)] and hydrogen [Stenlåås et al (2004) and Rosati and Aleiferis (2009)]. The use of gasoline, diesel, bio-fuels and mixtures of the above are discussed in more detail in the following sub-sections.

2.1.3.1 Gasoline

Gasoline has been demonstrated to be a suitable fuel for HCCI combustion in both 2-stroke [Osborne et al (2003)] and 4-stroke [Koopmans and Denbratt (2001) and Wang et al (2008)] engines, largely because it is a volatile fuel and hence homogeneous mixtures can be formed easily. It is generally reported however that the main drawback of using gasoline as a HCCI fuel is its relative high resistance to auto-ignition. The study by Amann et al (2005) showed that when practical limits are applied to the control strategy the most suitable gasoline blend was that with a medium octane rating (77.0 RON) as the speed-load window achievable was the largest. Nevertheless the variations in commercially available gasoline seen between summer and winter and between different manufactures can have an effect on the HCCI combustion. The work by

Angelos et al (2007) using 12 different gasoline blends representative of the variation in commercial gasoline showed that although the lower load limit was unaffected by the fuel properties the upper load limit was affected, but the differences were not constant across the different speeds tested.

It has, though, been suggested and reported by other authors that the use of the traditional gasoline ratings (RON and MON) is not suitable for describing the auto-ignition properties of gasoline and gasoline like fuels. Shibata et al (2004) suggests that the presence of a low temperature heat release region has a considerable effect on HCCI combustion performance. Shen et al (2007) suggests that the fuel chemistry such as the quantities of aromatics, n-paraffins and iso-paraffins along with the 10% distillation temperature has a greater effect on HCCI combustion and emissions than RON and MON. Though there is no constant correlation across all engine operating conditions, the optimum fuel properties are dependent on both the speed and load at which it is being used. Shibata and Urushihara (2007) go further and have developed HCCI auto-ignition fuel indices that are based on the octane rating (RON or MON) but take into account the volumetric proportions of n-paraffins, iso-paraffins, olefins, aromatics and oxygenates. These fuel indices better predicted the HCCI combustion phasing than the octane ratings alone.

2.1.3.2 Diesel and Diesel Blends

Diesel is one of the two most commonly used internal combustion engine fuels (the other being gasoline) and therefore is of interest as an HCCI fuel because of its wide availability. Huang et al (2008) have successfully demonstrated the use of diesel as an HCCI fuel. However it is widely reported [Kawano et al (2005) and Helmantel and Denbratt (2006)] that diesel ignites too easily due to its propensity to auto ignite and therefore has limited use as an HCCI fuel. The work by Milovanovic et al (2004b) suggests that bio-diesels may be a better fuel than conventional crude-derived diesels. This is because they show less variation in combustion phasing with changes in equivalence ratio, combustion efficiency can be maintained for leaner mixtures and they are more tolerant to EGR.

There have been many studies conducted where diesel is blended with another fuel to improve the combustion and emission performance with respect to HCCI combustion. One of the fuels that has been blended with diesel is ethanol. The study by Kim et al (2008) used ethanol addition to improve mixture formation and reduce emissions, while Pidol (2008) reported an increase in the HCCI operating range with ethanol addition.

The other blend-in fuel to be extensively investigated is gasoline such as in the study by Ryan et al (2004). The study on partially pre-mixed combustion in a light-duty diesel engine by Weall and Collings (2007) showed that the load achievable with good emissions levels could be increased with a blend of $50\%_{Vol.}$ gasoline and $50\%_{Vol.}$ diesel compared to pure diesel. A reason for this is that the addition of gasoline increased the ignition delay and the fuels volatility

allowing for more pre-combustion mixing. However there was a reduction in combustion stability for high proportions of gasoline at low load. The study by Christensen et al (1999) using port injected gasoline and diesel blends in a variable compression ratio HCCI engine can be considered in two different ways. If the results are interpreted as adding diesel to gasoline the required compression ratio and/or intake temperature can be reduced for a constant combustion phasing at the expense of increased emissions and reduced efficiency. However if it is thought of as adding gasoline to diesel the emissions are improved through improved fuel vaporisation coming from the increased volatility of gasoline and the raised inlet temperatures required for the constant combustion phasing. The low pressure port injection system used in this study also exacerbates the problem of the reduced volatility of diesel and can lead to increased emissions through poor mixture preparation.

The work by Zhong et al (2005 and 2006) and Xu et al (2007) on the same port injected single-cylinder HCCI engine shows that the addition of diesel to gasoline (referred to as 'Dieseline') can be beneficial. The addition of diesel shows a significant advance in combustion phasing for the same operating conditions. The load window is extended through the improved ignitability of dieseline. The lower load limit is reduced through the use of leaner mixtures (λ) and/or increased EGR, with the upper load limit being increased by the use of less EGR (less internal heating is required with dieseline). The combustion stability is also shown to be increased with the addition of diesel. The hydrocarbon and carbon monoxide emissions can be reduced through more complete combustion, but an increase in NO_X emissions is observed for some operating conditions through an increase in in-cylinder temperature brought about by the more complete combustion. No smoke/PM data is presented for these studies but is expected to be significant

because of the low PFI injection pressures used being insufficient for the complete atomisation of the added diesel fuel.

2.1.3.3 Bio-Fuels

Bio-fuels are considered here to be fuels that can be derived from bio-sources, even though in the particular studies presented below they may have been derived from conventional crude stocks. These bio-fuels are normally oxygenated hydrocarbons, with the most common two being methanol and ethanol. Both methanol and ethanol have high octane ratings (100+ RON) and high enthalpies of vaporisation, which would intuitively suggest that these fuels are not particularly suited to HCCI combustion. Nevertheless HCCI combustion has been demonstrated successfully with ethanol [Zhang et al (2006) and Maurya and Agarwal (2008)] and non-dehydrated ethanol [Hunter Mack et al (2009)].

The study by Gnanam et al (2006) reports that actually ethanol shows advanced combustion compared to iso-octane, at an engine speed of 1035 RPM with an intake temperature of 136 °C ethanol advances combustion by 2.7 CAD. Though in this study PFI injection was used along with a constant charge temperature irrespective of fuel used, this negates the increased enthalpy of vaporisation of ethanol. Oakley et al (2001) demonstrates that ethanol and especially methanol can achieve a larger lambda-EGR operating region than gasoline because the combustion phasing is less sensitive to lean mixtures and increased EGR. Likewise ethanol and methanol showed advanced combustion phasing compared to gasoline. Similar to the study by Gnanam et al (2006) attempts are made to maintain a constant inlet charge temperature (320 °C) and this again helps to negate the effect of increased enthalpy of vaporisation.

The study by Xie et al (2006) was conducted with an ambient inlet air temperature but the methanol and ethanol fuel blends still showed advanced combustion phasing at an engine speed of 2000 RPM, but the mixtures would not auto-ignite at lower engine speeds. The alcohol fuel blends however did still demonstrate a greater tolerance to lean mixtures compared to gasoline. The NO_X emissions are also shown to be reduced with alcohol fuels because of the reduced combustion temperatures. In this study however the alcohol blends did show reduced combustion stability for some operating points, so if practical limits are applied ($COV_{IMEP} \leq 5\%$) the usable speed-load range could be smaller for alcohol fuels compared to standard gasoline.

2.2 Spark Ignition Combustion

Spark ignition combustion has long been established as a practical combustion system because a wide range of (volatile) fuels can be used, provided a suitable combination of compression ratio and spark timing is chosen. These fuels include gasoline [Han and Chung (1999) and Okamoto et al (2002)], ethanol [Kapus et al (2007) and West et al (2007)], methanol [Ebersole and Manning (1972) and Menrad et al (1977)], natural gas [Evans et al (1984) and Fleming and O'Neal (1985)] and hydrogen [Kim et al (1995) and Shudo et al (1999)]. Because homogeneous mixtures are used there is very little soot or particulate matter emitted, unlike conventional compression ignition (Diesel) combustion.

The thermal efficiency of spark ignition combustion is normally lower than that achieved with conventional compression ignition combustion. The occurrence of knocking combustion limits the maximum compression ratio, which tends to be lower than those used in compression ignition combustion, thus the fundamental thermodynamic efficiency is reduced. With spark ignition combustion the load is controlled by throttling the intake air, which increase the pumping losses and reduces efficiency. Attempts have been made to reduce the pumping losses [Payri et al (1984), Elrod and Nelson (1986) and Negurescu et al (2001)] but the problem still remains. The NO_X emissions can be significant from spark ignition combustion because stoichiometric mixtures have to be used. This is so the Three Way Catalyst (TWC) used for the after treatment of the exhaust gas can function correctly.

Combustion phasing is controlled by the timing of the spark discharge. For maximum efficiency the combustion needs to be phased so the optimum balance of compression and expansion work is obtained. The least amount of spark advance that achieves this is referred to as the MBT timing, minimum advance for best torque. However it is sometimes required that the spark timing is retarded from this value to avoid excessive NO_X emissions or knocking combustion if the compression ratio is too high. Exhaust after-treatment catalyst light-off can also be improved if considerably retarded spark timings are used, as the retarded combustion increases the exhaust temperature.

2.2.1 Direct Injection Technology

A technique for reducing fuel consumption that is currently undergoing considerable investigation is direct fuel injection. This is where the fuel is injected directly into the cylinder, rather than being drawn in with the fresh air charge. Though direct fuel injection is currently receiving much attention it is not a new technology and has previously been used in the 1950's to improve power output. Direct injection is considered to be attractive because through its use part load fuel consumption can be improved by using stratified combustion and WOT load can be increased through increased volumetric efficiency. Direct injection has other benefits and these include reduced hydrocarbon emissions at engine start-up. The study by Koga (2001) showed that by injecting the fuel directly into the cylinder, fuel build-up in the cold intake manifold/port is eliminated.

Significant problems are associated with direct injection combustion systems. Because the fuel is injected directly into the in-cylinder flow structure, rather than into the air stream that becomes the in-cylinder flow, mixture preparation and combustion is susceptible to variations in the flow structure. The study by Adomeit et al (2007) on modelling stratified combustion in a wall guided direction injection engine states that fluctuations in the in-cylinder flow can lead to serious problems such as mis-fires. The reduced time between start of injection and spark discharge for direct injection compared to standard port injection can lead to mixture preparation problems. Typically the amount of fuel evaporated before the onset of combustion is reduced, leading to increased emissions originating from overly rich (NO_X, HC and PM) and overly lean (HC and CO) regions. Significant amounts of fuel impingement onto the combustion chamber

surfaces should also be avoided. If the fuel does not evaporate from these surfaces before the onset of combustion significant amounts of hydrocarbon and particulate matter emissions can be created, as shown by Li et al (1999) and Noyori (2006) respectively.

2.2.1.1 Direct Injection Concepts

There are three basic concepts for gasoline direct injection, with these being wall guided, air guided and spray guided. The first generation of direct injection technology to be investigated was the Wall-Guided concept. This is where a bowl in the piston crown directs the injected fuel towards the spark plug, so a combustible mixture is formed around the spark plug at the time of spark discharge. This is demonstrated by Noma et al (1998), but this concept has significant drawbacks. Yang and Kenney (2002) describe many of the problems with the wall-guided (referred to as bowl-in-piston) injection system. These include significant amounts of cylinder wall wetting and fuel impingement onto the piston bowl increasing soot, CO and possibly hydrocarbon emissions. The bowl shape also significantly increases the surface area of the piston crown, which in turn increases the heat loss from the cylinder and reduces efficiency. The bowl shape also increases the mass of the piston, resulting in increased inertial losses.

The Air-Guided concept [Kim et al (1999) and Alger et al (2000)] was put forward to reduce the fuel impingement problems associated with the wall-guided system. The air-guided system uses a similar injection pressure (~50 bar) to the wall-guided system but the fuel is transported to the spark plug region by the motion of the in-cylinder charge. This system however has not seen universal acceptance.

The latest direct injection concept to be investigated and implemented is the Spray-Guided system, which is also referred to as the second generation direct injection system. With this system the spray pattern generated is of such a shape that the injected fuel is directed towards the spark plug electrodes. This system uses higher injection pressures than the wall-guided system, typically around 150 bar. This system in demonstrated by Honda et al (2004). Schwarz et al (2006) reports significant improvement of the stratification range, fuel consumption and emissions compared to the first generation DI systems while Honda et al (2004) reports reduced wall wetting.

2.2.1.2 Stratified Combustion

In an attempt to improve the part load efficiency of spark ignition engines the concept of stratified charge was investigated. This is where the engine is operated with a more open throttle position (to reduce pumping losses) and the load is controlled by the amount of fuel injected. With this concept the cylinder is filled mostly of fresh air (and possibly EGR), with a combustible mixture ($\lambda \approx 1$) being generated around the spark plug by directly injecting the fuel.

Stratified combustion is not without its problems however. Sandquist and Denbratt (1999) report increased levels of hydrocarbon and soot emissions, which likely occur from rich zones caused by under mixing and from wall wetting. Szekely and Alkidas (2005) show that in their study using a spray-guided DI system the fuel consumption, hydrocarbon emissions and combustion stability are dramatically affected by small changes in injection and spark timings. It was shown that generally the end of injection timing needed to be constrained to a region of around 10 CAD, while the spark timing should not be varied by more than 3 CAD. This is likely to cause

problems when transitioning from stratified to homogeneous combustion and vice-versa. Despite these problems Yang et al (2000) reports that a particular light load, stratified, operating point showed a reduction in net specific fuel consumption of 16 – 19% compared to homogeneous operation through reduced pumping losses and increased specific heats ratio.

Using stratification techniques causes the exhaust stream to contain significant amounts of oxygen. This means that a normal three way catalyst cannot be used for the reduction of NO_X. Instead more complex systems such as NO_X traps and selective catalytic reduction (SCR) systems need to be used, which normally results in a fuel consumption penalty.

2.2.1.3 Volumetric Efficiency Improvement

By injecting the fuel directly into the cylinder the evaporating fuel causes the temperature to drop in the cylinder, resulting in a reduced in-cylinder pressure. This can be utilised at wide open throttle (WOT) to causes a greater pressure drop between the cylinder and the atmosphere. This increased pressure drop causes more air to be drawn into the cylinder increasing the volumetric efficiency. This has been demonstrated by Shimotani et al (1995) and Yang and Anderson (1998). Yang and Anderson reported an increase of 5 – 8% in IMEP by using direct injection compared to standard port injection. A part of this increase was caused by an increase in volumetric efficiency and the other by the lower in-cylinder temperature suppressing the onset of knocking combustion. This can be a useful technique for increasing engine load but can cause cold start problems, especially for fuels with high enthalpies of vaporisation such as methanol and ethanol.

2.2.2 Use of Bio-Fuels

There has been a considerable amount of research already conducted on the use of ethanol in spark ignition engines, but the majority of this research is conducted on PFI engines rather than direct injection engines. However there is no information available in the literature on the use of 2,5 di-methylfuran, either neat, blended with gasoline or as a gasoline fuel additive.

Ethanol and in particular bio-ethanol has been considered as an attractive fuel for internal combustion engines due to its renewable nature and for the possibility of reducing net CO_2 emissions. Other attractive properties include increased octane rating and enthalpy of vaporisation compared to standard gasoline, which allows for the use of increased compression ratios, increasing engine efficiency. However these properties can cause problems if suitable changes to the engine calibration are not made. It is reported by Hara et al (2006) that ethanol has a faster laminar flame speed than gasoline, 39 cm/s compared to 33 cm/s. This 18% increase in laminar flame speed would suggest that the combustion of mixtures containing ethanol would be faster than that of pure gasoline. However in an engine this possible reduction in combustion duration may not be realised as the effective flame speed is a function of both the laminar flame speed and the turbulent combustion speed of the gas mixture, which could be up to two orders of magnitude faster.

The study by Al-Farayedhi et al (2000) using a PFI injection strategy showed that the addition of ethanol to gasoline reduced the CO emissions, particularly for rich mixtures because of an increase in the available oxygen that is contained in the ethanol fuel molecule. It was also reported that the addition of $10\%_{Vol.}$ ethanol resulted in a reduction in NO_X emissions, but further increase in ethanol content caused an increase in NO_X emissions though no data was given on combustion phasing.

The PFI study by Nakata et al (2006) and the DI study by Wallner et al (2008) both show that engine output and efficiency can be increased by the use of ethanol blends through the use of more favourable/MBT spark timings. As the ethanol blend ratio was increased the NO_X emissions reduced with the cause being given as the increased enthalpy of vaporisation lowering the pre-combustion temperatures and the lower flame temperature of ethanol reducing the in-cylinder temperature as shown by a reduction in exhaust temperature (Wallner). Both studies showed a reduction in hydrocarbon emissions for the ethanol blends, with the reduction increasing as the blend ratio was increased. The reason given for this was the reduction of the higher boiling point gasoline fractions in the fuel blend. Though this reduction could partially be attributed to the reduced sensitivity an FID has towards oxygenated hydrocarbons.

2.2.3 Particulate Matter Emissions

It would appear that spark ignition engines do not emit vast amounts of particulate matter emissions, as when compared to diesel engines there is no black smoke produced. Though generally the large carbon particles associated with black 'diesel smoke' are not emitted, any particles that are smaller than 2.5 μm in diameter are considered a health risk [Dockery et al (1993)]. The particulate emissions from DISI engines are now a regulated emission. Euro V (2009 onwards) regulations only includes limits for particle mass, but Euro VI (2014 onwards) will also include limits on particulate number. This is because direct injection engines, particularly first generation, emit more particulate matter emissions than PFI engines [Hall and Dickens (1999) and Graskow et al (1999)].

The increase in PM from direct injection engines is caused by two main factors. The first being the increase in wall wetting and fuel impingement onto the piston crown resulting from the fuel being injected directly into the cylinder. The second factor is that the time between injection and spark discharge is reduced, thus reducing the time available for mixture preparation with the PM resulting from the rich regions. The study by Maricq et al (1999) shows that for a load of 3.5 bar BMEP at 2500 RPM using homogeneous mixtures (EoI=317° $bTDC_{COMB}$) a 19 CAD advancement (21 – 40° $bTDC_{COMB}$) in the spark timing resulted in a near 3 times increase in total number concentration. For the same load point using stratified mixtures (EoI=68° $bTDC_{COMB}$) a 15 CAD advancement (18 – 33° $bTDC_{COMB}$) in the spark timing resulted in a 70 % increase in total number concentration. These increases are also accompanied by an increase of 10 – 20 nm in diameter for the particle corresponding to the peak number count. Retarding

the spark timing has two effects, the first being an increase in mixing time and the second being increased exhaust temperatures. The increased exhaust temperature can lead to reduced total PM emissions by the increased burn-up of the initial nucleation particles and a reduction in the hydrocarbon emission that can adsorb onto the surface of existing particles during the expansion and cooling of the exhaust gas.

The injection timing also has significant effect on the mixing time and hence total number concentrations as the late stratified injection timing showed a 43 times increase in total number concentration at the same spark timing (29° $bTDC_{COMB}$) in the study by Maricq et al (1999). An increase in the in-cylinder motion can help mixing and reduce the total PM emitted. Mehta et al (2001) reported that the use of swirl valves resulted in the lowest PM mass loadings when early injections were used as well as low tumble conditions generally producing the highest PM concentrations.

The use of alcohol/gasoline fuel blends can have a significant effect on the PM emissions. In a study by Price et al (2007a) that used gasoline/methanol and gasoline/ethanol blends (0, 30 and 85$\%_{Vol.}$ alcohol) it was reported that the 85% alcohol blends showed a significant reduction in the accumulation mode particle concentrations (similar to background levels), but the nucleation mode showed a considerable increase. It was suggested that the addition of alcohol caused a reduction in the concentration of the intermediary soot precursor species. The reason for the increased nucleation mode was given that with a reduction in soot particles (accumulation mode) the surface area available for unburned hydrocarbons to adsorb onto was reduced and hence the HC self nucleated. The idea that the reduced accumulation mode is caused by the

reduction in soot precursors is supported by the study by Abrantes et al (2009), where a 92% reduction in polycyclic aromatic hydrocarbons (PAH) is observed for a vehicle fuelled with ethanol compared to a vehicle fuelled with gasohol.

2.3 2,5 Di-Methylfuran

In this study a novel bio-fuel is used and compared to bio-ethanol. This new fuel is 2,5 di-methylfuran (DMF), which is receiving considerable research attention now that a commercially viable production method has been proposed and developed by the Department of Chemical and Biological Engineering at the University of Wisconsin-Madison [Román-Leshkov (2007)]. DMF is regarded as a possible fuel for the future of internal combustion engines because it can be derived from bio-mass (fructose), it has a 40% higher energy density and requires less energy to produce than bio-ethanol [Román-Leshkov (2007)]. 2,5 di-methylfuran is a mono-oxygenated ring compound containing six carbon atoms that is a member of the Furan group of compounds, the structure is shown in Figure 2.1.

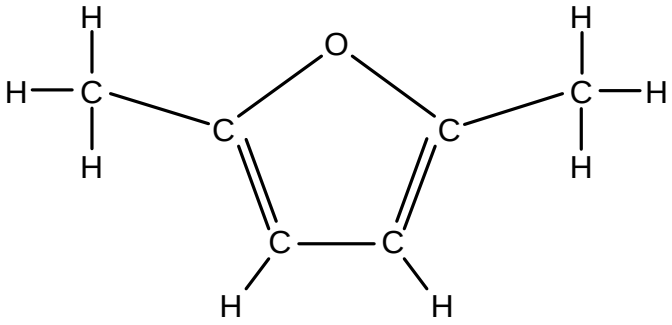

Figure 2.1 Molecular structure of 2,5 di-methylfuran

DMF has properties that make it a possible gasoline replacement; such as high octane rating, good volatility and acceptable boiling point, as shown in Table 3.6, Chapter 3. Despite this there is very little information available in the literature about its use as a fuel. Furans though have previously been used as octane enhancers in gasoline [Gouli et al (1998)].

2.4 Summary

A review of the literature relating to aspects of HCCI and spark ignition combustion has been conducted with the most important and relevant aspects being presented above. The aspects of HCCI combustion included are possible control methods including the trapping of exhaust residuals and direct fuel injection, the source of emissions and the use of conventional and oxygenated fuel blends. The areas of spark ignition combustion covered include the use of, and the problems associated with direct fuel injection, the use of oxygenated fuel blends and particulate matter emissions. This is used as a basis for the investigations presented in the following chapters of this thesis.

CHAPTER 3

3 Experimental Setup and Techniques

This chapter gives details on the equipment used in this study, including setup and operation. The engine control methods are described along with details being given on the important data processing techniques and calculations used in this study.

3.1 Single Cylinder Engine

The engine used in this study is a single cylinder four-stroke engine fitted with a four valve spray guided direct injection cylinder head.

3.1.1 General Overview

The basic geometry of the engine is shown in Table 3.1. The engine is fitted with both intake and exhaust plenums to reduce the pressure fluctuations in the intake and exhaust ducts respectively. The engine is pictured in Figure 3.1, showing the intake plenum (right) and exhaust plenum (left). The engine is fitted with a variable cam timing system that is described in more detail in Section 3.1.2.

Table 3.1 Basic engine geometry

Bore (mm)	90.0
Stroke (mm)	88.9
Swept Volume (cm^3)	565.6
Connecting Rod Length (mm)	160.0
Compression Ratio (Geometric)	11.5:1

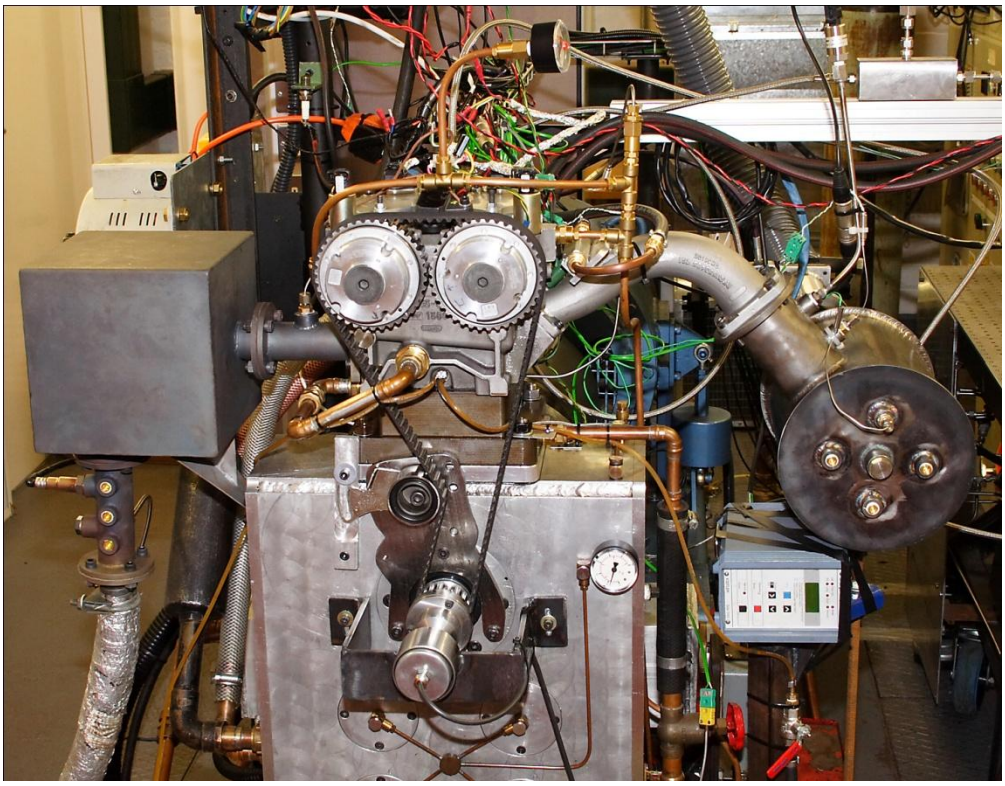

Figure 3.1 Single cylinder engine

The engine is coupled to a DC dynamometer, which is operated in constant speed mode; a speed of 1500 RPM is used for this study. During stable operation the speed is maintained within ±20 RPM whilst during unstable operation this can increase to ±200 RPM. Before any investigations are conducted the engine is warmed up at low load in spark ignition mode until the oil and water are at their operating temperatures, 85±5 °C and 95±3 °C respectively.

3.1.2 Combustion System

The combustion system for this engine consists of a centrally mounted, six-hole injector, with the spark plug being mounted beside the injector at an angle of 18 degrees to the cylinder axis, as shown in Figure 3.2 below. The orientation of the spray plumes is shown in Figure 3.3. It can be seen that the nozzle pattern consists of two groups of three holes, with the line of symmetry coinciding with the crankshaft axis. Spray plumes 1 and 6 pass either side of the spark plug.

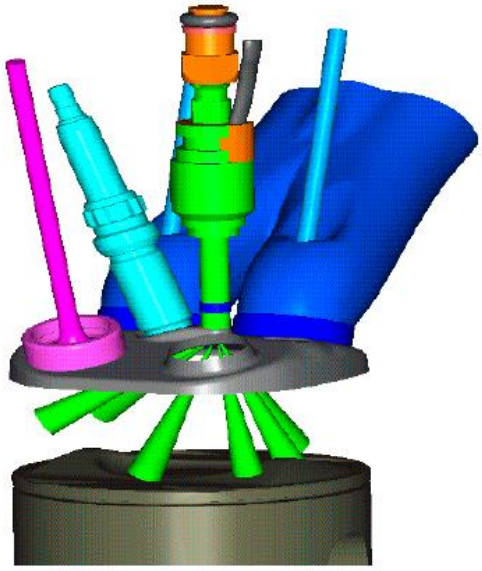

Figure 3.2 Layout of combustion system [Sandford et al (2009)]

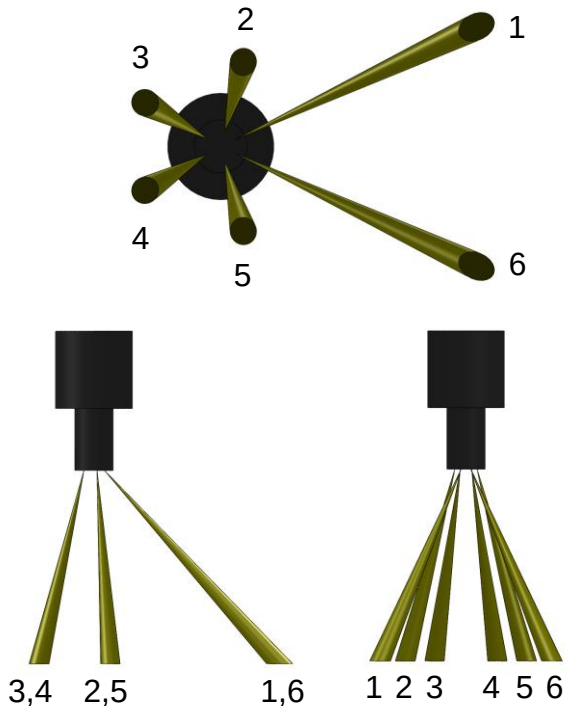

Figure 3.3 Injector spray plume orientation

3.1.3 Crankshaft Encoder Setup

The timing of the once per revolution signal generated by the crankshaft encoder needs to be accurately known as it is used by the engine control software (for injection and spark timings) and the variable valve timing software. The timing of this signal (relative to combustion TDC) is obtained by setting a spark timing of 0º $bTDC_{COMB}$ through the engine control software, and measuring the actual position of the spark by using a stroboscope and the 1/degree markings on the engine flywheel. Once this offset is obtained it can be entered into the engine control software so the 0º $bTDC_{COMB}$ spark actually occurs at TDC. The 1/degree markings on the flywheel are verified by measuring the position of the piston (relative to TDC) at various positions and calculating the angular distance from TDC from the crankshaft geometry.

3.1.4 Valve Train

For this study a variable cam timing system is fitted to the engine. Two different sets of camshafts are used; one set for HCCI and the other for spark ignition operation. Details of these are given below.

3.1.4.1 Variable Cam Timing (VCT) System

The variable cam timing (VCT) system fitted to this engine uses crankcase oil pressure to change the off-set of the camshaft relative to the camshaft pulley. The camshaft timing can be retarded by a maximum of 50 crank angle degrees for both the intake and exhaust camshafts. A custom LABVIEW script, in conjunction with a National Instruments counter-timer card (model 6202) is used to control the VCT system. The software monitors the camshaft position (relative to the cycle marker) once a cycle (two revolution of the crank shaft) and makes adjustments to the cam timing by changing the pulse width of the signal sent to the VCT oil control solenoids. Typically for stable engine operation the cam position can be maintained to within ±0.1 CAD. Figure 3.2 shows the VCT cam pulleys, oil control solenoids and cam position sensors in more detail.

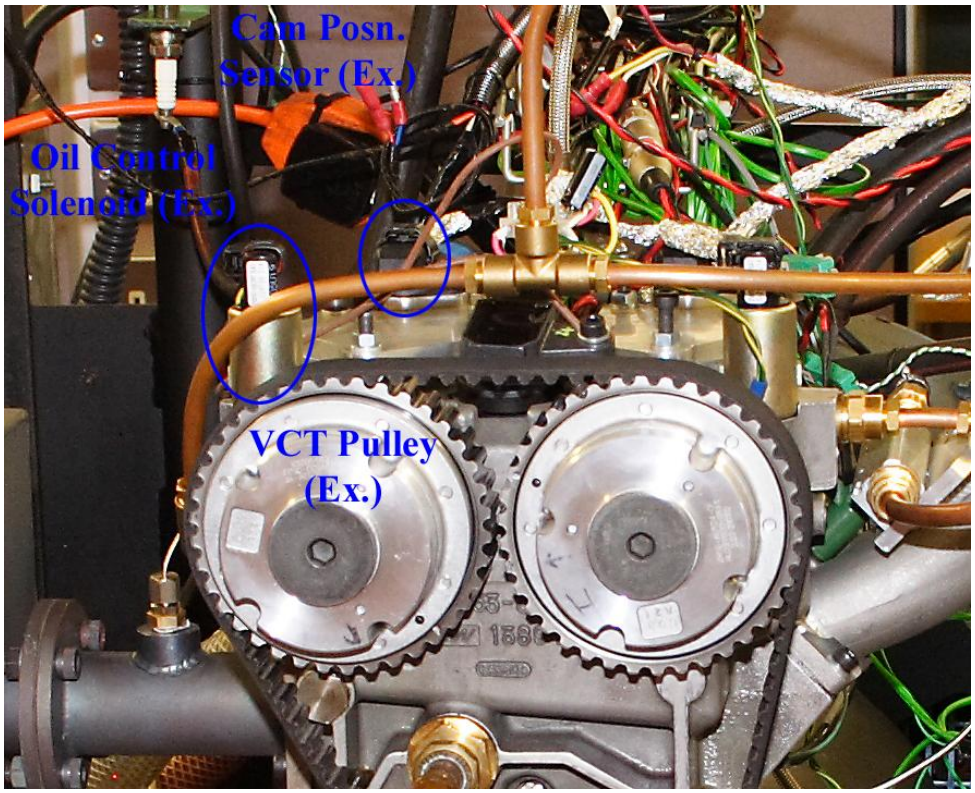

Figure 3.4 VCT System

3.1.4.2 Spark Ignition Camshafts

The geometry of the intake and exhaust camshafts used for the spark ignition investigations are shown in Table 3.2. These values are typical for a production engine of this cylinder size.

Table 3.2 Camshaft geometry – Spark ignition

	Intake	Exhaust
Maximum Lift (mm)	10.5	9.3
Duration (CAD)	250	250

3.1.4.3 HCCI Camshafts

The HCCI load control method chosen for this study involves the use of trapping exhaust residuals in the cylinder. This is achieved by closing the exhaust valve early and opening the intake valve late. To allow this strategy to work successfully the duration of the intake and exhaust camshafts have to be reduced (compared to SI) so the compression and expansion strokes are not adversely affected. This reduced duration has to be accompanied with a reduction in maximum valve lift to maintain acceptable valve acceleration values. The geometry of the intake and exhaust camshafts used for the HCCI investigations are shown in Table 3.3.

Table 3.3 Camshaft geometry – HCCI

	Intake	Exhaust
Maximum Lift (mm)	2.65	2.10
Duration (CAD)	130	110

3.1.5 Fuel System

The engine used in this study is fitted with a port fuel injection (PFI) system as well as a direct injection (DI) system. The PFI system is primarily for engine warm-up, but is also used to assess the mixture preparation performance of the DI system, such as wall wetting and fuel evaporation.

The DI fuel system is based on a free piston accumulator. The fuel is delivered from a 'day-tank' via an electric pump to the volume in the top of accumulator cylinder above the piston, the top of the cylinder is also connected to the DI injector. The space bellow the piston is pressurised with oxygen free nitrogen, supplied via a standard compressed gas cylinder (British

Oxygen Company, size W) and regulated by a standard gas regulator. The system also contains a circuit that allows for any unused fuel to be delivered back to the day tank along with the ability for the complete system to be flushed with compressed gas (nitrogen). The entire system consists of ¼-inch, seamless, stainless steel tube and stainless steel compression fittings. The system is manually controlled by operating the appropriate valves. The fuel pressure used throughout this study is 150 bar gauge.

3.1.6 Lambda Meter System

The lambda meter system used on this engine comprises of an ETAS Lambda Meter, model LA3 and a Bosch heated wideband oxygen sensor. This particular lambda meter allows the pre-programmed fuel properties to be changed to suit the fuel being used. These parameters are H/C, O/C and stoichiometric air-fuel ratios. This is particularly important when oxygenated fuels are used. The lambda control is open loop, with the engine operator adjusting the injection pulse width to achieve the desired value.

3.1.7 Control

The injection and spark timing parameters are controlled by a LABVIEW script using a National Instruments counter-timer card (model 6602). The start of injection timing and injection pulse width, along with the spark timing and coil charge time can be adjusted in real-time whilst the engine is running. The system is capable of controlling two separate injections per cycle, with these two injections having independent pulse widths.

Load control for spark ignition is achieved by the operator adjusting a butterfly throttle valve that is situated in the inlet track. For HCCI operation in this study the load is controlled by the mixture strength (λ) and the amount of trapped residuals (ER), via the VCT control system. In both cases the load control is open loop; however IMEP is calculated online by the high-speed data acquisition software (see Section 3.3.1). IMEP is calculated from the in-cylinder pressure, which is measured with a Kistler water cooled pressure transducer type 6041A, flush fitted with the cylinder head wall, connected to the data acquisition system via a Kistler 5011 charge amplifier.

The temperatures at various points on the engine (e.g. intake, exhaust, and engine oil and coolant) were all measured using type 'K' thermocouples. The engine coolant temperature was controlled by using a Proportional Integral Derivative (PID) controller to drive a solenoid valve that regulated the flow of cold water through a heat exchanger. The oil temperature was maintained by using a heat exchanger connected to the engines cooling system (hot water side).

3.2 Emissions Measurement

In this study both gaseous and particulate matter emissions are measured. A description of the measurement equipment and its operation is given in the following sub-sections.

3.2.1 Gaseous Emissions

During this study two different Horiba tower type exhaust gas analysers are used, a MEXA-1600DEGR and a MEXA-7100DEGR. In relation to simple emissions measurement both of the systems operate in the same way and use the same type of analyser modules the results from

both systems are directly comparable. The different exhaust gas components measured and the measurement method used are listed in Table 3.4.

Table 3.4 Exhaust emission measurement methods

Emission	Measurement Method
Total hydrocarbon	FID (Hot)
CO	NDIR (Dry)
CO_2	NDIR (Dry)
NO_X	CLD (Dry)

The exhaust is sampled downstream of the exhaust plenum via a heated line (and heated pre-filter for the MEXA-7100DEGR system). Both the heated line and pre-filter are maintained at a temperature of 191°C. At the start of a test schedule, before any measurements are taken the analyser modules are calibrated by the use of suitable bottled span and zero calibration gases.

3.2.2 Particulate Matter Emissions

In this study two different types of particulate matter emissions measurements are made. The first method measures the smoke level in the exhaust by filter blackening. For this an AVL 415S Smoke Meter is used, which samples the exhaust stream via a heated line. Three consecutive measurements, 30 seconds in duration, are taken and then averaged. The results are in the range of 0-9 with the units of Filter Smoke Number (FSN), a value of 0 represents a clean filter paper and a value of 9 represents a completely blackened filter paper.

The second type of PM emissions measurement method used is to measure the size and number distribution of the particles in the exhaust stream. This is achieved by using a Scanning Mobility Particle Sizer (SMPS). The particular instrument used is manufactured by TSI and comprises of a model 3080 particle classifier, a model 3081 Differential Mobility Analyser (DMA) and a model 3775 Condensing Particle Counter (CPC). The important SMPS settings used in this study are listed in Table 3.5.

Table 3.5 SMPS settings

Parameter	Value
Sample Flow Rate (l/min)	0.5
Sheath Flow Rate (l/min)	5.0
Scan Time (s)	120
Minimum Particle Diameter (nm)	10.7
Maximum Particle Diameter (nm)	487.0
D_{50} (nm)	978.9

A heated (80°C) rotating disk diluter is used, set a dilution ratio of 50:1. This dilution ratio is chosen as it is a compromise between sufficiently particle counts for reliable measurement and a ratio that is large enough so the measurements are insensitive to fluctuations in the dilution ratio. When only the solid carbon particles are to be measured a thermo-denuder is used, set to a temperature of 300°C. This is to drive-off the hydrocarbons species that are adsorbed onto the surface of the carbon particles, and those that form liquid particles directly.

3.3 Data acquisition System

A brief description is given below on the two data acquisition systems used for this study. The first is a high speed system for cycle resolved parameters and the second is a low speed system for the measurement of steady-state parameters.

3.3.1 High Speed

The high speed data acquisition system records cycle resolved data, primarily in-cylinder pressure and intake pressure. The outputs from the camshaft position sensors are also recorded for the purpose of checking the correct operation of the VCT system. The system consists of a custom LABVIEW script and a National Instruments data recording card, model 6251. The input signals are connected to the data acquisition card via a National Instruments breakout box, model BNC 2090. The data is recorded with a resolution of 0.5 CAD, for 100 consecutive cycles for the HCCI investigations (Chapter 4) and for 300 consecutive cycles for the spark ignition studies (Chapters 5 – 7).

3.3.2 Low Speed

The low speed data acquisition system records the signals that have a time period greater than an engine cycle. These signals are principally temperature (intake, exhaust, etc), volumetric intake airflow, the atmospheric conditions (temperature, pressure and humidity) and the output from the emissions tower. The signals from the thermocouples were passed through a thermocouple amplification circuit before going to the data recorder. The acquisition system consists of a custom LABVIEW script and a National Instruments data recording card, model 6220. The data

is recorded at a rate of 10 Hz, for 10 seconds for the HCCI investigations and for 30 seconds for the spark ignition studies. These approximate to the times required for the high speed data to be recorded for the respective investigations.

3.4 Data Processing

Data processing involves the manipulation of the data recorded by the high and low speed data acquisition systems. The data is processed by the use of a custom MATLAB script developed by the author. Parameters such as IMEP, presented as net IMEP, heat release rate, rate of pressure rise and maximum in-cylinder pressure are calculated for every recorded cycle and then averaged. The method used for the calculation of IMEP is the standard methods that can be found in any text on the subject, such as Stone (1999). Details on some of the less standard calculations, such as the estimation of ER rate, are given in the following sub-sections.

3.4.1 In-Cylinder Pressure Referencing

Piezo-electric pressure sensors are very effective at measuring the in-cylinder pressure. However the signal from the sensor can be susceptible to drift caused by temperature fluctuations, therefore the signals from the sensor need to be pegged to a reference. A commonly used method for this is based on the assumption that at intake BDC the in-cylinder pressure is the same as the intake pressure. Referencing is achieved by shifting the in-cylinder pressure trace for each individual cycle, so that the pressure at BDC_{INTAKE} is equal to the intake pressure at the same crank angle.

3.4.2 Heat Release Analysis

In this study heat release analysis is conducted in two parts with the first being the calculation of net heat release rate (Equation 3.1), as described in Stone (1999). The second part is the cumulative summation and normalisation of the heat release rate to obtain the mass fraction burned (MFB) data (Equation 3.2).

$$\frac{dQ_n}{dQ_\theta} = \frac{\gamma}{\gamma - 1} p \frac{dV}{d\theta} + \frac{1}{\gamma - 1} V \frac{dp}{d\theta}$$

Equation 3.1

where γ is approximated to be the polytropic exponent of compression and expansion, for which a different value is calculated for the respective parts of the cycle.

$$MFB = \frac{\sum_0^n \frac{dQ_n}{dQ_\theta}}{\sum_0^N \frac{dQ_n}{dQ_\theta}}$$

Equation 3.2

3.4.3 Combustion Efficiency

Combustion efficiency is evaluated from the exhaust gas composition (carbon monoxide and hydrocarbons) and is effectively calculated as combustion inefficiency, as shown in Equation 3.3, which is a simplified version to that used by Christensen and Johansson (2000).

$$\eta_{combustion} = 1 - \frac{x_{CO} Q_{LHV_{CO}} + x_{HC} Q_{LHV_{fuel}}}{\left[\dot{m}_{air} \Big/ (\dot{m}_{air} + \dot{m}_{fuel}) \right] Q_{LHV_{fuel}}}$$

Equation 3.3

where x_{CO} and x_{HC} are the mass fractions of CO and HC respectively and Q_{LHVco} and $Q_{LHVfuel}$ are the lower heating values of carbon monoxide and the fuel used respectively. The calorific value of the unburned hydrocarbons is assumed to be that of the fuel used. This is because the hydrocarbons are not speciated and hence the actual aggregated hydrocarbon calorific value is unknown.

3.4.4 Fuel Consumption

Due to the nature of the high pressure (DI) fuel system; fuel usage cannot be directly measured by the use of simple techniques, such as a mass balance or a burette. Fuel consumption is calculated from the inducted air flow rate and the air-fuel ratio. The volumetric inducted air flow rate is measured with a positive displacement rotary flow meter, which is converted to a mass flow rate by using the ideal gas law and by knowing the ambient air pressure and temperature. The inducted air mass flow rate is then divided by the gravimetric air-fuel ratio, which is calculated from the gravimetric stoichiometric air-fuel ratio and the recorded lambda value.

3.4.5 ER Rate for HCCI Combustion

For the HCCI investigations the ER rate is estimated by the method described by Risberg et al (2004). The mass trapped in the cylinder at the point of exhaust valve closing is estimated using the ideal gas law. At EVC the in-cylinder pressure is known along with the trapped volume (from crankshaft geometry), with the in-cylinder temperature being estimated to be the same as the exhaust temperature. From this the mass of trapped exhaust gas (ER) can be estimated, with the ER rate being given as a percentage of the total mass of trapped charge.

3.4.6 In-Cylinder Temperature

The in-cylinder temperature is only calculated for the HCCI investigations. This is due to the difficulties in estimating the amount of trapped exhaust residuals when a positive valve overlap valve timing strategy is used, like for the spark ignition investigation in this study. The in-cylinder temperature is estimated using the ideal gas law and by knowing the total trapped mass (fresh charge + ER), total in-cylinder volume (from crankshaft geometry) and the in-cylinder pressure. In calculating the temperature the blow-by losses are considered to be zero.

3.5 Fuel Properties

The pertinent properties of the unblended fuels used in this study are listed in Table 3.6. It should be noted that when the fuels are blended with gasoline no attempt is made to maintain the properties of the standard gasoline, such as octane rating and stoichiometric air-fuel ratio. It should also be noted that the 2,5 di-methylfuran used in this study originated from crude-oil rather than a bio-source, but is still representative of the bio-derived fuel.

Table 3.6 Table of fuel properties

	Standard Gasoline	Ultra Low Sulphur Diesel	Bio-Ethanol	2,5 Di-Methylfuran
Octane No. (RON)	95.8	-	~110 [1,2]	119 [3,4]
Cetane No.	-	54.1	-	-
LCV (MJ/kg)	43.0	42.7	26.8	33.3 [3]
$AFR_{Stoich.}$	14.48	-	8.96	10.73
H/C ratio	1.835	-	3.000	1.333
O/C ratio	0	-	0.500	0.167
Enthalpy of Vaporisation (kJ/kg)	372	-	919.6[5]	331.4[6]
Enthalpy of Vaporisation (for stoichiometric mixture) ($kJ/kg_{Mixture}$)	24.0	-	92.3	28.3
Density @15°C	0.7387	0.8333	0.7904	0.9
IBP (°C)	28.6	164.6	78	93
FBP (°C)	196.3	352.4		
Vapour Pressure @20°C (kPa)	87.8	-	5.9 [7]	2.9 [6]
Laminar Flame Velocity (cm/s)	~33 [8]	-	~39 [8]	~43 [9]

1.Nakata et al (2006)
2.Taniguchi et al (2007)
3.Román-Leshkov et al (2007)
4.Mousdale (2008)
5.Majer et al (1985)
6.Verevkin and Welle (1998)
7.Kar et al (2008)
8.Hara et al (2006)
9.Wu et al (2009)

3.6 Analysis of Uncertainties in the Recorded Data

The purpose of this section is to provide a guide to the accuracy of the measurements made during this study. The data presented is generally assembled from the relevant manufacture's instruction manuals and product literature. The instruments covered include the dynamometer, valve timing control system, in-cylinder pressure sensor and the emissions measurement equipment.

The dynamometer control is achieved by using a Mentor II Digital DC Drive manufactured by Control Technologies. The resolution accuracy of the encoder used is better than 0.01% and the drive has a speed holding accuracy of 0.1%.

The steady state positional (valve timing) accuracy of the variable cam timing (VCT) system for stable operating conditions is typically ± 0.1 CAD, as shown by the on-screen position off-set error graph and from the cam position trace recorded by the high speed data acquisition system.

The in-cylinder pressure was measured using a Kistler 6041A water cooled pressure sensor connected to a Kistler 5011B charge amplifier. The linearity error of the pressure sensor is given by the manufacturer as less than ± 0.5% of the full scale. With cooling the sensor has a sensitivity shift of less than ± 0.5%. The manufacturer also gives information on the short term drift and change in IMEP value when compared to a reference sensor in a test engine operating at a load of 9 bar IMEP at an engine speed of 1500 RPM, these values are less than ± 0.25 bar

and less than ± 2% respectively. The linearity error of the charge amplifier is given as less than ± 0.05% of the full scale.

The gaseous emissions were measured with either a MEXA-1600DEGR or a MEXA-7100DEGR, both of which are manufactured by Horiba Instruments Limited. Both analyser systems are accurate to ± 1% of the full scale, while the MEXA-7100DEGR has a zero/span drift of no more than ± 1% of the full scale measured over a period of 8 hours.

The condensing particle counter (TSI Incorporated, Model 3775) that forms part of the SMPS system (Section 3.2.2) has a particle count accuracy of ± 10% for particle concentrations lower than $5x10^4$ particles/cm^3 and ± 20% for particle concentrations lower than 10^7 particles/cm^3.

To help eliminate the problems caused by random events and noise in the data signals and acquisition system the data is collected for a number of cycles and then averaged as described in previously in Section 3.3.

CHAPTER 4

4 The Effect of Conventional and Bio-Fuel Blends on Gasoline HCCI Combustion and Emissions Performance

In this chapter the effects of adding conventional ultra low sulphur diesel (ULSD) and bio-fuels (ethanol and 2,5 di-methylfuran) to standard 95 RON gasoline on HCCI combustion and emissions are investigated in a direct injection spark ignition (DISI) engine.

4.1 Dieseline HCCI

In this section diesel/gasoline blends are investigated, which are referred to as ‘Dieseline’. The concept of ‘Dieseline’ comes from the strategy of modifying the fuel properties to make it more suitable for HCCI combustion. Gasoline and diesel are currently the most commonly used automotive fuels, but their properties are not perfectly suited to HCCI combustion. Gasoline with a high Octane rating (~90-100) does not ignite readily, and with diesel having a high Cetane rating (~50-60) ignites and combusts too easily. With dieseline being a mixture of the two fuels, the combined fuel properties are more suited to HCCI combustion.

Gasoline is used as the main bulk fuel because it is very volatile, and thus produces a homogeneous mixture. Diesel is then blended with the gasoline to increase its Cetane number and thus making it more suitable for compression ignition [Weall and Collings 2007]. The benefits of dieseline have previously been investigated with a PFI engine by Zhong et al (2005 and 2006), and more recently by Xu et al (2007).

Direct injection (instead of PFI) was chosen for this study for the following reasons; with the first reason being that it better represents current and future trends for engine technology [Cole et al (1998)], with direct injection being used to increase the power density of SI engines [Wyszynski et al (2002)]. Secondly, with diesel fuel having a low volatility, much higher injection pressures (compared to conventional gasoline PFI systems) are required for creating a homogeneous mixture [Bhusnoor et al (2007)]. Also, with a DI system, changing the start of injection/injection strategy can to a certain degree change the combustion phasing [Urushihara et al (2003)]. Clearly, the relatively higher injection pressure of the in-cylinder direct injection will help the atomisation of dieseline fuel which in comparison with gasoline will have a lower volatility (depending on the diesel blending ratio).

Two different splash blends of diesel/gasoline are examined, with the blends being 10 and 20% ULSD in gasoline as well as standard gasoline. These are designated as Dx, with ‘x’ representing the percentage by mass of diesel in the dieseline blend.

The valve timing strategies used in this study are that the exhaust valve is closed before TDC_{GE}, and the intake valve is opened after TDC_{GE}. EVC and IVO are symmetric about TDC_{GE}. The early closing of the EV and the late opening of the IV cause exhaust gas residuals to be trapped in the cylinder (internal EGR). This is done to raise the temperature of the in-cylinder charge causing it to combust more easily. Also high levels of ER can slow down combustion lowering peak in-cylinder pressures and temperatures. [Yao et al (2005)]. Figure 4.1 below shows the valve lift profiles for both minimum and maximum NVO used in this study, overlaid on a representative in-cylinder pressure trace.

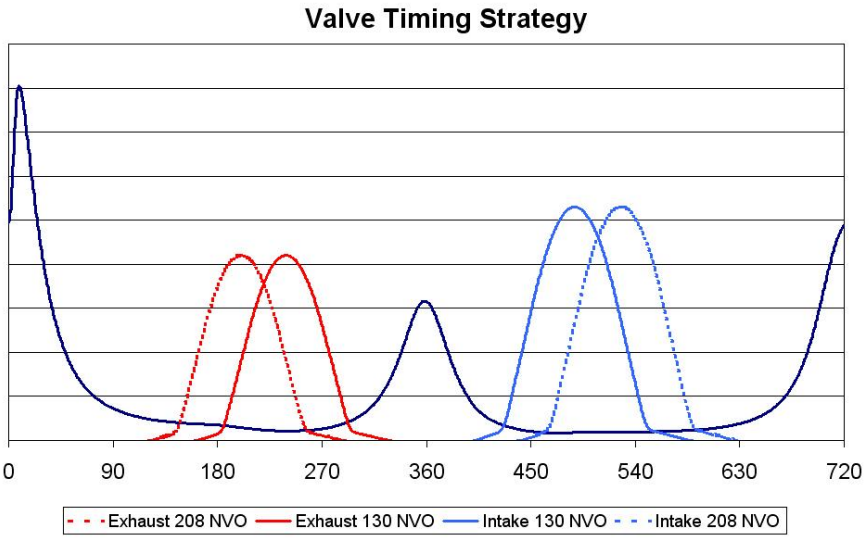

Figure 4.1 HCCI, Valve timing diagram

The NVO values used in this study ranged from 130 – 200CAD in 10CAD steps and 208CAD. Four values of Start of Injection (SoI) were used for all of the NVO values presented above, and these were 360, 330, 300, and 270 CAD $bTDC_{COMB}$ and denoted as 360SoI, 330SoI, 300SoI, and 270SoI respectively. The injection duration was not kept constant because the amount of fuel delivered was controlled by injection duration. The injection duration varied from

approximate 6 – 10 CAD depending on valve timing, desired lambda value, and fuel used. It should be noted that the rich mixture limit was chosen to be slightly lean (excess air) of $\lambda = 1$ as to avoid slight variations in the mixture stoichiometry causing noticeable differences in the CO emissions produced. The criteria for defining the operating region in this study are that the rate of pressure rise is below 5 bar/CAD, and the COV_{IMEP} is lower than 5%. The limit for the rate of pressure rise was chosen to reduce the level of combustion noise, and to reduce the loading applied to the engine components with it being an SI engine. The COV_{IMEP} limit was selected as it is widely accepted that 5% COV_{IMEP} is the point at which end users can start to detect unstable operation. It should be noted that these criteria were not met by all of the NVO/SoI combinations presented above for all fuels, and therefore those outside of either of the ranges are not presented here.

4.1.1 Operating Window expansion

The IMEP-Lambda operating regions for ULG95, D10 and D20 are shown in Figure 4.2. Also shown are the points used for the combustion and emissions comparison, these points are arranged to compare a range of approximately constant load points for the three fuels. Only the points with best fuel consumption (for each fuel) are presented. The operating region is generated from running the engine at the valve timings and injection timings listed previously, and varying the mixture strength until the rate of pressure rise was over the limit of 5 bar/deg (for low λ) or the combustion became unstable with COV > 5% (for high λ), as shown in Figure 4.2. The operating region is then the area that covers all of these points.

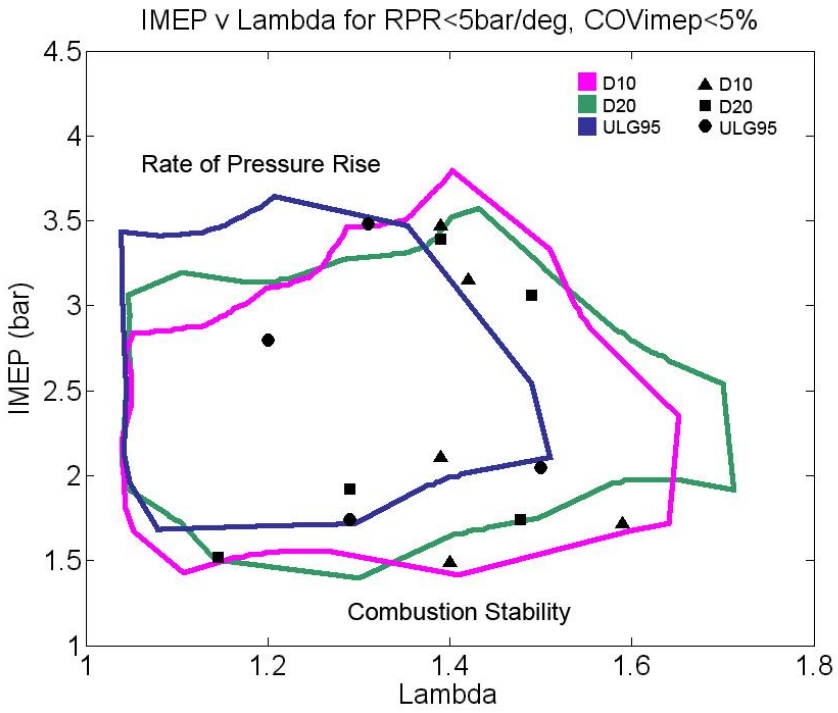

Figure 4.2 HCCI – Dieseline, Load window comparison

It can be seen that by adding a small quantity of diesel to the fuel the upper load limit can be marginally increased (4% increase in IMEP for D10 compared to gasoline), the lower load limit reduced (16% and 19% reduction in IMEP for D10 and D20 respectively, compared to gasoline), and leaner mixtures can be used. D10 shows an increase in the upper load limit because stable lean combustion can be achieved at a reduced NVO (and thus reduced ER rate) allowing more fresh charge into the cylinder, while the reduced mixture strength has allowed excessive rates of pressure rise to be avoided. With an increase in diesel fuel concentration, D20 does not show this increase in upper load limit because stable combustion could be achieved for only the earliest SoI (360º $bTDC_{COMB}$). However with early injection, combustion is advanced, which results in more heat transfer loss and worse combustion phasing and thus reducing the load produced. It is clear in Figure 4.2 that the lower load limit is extended with both D10 and

D20. This is because stable combustion can be achieved for leaner mixtures at the same valve timings compared to gasoline. Diesel blending increases the fuels ignitability; however the mechanism is still unclear and will be discussed in Section 4.1.5.

4.1.2 Combustion

The addition of diesel to the gasoline causes the start of combustion (SoC) to advance. Figures 4.3-4.5 show the 5% MFB values for the three fuels tested with an injection timing of 360º bTDC$_{COMB}$, plotted against the engine operating conditions (NVO/SoI) for the Load/Lambda windows presented in Figure 4.2. If the overlapping operating points (same NVO and SoI) are compared it can be seen that D10 advances combustion typically by 2 CAD, and D20 by 3 CAD, compared to gasoline.

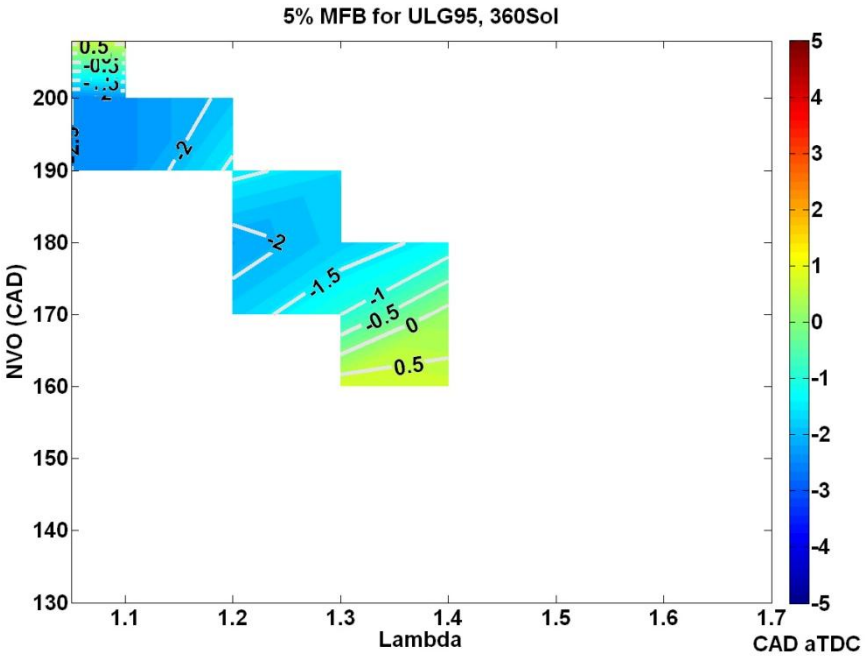

Figure 4.3 HCCI – Dieseline, 5% MFB for ULG95, 360SoI

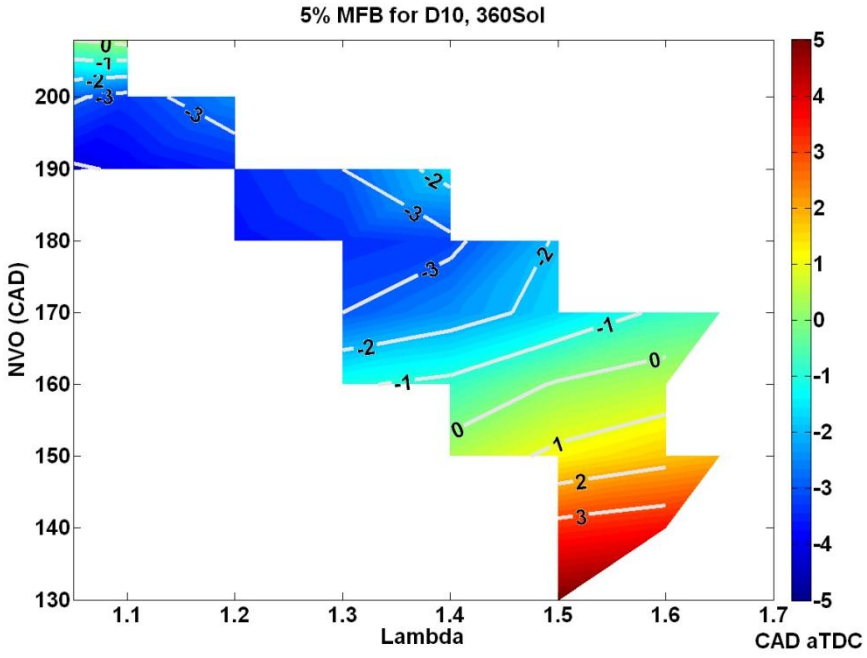

Figure 4.4 HCCI – Dieseline, 5% MFB for D10, 360SoI

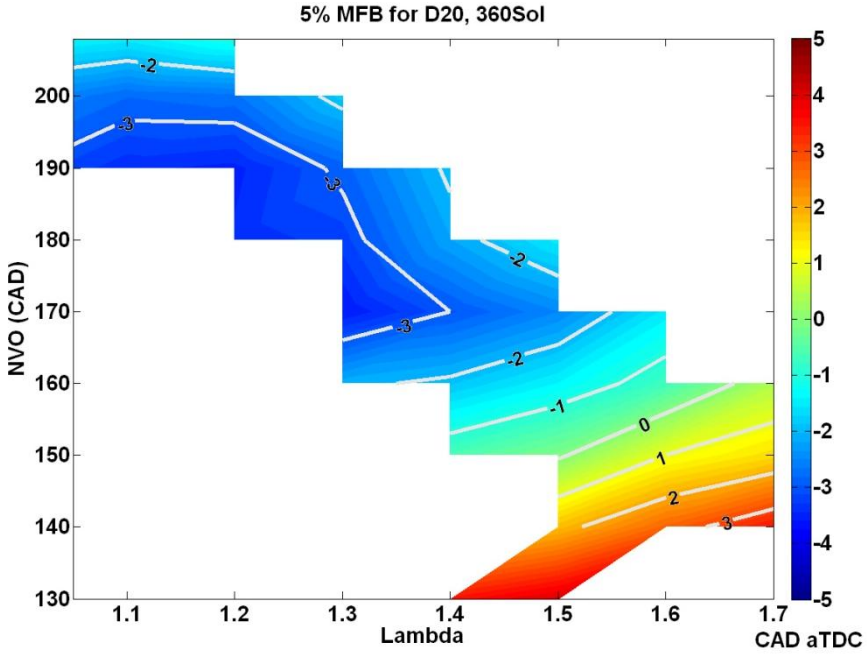

Figure 4.5 HCCI – Dieseline, 5% MFB for D20, 360SoI

This advance in combustion timing is because D10 and D20 ignite at a lower temperature than that of gasoline. The in-cylinder temperatures at the point of 5% MFB for the three fuels (at the engine operating conditions as Figures 4.3-4.5) are shown in Figures 4.6-4.8. The in-cylinder temperature calculation is described in Chapter 3, Section 3.4.4. It can be seen that at overlapping operating points D10 and D20 typically ignites at a temperature 50K and 60K lower than that of gasoline respectively.

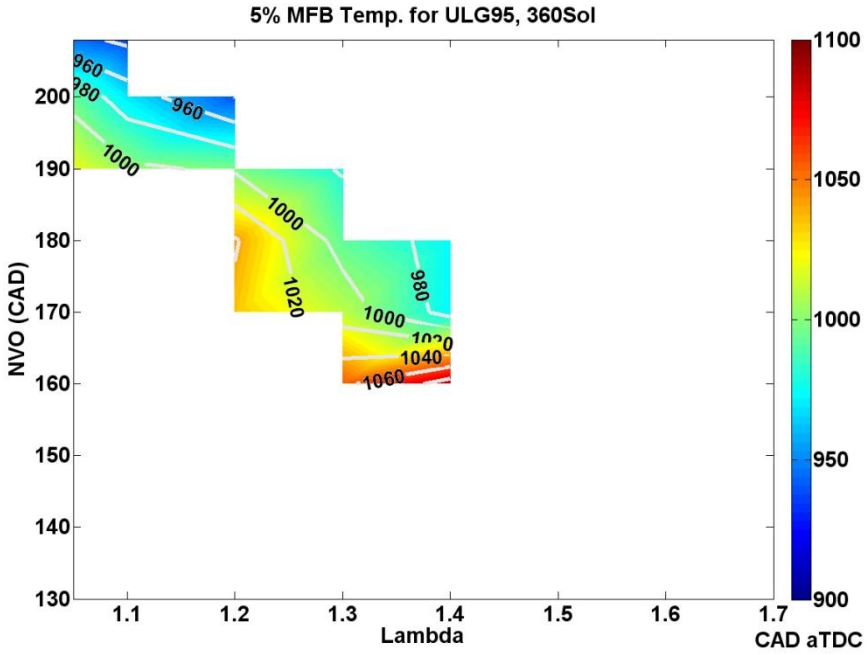

Figure 4.6 HCCI – Dieseline, In-cylinder temp. at 5% MFB for ULG95, 360SoI

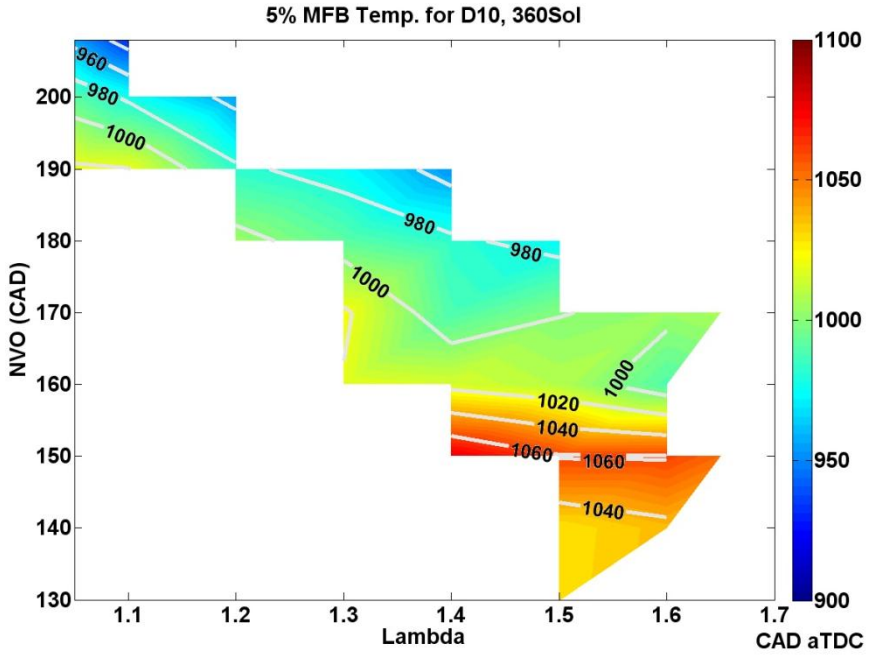

Figure 4.7 HCCI – Dieseline, In-cylinder temp. at 5% MFB for D10, 360SoI

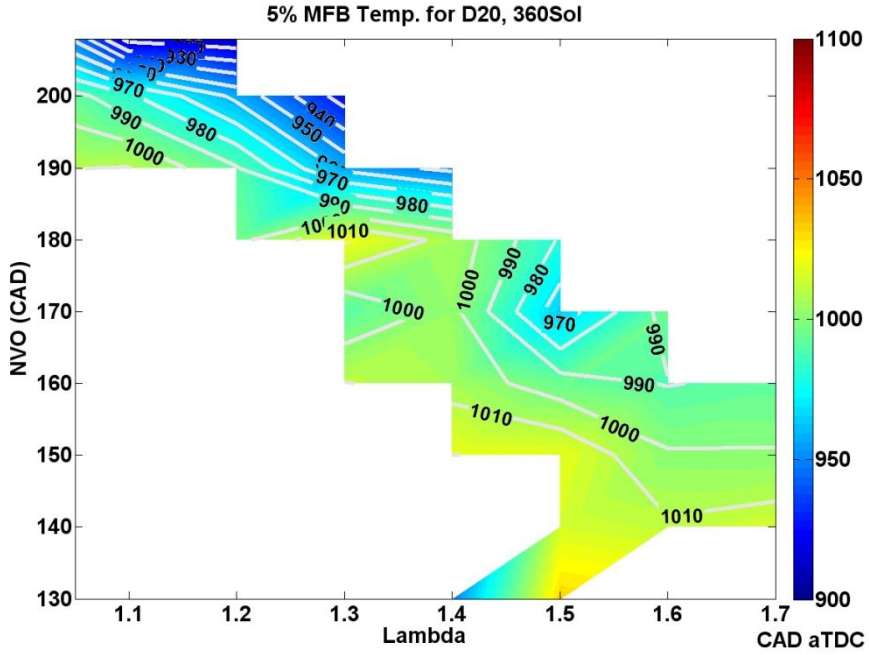

Figure 4.8 HCCI – Dieseline, In-cylinder temp. at 5% MFB for ULG95, 360SoI

With Dieseline having greater ignitability (combustion is advanced for the same inlet conditions), leaner mixtures (accompanied with a decrease in ER) of Dieseline can be used to achieve the same load as gasoline, but with combustion retarded and slowed compared with pure gasoline resulting in reduced rates of pressure rise and maximum in-cylinder pressures, which gives the possibility of load extension. The 5% MFB timing and 5-50% MFB duration are shown in Figures 4.9 and 4.10 respectively for the combustion and emissions comparison points.

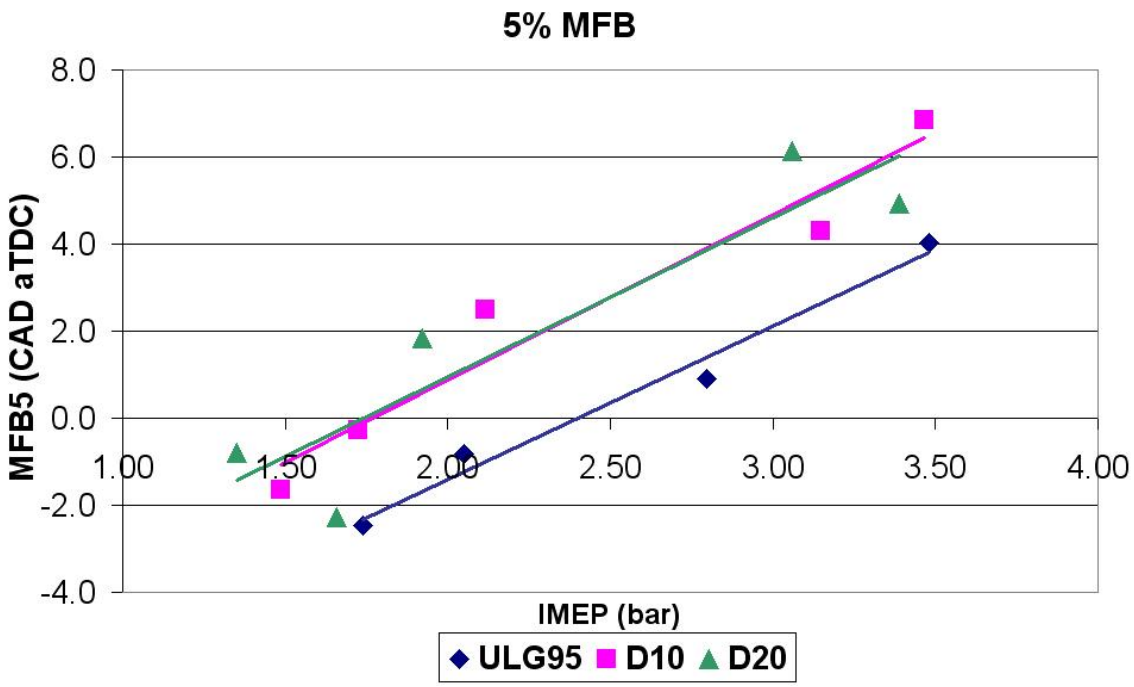

Figure 4.9 HCCI – Dieseline, 5% MFB timing

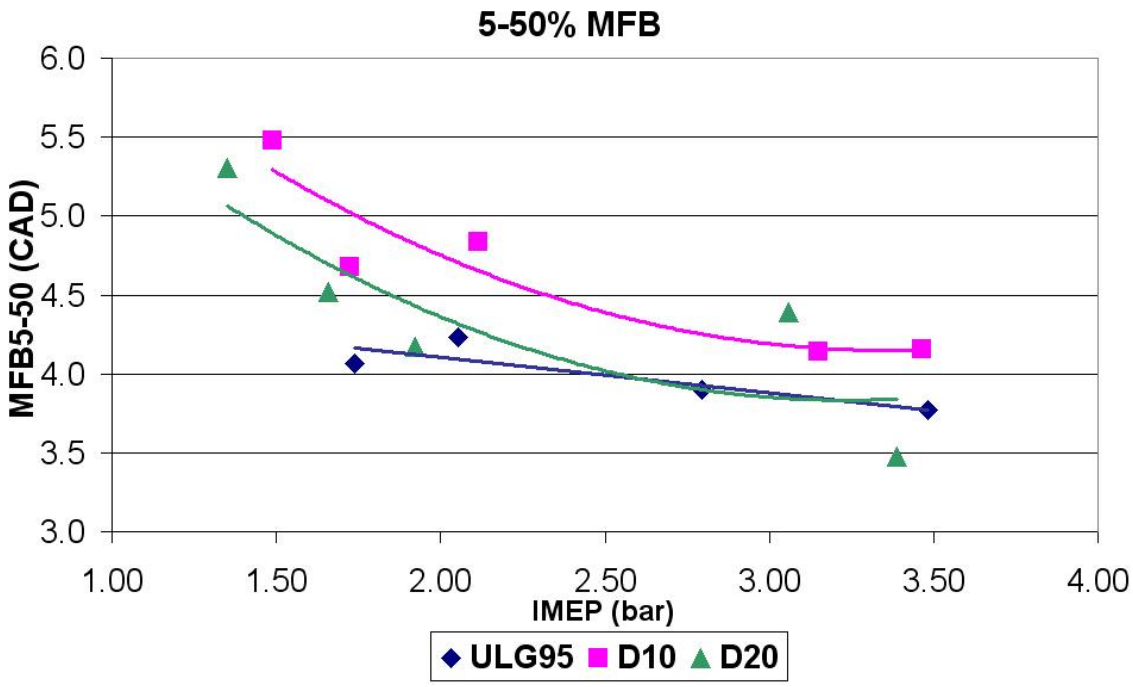

Figure 4.10 HCCI – Dieseline, 5-50% MFB duration

It can be seen that the D10 combustion is retarded by approximately 2 CAD and the 5-50% MFB duration is increased by 0.5 CAD compared to gasoline. The combustion timing for D20 is the same as that for D10, but the duration generally lies somewhere between that of ULG95 and D10. This is because the mixture strength (λ) for D20 was similar to that of D10, reducing the mixture strength resulted in reduced combustion stability. With D20 having improved ignitability over D10, similar mixture strengths resulted in faster combustion for D20 compared with D10.

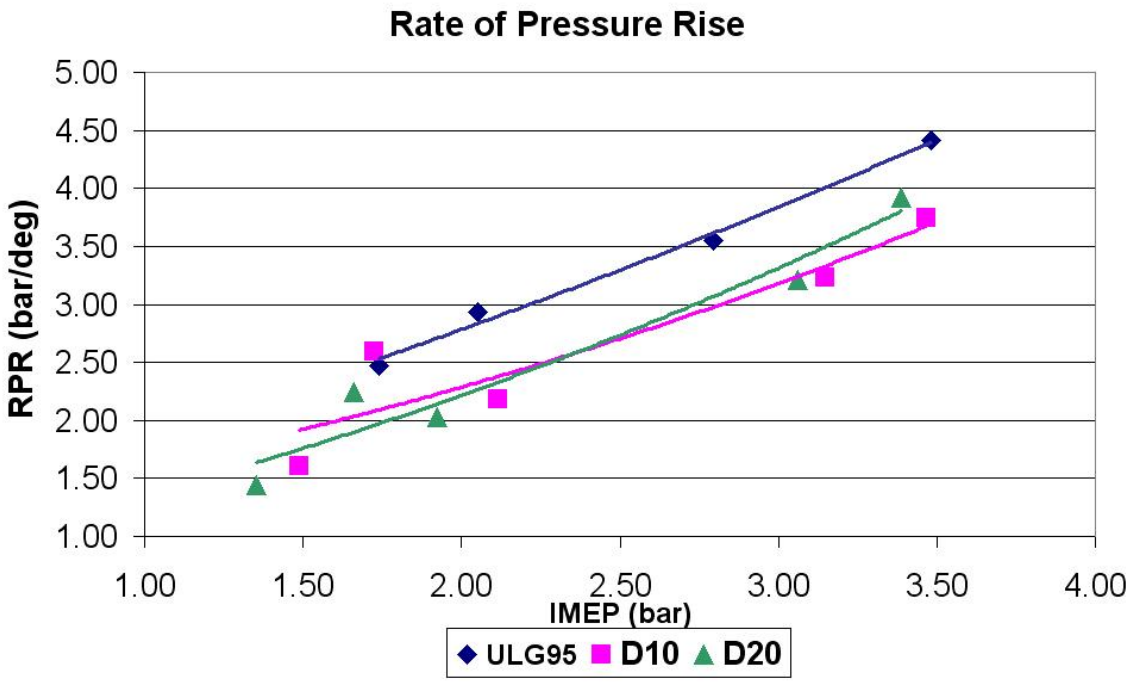

Figure 4.11 HCCI – Dieseline, Rate of pressure rise

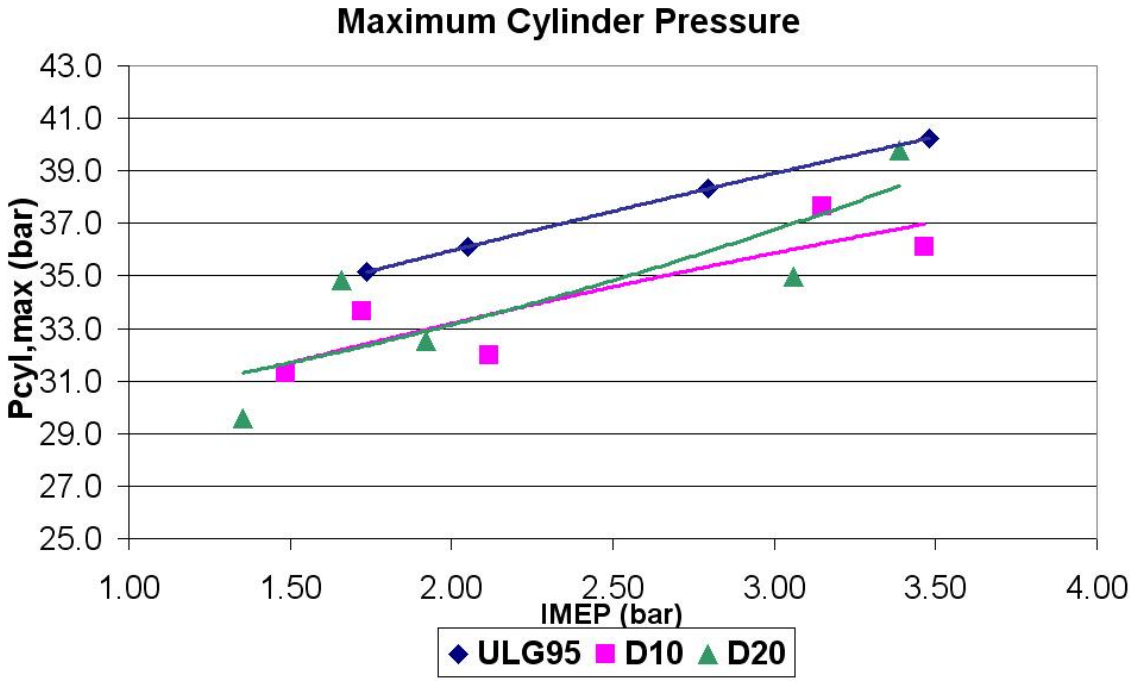

Figure 4.12 HCCI – Dieseline, Peak in-cylinder pressure

Rates of pressure rise and peak cylinder pressures are shown in Figures 4.11 and 4.12 respectively. It can be seen that both D10 and D20 have lower rates of pressure rise and reduced peak pressures across the load range compared to gasoline. Though at higher loads, D20 has higher rates of pressure rise and peak pressures than D10. This shows the same trend as the 5% MFB and 5-50% MFB values. Retarded and slower combustion has led to lower rates of pressure rise and reduced peak pressures (especially for D10).

Combustion stability is shown in Figure 4.13, in the form of the coefficient of variation of IMEP. It can be seen that the leaning of the D10 and D20 mixtures has not adversely affected the combustion stability at high loads, but at lower loads there is a decrease in combustion stability.

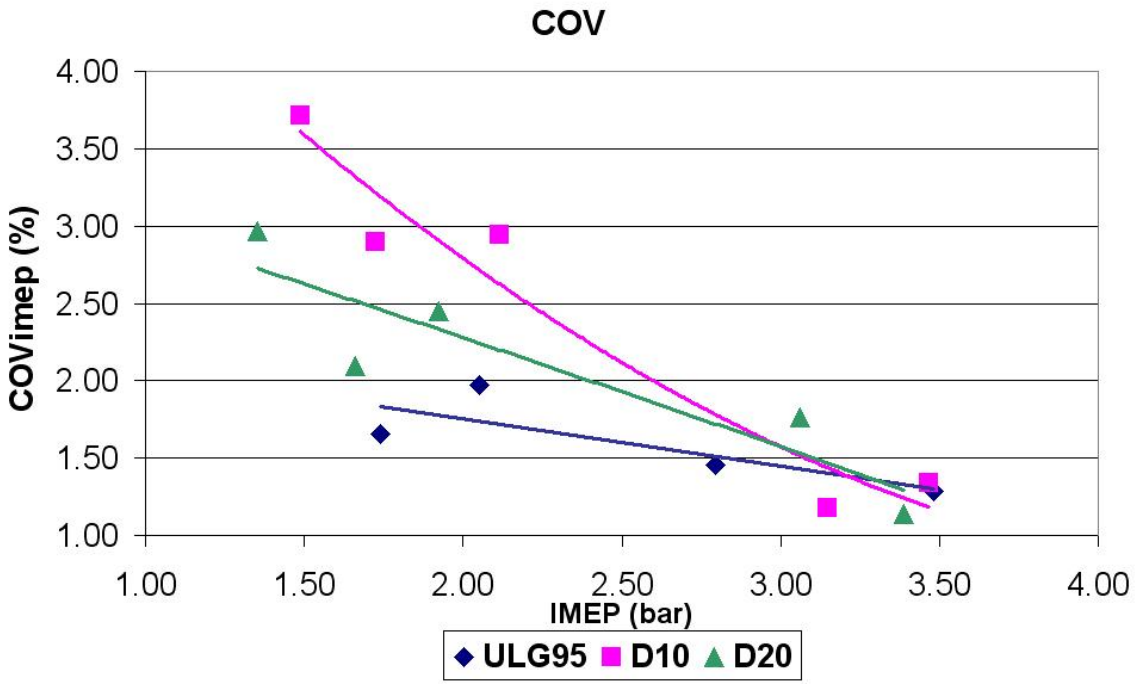

Figure 4.13 HCCI – Dieseline, Combustion stability

4.1.3 Emissions

The addition of diesel fuel to gasoline shows an improvement in the specific NO_X emissions, as shown in Figure 4.14. This can be attributed partially to D10 and D20 operating with a leaner mixture, reducing the combustion violence and peak temperatures, but also the retarded and slowed combustion will result in lower in-cylinder temperatures.

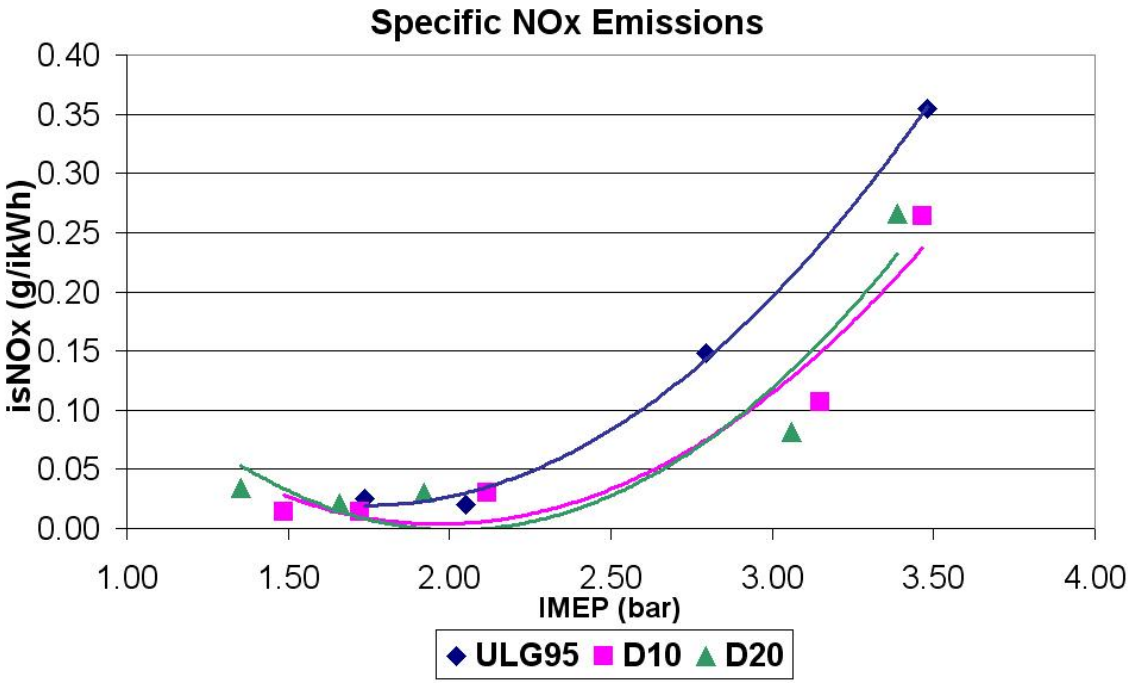

Figure 4.14 HCCI – Dieseline, Indicated specific NO_X emissions

The reduction in NO_X emissions is accompanied by an increase in hydrocarbon emissions as shown in Figure 4.15. This increase in hydrocarbon emissions can be attributed to the injection timing of D10. The 360SoI might cause part of the fuel to impinge onto the piston crown, and increase the HC emissions. Lower combustion temperature gives another contribution to the relatively high HC emission. In HCCI combustion there seems to exist an HC – NO_X trade-off that is similar in nature to the diesel NO_X – Soot trade-off, and is related to combustion temperature. This will be discussed further in Section 4.3.

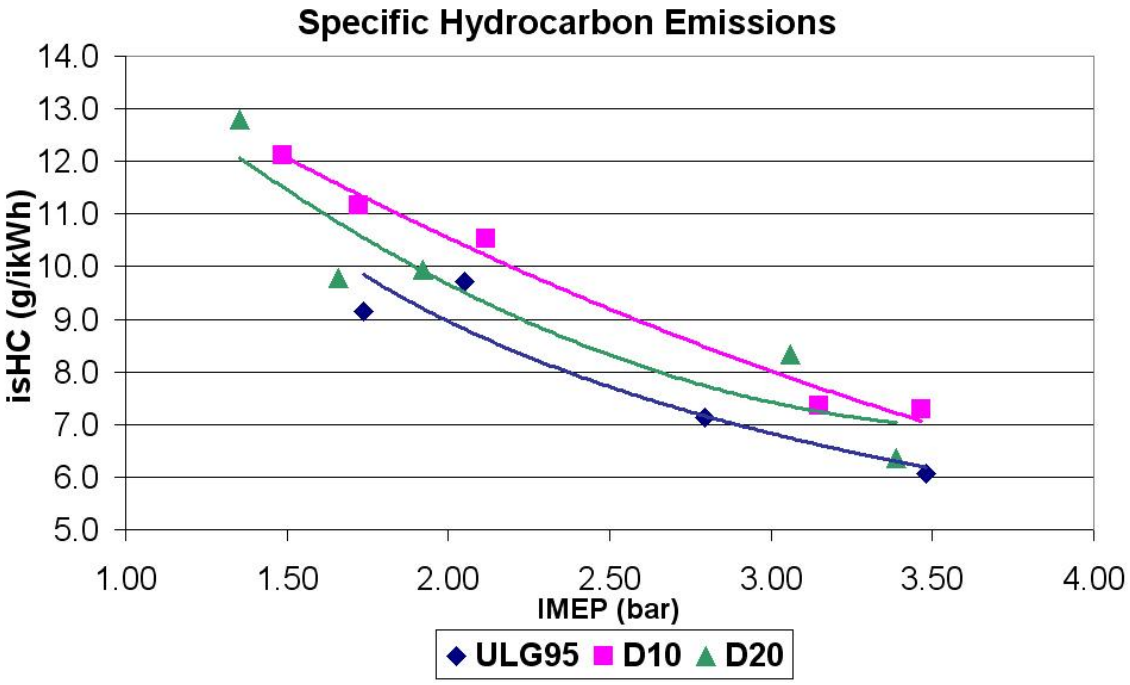

Figure 4.15 HCCI – Dieseline, Indicated specific hydrocarbon emissions

The carbon monoxide emissions are shown in Figure 4.16. For high loads the CO emissions for D10 and D20 are similar to those of gasoline which suggests that there is sufficient temperature for complete combustion. For lower loads D10 and D20 show an increase in CO emissions, this is because the combustion mixtures are leaner resulting in insufficient combustion temperatures for complete combustion.

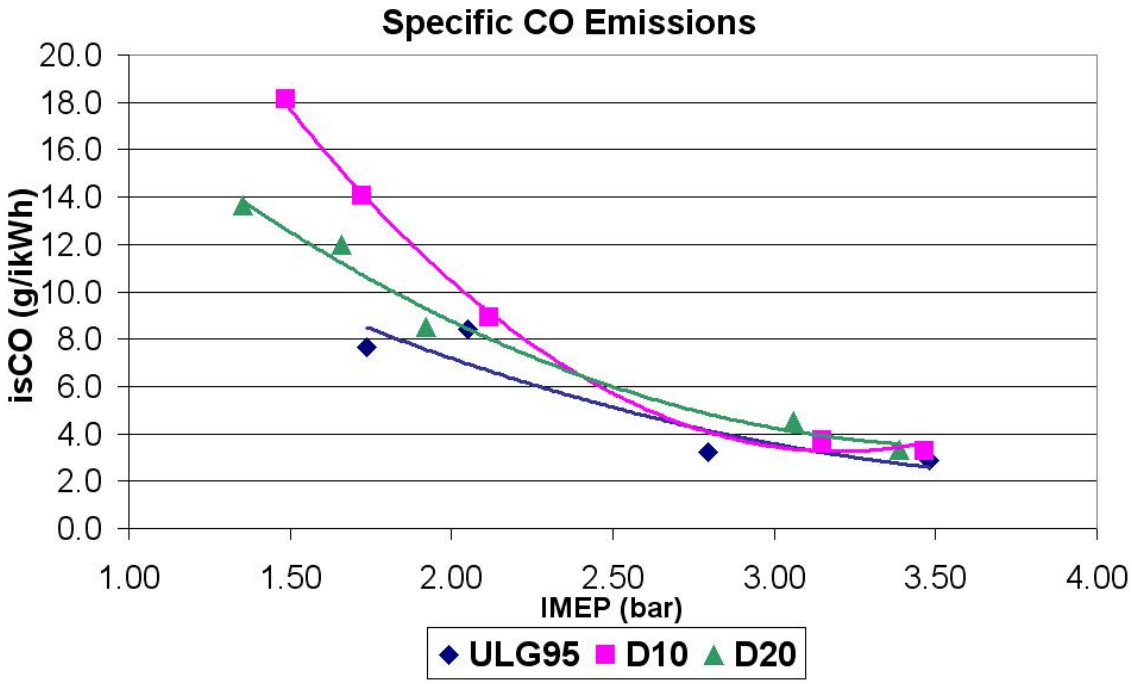

Figure 4.16 HCCI – Dieseline, Indicated specific carbon monoxide emissions

The smoke emissions (measured as FSN) for D10 up to 2 bar IMEP are virtually the same as that of gasoline and are almost zero. At higher loads the D10 smoke emissions differ significantly from those of gasoline but are still very low (bellow 0.050 FSN). With increasing the diesel content, D20 has significantly higher smoke emissions than gasoline, though are still low. Smoke emissions are shown in Figure 4.17. This increase in smoke can be attributed to the low volatility of diesel fuel and the relatively low (compared to common-rail diesel) injection pressure. This means that it is more difficult for the diesel droplets to break-up and evaporate to form a homogeneous mixture, resulting in rich spots within the mixture. This will be made worse with injection timings that occur later in the NVO period. This is because the in-cylinder temperature at the start of injection will be lower, thus reducing the fuels ability to evaporate.

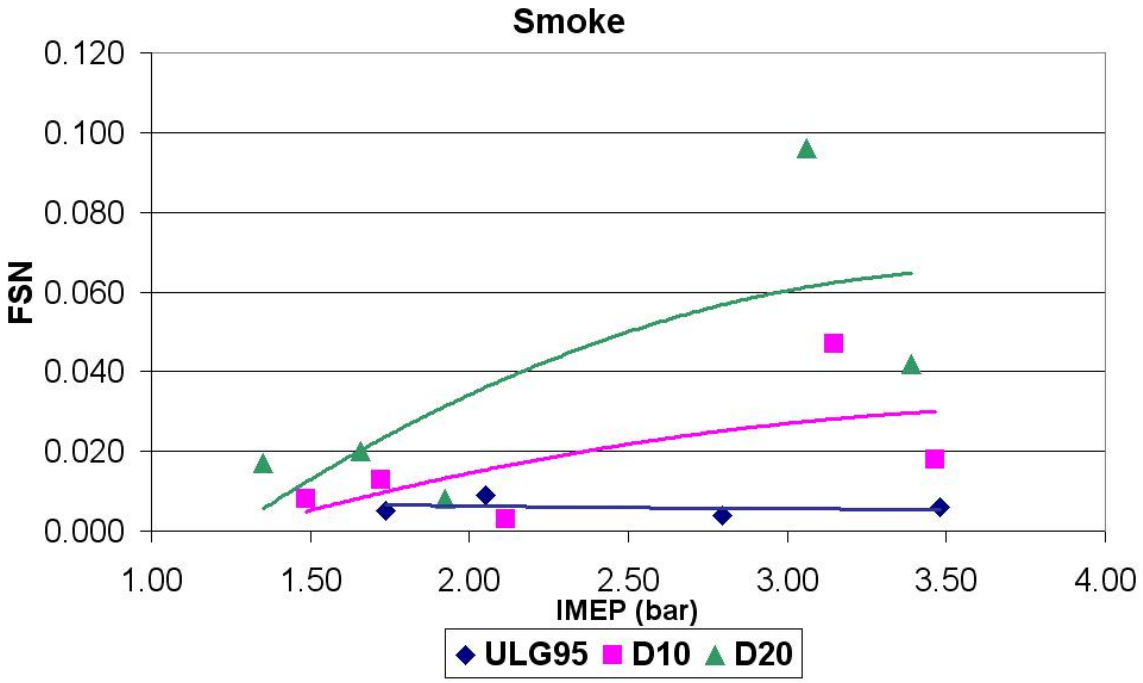

Figure 4.17 HCCI – Dieseline, Smoke emissions

4.1.4 Efficiency

The specific fuel consumption for D20 as shown in Figure 4.18 is similar to that of standard gasoline. However D10 shows an improvement in fuel consumption in the middle of the load range. This can be attributed to D10 generally having a retarded start of combustion timing. This results in more energy being released after TDC, and thus higher loads for the same energy input. Although D10 shows reduced fuel consumption in the middle of the load range, all three fuels show very similar peak indicated efficiencies. The maximum indicated efficiencies achieved (from within the operating region shown in Figure 4.2) for the three fuels are gasoline – 0.37, D10 – 0.36, and D20 – 0.37.

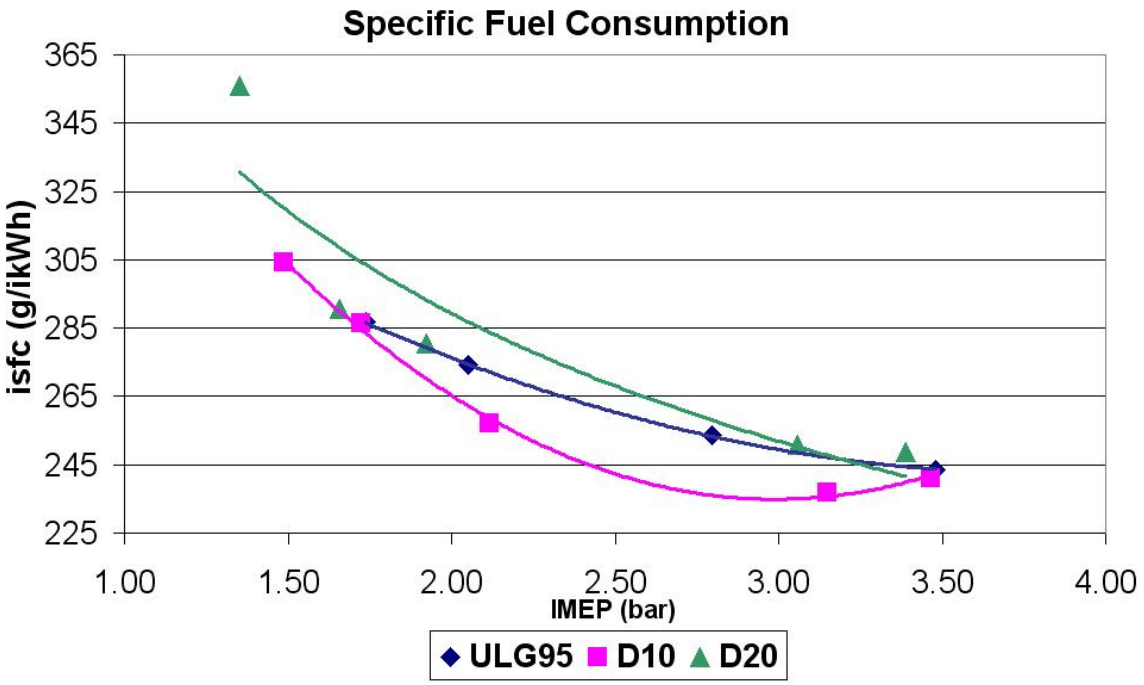

Figure 4.18 HCCI – Dieseline, Indicated specific fuel consumption

4.1.5 Discussion of Dieseline Combustion

It can be clearly seen from the results that dieseline has improved ignitability compared to "single component" gasoline. As predicted by the Arrhenius formula [Sazhina et al (1999)], the cylinder charge needs to reach a critical condition before combustion can take place, with this condition being decided by temperature, concentration and composition. For an absolutely homogeneous charge all of the cylinder contents need to reach this critical condition before combustion can commence in any part of the cylinder. However, for an inhomogeneous charge, even if the average condition is the same (and below the critical condition), once some peak spots which are caused by the inhomogeneity exceed the critical condition, combustion occurs in these spots and consequently increase the temperature and pressure in the whole cylinder. By these means, adequate inhomogeneity enhances the ignitability of "homogeneous" charge compression ignition and shows benefits to the combustion control.

Clearly, dieseline introduces more inhomogeneity into the mixture by the long chain hydrocarbon molecules, which improves the HCCI performance. This inhomogeneity induced by dieseline is likely to be caused by the poor volatility of the long chain hydrocarbon molecules of the diesel fuel. This is not helped by the relatively low injection pressures used in this study. It is likely that the diesel remains as small droplets creating spots of locally rich mixture. Further optical study is required to investigate this claim.

But, what is still not clear is whether dieseline performs more like gasoline, diesel, or a mixture of the two fuels. From the in-cylinder pressure trace and heat release rate analysis, as shown in Figure 4.19 (average of 100 cycles, the COV_{IMEP} values were 4.3%, 1.7% and 2.1%, for ULG95, D10 and D20 respectively.), no sign was shown of any LTC as is the case for normal diesel fuel. This means that with up to 20% diesel addition the fuel is more gasoline like than a gasoline/diesel mixture. This agrees with what has been shown in previous research [Akira and Shoji (2007)]. When a high Cetane number fuel (n-heptane) was added into a high octane number fuel (gasoline), the mixture showed a more diesel-like character, but before a critical value was reached, no sign of LTC combustion could be observed from HRR analysis. This is also the outcome found by Christensen et al (1999); in their study 35% diesel was required before any LTC was visible. However the work by Ryan et al (2004) does show LTC for mixtures as low as 20% diesel in gasoline, though they used lower rates of ER (maximum of 50%) compared to this study (50-75% approx).

One explanation for the lack of LTC with low concentrations of diesel (less than 30%) is that the values of HRR in the LTC region are small even for diesel when compared to the HRR values for the main combustion. When the diesel is diluted (by being added to gasoline) there is going to be less diesel in the cylinder and thus the energy released in the LTC region is also going to be reduced. This reduced value could then be masked by noise on the in-cylinder pressure trace and heat loss effects not accounted for in the heat release analysis. To resolve this issue higher precision pressure traces are required, and heat loss/transfer must be factored into the heat release analysis. Optical spectroscopy measurements (with sufficient resolution and low background noise) may also show the presence of a LTC region for low concentrations of diesel.

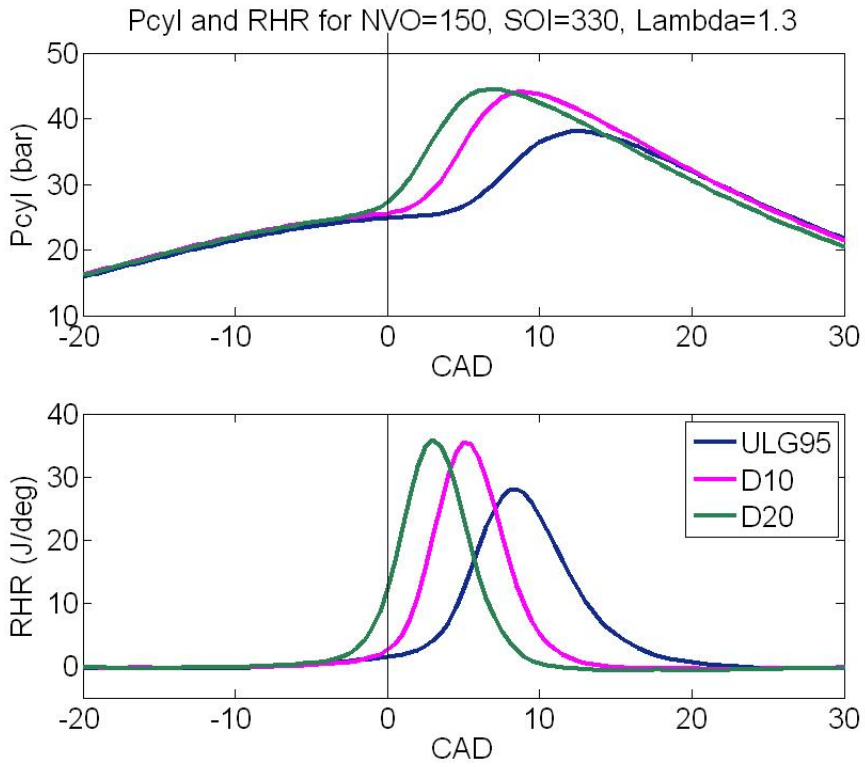

Figure 4.19 HCCI – Dieseline, In-cylinder pressure trace and HRR for D20, D10 and ULG95

4.2 Bio-Fuels HCCI

Bio-fuel/gasoline blends are investigated because HCCI combustion is regarded as a future solution to the simultaneous reduction in exhaust emissions and increase in engine efficiency, but is some time away from being production ready [Stanglmaier and Roberts (1999), Epping et al (2002) and Johansson et al (2009)]. By the time HCCI capable engines reach production bio-fuels are likely to form a major part of the automotive fuel supply as either pure bio-fuels or as a substitute for fossil fuel derived hydrocarbons for CO_2 reduction.

It is expected that the bio-fuels tested, namely bio-ethanol and 2,5 di-methylfuran will have a negative impact on the load-lambda window achievable because of their high octane ratings and increased charge cooling effects, with the latter being particularly relevant to ethanol. Ethanol has an octane rating of ~110 RON [Nakata et al (2006), Turner et al (2007) and Taniguchi et al (2007)] and with DMF having a rating of 119 RON [Román-Leshkov et al (2007) and Mousdale (2008)]. This suggests that the bio-fuels (and blends of) will have reduced ignitability because of the higher auto-ignition temperatures associated with increased octane rating compared to standard gasoline and hence a reduced load-lambda window will result.

Previous studies on ethanol HCCI however have shown that ethanol advances combustion (compared to gasoline or PFR equivalents) despite the above negative effects. Though the way in which these tests were conducted negated some of the negative effects of ethanol, in particular charge cooling. The study by Gnanam et al (2006) used heating to maintain charge temperature despite the fuel being used. Yap et al (2004) used PFI injection and intake heating, which combined, significantly reduces the effects of charge cooling and increased auto-ignition temperature, with a similar load window to standard gasoline being reported. The study by Xie et al (2006) showed a similar speed-load window for ethanol and ethanol/gasoline blends compared to gasoline but did report problems a low speed (similar speeds to this study) caused by problems with auto-ignition. Also if the same COV_{IMEP} limit as used in this study ($\leq 5\%$) is applied to the work by Xie and co-workers then the speed-load window would be reduced and smaller to that of standard gasoline.

In this study the intake air was heated, but only to a temperature of 35±1 °C and therefore it can be considered as unheated. The intake heating was in order to remove day-to-day fluctuations in the atmospheric temperature and to negate the problem of extended periods of engine testing increasing the temperature in the test cell. The injection of the fuel directly into the cylinder (as used in this study) will also highlight the problem of charge cooling, because all of the heat recovery will come from within in the cylinder and hence lower the temperature of the in-cylinder contents.

The valve timing and injection strategies used in this study are the same as those used for the dieseline study (Section 4.1). The same limits for defining a suitable operating point are also employed, that is RPR $\leq$ 5 bar/CAD and $COV_{IMEP} \leq 5\%$. The Fuel blends used in this study are $10\%_{Vol.}$ 2,5 di-methylfuran in gasoline (DMF10), $10\%_{Vol.}$ ethanol in gasoline (E10) and standard gasoline (ULG95)

4.2.1 Effects on Operating Window

The IMEP-Lambda operating regions for ULG95, DMF10 and E10 are shown in Figure 4.20. Also shown are the points used for the combustion and emissions comparison, these points are arranged to compare a range of approximately constant load points for the three fuels. Only the points with the highest indicated efficiency (for each fuel) are presented. The operating region is defined and generated in the same way as that in the Dieseline study (see Section 4.1.1).

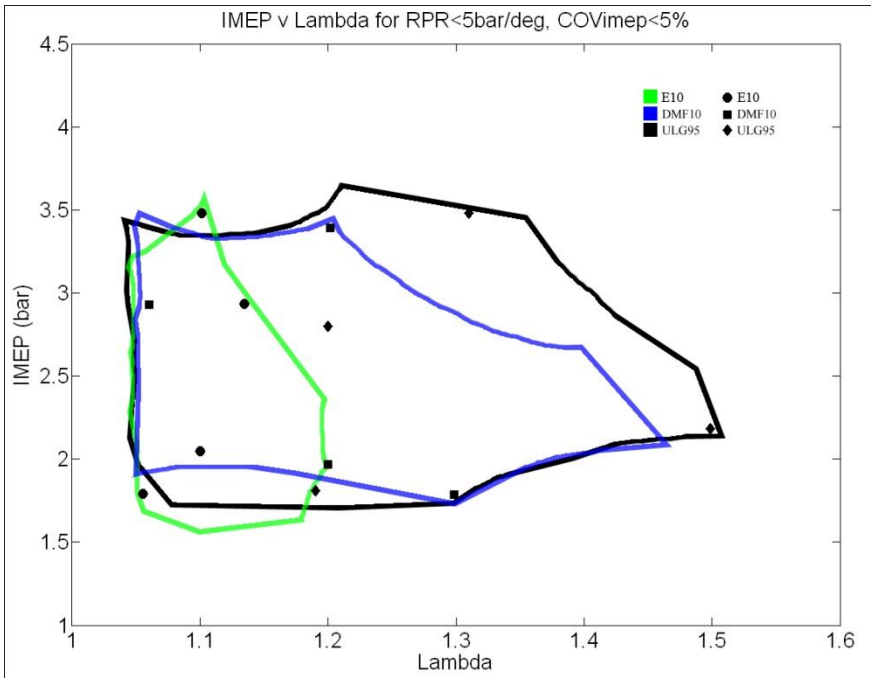

Figure 4.20 HCCI – Bio-fuels, Load window comparison

It can be seen that the addition of 10%$_{Vol.}$ of DMF to gasoline has only a minor effect on the load-lambda window achievable. The low load limit is the same as that for gasoline with a slight (~0.25 bar IMEP) reduction in the upper load limit which is caused by the combustion of DMF10 becoming too unstable when lean mixtures (required to reduce the rate of pressure rise) and low (~50%) ER levels are used.

The load range achievable when 10%$_{Vol.}$ of ethanol is added to gasoline is not greatly affected. The upper load limit is the same, with a slight reduction in the lower load limit caused by a 1 percentage point increase in COV_{IMEP} for high ER levels (~75%). The lean limit however is significantly reduced from λ=1.5 for gasoline to λ=1.2 for E10. This is caused by the reduction in combustion stability/increase in miss-fires for lean mixtures.

4.2.2 Combustion

The start of combustion (defined as 5% mass fraction burned) for two different NVO values (and hence ER rates) representing a high load (3.3 bar IMEP for gasoline, λ=1.2) and low load (1.6 bar IMEP for gasoline, λ=1.2) condition respectively are shown in Figure 4.21 and 4.22. It can be seen for the high load case that the addition of DMF causes the start of combustion to be retarded by approximately 1 CAD. When ethanol is added to gasoline SoC is further retarded by another 2 CAD, despite both of the fuels having a similar octane rating. This difference therefore is likely to be caused by the difference in charge cooling effects of the two fuels. The enthalpy of vaporisation for a stoichiometric mixture of ethanol is over three times greater than that for DMF, 92.3 $kJ/kg_{mixture}$ compared to 28.3 $kJ/kg_{mixture}$ respectively (see Table 3.6). This suggests that the in-cylinder temperature after the injection of the ethanol blended fuel is likely to be lower and hence a longer rime is required for heat recovery and hence auto-ignition temperature to be reached. The relative differences between fuels remains constant for both of the SoI's shown, 360° $bTDC_{COMB}$ (early timing) and 270° $bTDC_{COMB}$ (late timing).

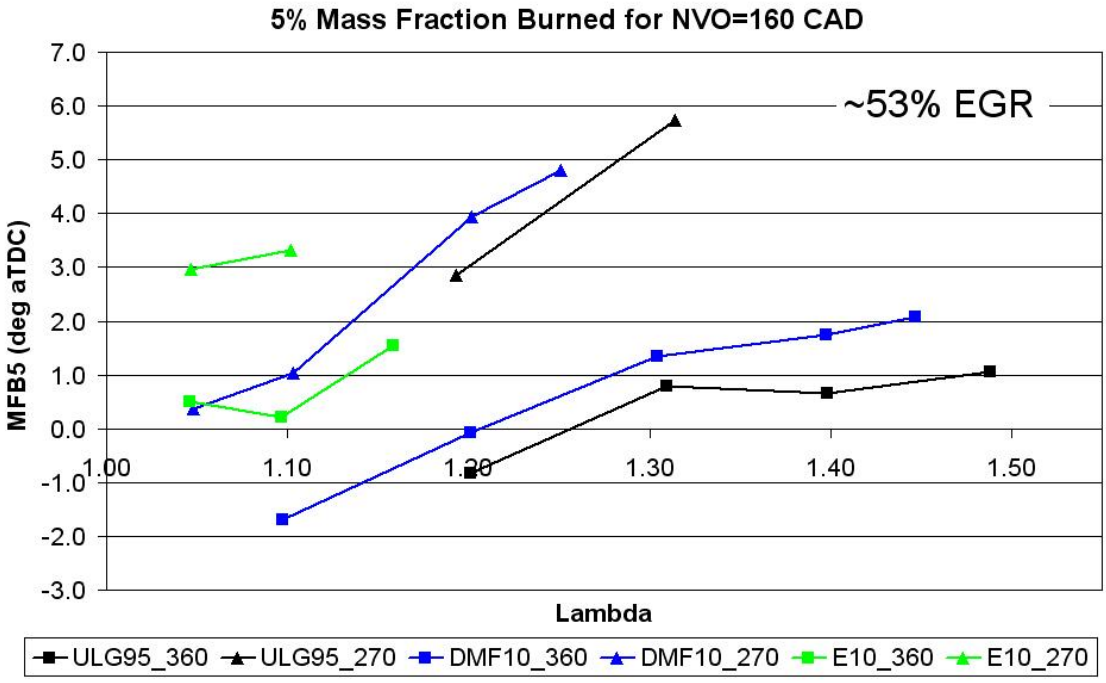

Figure 4.21 HCCI – Bio-fuels, Combustion phasing (NVO = 160)

For the low load condition the retardation of the SoC for the ethanol blend compared to standard gasoline is somewhat similar to that seen for the high load condition, ~2-3 CAD. However the DMF blend shows identical ignition timings to that of the ethanol blend. The difference in enthalpies of vaporisation as previously discussed would suggest that the SoC for the ethanol blend would be more retarded than that of the DMF blend. However for the low load condition the ER level is increased from ~53% to ~65% causing a reduction in the fresh charge inducted, so for the same mixture strength (λ) less fuel is injected. This reduced fuel mass means that the actual difference in temperature drops caused by the fuel evaporating for the two blends is lower. With the temperature drop difference (between fuel blends) being reduced the octane rating of the fuel blend becomes more significant and with the octane ratings being similar for both ethanol and DMF the ignition timings are therefore also similar.

Another explanation for this is that DMF is less tolerant to ER than both gasoline and ethanol. The relative difference in ignition timing for the ethanol blend compared to gasoline remains the same for the two ER rates. However the ignition retardation (compared to gasoline) for the DMF blend increases as the ER rate is increased.

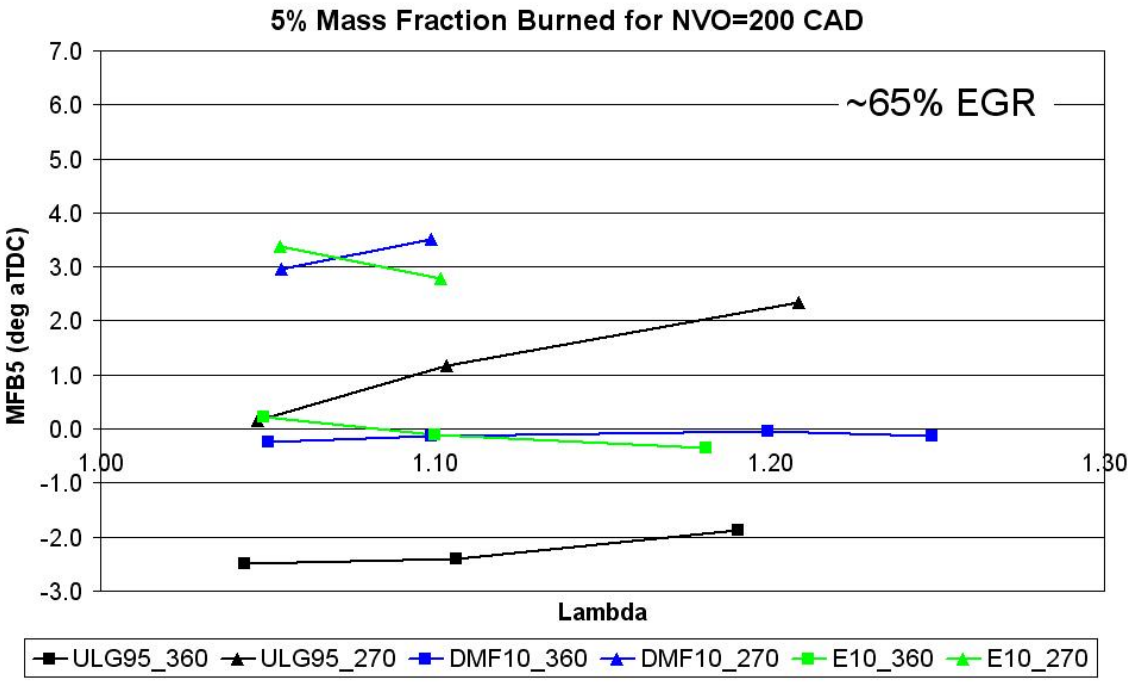

Figure 4.22 HCCI – Bio-fuels, Combustion phasing (NVO = 200)

The reduced ignitability for the DMF and ethanol blends compared to standard gasoline is the cause of the reduced load-lambda windows for these blends as shown in Figure 4.20. This reduction in ignitability is also evident when the starts of combustion for the combustion and emissions comparison points are examined in Figure 4.23. The ignition timings for the ethanol and DMF blends are generally retarded compared to standard gasoline and this is despite an increase in mixture strength (λ). The advance in ignition timing seen for the ethanol blend at the highest load point (~3.5 bar IMEP) is because the mixture is enriched still further.

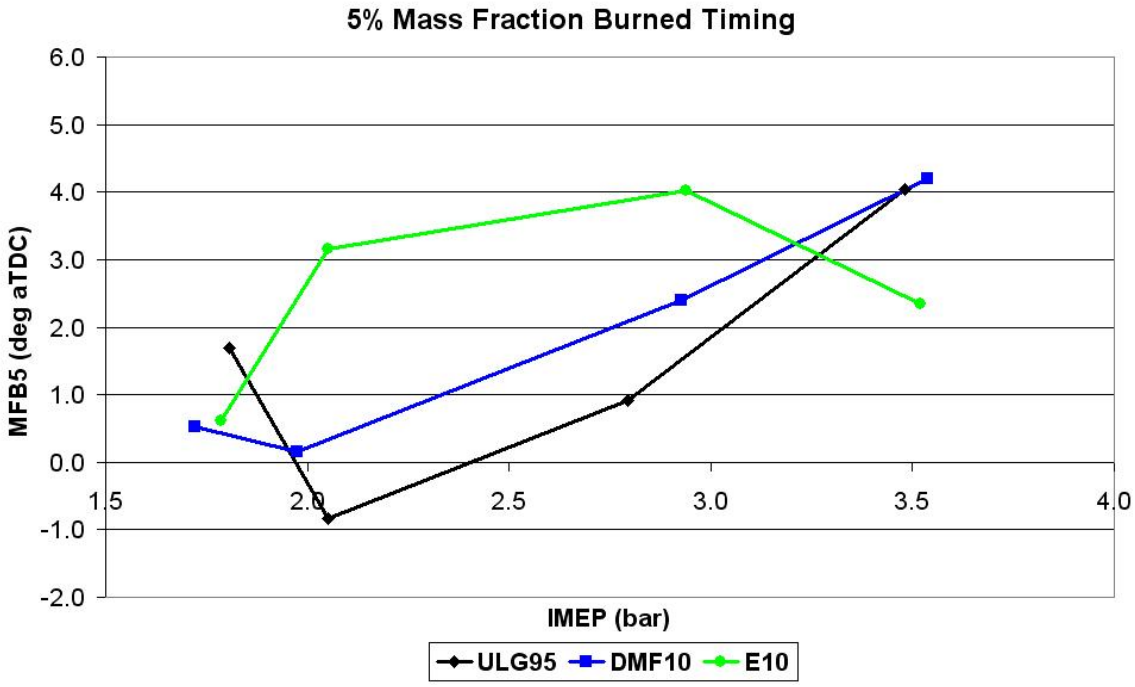

Figure 4.23 HCCI – Bio-fuels, 5% MFB timing

If combustion duration is examined (presented as 5-50% MFB, Figure 4.24) it can be seen that the retarded combustion of the ethanol blend causes an increase in combustion duration. This is because the combustion is occurring in a larger volume and hence the temperature rise is reduced causing the combustion to be less well promoted than if the temperature was increased. The DMF blend shows a similar combustion duration to that of standard gasoline (and faster than the ethanol blend).

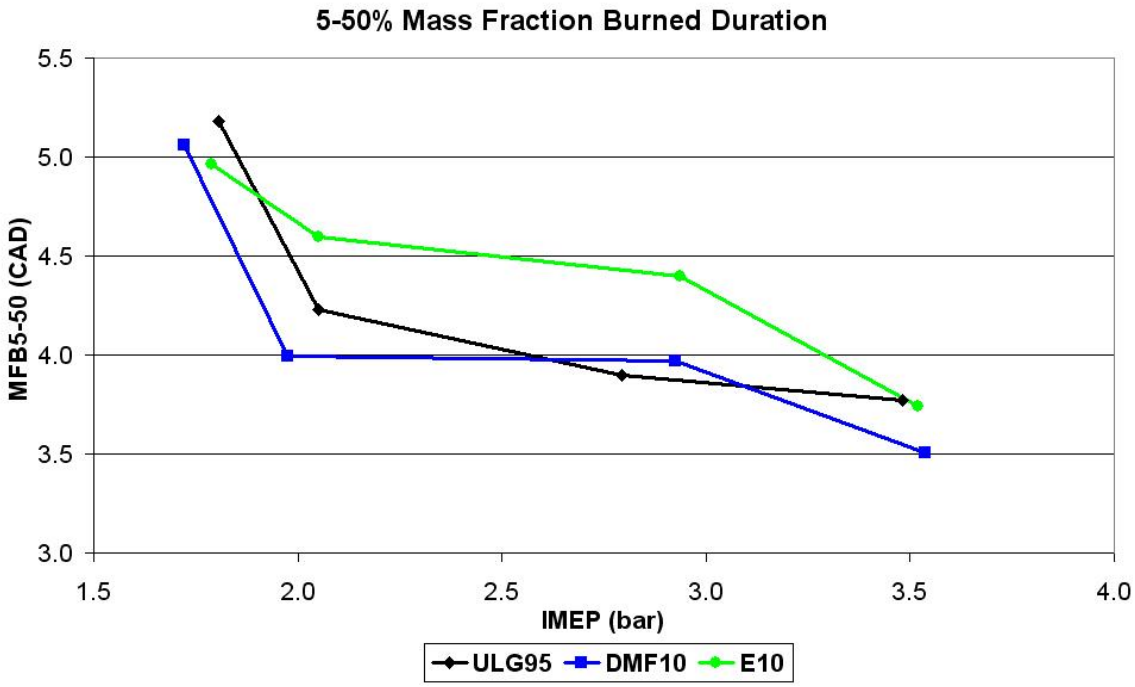

Figure 4.24 HCCI – Bio-fuels, Combustion duration

The increased combustion duration seen for the ethanol blend causes a reduction in combustion stability, as seen by the factor of two increase in COV_{IMEP} presented in Figure 4.25. The DMF blend shows similar levels of combustion stability to that of standard gasoline, as suggested by the similarity shown towards combustion duration. For both the ethanol and DMF blends there is a reduction in stability seen for the highest load point (~3.5 bar IMEP) that is not a direct

result of poor/low temperature combustion as seen for the increase at the lowest load point (~1.7 bar IMEP). Instead slightly incomplete combustion from the previous cycle causes a slight increase in quantity of fuel present in the cylinder, so the combustion in the following cycle is more vigorous causing a noticeable change in the load produced for that cycle, increasing the COV_{IMEP}. This can also explain the increase in the rate of pressure rise (RPR) for the ethanol blend for 3 bar IMEP and above and for the DMF blend at 3.5 bar IMEP as shown in Figure 4.26. Below 3 bar IMEP the rate of pressure rise for all three fuel blends is comparable.

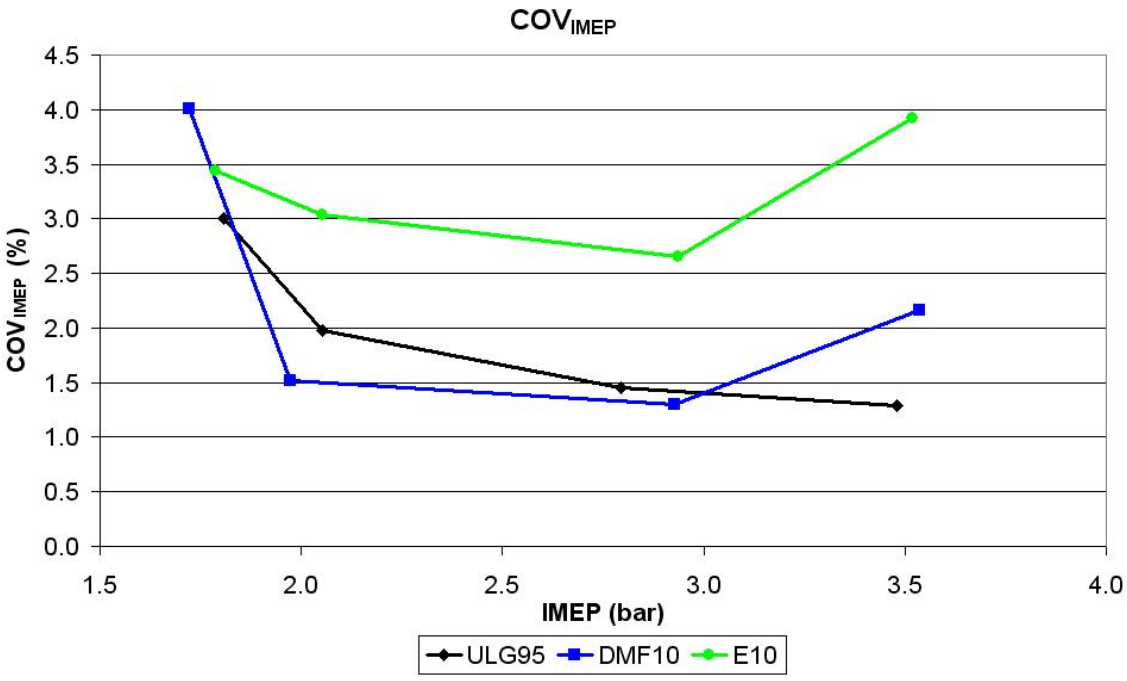

Figure 4.25 HCCI – Bio-fuels, Combustion stability

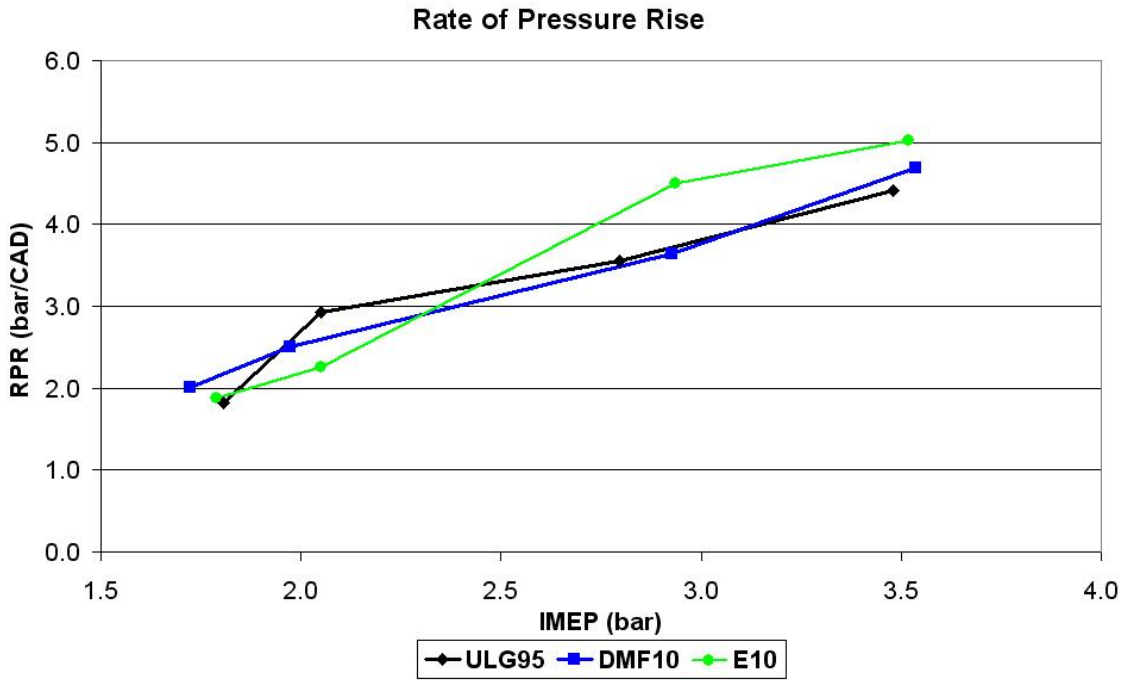

Figure 4.26 HCCI – Bio-fuels, Rate of pressure rise

Combustion efficiency (see Section 3.4.3 for calculation method) is presented in Figure 4.27. It can be seen that combustion efficiency is generally maintained despite the increased octane ratings of ethanol and DMF. The difference between any two fuel blends at a particular load is generally no greater than half of one percentage point.

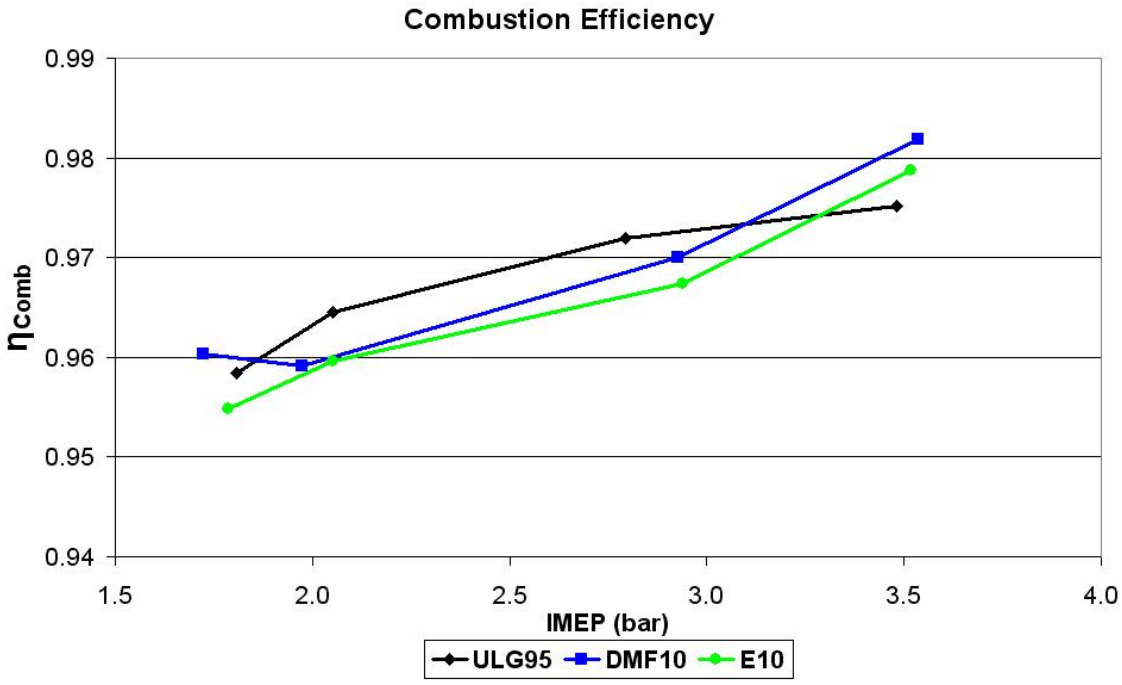

Figure 4.27 HCCI – Bio-fuels, Combustion efficiency

4.2.3 Emissions

It can be seen that the slightly richer mixtures required for DMF have led to increased NO_X emissions as shown in Figure 4.28 and this is despite the slightly retarded combustion phasing. The increase is moderate (<0.1 g/ikWh) for loads below 3 bar IMEP but more significant for 3.5 bar IMEP. The ethanol blend shows comparable NO_X emissions for loads below 3 bar IMEP despite the richer (and therefore, higher heat release rates) mixture (λ) required. This is caused by a combination of the relatively retarded combustion phasing and that ethanol has a lower adiabatic flame temperature compared to that of standard gasoline. The significant increase of 80% and 74% respectively in NO_X emissions seen at ~3.5 bar IMEP for the ethanol and DMF blends is caused by the mechanism described in the discussion relating to the increased rate of

pressure rise at the same load point. That is a cycle where the combustion is not fully complete is followed by a cycle of more vigorous combustion raising the in-cylinder temperature and hence promoting NO_X formation.

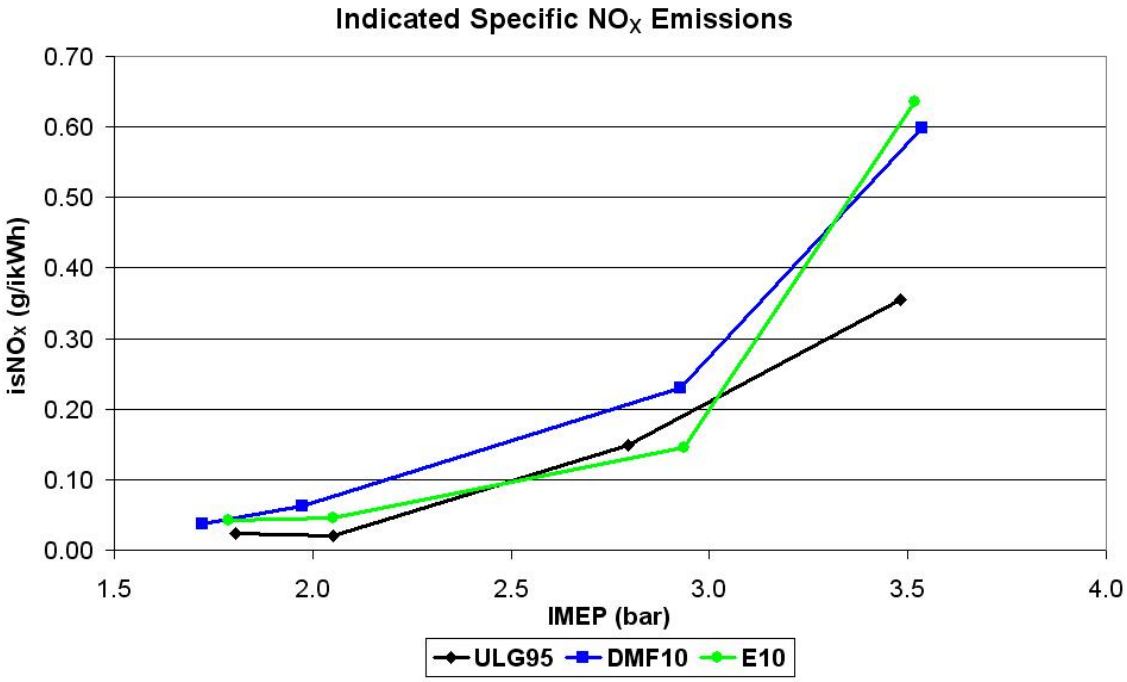

Figure 4.28 HCCI – Bio-fuels, Indicated specific NO_X emissions

The increase in in-cylinder temperature that was responsible for the increase in NO_X emissions has caused a reduction in hydrocarbon emissions through the promotion of complete combustion as shown in Figure 4.29. This is because there seems to exist a temperature related NO_X – HC trade-off similar to the NO_X – Soot trade-off seen with Diesel engines. This will be discussed further in Section 4.3.

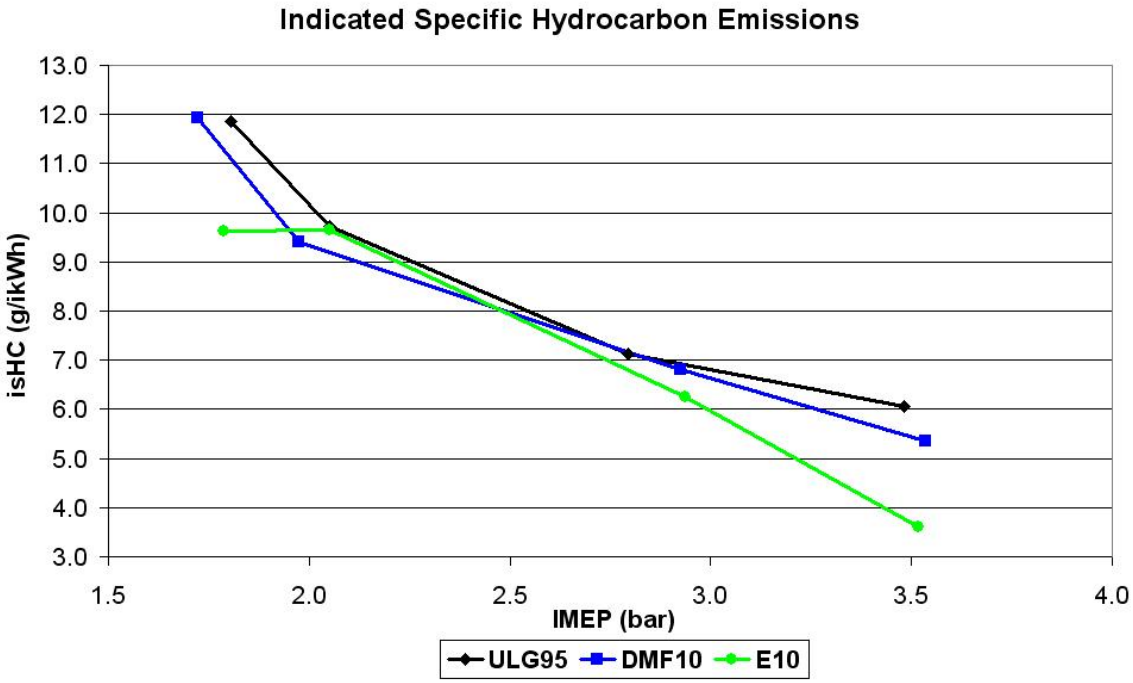

Figure 4.29 HCCI – Bio-fuels, Indicated specific hydrocarbon emissions

As suggested by the similar combustion efficiencies for all fuel blends the carbon monoxide emissions (Figure 4.30) are not adversely affected by the addition of ethanol or DMF despite the increase in mixture strength (λ) required.

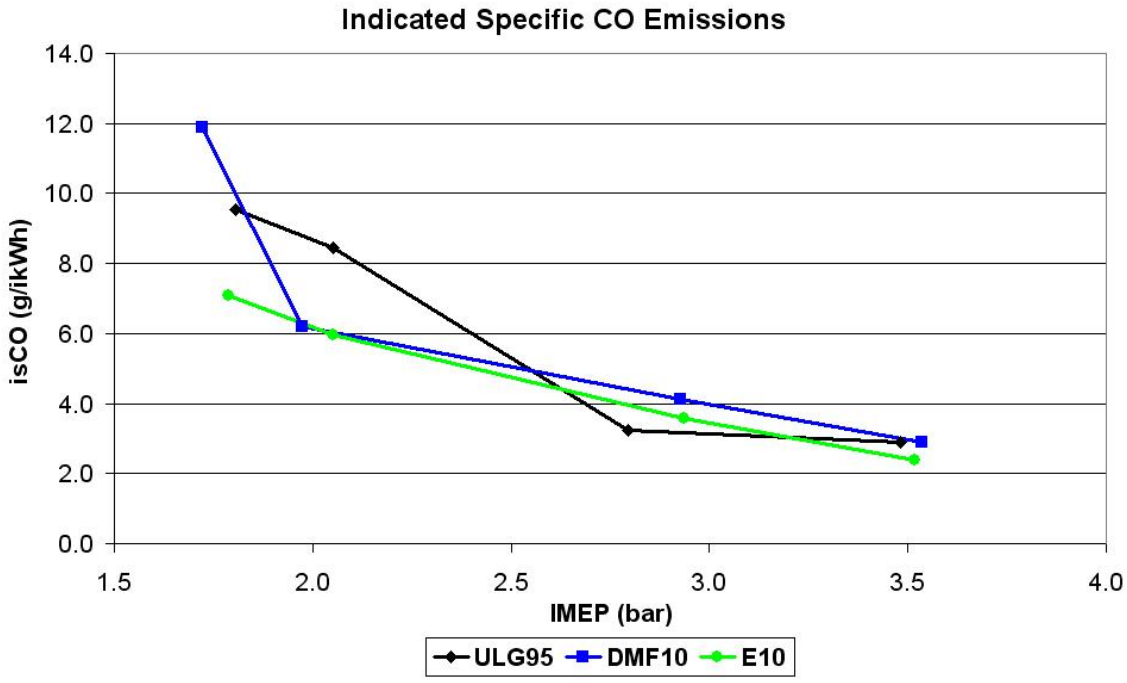

Figure 4.30 HCCI – Bio-fuels, Indicated specific carbon monoxide emissions

4.2.4 Efficiency

Indicated efficiency is presented in Figure 4.31 instead of indicated specific fuel consumption because with DMF and ethanol being oxygenated compounds their gravimetric calorific values are reduced (relative to gasoline) and hence a greater fuel mass is required for the same energy delivery. It can be seen that the ethanol and DMF blends have reduced efficiency compared to gasoline. This is attributed to the increased charge cooling effects of ethanol and DMF compared to gasoline increasing the 'gas spring' [Kornhauser and Smith (1987)] losses. The fuel injection occurs during the expansion following re-compression while the valves are closed. This means that the evaporating fuel cools the trapped gas and hence reduces the pressure (valves are closed so no mass transfer) and increases the hysteresis between the compression and

expansion of the gas. This results in less work being recovered during the expansion of the compressed gas, hence increasing the losses.

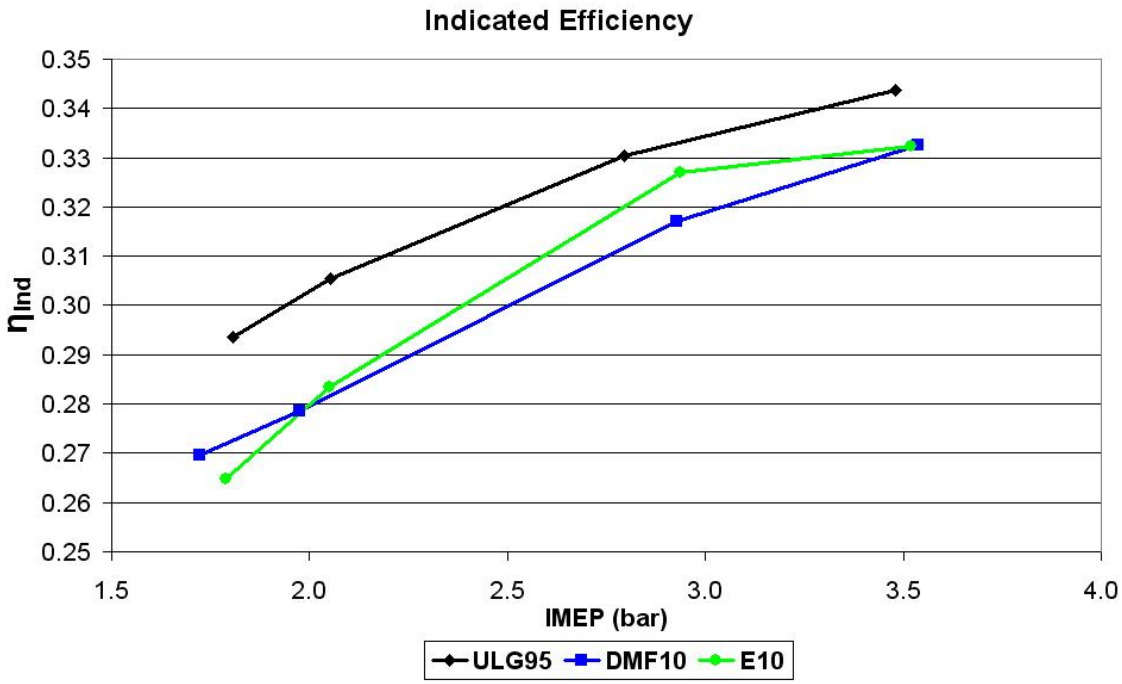

Figure 4.31 HCCI – Bio-fuels, Indicated efficiency

4.3 NO_X – HC Trade-Off

As previously discussed in this chapter, HCCI combustion appears to show a trade-off between NO_X and hydrocarbon emissions. If the engine calibration is changed (whilst maintaining the same load) to reduce one of these emissions an increase will be seen in the other, whether the change in calibration be a different mixture strength (λ), ER rate, injection timing or a combination of the above.

This trade-off appears to be related to in-cylinder temperature as shown in Figure 4.32. In this figure the NO_X and HC emissions for a load of 2.9±0.1 bar IMEP, for standard gasoline, D10 and D20 are plotted against maximum in-cylinder temperature. The hydrocarbon emissions show a linear reduction with increasing temperature, while the NO_X emissions show the well known exponential relationship towards temperature [Narayan and Rajan (2004)]. It can be seen that if a particular engine calibration produces a relatively high NO_X level and attempts are made to reduce this by increasing excess air, ER or retarding the start of injection timing an increase in hydrocarbon emissions will be seen. It is proposed that this increase in hydrocarbon emissions is caused by the reduced in-cylinder temperature increasing the thickness of the quench layers covering the combustion chamber surface and that the reduced temperature (including combustion chamber surface) slowing down and reducing the evaporation of impinged fuel. This emissions trade-off is similar to the well documented NO_X – Soot trade-off seen with Diesel (CI) engines [Han et al (1996) and Uludogan (1996)].

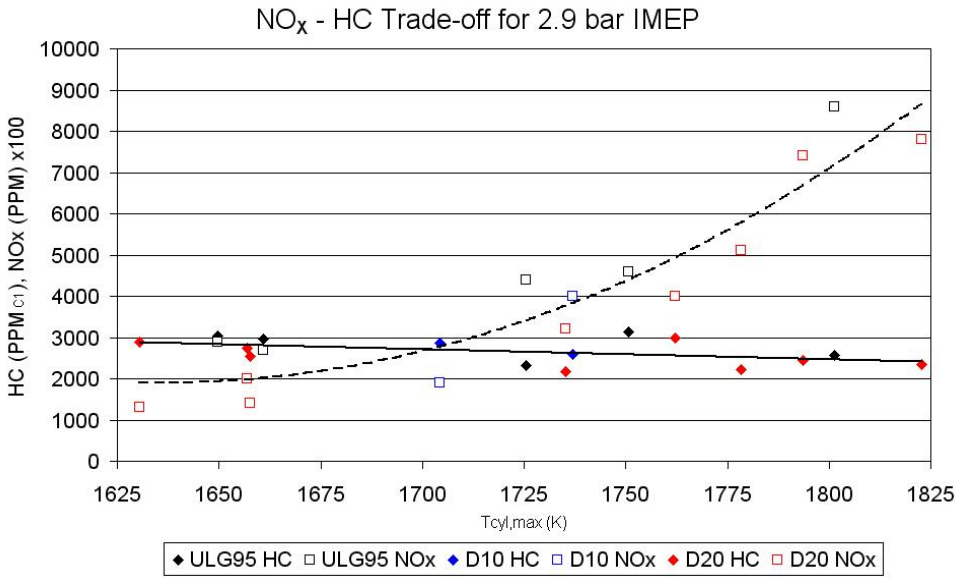

Figure 4.32 HCCI, NO_X – HC trade-off (IMEP = 2.9 bar)

In general both the NO_X and hydrocarbon emissions are heavily dependent on the in-cylinder temperature, as shown by Figure 4.33. In this figure the NO_X and HC emissions for standard gasoline, D10 and D20 shown in Figure 4.2 (representing a load range of ~1.4-3.5 bar IMEP) are plotted against maximum in-cylinder temperature. There are more points available from the dieseline study but many of these points have high levels of combustion instability (COV_{IMEP}), which is likely to artificially increase HC emissions through poor combustion cycles and NO_X emissions by significantly advanced combustion that follows cycles with poor combustion (unburned hydrocarbons causing uncontrolled mixture enrichment). The data from the bio-fuel blends study (Section 4.2) is also omitted because of the problems associated with measuring oxygenated hydrocarbons with an FID (see Chapter 5, Section 5.2.2 for further discussion).

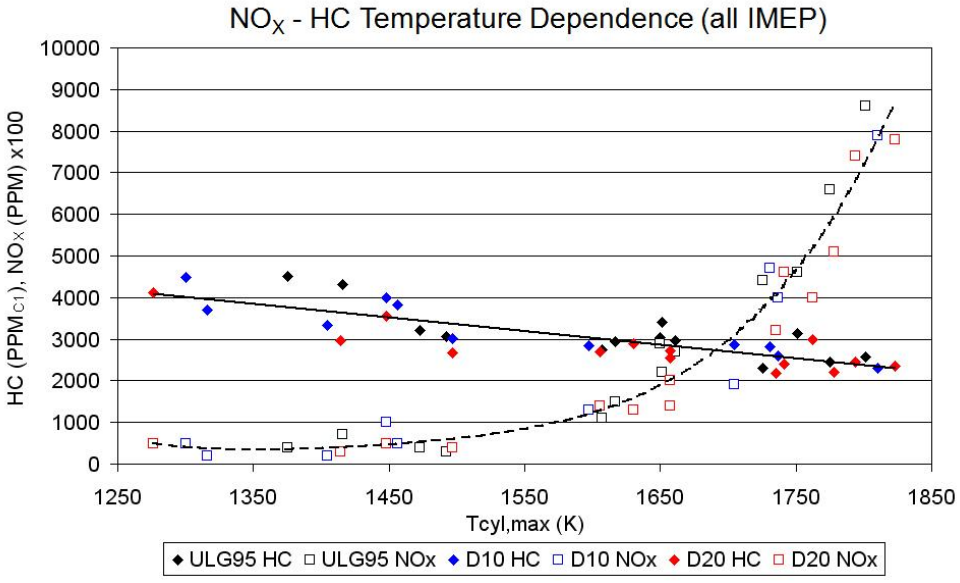

Figure 4.33 HCCI, NO_X – HC temperature dependence (all loads)

Due to the exponential temperature dependence for NO_X and the linear relationship for hydrocarbon emissions, a relatively small increase (compared to NO_X reduction) in hydrocarbon emissions can lead to a significant reduction in NO_X emissions. For example at a load of 1.7 bar IMEP a 25% increase in HC emission results in a 40% reduction in NO_X emissions. More significantly as the engine load is increased this ratio of HC increase to NO_X reduction can be reduced. This is demonstrated for a load of 2.9bar IMEP where a 20% increase in HC emission results in a substantial 80% reduction in NO_X emission. This could allow for the simplification of the exhaust after-treatment systems required for HCCI equipped vehicles. A passive diesel oxidation catalyst (DOC) for HC reduction could be used instead of an active lean NO_X trap or selective catalytic reduction (SCR) catalyst system for NO_X reduction.

This trade-off has been documented by other authors [Juttu et al (2007)], with some attempting to reduce the trade-off by better mixture preparation, Nordgren et al (2004) and Steeper and De Zilwa (2007). The emissions increase through poor mixture preparation is caused by HC emissions coming from over lean regions and an increase in NO_X coming from rich hot spots. However the mixture preparation related emissions are in addition to the emissions coming from perfectly homogeneous combustion which will still be subject to the fundamental trade-off presented above.

4.4 Summary

This study has shown that adding a small quantity of diesel to standard gasoline can significantly improve the fuels combustion performance with respect to HCCI combustion. This improved combustion performance, namely increased ignitability allows the load window to be increased with both improved upper and lower load limits. This is brought about by the diesel addition maintaining acceptable combustion stability for leaner mixtures.

The ability to operate with leaner mixtures reduces the mechanical loading on the engine through reducing combustion severity and maximum in-cylinder pressures. Leaner mixtures also lower the in-cylinder temperature so the NO_X emissions are reduced. However this is accompanied by a slight increase in hydrocarbon emissions and smoke. The retarded combustion brought about by the leaner mixtures results in improved engine efficiency through better combustion phasing.

It is proposed and discussed that the improved ignitability seen with the addition of diesel is actually brought about by introducing inhomogeneity in the mixture. This inhomogeneity is caused by the long chain diesel fuel molecules and the possibility of diesel fuel droplets brought about by the relatively low injection pressures used. However a low temperature combustion regime is not seen in this study.

The addition of ethanol and 2,5 di-methylfuran to gasoline shows a reduction in the load-lambda window achievable that it brought about by reduced ignitability. This reduction in ignitability is caused by the increased octane rating and enthalpy of vaporisation of the blend-in fuels. The reduced ignitability of the ethanol blend causes a noticeable decrease in combustion stability. Furthermore both bio-blends show increased rates of pressure rise and NO_X emissions for the highest load point presented (3.5 bar IMEP). This is brought about by the reduced combustion stability giving rise to over rich (relative to the 100 cycle average) cycles and therefore overly vigorous combustion.

The bio-fuel blends show reduced indicated efficiency which is attributed to increased 'gas spring' losses. This is brought about by the increased enthalpies of vaporisation and increased injection duration required due to the oxygenated nature of the fuels causing a reduction in in-cylinder pressure during the expansion of the re-compressed trapped exhaust gasses.

Evidence and discussion is presented on the existence of a fundamental NO_X – HC trade-off for HCCI combustion that is related to in-cylinder temperature and is akin to the NO_X – Soot trade-off seen with conventional compression ignition combustion.

CHAPTER 5

5 The Effect of Bio-Fuels on Direct Injection Spark Ignition (DISI) Combustion – Part Load

This chapter investigates the effect of using bio (oxygenated) fuels on combustion and regulated emissions in Direct Injection Spark Ignition (DISI) combustion at part load conditions (3.4 bar IMEP, 1500 RPM). Preliminary investigations were carried out to find a suitable valve and spark timing strategy. Both conventional (Ethanol) and novel (2,5 Di-methylfuran) bio-fuels are investigated and compared to standard 95 RON gasoline. The repeatability of the ethanol data is also examined with relation to explaining the trends found in the ethanol data.

5.1 Engine Baseline

Before any comparisons can be made between bio-fuels and gasoline a suitable testing point has to be found (at 1500 RPM, 3.4bar IMEP). A valve and spark timing combination is considered suitable if the COV_{IMEP} is lower than 3% whilst maintaining low NO_X emissions and low specific fuel consumption. The combination of valve timing strategy and spark timing that satisfied these conditions is shown in Table 5.1. This chosen setup has a relatively late exhaust valve closing but this allows for some of the expelled exhaust gas to be drawn back into the cylinder, which helps suppress NO_X formation.

Table 5.1 Engine spark ignition baseline setup

Intake Valve Opening	376° $bTDC_{COMB}$
Intake Valve Closing	126° $bTDC_{COMB}$
Exhaust Valve Opening	146° $aTDC_{COMB}$
Exhaust Valve Closing	324° $bTDC_{COMB}$
Injection Timing	280° $bTDC_{COMB}$
Spark Timing	34° $bTDC_{COMB}$

5.2 Investigation into the effects of Bio-Ethanol/Gasoline Blends

For this study two different injection strategies are used. The first is a standard single homogeneous injection and the second is a split injection strategy. The split injection strategy is used to investigate if this would lead to better mixing between the inducted air and injected fuel. If better mixing is achieved it is expected that the combustion stability is improved along with reduced CO and HC emissions. The start of injection for the first injection in the split strategy is set for 5 CAD after the intake valve opens. This is to allow for the greatest mixing time (time between injection and spark discharge) and for the injection spray to interact with the tumbling intake air to aid mixing. The second injection is set to finish approximately 5 CAD before the intake valve closes. This is to allow the spray to still interact with the remaining tumbling in-cylinder motion, whilst allowing the first spray plume to break-up and stopping the two spray plumes from interacting and reduce mixing. The duration of the two injections are set to be equal in terms of crank angle degrees of opening. In the following text the two injection strategies will be referred to as 280SoI for the single injection and 371/141SoI for the split injection.

The engine configuration for the part load tests is shown in Table 5.2.

Table 5.2 Engine configuration for part load spark ignition operation

	Single Injection	**Split Injection**
Engine Speed (RPM)	1500	
IMEP (bar)	3.4	
λ	1.0	
IVO (° $bTDC_{GE}$)	16	
EVC (° $aTDC_{GE}$)	36	
SoI (° $bTDC_{COMB}$)	280	371/141
Spark Timing (° $bTDC_{COMB}$)	19, 24, 29, 34, 39	

Five different splash blends of ethanol/gasoline are examined, the blends being 10, 20, 30, 50 and 85%$_{Vol.}$ bio-ethanol in gasoline as well as standard gasoline and pure bio-ethanol. These are designated as Ex, with 'x' representing the percentage by volume of bio-ethanol in the ethanol/gasoline blend.

5.2.1 Combustion Performance

The 10% mass fraction burned timings plotted against fuel blend for the range of spark timings used are shown in Figure 5.1.

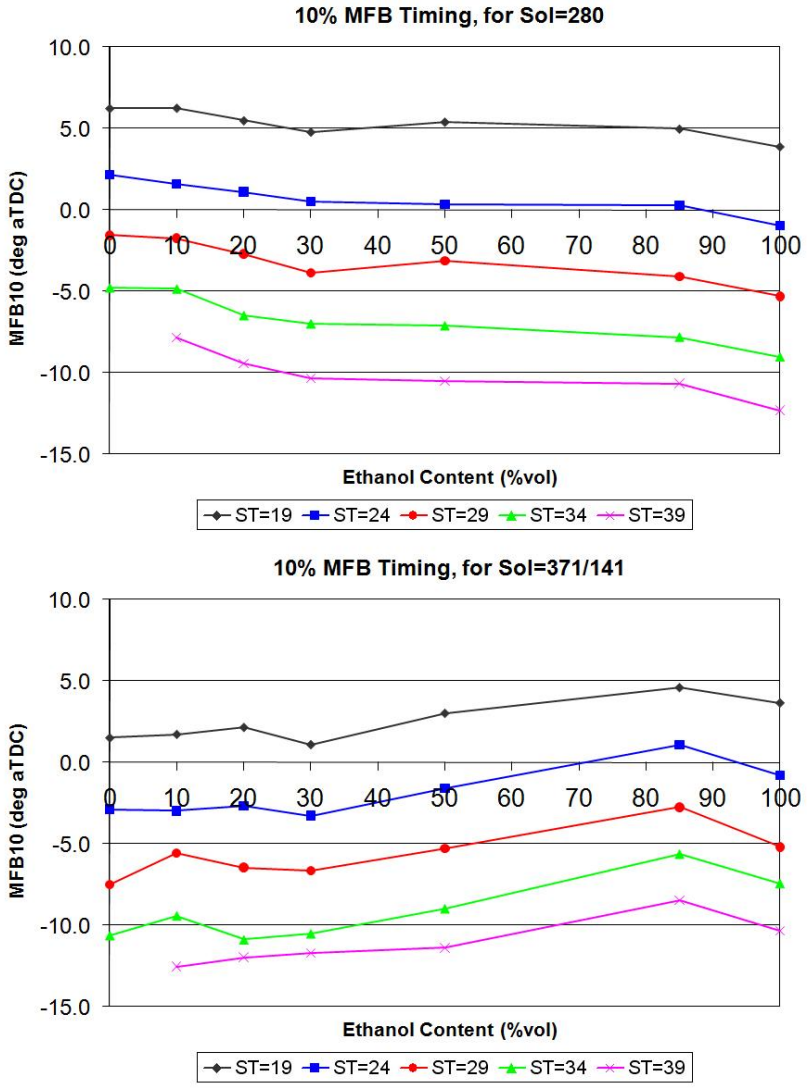

Figure 5.1 Part load SI, 10% mass fraction burned

It can be seen that for the 280SoI case SoC (defined as 10% MFB) is advanced as the ethanol content is increased. This is showing that the ignition delay (defined as the time between spark discharge and 10% MFB) is reduced with the addition of ethanol (Figure 5.2). Though there is a generally flat region between E30 and E85. The reduction in ignition delay can be attributed to a faster laminar flame speed for ethanol compared to gasoline, ~39 m/s compared to ~33 m/s respectively (Table 3.6).

For the 371/141SoI case it can be seen that generally as the ethanol content is increased the SoC is retarded, though for standard gasoline the combustion is advanced for the 371/141SoI case compared to the 280SoI case. This retardation is attributed the reduction in in-cylinder temperature caused by the evaporating fuel. The late second injection means that there is little time for heat recovery from the in-cylinder surfaces, resulting in lower temperatures prior to spark discharge.

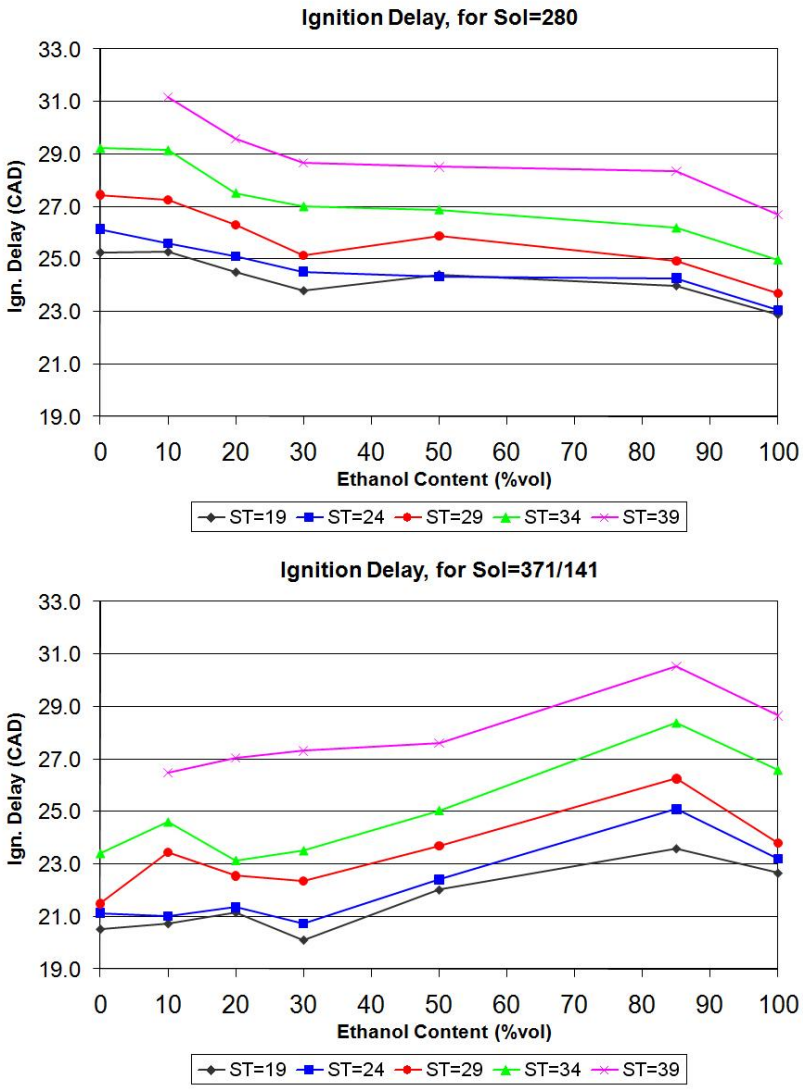

Figure 5.2 Part load SI, Ignition delay

Combustion duration, defined as 10-90% MFB duration, is shown in Figure 5.3. It can be seen that for both injection strategies the combustion duration generally follows the same trend as that of the start of combustion. This suggests that ethanol has little effect on the main combustion event, with the increase in laminar flame velocity being masked by the turbulent in-cylinder motion.

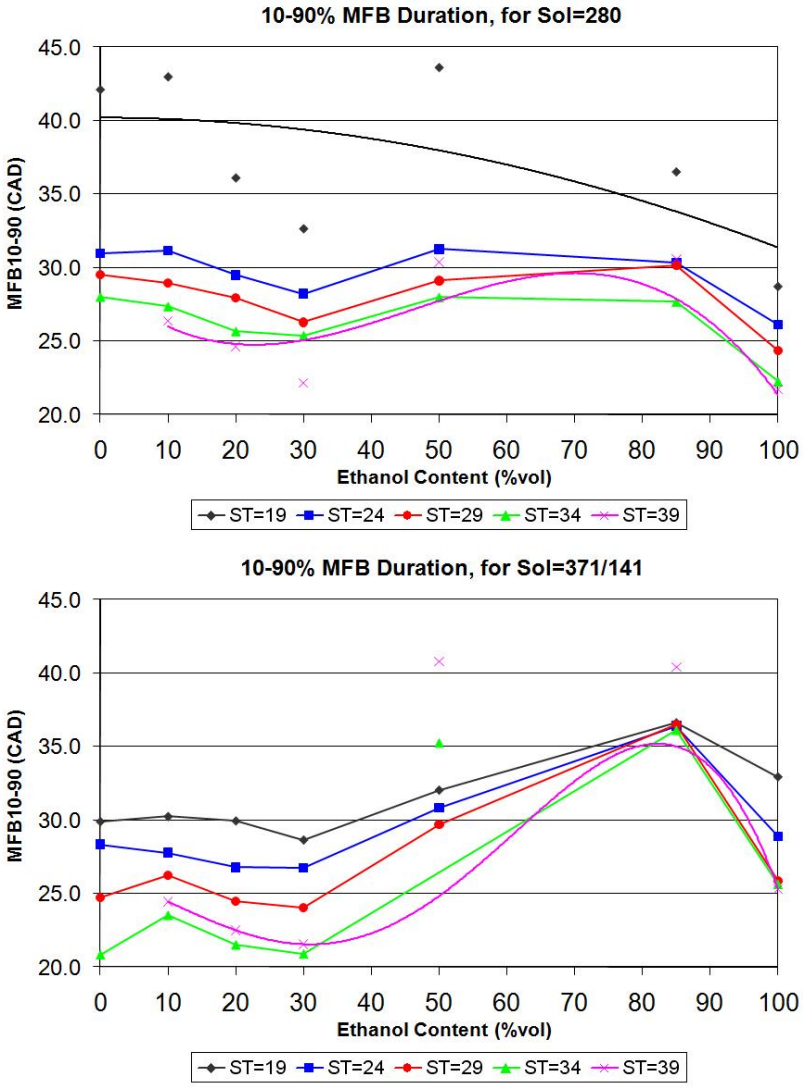

Figure 5.3 Part load SI, Combustion duration

Combustion stability is presented here as COV of IMEP and is shown in Figure 5.4. Combustion stability generally follows the same trend as that of combustion duration for both injection strategies. This can be correlated to in-cylinder flow. The faster the combustion is, the less time there is for the flame front to be influenced by in-cylinder motion, and hence resulting in greater stability.

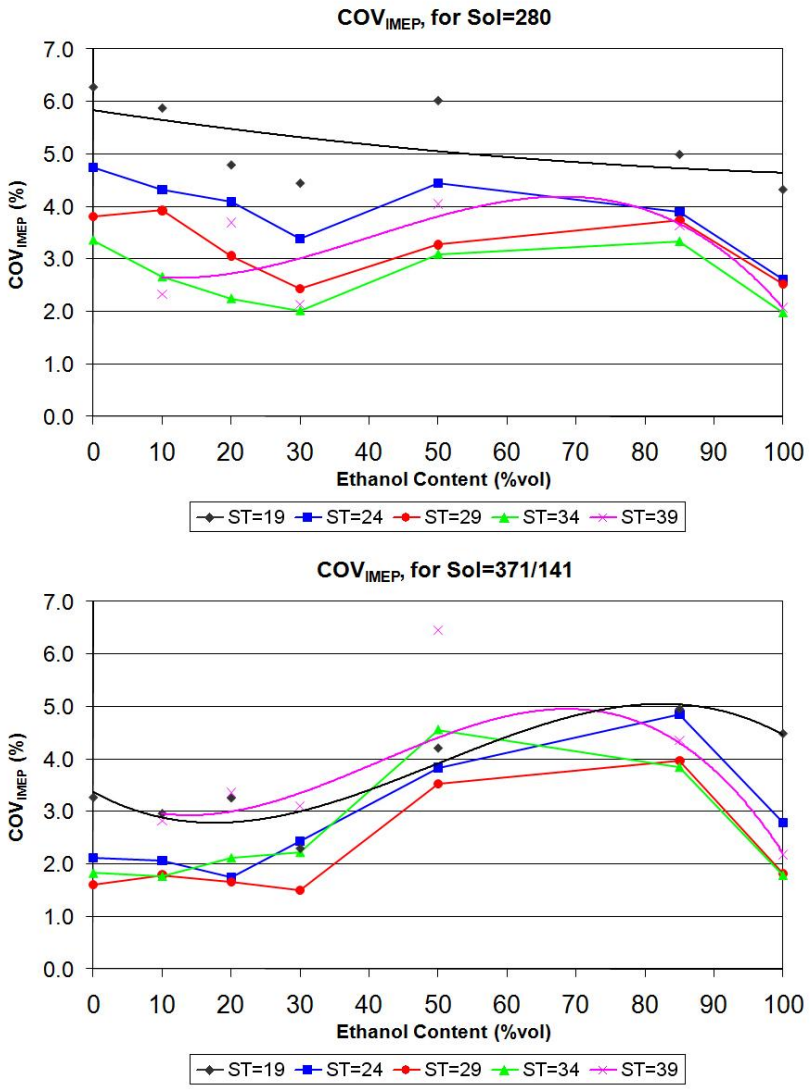

Figure 5.4 Part load SI, Combustion stability

Combustion efficiency (calculated from CO and HC in the exhaust stream, see Section 3.4.3.) is presented in Figure 5.5. It can be seen for the 280SoI case combustion efficiency generally improves with increased ethanol content. The combustion efficiencies for the 371/141SoI case up to E50 are almost identical to those of the 280SoI case but there is a considerable reduction for E85 and E100. This is thought to be caused by fuel impingement on the piston and will be discussed in more detail in the section on carbon monoxide emissions. A certain amount of

caution however has to be applied to the combustion efficiency data because of the problems associated with measuring oxygenated hydrocarbons; more detail is given on this in the discussion of hydrocarbon emissions (Section 5.2.2).

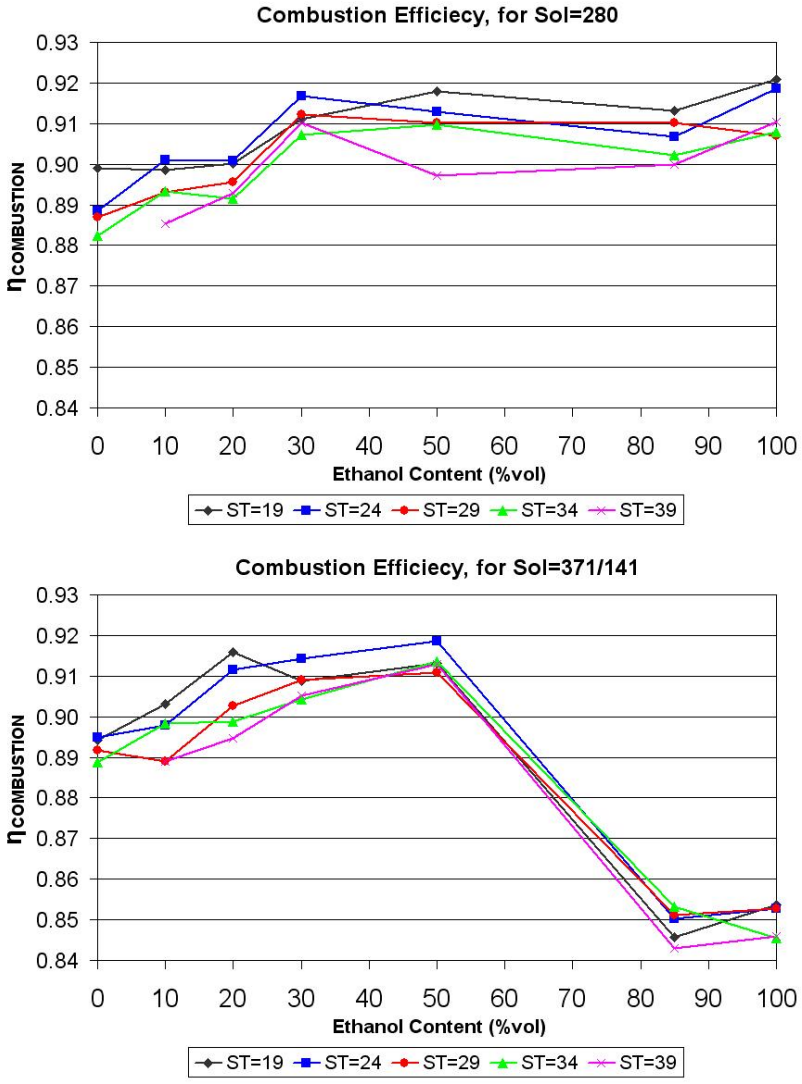

Figure 5.5 Part load SI, Combustion efficiency

It is generally reported in the literature [Nakata et al (2006), Wallner et al (2008) and Salih et al (1992)] that the in-cylinder temperatures reduce with the addition of ethanol, because ethanol has a lower adiabatic flame temperature and the higher heat of vaporisation increasing charge cooling. Peak in-cylinder temperature can be inferred from peak in-cylinder pressure. This is because the mass flow into the engine is similar for all operating points (same load) and with peak pressure phasing being similar and close to TDC any change in volume at peak pressure is going to be insignificant when compared to the total volume. Peak in-cylinder pressure is presented in Figure 5.6. In this study it can be seen that indeed for the 371/141SoI case as the ethanol content is increased the peak in-cylinder pressure (and therefore temperature) reduces. However for the 280SoI case the peak in-cylinder pressure (and therefore temperature) increases with the addition ethanol. This is caused by the observed trends in start of combustion, if the combustion is advanced the combustion occurs in a smaller volume and hence the temperature rise is greater for a given energy release.

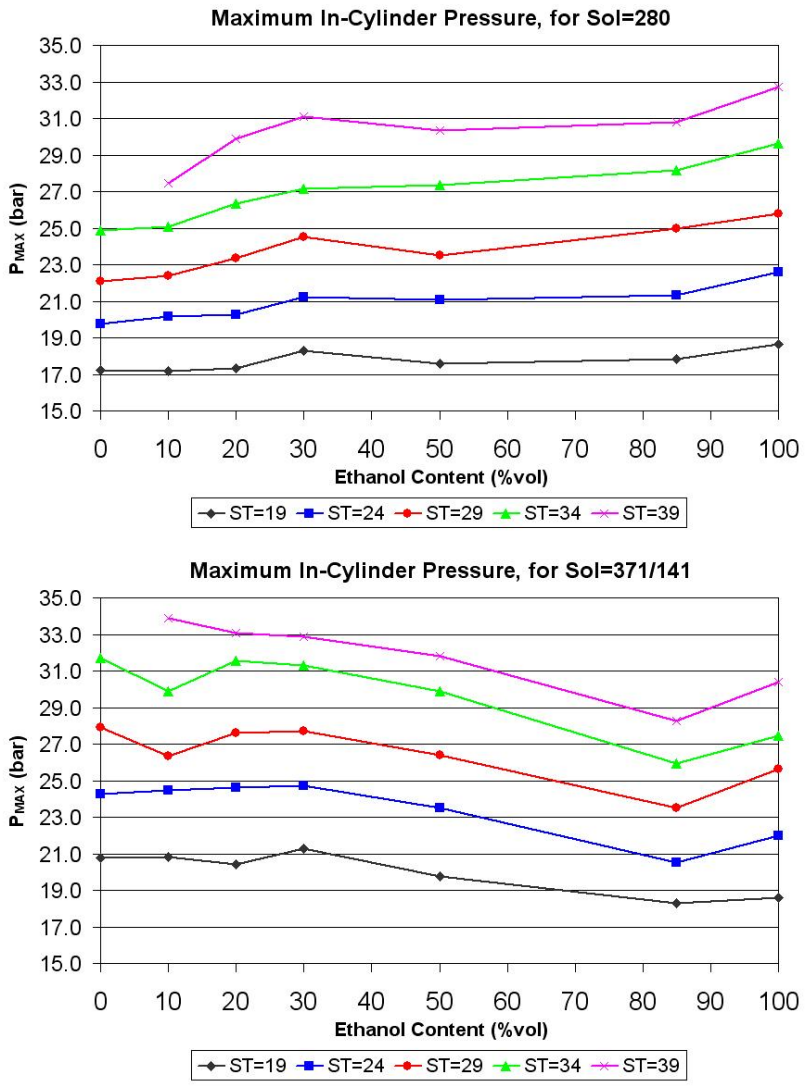

Figure 5.6 Part load SI, Peak in-cylinder pressure

Exhaust temperature is an important parameter as it can affect the oxidation of HC and CO late in the expansion stroke and the effectiveness of exhaust after treatment devices. Exhaust temperature is shown in Figure 5.7. It can be seen for the 280SoI case that as the ethanol content is increased up to 85% the exhaust temperature reduces, it then increases slightly for pure ethanol. Likewise advanced spark timings lead to lower temperatures. This is mainly because of combustion phasing and the time available for the cylinder gas to cool. With advanced

combustion there is more time between the end of combustion and the exhaust valve opening for the gas to cool and hence this results in a lower exhaust temperature. However the combustion phasing for E30-E85 is almost constant, whereas the exhaust temperature reduces for these fuel blends. This may be because ethanol has a lower adiabatic flame temperature.

For the 371/141SoI case the exhaust temperature is generally unaffected by ethanol addition up to E30. This is because up to E30 the combustion phasing and in-cylinder temperatures remain constant. The exhaust temperature reduces for E50 and then increases again as the ethanol content increases. The exhaust temperature for pure ethanol is similar to that of pure gasoline. This is due the competing factors of reduced in-cylinder temperature and retarded combustion phasing. It is also noted that the exhaust temperatures for up to E30 are lower for the 371/141SoI case compared to the 280SoI case. This is again following the trend of combustion phasing, with the 371/141SoI case having more advanced combustion.

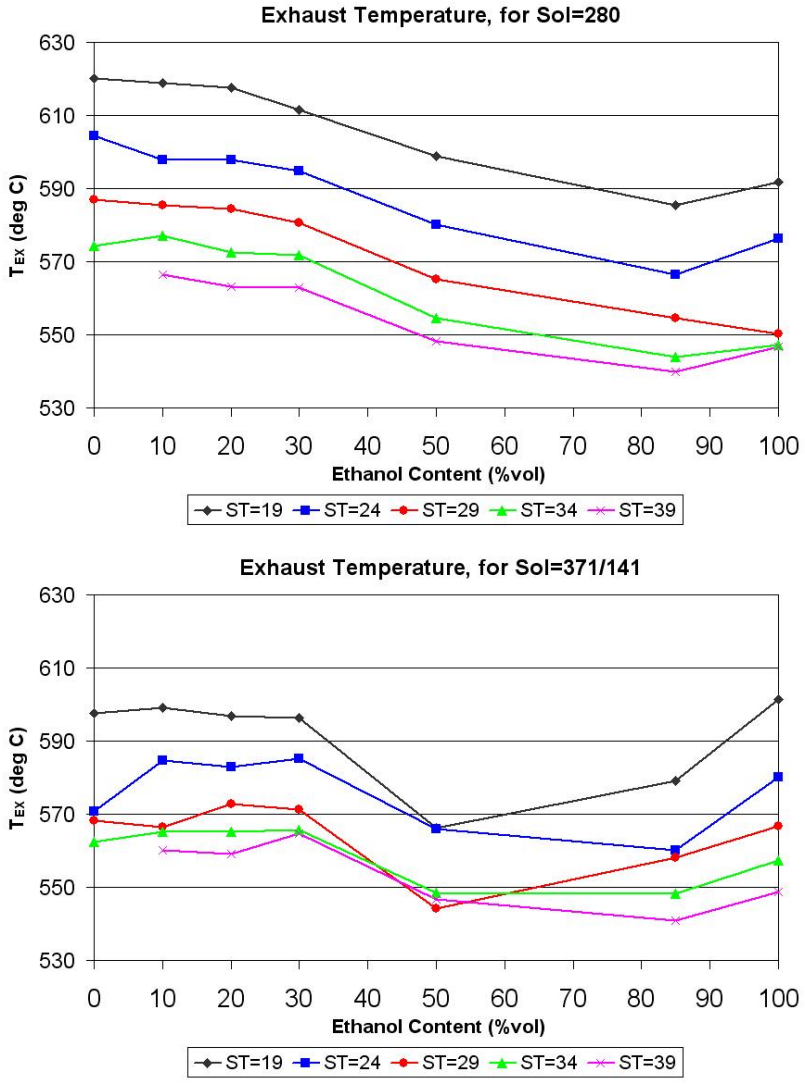

Figure 5.7 Part load SI, Exhaust temperature

5.2.2 Emissions

The level of NO_X emissions is exponentially dependant on the in-cylinder temperature, as the in-cylinder temperature increases the rate of NO_X formation is increased. For the 371/141SoI case this trend is observed, with the NO_X (Figure 5.8) plot having the same shape as the peak in-cylinder temperature plot.

For the 280SoI case there is also a general reduction in NO_X emissions. However there is a small peak at E30, which gets more pronounced as the spark timing is advanced, with the level then reducing as the ethanol content is increased. The peak at E30 can be related to increase in peak in-cylinder temperature seen between pure gasoline and E30. The trend between E30 and E85 could be because of the reduction in flame temperature as seen by the reduction in exhaust temperature. The NO_X level then increases slightly for pure ethanol and this is because of the combustion being advanced compared to that of E85.

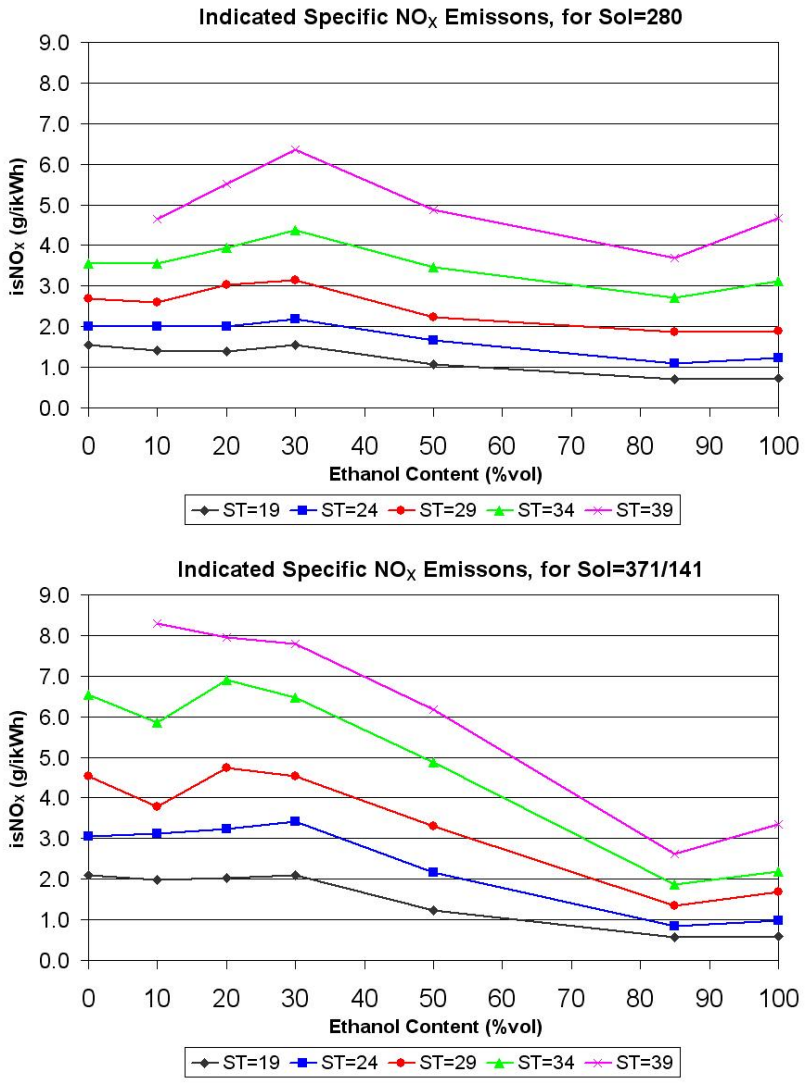

Figure 5.8 Part load SI, Indicated specific NO_X emissions

The hydrocarbon emissions are shown in Figure 5.9. It can be seen that both injection strategies lead to very similar (in both shape and value) trends for HC emissions versus both fuel blend and spark timing. There is an almost linear reduction in HC emissions with the increase in ethanol content. There are three factors influencing this, the completeness of combustion, the molecular weight of the fuel, and the ability of an FID emissions analyser to detect oxygenated hydrocarbons. This is reported by Wallner et al (2008) and Price et al (2007a) cites the work by

Cheng et al (1998), who gives response values (referenced to n-heptane) for various hydrocarbon species. The data presented shows that the response for alcohols such as methanol and ethanol are 50% and 75% respectively, with aldehydes such as n-butanal and n-heptanal having responses of 78% and 90% respectively. Whereas non-oxygenated hydrocarbons such as aromatic and alkane species give a much higher response, with benzene and toluene having responses of 99% and 101% respectively and methane and propane giving responses of 102% and 99% respectively. It can be seen that the spark timing has a small effect on the measured hydrocarbon levels, with advanced spark timings giving rise to increased hydrocarbon emissions. This is attributed to the higher in-cylinder pressure (associated with advanced combustion) forcing a greater quantity of unburned fuel into the crevice volumes. This is compounded by the reduction in exhaust temperature associated with advanced combustion causing the oxidation of the trapped fuel/partial combustion products to be lower.

However because of the similarity of emissions for both injection strategies, the reduction in the fuels molecular weight caused by the addition of ethanol and the reduced ability of an FID to detect oxygenated hydrocarbons are the main causes of the trends seen in this study and most likely mask the true nature of the hydrocarbon emissions.

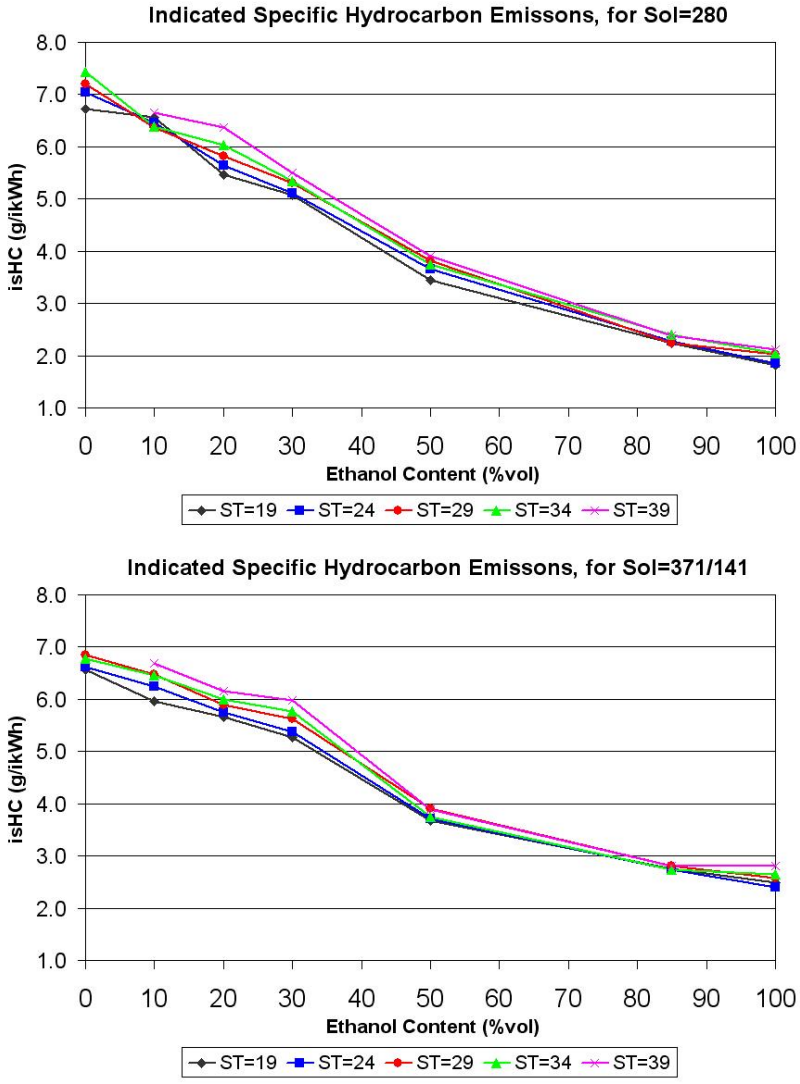

Figure 5.9 Part load SI, Indicated specific hydrocarbon emissions

The carbon monoxide emissions (Figure 5.10) for the 280SoI case show a general reduction as the ethanol content is increased. This is attributed to an increase in the available oxygen (particularly for rich mixture areas) associated with the oxygenated nature of ethanol [Al-Farayedhi et al (2000)]. For the 371/141SoI case the CO emissions are again reduced, but only up to E50. There is a significant increase for E85 and for pure ethanol. This is attributed to more

fuel impinging on the piston crown caused by the longer injection durations required for the ethanol blends, coupled by a reduction in the fuels volatility (vapour pressure).

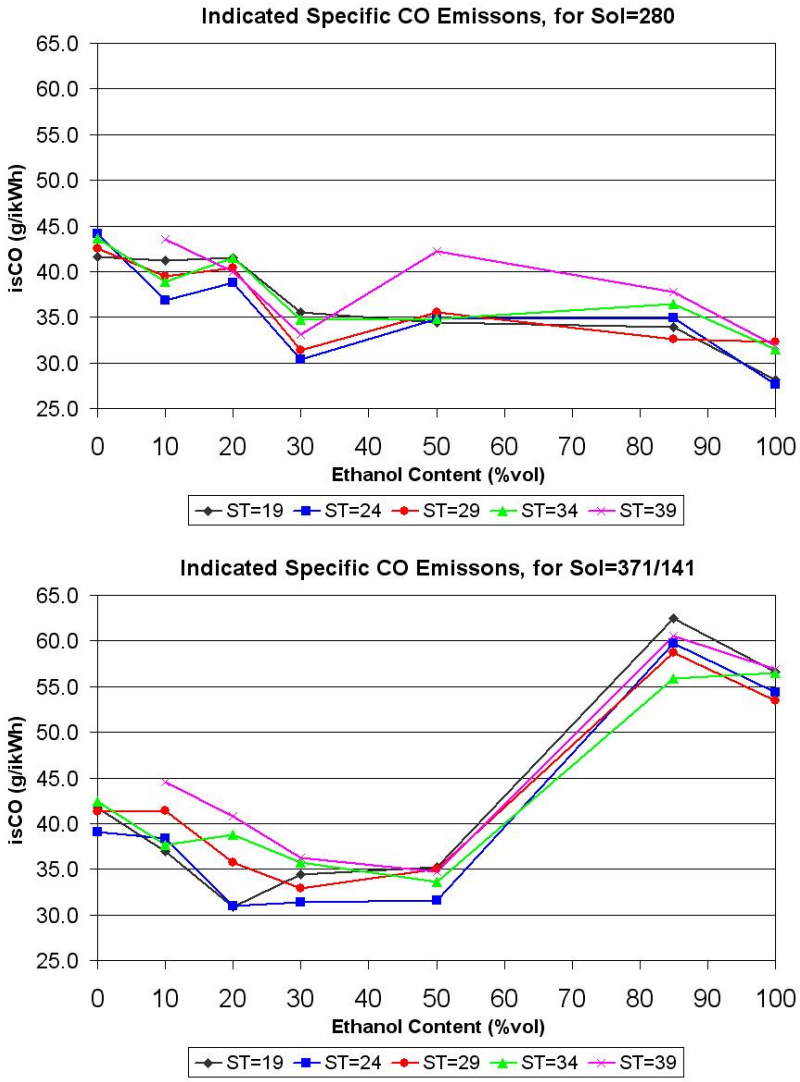

Figure 5.10 Part load SI, Indicated specific carbon monoxide emissions

5.2.3 Efficiency

Indicated efficiency is being presented here instead of specific fuel consumption because of the varying degree of oxygenation of the fuels used and the impact this has on the resulting gravimetric calorific value (~43 MJ/kg for gasoline and ~27 MJ/kg for ethanol).

Indicated efficiency is presented in Figure 5.11. For the 280SoI case it can be seen that as the ethanol content is increased the indicated efficiency also increases. This can be attributed to the increase in combustion efficiency shown previously in section 5.2.1. It can be seen that in general as the ethanol content is increased the spark timing has to be retarded (although these speak timings are not necessarily MBT timings) to achieve the highest efficiency. This is because as the ethanol content is increased the ignition delay and combustion duration are both reduced, resulting in the need to delay the start of combustion. For the 371/141SoI case indicated efficiency is generally unaffected by ethanol addition.

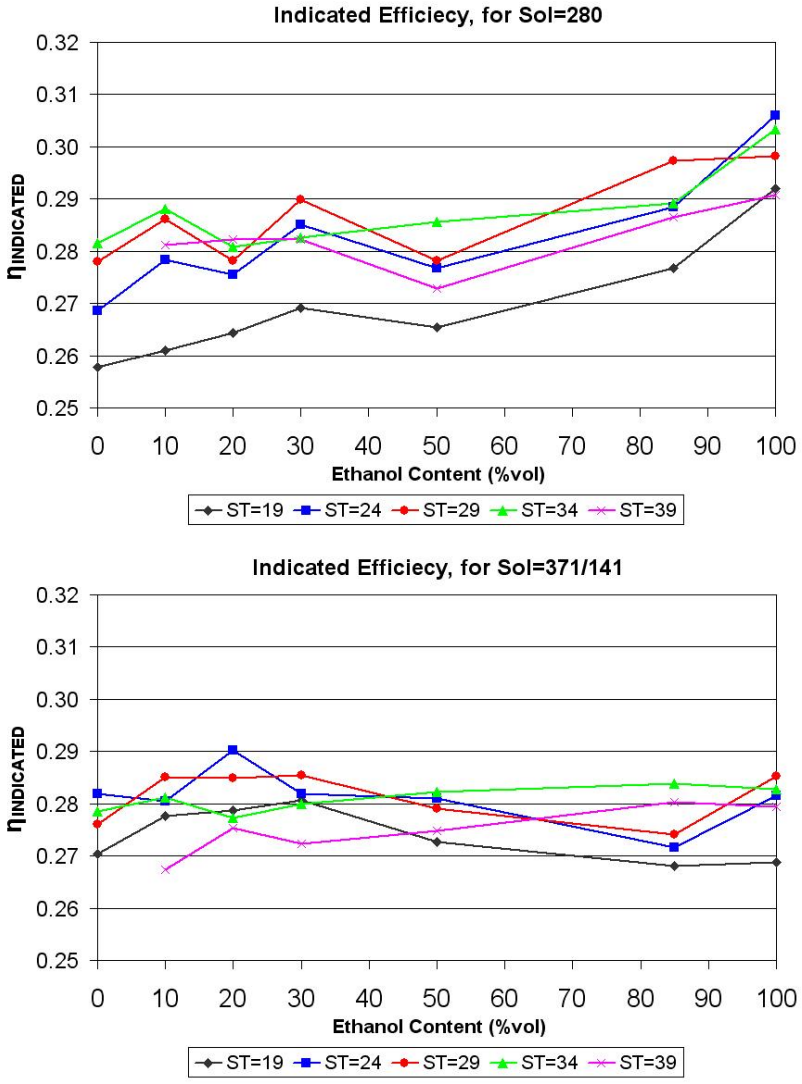

Figure 5.11 Part load SI, Indicated efficiency

5.3 Repeatability of Bio-Ethanol Data

The data in section 5.2 was collected over a number of different days. This was due to the time required to conduct all of the tests points for all of the fuels was greater than that available in a single day of testing. The fuel blends were tested on three different and non-consecutive days. E10, E20 and E30 were tested in the first group, standard gasoline and pure ethanol in the second group, and E50 and E85 were tested in the third and final group. This may have led to trends in the data with respect to fuel blend that were caused by day-day variations rather than actual differences caused by the changing fuel properties. In the following section data repeatability is investigated. A reduced number of fuel blends (E10 and E30 are not tested) and three spark timings representing a long, medium and short mixing time, of 19°, 29°, and 39° $bTDC_{COMB}$ respectively are repeated on two separate and non-consecutive days. This data is averaged along with the original data and presented in the following figures. The error bars represent ±1 standard deviation from the mean.

Figure 5.12 shows the 10% MFB timing. For the 280SoI case the repeated data shows the same trend (with respect to both fuel blend and spark timing) as the original data and has low spread. The length of the error bars equate to approximately 1 CAD which is small considering the data is only recorded at a resolution of 0.5 CAD. The 371/141SoI case again shows the same trends as the original data, however the error bars are slightly greater representing approximately 2 CAD for E85 and E100. This still does however suggest that the start of combustion is affected by the reduced in-cylinder temperatures associated with the late second injection.

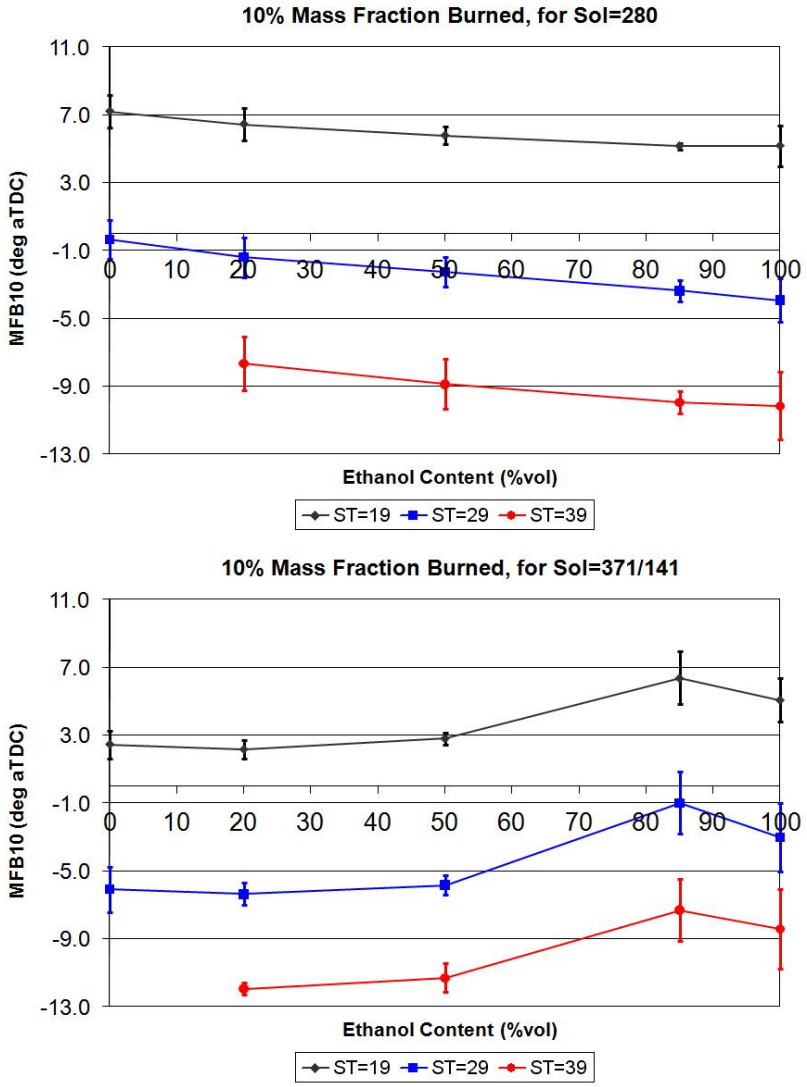

Figure 5.12 Part load SI repeatability test, 10% mass fraction burned

The combustion duration as shown in Figure 5.13 does show similar trends to that of the original data including the peak at E85 for the split injection case. However there is a significant amount of spread in the data at some, but not all points. This can be attributed to the problem of calculating the 90 percentile of the mass fraction burned profile. At this point the gradient of the curve is very shallow and any noise in the trace could cause the analysis code to select a point some crank angle degrees away from the real point, and hence cause the spread in the data.

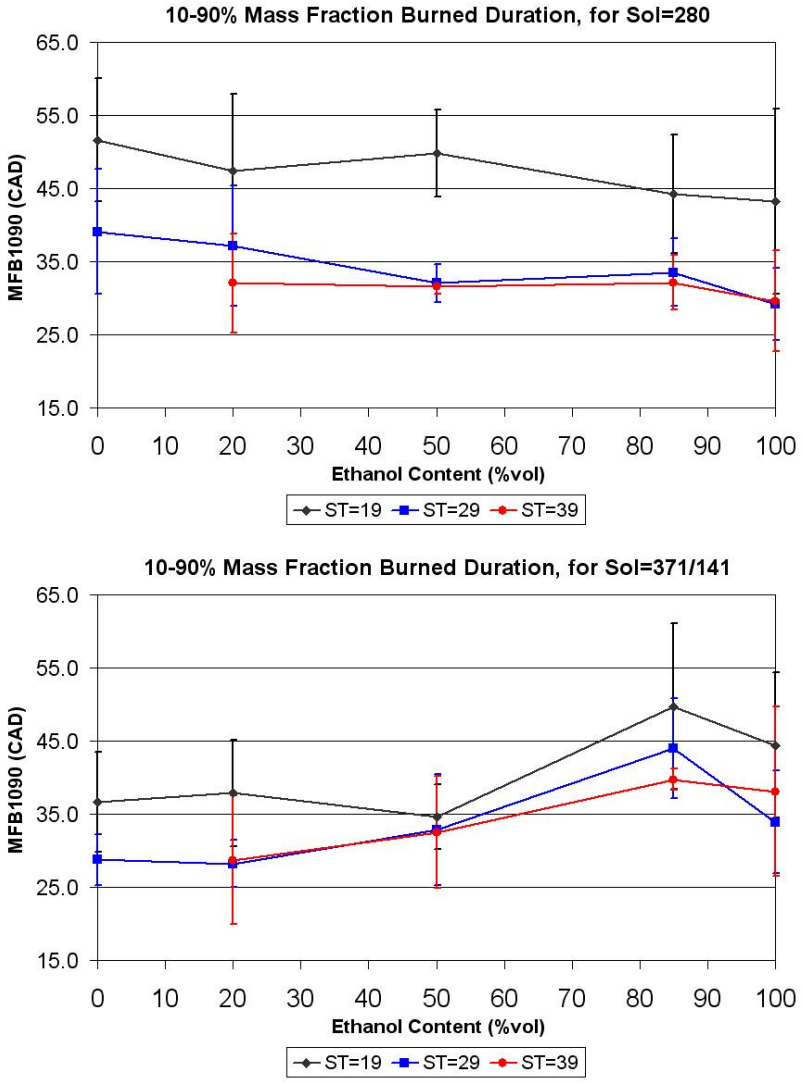

Figure 5.13 Part load SI repeatability test, Combustion duration

Maximum in-cylinder pressure (pseudo in-cylinder temperature) and exhaust temperature are presented in Figures 5.14 and 5.15 respectively. These again show good correlation with the original data in terms of both trend and actual values whilst also having low spread.

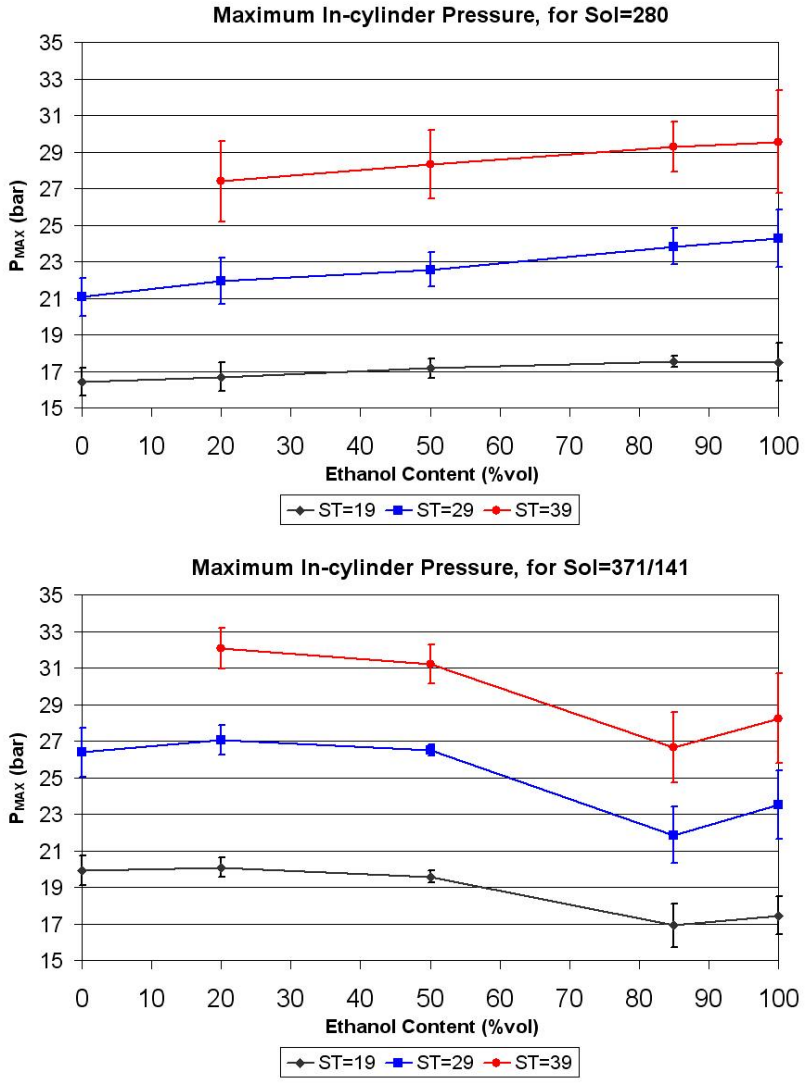

Figure 5.14 Part load SI repeatability test, Peak in-cylinder pressure

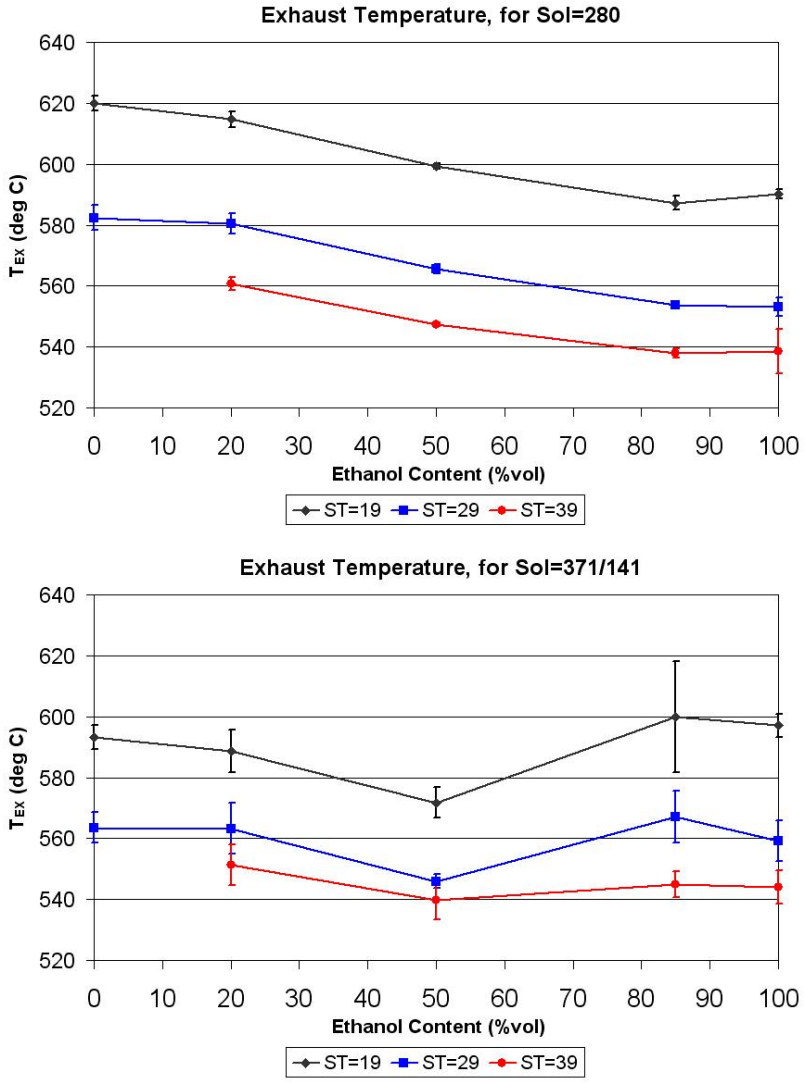

Figure 5.15 Part load SI repeatability test, Exhaust temperature

In-cylinder pressure and exhaust temperature are a function of in-cylinder temperature, combustion phasing and duration, and adiabatic flame temperature. With the repeatability test data showing good correlation with the original data and having low spread suggest that the combustion phenomena observed is correct and repeatable. This is despite some of the presented data not agreeing with previously published studies, namely being the in-cylinder temperature (presented here as in-cylinder pressure).

5.4 Investigation into the effects of 2,5 Di-methylfuran/Gasoline Blends

In this section splash blends of 2,5 di-methylfuran (DMF) and gasoline are compared to splash blends of ethanol and gasoline. The load and engine operating conditions are the same as that for the single injection strategy in Table 5.2, except only three spark timings are used, with these being 19°, 29°, and 39° $bTDC_{COMB}$. The blends studied are DMF20 (20%$_{Vol.}$ DMF) and DMF50 (50%$_{Vol.}$ DMF), E20, E50, and standard gasoline. All tests were conducted on the same day to avoid any problems caused by day-day variations in atmospheric conditions.

5.4.1 Combustion Performance

From the start of combustion (10% mass fraction burned, Figure 5.16) it can be seen that the blends of DMF have similar ignition properties to ethanol blends of the same ratio. This implies that the mixture in the vicinity of the spark plug at the point of spark discharge for the DMF blends is of similar ignitability to that of the ethanol blends despite both fuels being different in structure.

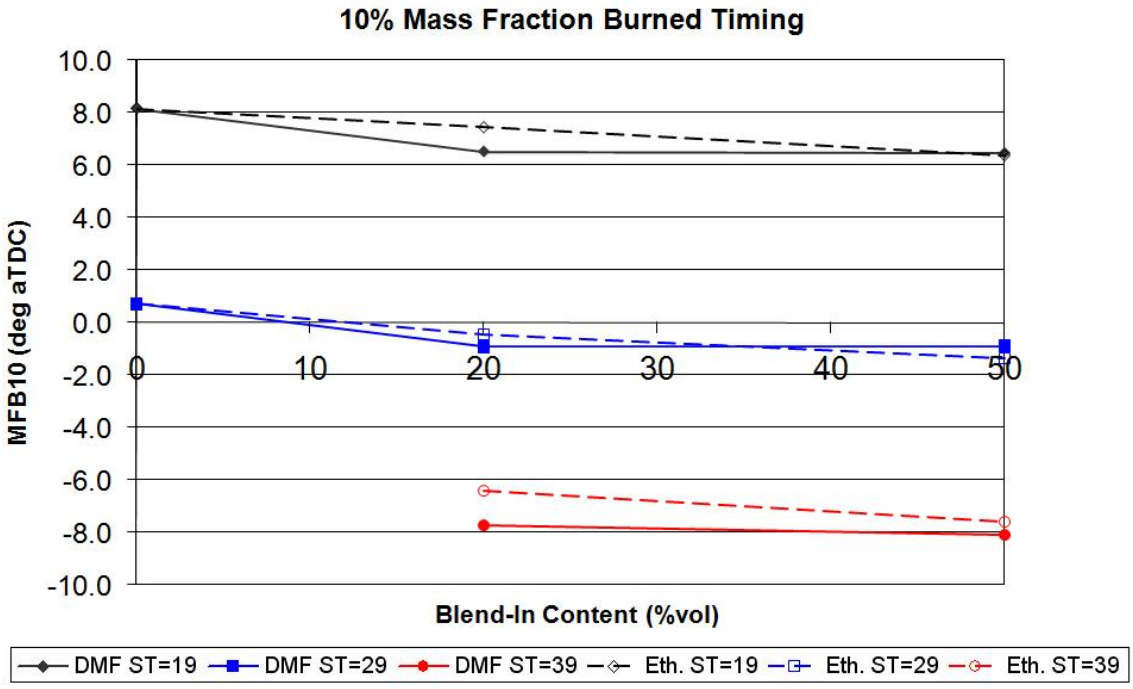

Figure 5.16 Part load DMF SI, 10% mass fraction burned

However it would be expected that the DMF blends would show more advanced combustion than the corresponding ethanol blends because of its faster laminar flame speed, ~43 m/s compared to ~39 m/s for ethanol (Table 3.6). DMF does though show a reduced ignition delay (defined as the time between spark discharge and 10% MFB) as shown in Figure 5.17 compared to gasoline, as predicted by the increased laminar flame speed (~43 m/s compared to ~33 m/s, Table 3.6).

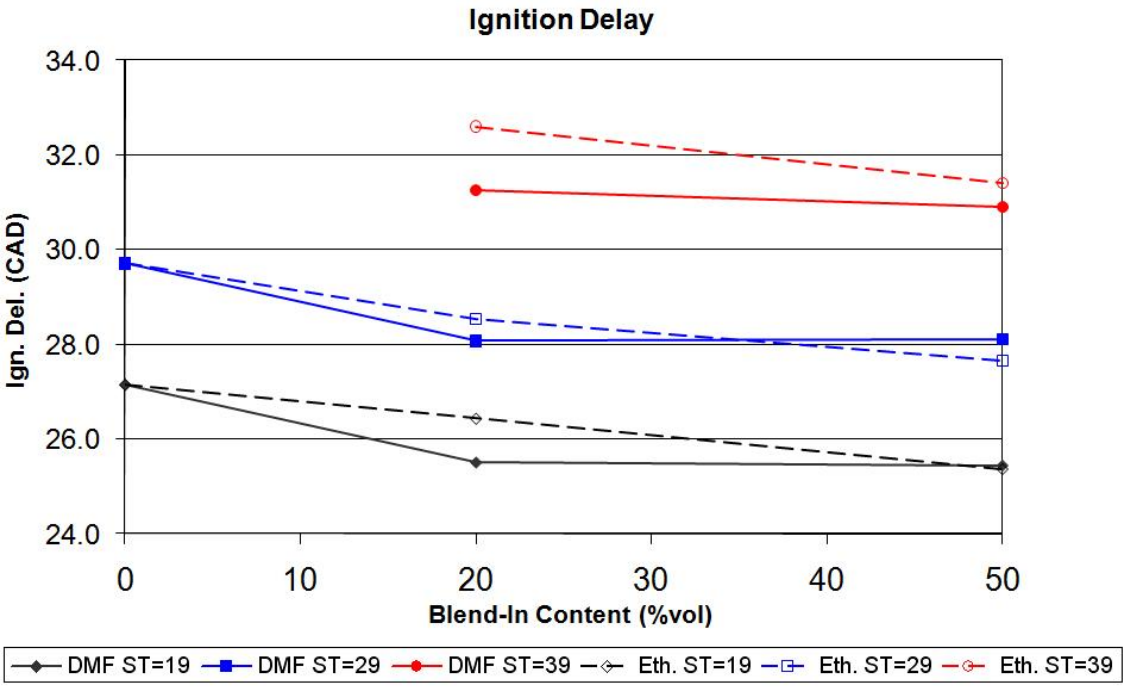

Figure 5.17 Part load DMF SI, Ignition delay

The faster laminar flame speed of DMF has a greater effect on the combustion duration (10-90% MFB, Figure 5.18) where it can be seen that the addition of DMF reduces the combustion duration. It can be seen that the DMF blends generally show reduced combustion durations than the equivalent ethanol blends, as predicted by the differences in laminar flame speed.

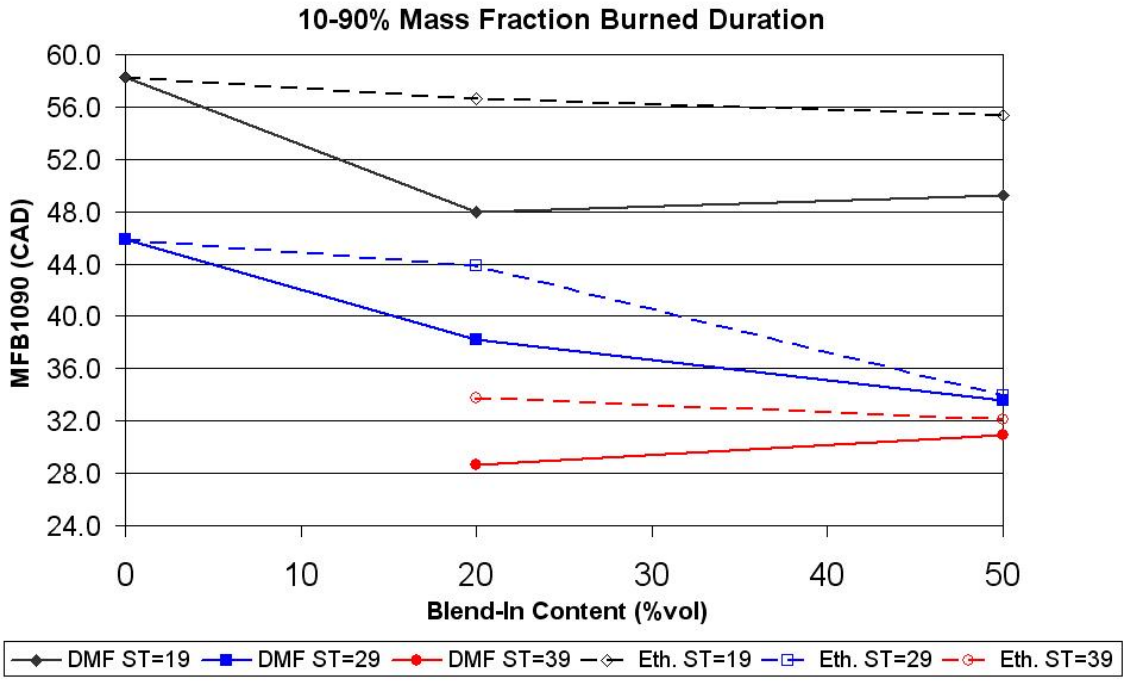

Figure 5.18 Part load DMF SI, Combustion duration

As expected the reduction in combustion duration has led to an improvement in combustion stability. Combustion stability is presented in Figure 5.19 as COV_{IMEP}.

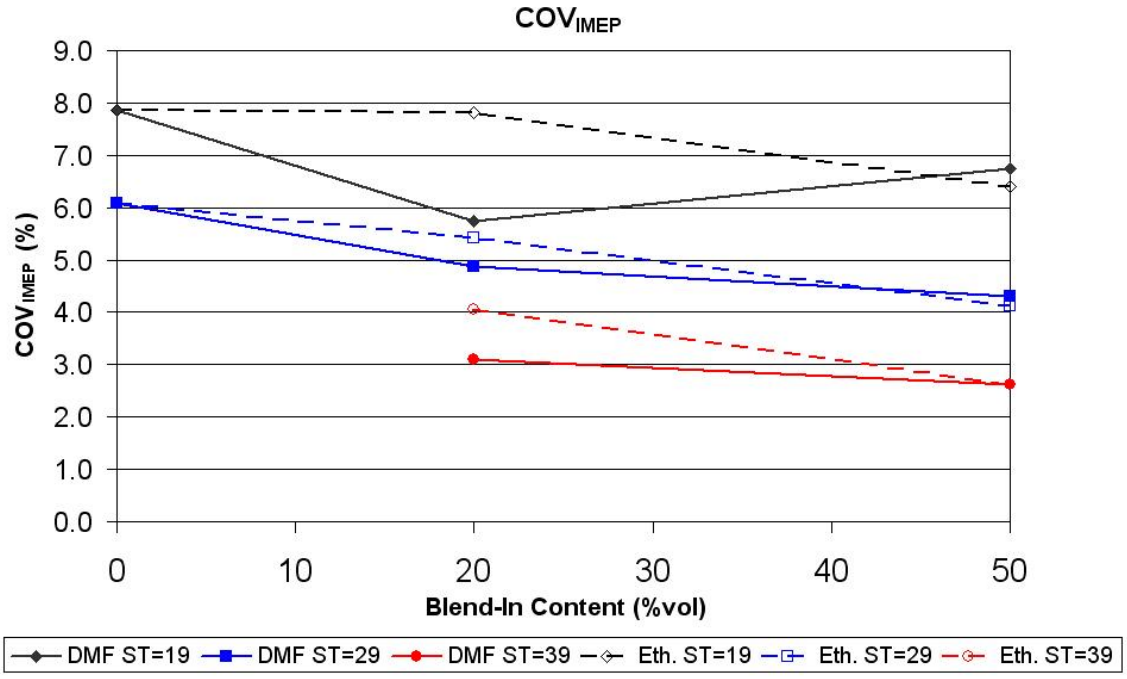

Figure 5.19 Part load DMF SI, Combustion stability

Combustion efficiency is presented in Figure 5.20. It can be seen that the addition of DMF improves combustion efficiency, but not to the extent that ethanol addition does. This improvement is attributed to DMF being oxygenated. This means to a certain extent the oxygenated fuel molecule does not have to 'search for' as much oxygen as a non-oxygenated molecule. DMF has O/C and O/H ratios of 0.167 and 0.125 respectively, were as ethanol has O/C and O/H ratios of 0.5 and 0.167 respectively. This can explain why DMF improves combustion efficiency, but not to the same extent as ethanol. The calculated combustion efficiency has to be considered in conjunction with the uncertainties associated with the hydrocarbon emissions (as discussed in Section 5.2.2). If the hydrocarbon emissions were more accurately measured then the differences in combustion efficiencies for the ethanol and DMF blends would likely be less.

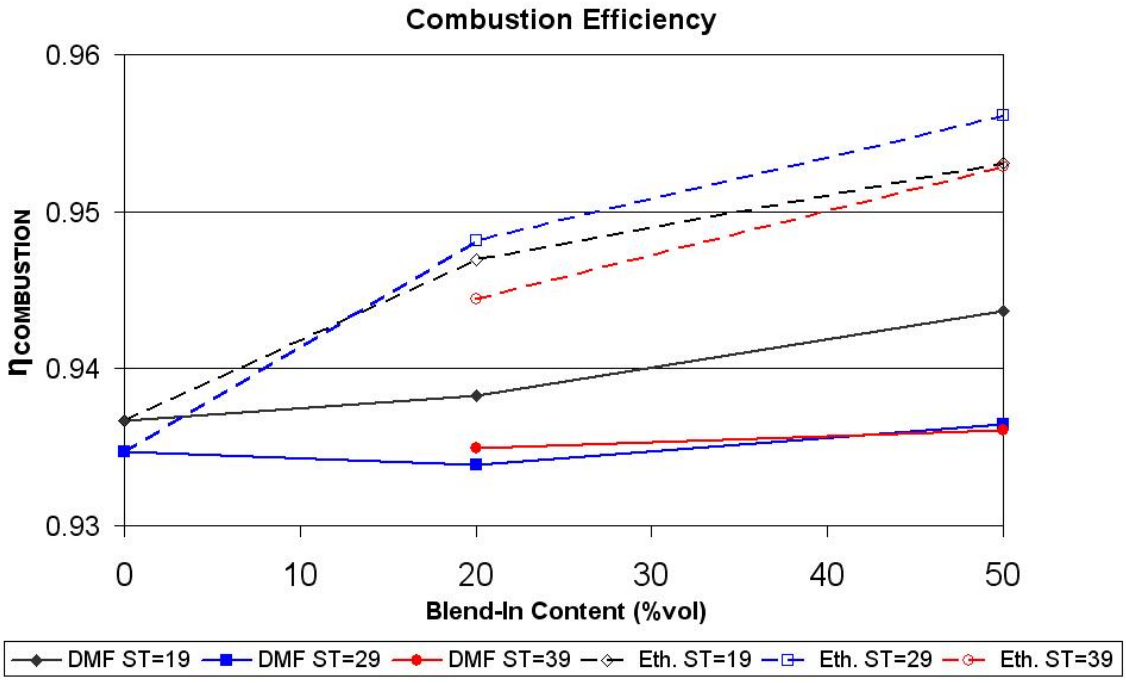

Figure 5.20 Part load DMF SI, Combustion efficiency

DMF shows an increase in peak in-cylinder temperature compared to standard gasoline (shown here as peak in-cylinder pressure, Figure 5.21). This could be attributed to a higher adiabatic flame temperature, but the increase is small and likely to be caused by the advanced and faster combustion seen with the addition of DMF. This increase in temperature is expected to cause an increase in NO_X emissions due to the exponential relationship of NO_X formation with temperature.

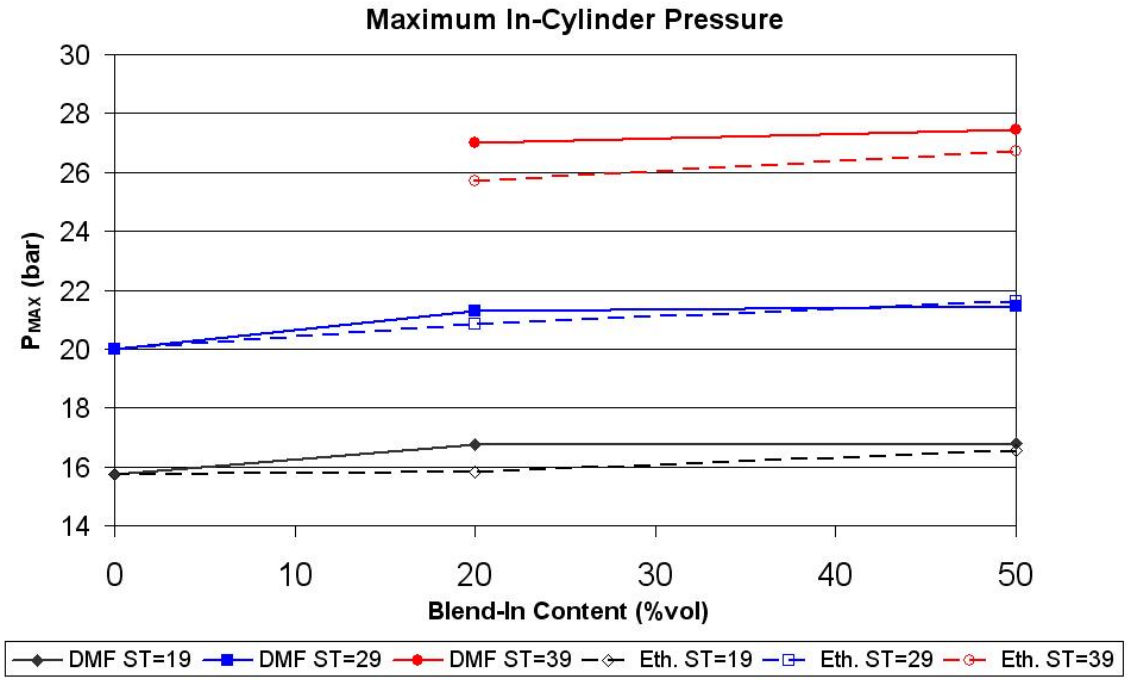

Figure 5.21 Part load DMF SI, Peak pressure

A better indicator of flame temperature is the exhaust temperature as shown in Figure 5.22. The advanced combustion leads to a greater time between end of combustion and exhaust valve opening. This gives more time for the cylinder contents to cool and hence lead to a lower exhaust temperature as seen with the ethanol blends. However the DMF blends generally led to a higher exhaust temperature despite the advanced and faster combustion leading to a greater time between the end of heat release and exhaust valve opening. This indicates that the flame temperature of DMF is higher than that of both ethanol and gasoline. However this goes against the theoretical study of Nabi et al (2002), who show that adiabatic flame temperature reduces linearly with increasing molecular oxygen weight percent.

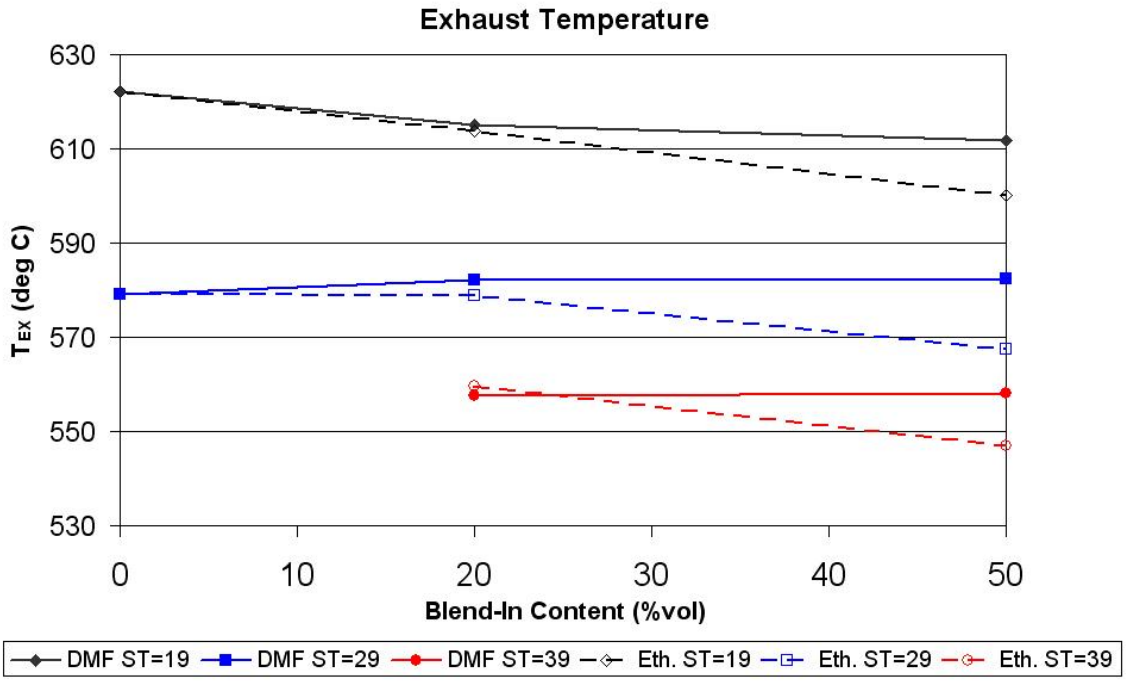

Figure 5.22 Part load DMF SI, Exhaust temperature

5.4.2 Emissions

The increase in in-cylinder temperature (inferred from in-cylinder pressure) has led to an increase in NO_X emissions for the DMF blends compared to standard gasoline. Whereas, the ethanol blends generally cause a reduction in the level of NO_X emissions. NO_X emissions are presented in Figure 5.23 below. This increase in NO_X emissions supports the idea that DMF has a higher adiabatic flame temperature compared to both gasoline and ethanol because of the relationship NO_X formation has with temperature.

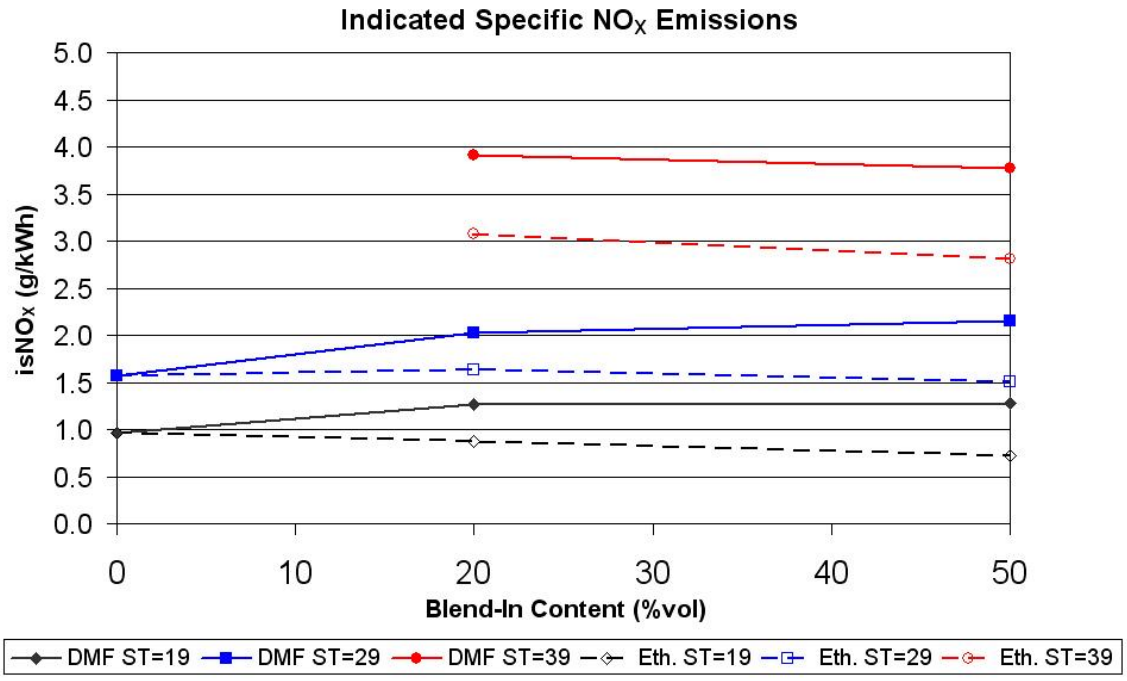

Figure 5.23 Part load DMF SI, Indicated specific NO_X emissions

The hydrocarbon emissions are presented in Figure 5.24. It can be seen that the addition of DMF has no effect on the level of emitted hydrocarbons, whereas the addition of ethanol causes a reduction in hydrocarbon emissions. This reduction has previously been discussed and is attributed to the inability of an FID to detect oxygenated hydrocarbons. However DMF has a C/O ratio that is three times greater than that of ethanol. This therefore suggests that the recorded level of hydrocarbon emissions for the DMF blends is closer to the real value than that for the ethanol blends but possibly still lower than the actual value. So as a result of this the observation that DMF addition has no effect on the hydrocarbon emissions could be in reality a slight increase in emissions with DMF addition.

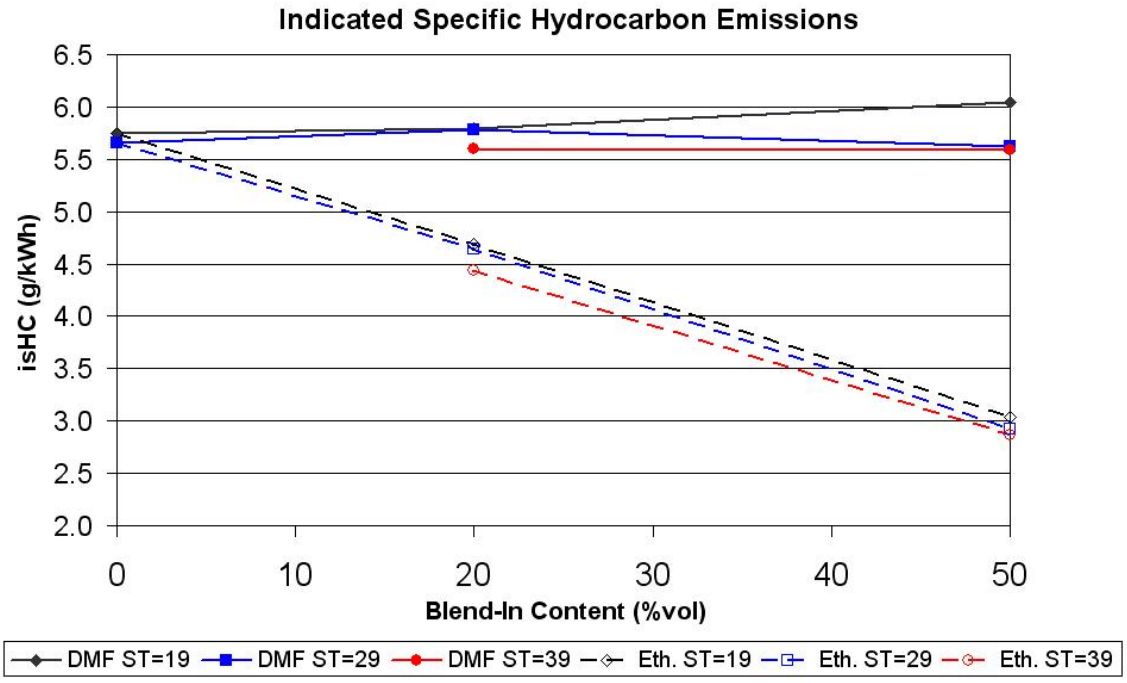

Figure 5.24 Part load DMF SI, Indicated specific hydrocarbon emissions

Despite DMF addition showing a slight increase in combustion efficiency, a minor increase in CO emissions is observed (Figure 5.25). This can be attributed to the incomplete decomposition and combustion of the DMF ring structure. This is also shown by the increase in particulate matter emissions as shown in Chapter 7.

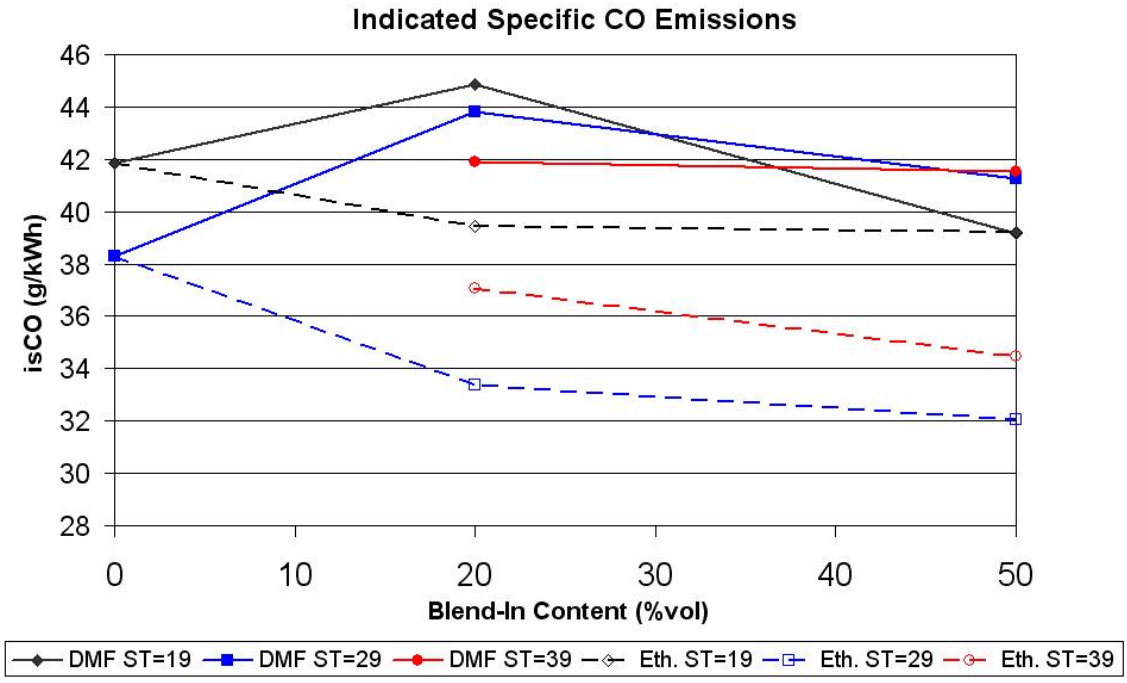

Figure 5.25 Part load DMF SI, Indicated specific carbon monoxide emissions

5.4.3 Efficiency

Once again indicated efficiency is presented in the place of indicated specific fuel consumption due to DMF being oxygenated and hence having a reduced calorific value compared to gasoline. It can be seen that the addition of DMF has little effect on the indicated efficiency (Figure 5.26), but the ethanol blends show a consistently higher efficiency that increases with blend ratio. This is attributed to the increase in combustion efficiency of the ethanol blends compared to the blends of DMF.

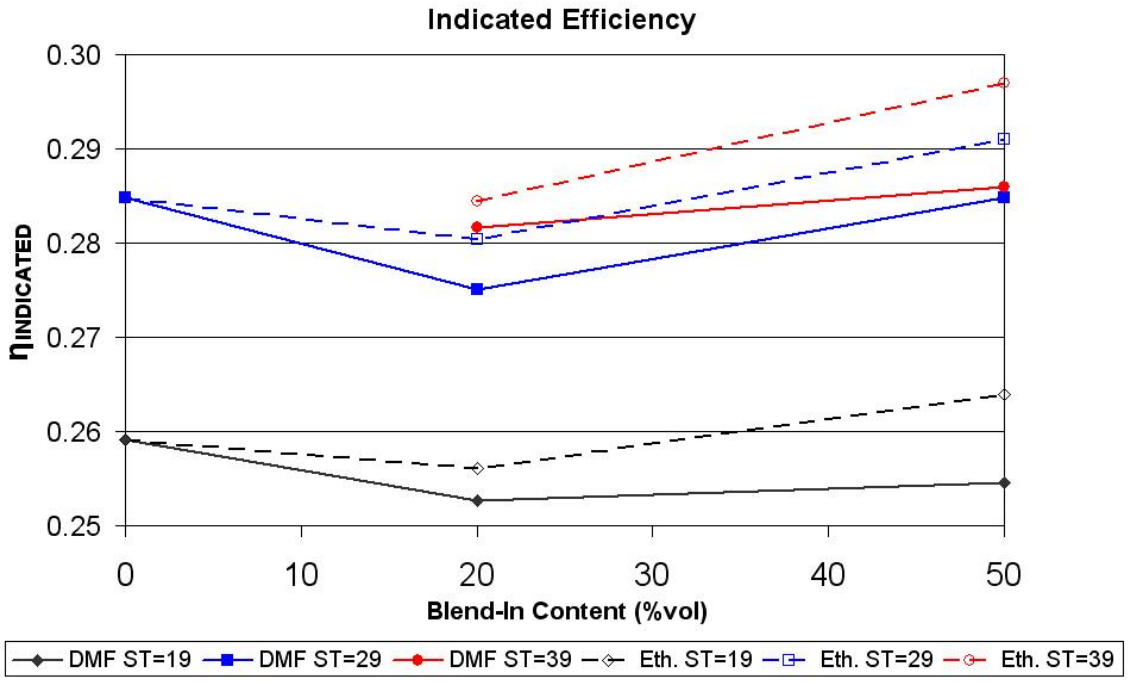

Figure 5.26 Part load DMF SI, Indicated efficiency

5.5 Summary

In this chapter the spark ignition performance of ethanol/gasoline and 2,5 di-methylfuran/gasoline blends have been investigated at part load (3.4 bar IMEP). It can be seen that any benefits or problems associated with the addition of either ethanol or DMF are dependent on the injection strategy used (single or split injection).

The addition of ethanol shows a reduction in ignition delay and faster combustion brought about by ethanol having a faster laminar flame speed. The combustion is more stable and combustion efficiency is improved with the reduction in carbon monoxide emissions. The NO_X emissions are reduced due to lower in-cylinder and flame temperatures, whilst a further reduction can be

realised by retarding the spark timing without sacrificing combustion stability. Engine efficiency (indicated) is increased, but the increase in fuel injected mass (due to the reduction in $AFR_{Stoich.}$) required for ethanol addition could lead to the fuel pump consuming more power and hence lowering brake efficiency. The split injection strategy used shows some of the above benefits but is generally limited to up to 30% ethanol content.

The addition of DMF also shows reduced ignition delay and faster combustion giving rise to improved combustion stability, which is attributed to a faster laminar flame speed. Combustion efficiency is improved because of the oxygenated nature of the DMF molecule. There is evidence to support the claim that DMF has a higher flame temperature than both gasoline and ethanol. The evidence for this is the increased exhaust temperature and higher NO_X emissions.

Some of the trends seen with increasing ethanol content are very much non-linear. This is caused by the evaporation properties of an ethanol/gasoline mixture varying non-linearly with ethanol content. The vapour pressure of an ethanol/gasoline mixture is not simply a linear combination of the two individual vapour pressures.

The trends in the hydrocarbon emissions with respect to ethanol and to a lesser extent DMF addition need to be considered in conjunction with the reduced sensitivity of an FID to detect oxygenated hydrocarbons. The observed reduction in hydrocarbon emissions with increasing ethanol content are most likely to be caused the reduced sensitivity of the FID rather than the improved combustion performance of the fuel blends.

CHAPTER 6

6 The Effect of Bio-Fuels on Direct Injection Spark Ignition (DISI) Combustion – Full Load

This chapter investigates the effect of using bio (oxygenated) fuels on combustion and regulated emissions in Direct Injection Spark Ignition (DISI) combustion at wide open throttle conditions. Both conventional (Ethanol) and novel (2,5 Di-methylfuran) bio-fuels are investigated and compared to standard 95 RON gasoline. A split injection strategy is investigated alongside the standard single injection for the ethanol blends. This is to investigate the combustion performance of an injection strategy that is intended to reduce PM emissions (Chapter 7).

For this study the valve timing and injection timing (single injection) are the same as those used for the part load tests (Chapter 5) and are shown in Table 6.1 for reference, likewise all tests are conducted with a stoichiometric mixture (λ=1). Two spark timings are used in this study, the first being the knock-limited spark timing for standard gasoline (7° $bTDC_{COMB}$) which will be referred to as retarded spark timing and the second is the knock-limited/MBT timing for the particular fuel blend used which will be referred to as advanced spark timing. These two spark timings are used to investigate the different fuel properties at the same conditions (gasoline knock-limited timing) and at a spark timing that gives maximum achievable efficiency for the given blend.

Table 6.1 Engine configuration for full load spark ignition operation

	Single Injection	Split Injection
Engine Speed (RPM)	1500	
IMEP (bar)	WOT	
λ	1.0	
IVO (° $bTDC_{GE}$)	16	
EVC (° $aTDC_{GE}$)	36	
SoI (° $bTDC_{COMB}$)	280	280/240
Spark Timing (° $bTDC_{COMB}$)	7, K-L/MBT	K-L/MBT

6.1 Investigation into the effects of Bio-Ethanol/Gasoline and 2,5 Di-methylfuran/Gasoline Blends

In this study three different blends of ethanol/gasoline are examined, the blends being 20, 50 and 85% bio-ethanol in gasoline as well as standard gasoline and pure ethanol. One DMF/gasoline blend of 50% DMF is investigated in addition to pure DMF. In addition to the direct injection tests, two different port injection (PFI) cases using standard gasoline are examined. The first PFI case uses the same injection timing as the DI cases (occurs while the intake valve is open) and for the second PFI case the injection occurs 16 CAD after the intake valve closes, to give the maximum time for the fuel to evaporate before entering the cylinder. These PFI tests are to evaluate the fuel evaporation and mixing performance of the direct injection system. All tests were conducted on the same day to avoid any problems caused by day-day variations in atmospheric conditions.

6.1.1 Load

With the engine being operated at a WOT condition the different fuel blends and spark timing combinations used led to differing engine loads to be produced. Engine load, presented here as indicated mean effective pressure (IMEP), is shown in Figure 6.1.

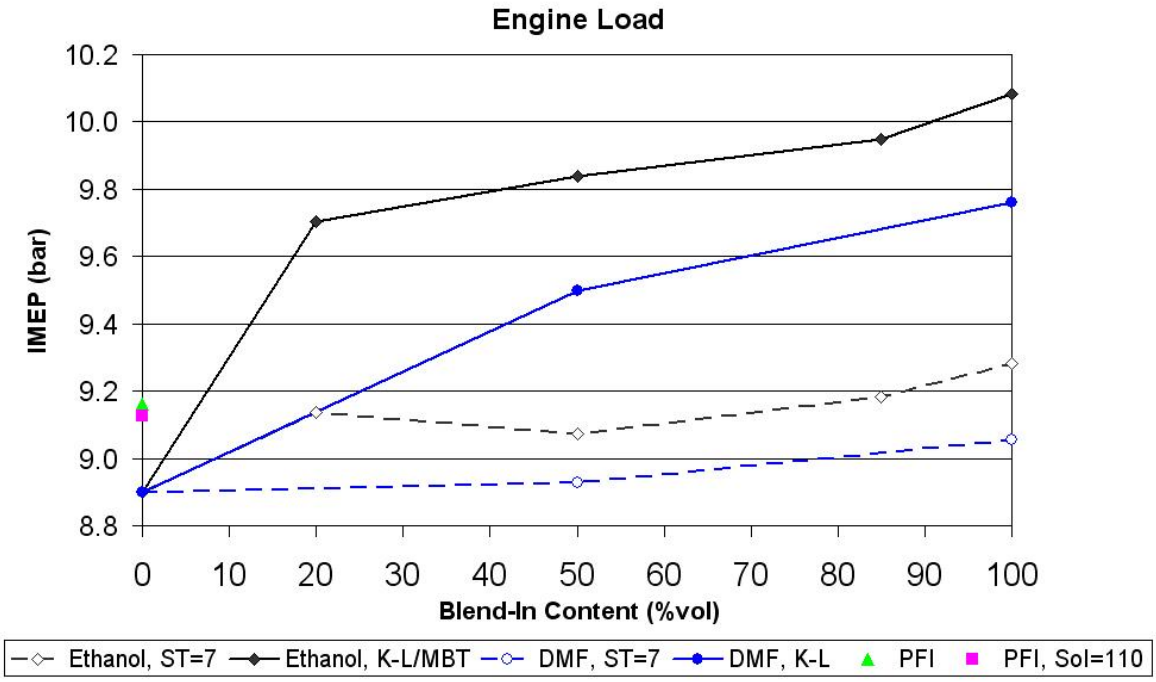

Figure 6.1 Full load SI, Engine load

It can be seen that for the constant spark timing (dashed line) that as the ethanol content is increased the load produced also increases. This is attributed to an increase in volumetric efficiency caused by the increased charge cooling effect of ethanol. Likewise as the DMF blend ratio is increased the load produced also increases. This is again attributed to an increase in volumetric efficiency. Volumetric efficiency is presented in Figure 6.2 as relative volumetric efficiency referenced to the closed valve PFI injection case. The peak in the ethanol curve at 50% volumetric ethanol content is caused by the non-linear behaviour of the vapour pressure of

ethanol/gasoline mixtures. The work by Kar et al (2008) shows that the vapour pressure of ethanol/gasoline mixtures increases up to 30% ethanol content and then reduces as the ethanol content is increased further. This coupled with the increased charge cooling (from increased enthalpy of vaporisation resulting from increased ethanol content) inhibits further evaporation, causing a peak in charge cooling potential to occur at around 50% ethanol content. The reduction in volumetric efficiency for the advanced spark timing is caused by higher in-cylinder surface temperatures arising from the higher in-cylinder temperatures associated with advanced combustion. The increased surface temperatures heat the incoming charge more causing it to expand more and thus a lower quantity is inducted. It can be seen for that for standard gasoline the two PFI cases produce a greater load than that of the DI case. This is attributed to improved mixing offered by the PFI injection compared to the direct injection; this will be discussed further in Section 6.1.2.

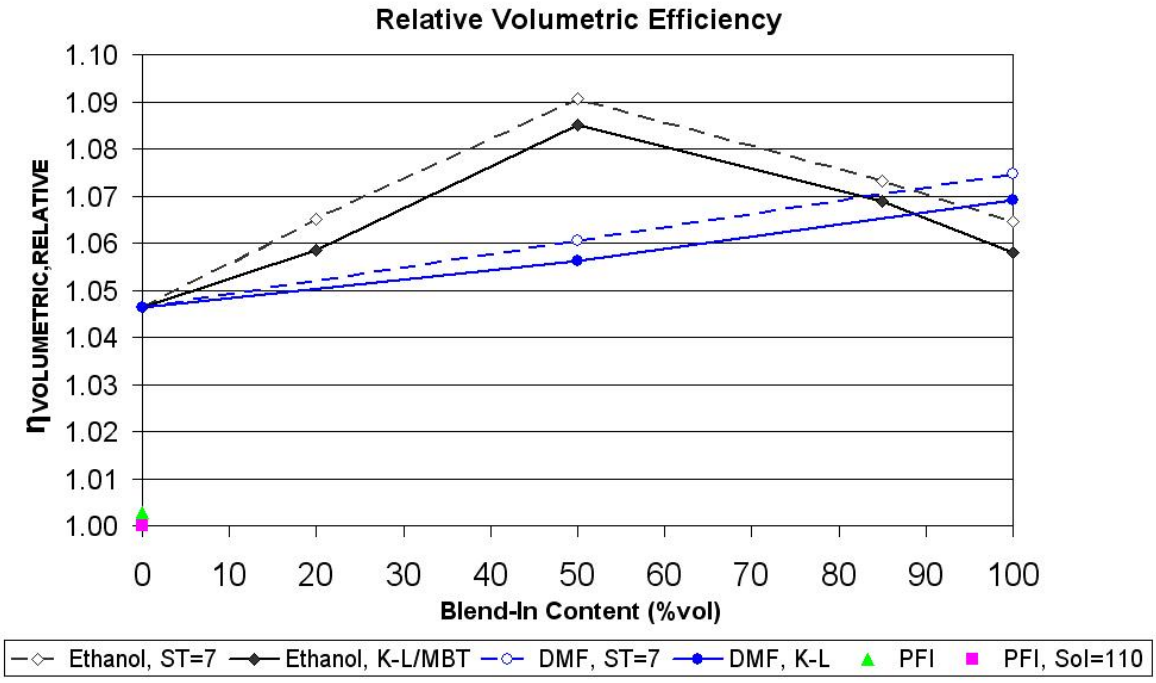

Figure 6.2 Full load SI, Relative volumetric efficiency

When the spark timing is advanced to either the knock-limited (K-L) or MBT timing there is a significant increase in the load produced because the combustion is either close to (K-L) or at the optimal timing (MBT). The load achievable for the ethanol blends is greater than that for the comparative DMF blends because MBT timing can be achieved for the ethanol blends of 50% and above whereas all of the DMF blends (including pure DMF) are knock-limited. Spark timing is shown in Figure 6.3.

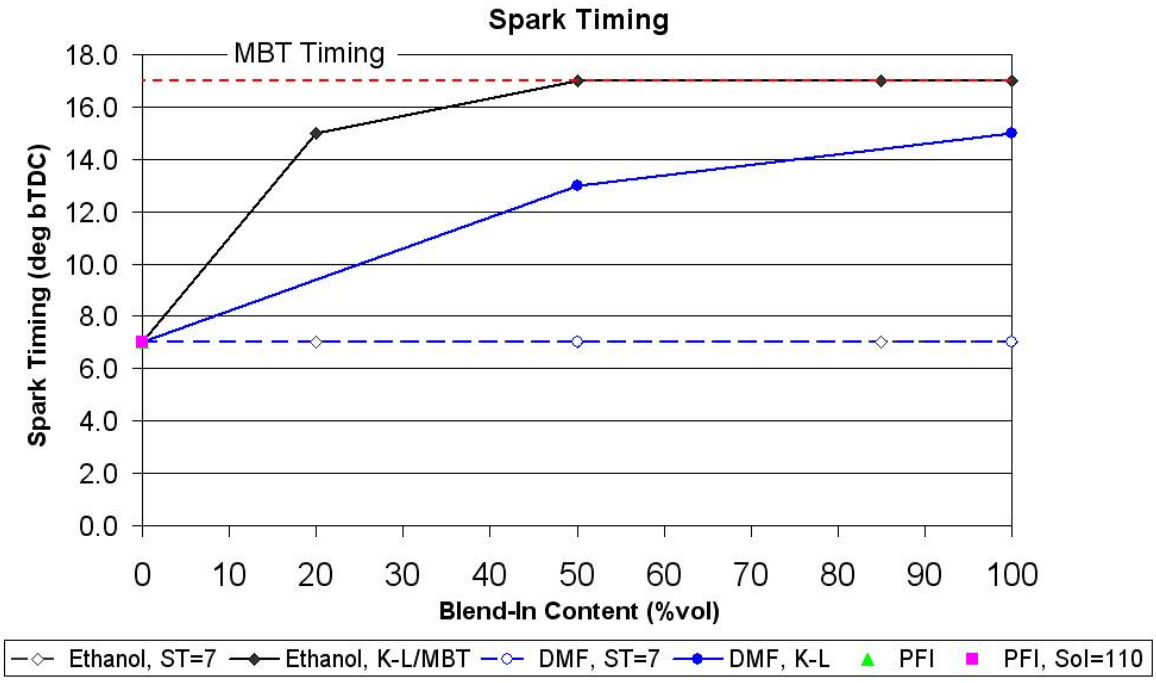

Figure 6.3 Full load SI, Spark timing

The literature [Roman-Leshkov et al (2007) and Mousdale (2008)] states that DMF has a higher research octane rating than ethanol and this would suggest that DMF (and blends of) would tolerate the same amount of spark advance as ethanol (and blends of), however this study suggests differently. This observed increase in knock tendency of DMF compared to ethanol is caused by the difference between the enthalpy of vaporisation of DMF and ethanol. The enthalpy of vaporisation for a stoichiometric mixture of DMF is less than a third of the value for that of an ethanol stoichiometric mixture, 28.3 $kJ/kg_{mixture}$ and 92.3 $kJ/kg_{mixture}$ respectively (see Table 3.6). With the fuel being injected directly into the cylinder and provided a significant amount of fuel is not impinged onto the piston and/or cylinder wall the evaporating fuel will lower the temperature of the in-cylinder charge. This lower temperature also results in a lower

in-cylinder pressure as combustion is initiated. This therefore means that the combustion can be advanced without the charge ahead of the flame front auto-igniting.

6.1.2 Combustion Performance

Ignition delay (defined as the time between spark discharge and 10% MFB) is presented in Figure 6.4 and it can be seen that there is a general reduction for the ethanol blends, with the trend being similar for both the advanced and retarded spark timings, with the two being offset by approximately 1 CAD in magnitude. This is caused by ethanol having a faster laminar flame velocity than that of gasoline, ~39 m/s compared to ~33 m/s respectively (Table 3.6). The non-liner trend of the ignition delay could be attributed to the non-linear nature of the vapour pressure and charge cooling potential of ethanol/gasoline mixtures affecting the in-cylinder temperature prior to spark discharge. The DMF blends show a slight linear reduction in ignition delay as the DMF content is increased. This is caused by the increased laminar flame velocity of DMF (~43 m/s, Table 3.6). The advanced spark timing shows a reduced ignition delay (for both ethanol and DMF blends) despite having a reduced mixing time (time between injection and spark timing) which would suggest an increase in ignition delay. This reduction in ignition delay however is a product of the advanced combustion. The advanced combustion significantly raises the in-cylinder temperature during combustion causing the temperature of the combustion chamber surface and exhaust valves to increase, which in turn heats up the fresh charge making it more ignitable and hence reducing the ignition delay. Comparing the DI and PFI injection strategies it can be seen that the PFI cases have a reduced ignition delay. This is because the fuel is drawn into the cylinder along with the fresh air and this increases the level of mixing compared to injecting fuel into the fresh air once inside the cylinder. It can be seen that the

closed valve PFI injection case (SoI=110° $bTDC_{COMB}$) has a slightly longer ignition delay. This is likely to be caused by some of the injected fuel impinging on the intake runner and the back of the intake valves causing inhomogeneity in the mixture. This also results in reduced combustion quality and load produced (Figure 6.1).

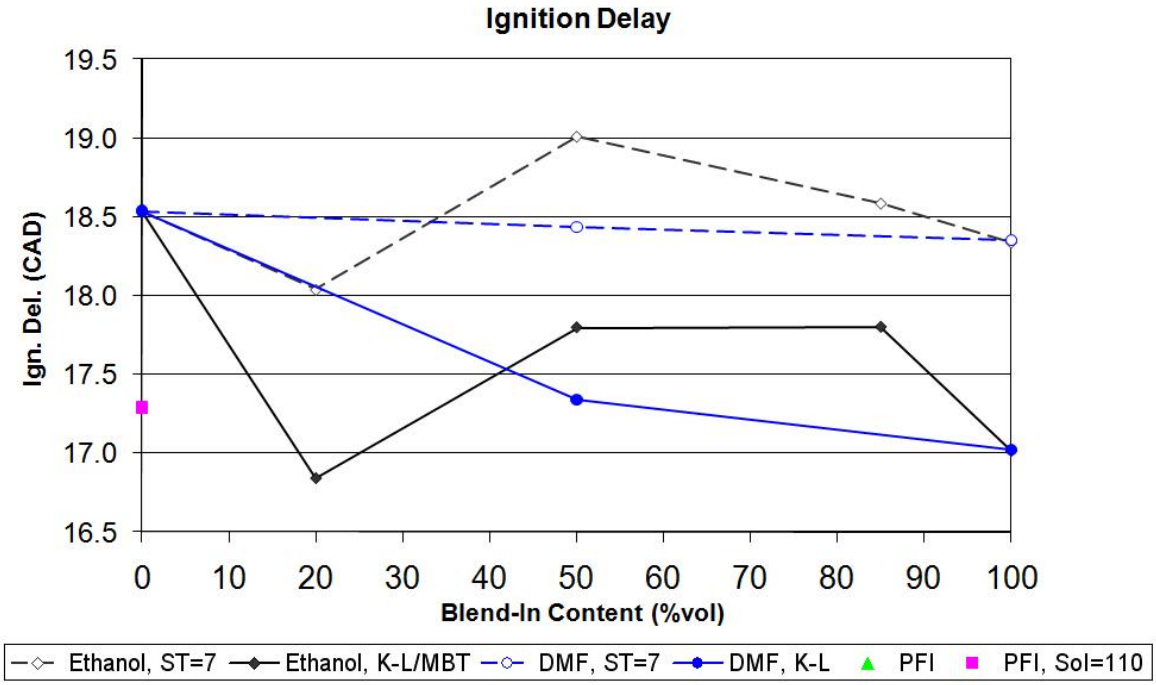

Figure 6.4 Full load SI, Ignition delay

Start of combustion (10% MFB) is shown in Figure 6.5 for reference. It can clearly be seen that advancing the spark timing leads to advanced combustion.

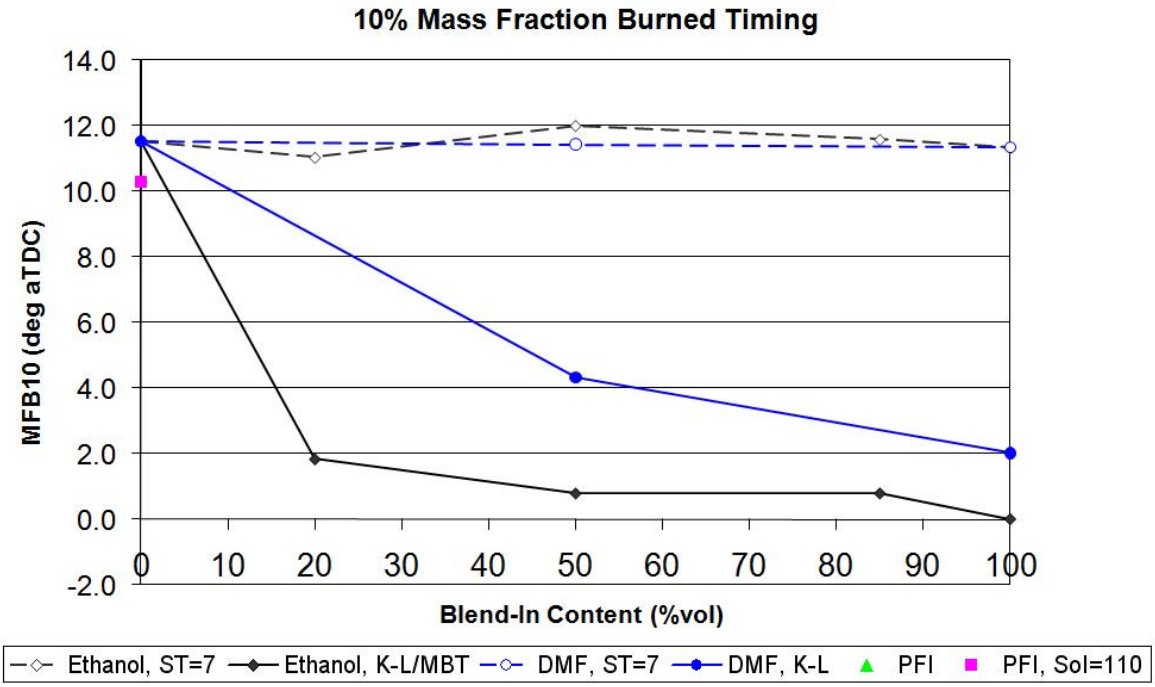

Figure 6.5 Full load SI, 10% mass fraction burned

Combustion duration is presented as 10-90% mass fraction burned in Figure 6.6. It can be seen that for the retarded spark timing as the ethanol content is increased the combustion duration is reduced. There are two mechanisms that contribute to this reduction; the first is increased laminar flame speed and the second mechanism is as the combustion is advanced more occurs in a smaller volume and hence increasing the temperature that further promotes combustion. The DMF blends also show a reduction in combustion duration as the blend ratio is increased. This reduction is also likely to be caused by an increased laminar flame velocity and advanced combustion phasing. When the spark timing is advanced there is a considerable reduction in the combustion duration. The main reason for this is because more of the combustion is occurring in a smaller volume leading to increased temperatures that in turn promote combustion.

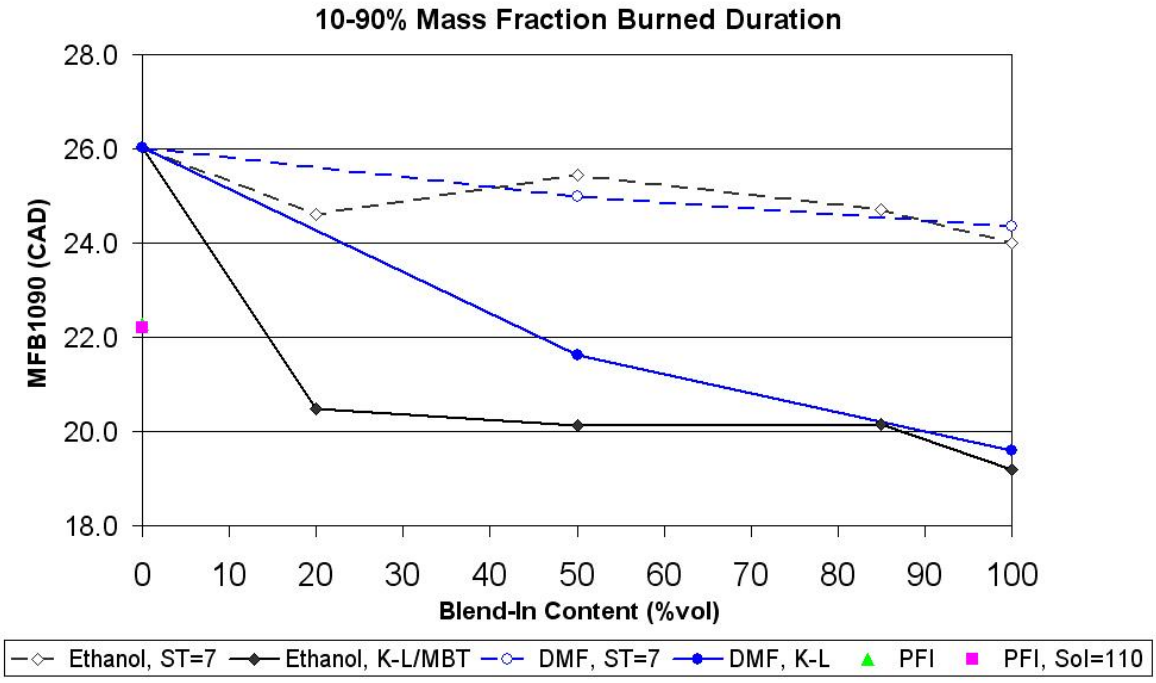

Figure 6.6 Full load SI, Combustion duration

Combustion stability presented as the coefficient of variation of indicated mean effective pressure is shown in Figure 6.7. For the retarded spark timings the addition of ethanol has no significant effect on combustion stability, but for the DMF blends the reduction in combustion duration has led to a slight increase in combustion stability. For the advanced spark timings the increase in combustion speed leads to improved combustion stability of both the ethanol and DMF blends. PFI injection shows significantly better combustion stability than DI injection and this is because with PFI injection the fuel is inducted along with the fresh air that forms the in-cylinder flow structure and therefore ensures good mixing, whereas with DI injection the fuel is injected into the in-cylinder flow structure and therefore the mixing is dependent on this structure which can be affected by the events of the previous cycle, hence reducing combustion stability.

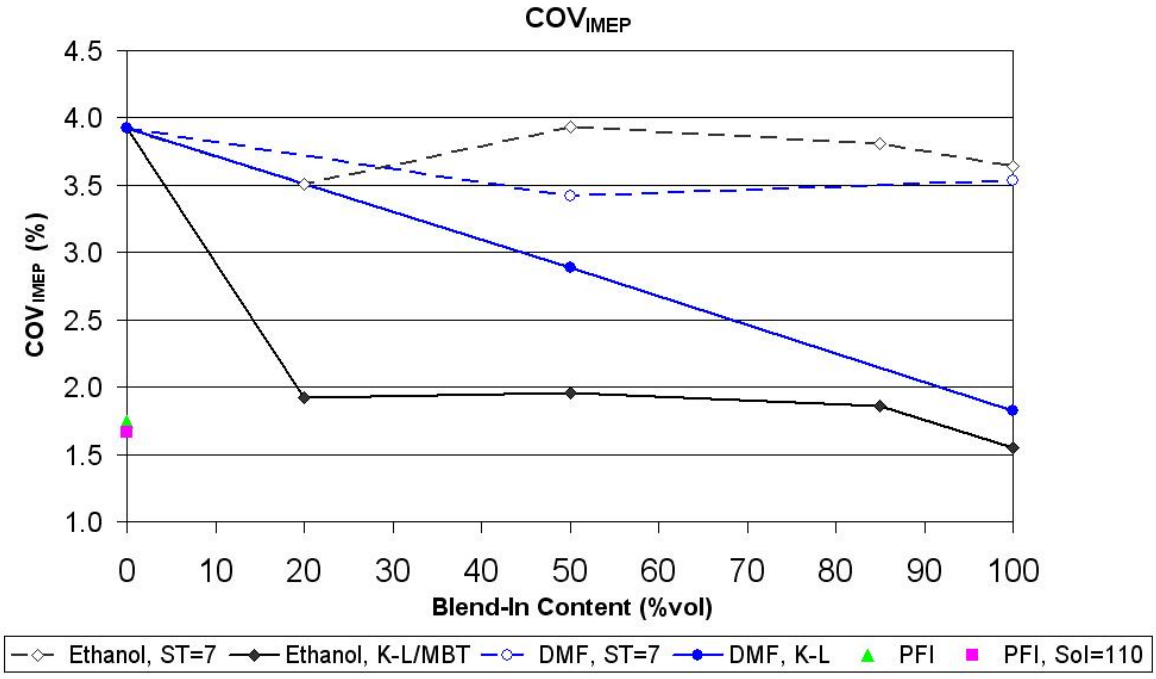

Figure 6.7 Full load SI, Combustion stability

Combustion efficiency (calculated from CO and HC in the exhaust stream, see Section 3.4.3.) is presented in Figure 6.8. It can be seen that the addition of ethanol generally improves the combustion efficiency. The retarded spark timing leads to a noticeable and significant increase in efficiency of approximately one percentage point and is caused by a reduced amount of partial combustion products being forced into the crevice volumes resulting from reduced lower in-cylinder pressures associated with retarded combustion. When retarded spark timings are used the addition of DMF to gasoline shows a significant improvement in combustion efficiency with pure DMF giving approximately one percentage point increase compared to standard gasoline. This is a result of DMF being oxygenated. However as the spark timing is advanced there is a slight reduction in combustion efficiency with DMF addition because of the higher in-cylinder pressures forcing more partial combustion products into the crevice volumes. For

standard gasoline direct injection shows a noticeable reduction (2-3 percentage points) in combustion efficiency that is caused by less than optimal mixture distribution. This is reinforced when the two different PFI strategies are compared, the closed valve injection case (SoI=110° $bTDC_{COMB}$) that provides the maximum time for evaporation but results in fuel impingement on the induction tract walls and intake valves resulting in a less homogeneous mixture has a reduced combustion efficiency. Once again caution has to be applied to the calculated combustion efficiency data because of the uncertainties in the hydrocarbon measurements (see Chapter 5, Section 5.2.2 for further discussion on this).

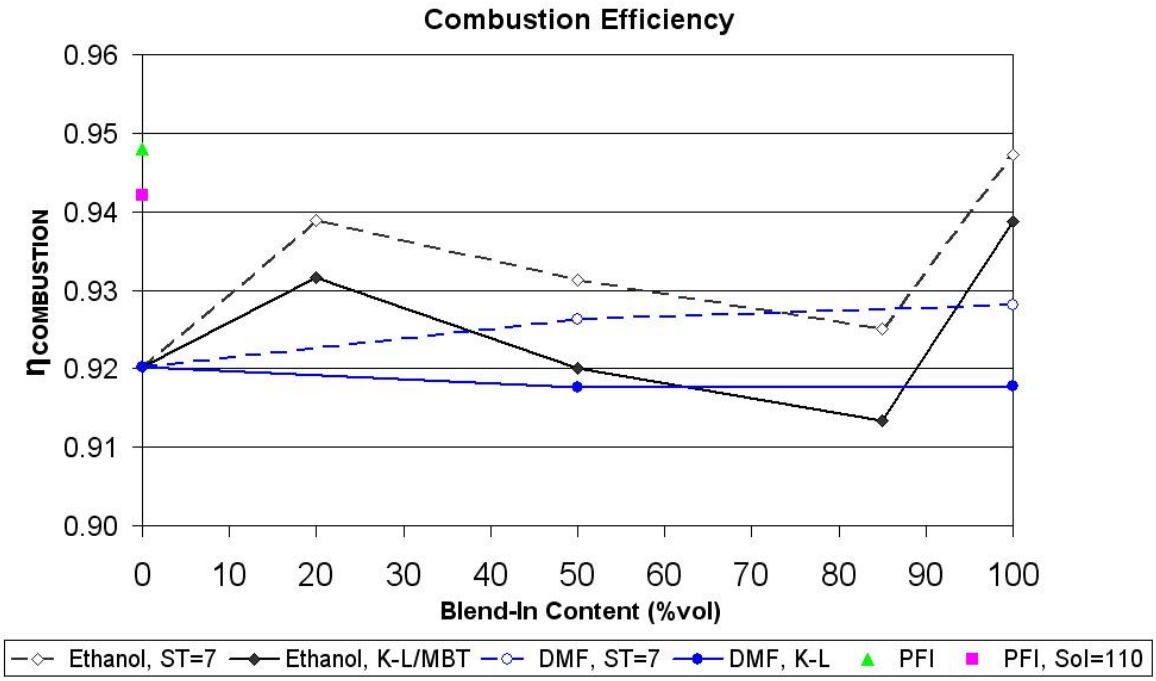

Figure 6.8 Full load SI, Combustion efficiency

Exhaust temperature can give an indication of flame temperature and has a bearing on CO and HC emissions due to post combustion oxidation of unburned fuel and combustion residuals. It can be seen in Figure 6.9 for the retarded spark timings as the ethanol content is increased the

exhaust temperature generally decreases. This is a combination of ethanol having a lower adiabatic flame temperature [Nabi et al (2002)] and the (slightly) advanced and faster combustion giving rise to more time between the end of combustion and exhaust valve opening leading to more cooling of the cylinder contents and hence a lower exhaust temperature. The change in the end of combustion timing accounts for the local minimum observed for E20. For the advanced spark timings a similar trend is also found and for the same reasons as above, with the significant difference in magnitude being caused by the 8-10 CAD difference in the advanced and retarded spark timings. For the DMF blends the retarded spark timing shows an increase in exhaust temperature as the blend ratio is increased. This is despite a slight advance in combustion timing and faster combustion that would suggest a reduction in exhaust temperature and thus indicating a higher flame temperature for DMF. This is in disagreement with the theoretical study by Nabi et al (2002), but does agree with the findings of the part load study (Chapter 5, Section 5.4). For the advanced spark timings there is a general reduction in exhaust temperature and this is caused by the combustion being advanced (due to advancing spark timing) as the blend ratio increases. Likewise the difference in temperature for the retarded and advanced cases is caused by the difference in time between end of combustion and exhaust valve opening.

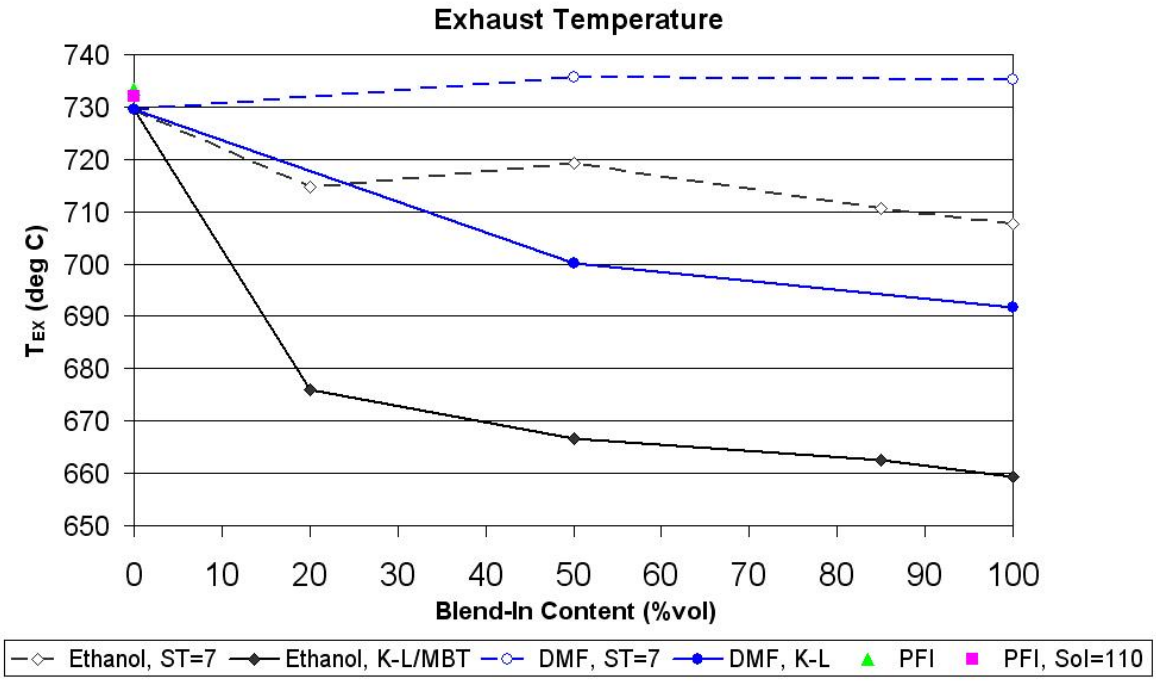

Figure 6.9 Full load SI, Exhaust temperature

Emissions

The emissions of oxides of nitrogen (NO_X) are presented in Figure 6.10 below. It can be seen that for the ethanol blends when the retarded spark timing is used there is a general reduction in NO_X emissions because of the reduced combustion temperature of ethanol. A similar trend is observed when advanced spark timings are used. The increase in magnitude is caused by the advanced combustion increasing the in-cylinder temperature and hence increasing NO_X production. The slight increase seen for pure ethanol with both ignition timings is caused by the slight advance in start of combustion seen with pure ethanol compared to E85. The DMF blends using retarded spark timings show a significant increase in NO_X emissions as the blend ratio is increased. This is partially caused by the slight advance in combustion seen with the addition of

DMF, but this advance is small and not likely to cause such an increase in NO_X production. This increase in NO_X emissions is evidence of DMF having a higher flame temperature than gasoline. When advanced spark timings are used with DMF the increase in NO_X emissions is a combination of advancing combustion raising in-cylinder temperature and an increase in flame temperature.

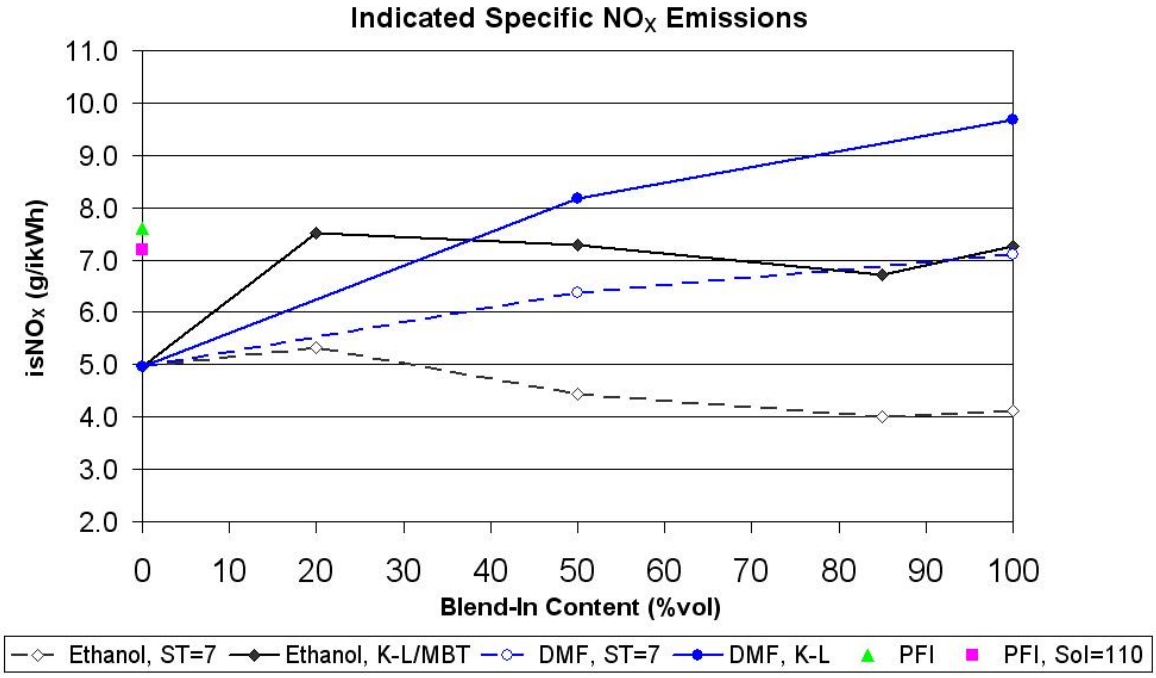

Figure 6.10 Full load SI, Indicated specific NO_X emissions

The hydrocarbon emissions are shown in Figure 6.11. It can be seen for the ethanol blends (both advanced and retarded spark timings) that there is a general reduction in hydrocarbon emissions as the ethanol content is increased. This could be an indication of more complete evaporation and better mixing, but is most likely caused by an FID's reduced sensitivity towards oxygenated hydrocarbons (Chapter 5, Section 5.2.2). The retarded spark timings show a reduction compared to the advanced spark timings and this is attributed to less unburned fuel being forced in to the

crevice volumes coupled with increased exhaust temperatures. It can be seen for the DMF blends as the blend ratio is increased for both spark timings the hydrocarbon emissions increase. This increase is a result of the incomplete combustion of the ring structure and this can also be seen when the particulate emissions (Chapter 7) are studied. The difference between the advanced and retarded spark timings is again caused by less unburned fuel being forced in to the crevice volumes coupled with increased exhaust temperatures increasing post combustion oxidation of the remaining cylinder contents.

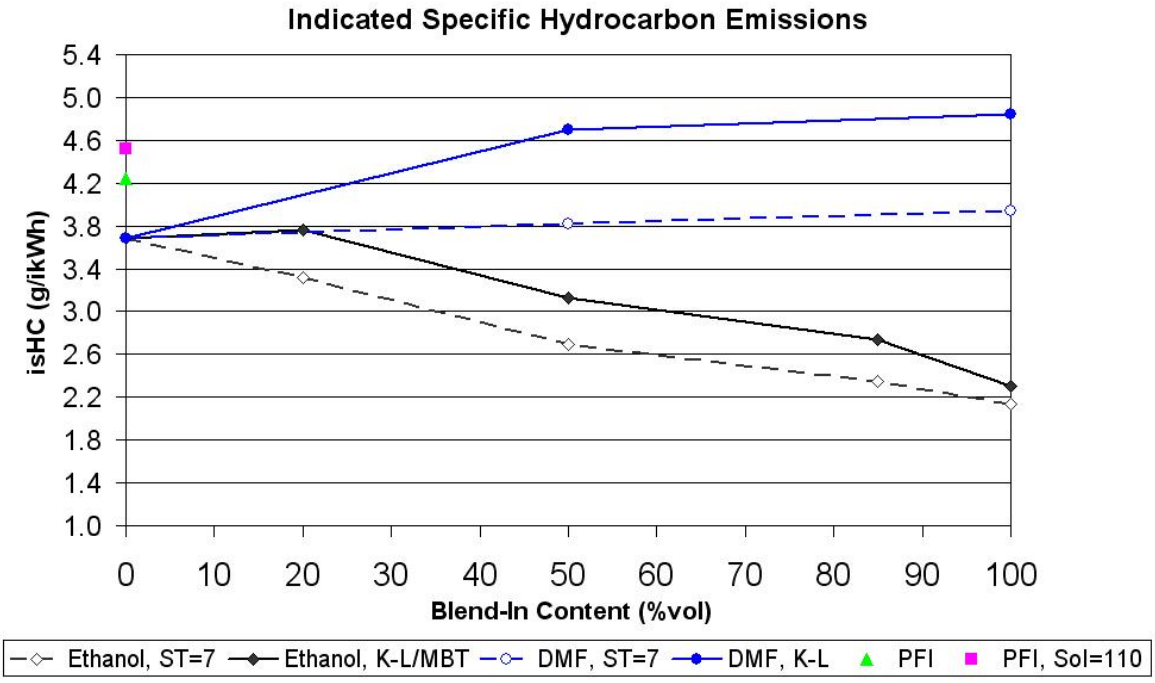

Figure 6.11 Full load SI, Indicated specific hydrocarbon emissions

Carbon monoxide emissions are presented in Figure 6.12. It can be seen that the addition of ethanol generally causes a reduction in CO emissions, with this reduction being attributed to the increased availability of oxygen (ethanol is an oxygenated molecule). The difference between the advanced and retarded spark timings is caused by the longer mixing time caused by the

retarded spark timing. For the DMF blends there is very little change in the CO emissions for all blend ratios, this is despite the increase in hydrocarbon emissions (Figure 6.11). This suggests that the post combustion oxidation of the remaining hydrocarbons in the cylinder is minimal but the oxidation of carbon monoxide to carbon dioxide is more significant. The difference between the advanced and retarded spark timings for both the ethanol and DMF blends is again caused by the differences in in-cylinder pressure and exhaust temperature as discussed above for the hydrocarbon emissions. Direct injection shows approximately a two times increase in CO emissions compared to Port injection. This is because of the inferior mixing and increased wall wetting that result from injecting the fuel directly into the cylinder and is one of the major problems with Direct injection.

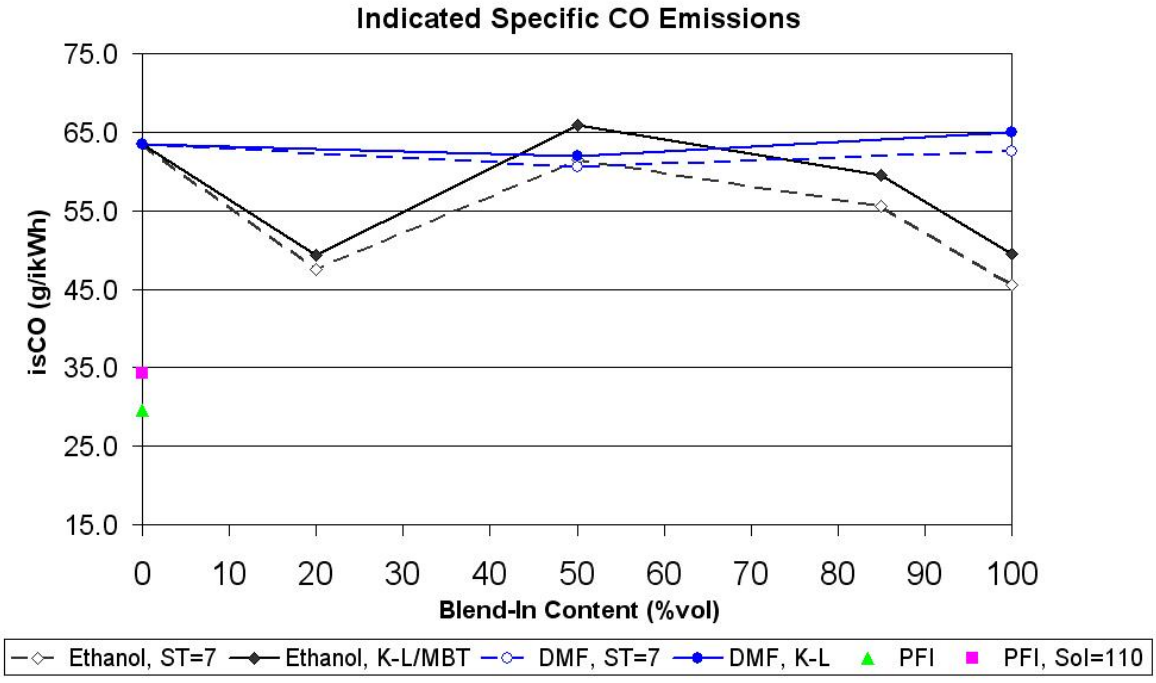

Figure 6.12 Full load SI, Indicated specific carbon monoxide emissions

6.1.4 Efficiency

Indicated efficiency is presented in Figure 6.13 in place of indicated specific fuel consumption due the different calorific values of the fuel blends used. It can be seen that as the ethanol blend ratio is increased for advanced spark timings indicated efficiency generally increases, with the increase being significant. One reason for this increase is for E50 and higher blends MBT spark timing can be achieved and hence increase efficiency. The trend for the retarded spark timings is similar except reduced in magnitude (2 percentage points), with this reduction being caused by the retarded spark timings giving rise to non-optimal combustion phasing. The DMF blends using the advanced spark timings show an increase in efficiency despite a reduction in combustion efficiency. This increase is because the advanced spark timings result in more optimal combustion phasing. The DMF blends (with advanced spark timings) have a lower efficiency than the ethanol blends because the spark timings are knock-limited whereas for the ethanol blends of 50% and greater are MBT timings. The noticeable increase seen for the PFI injection of standard gasoline compared to DI injection is caused by the increased combustion performance associated with PFI injection.

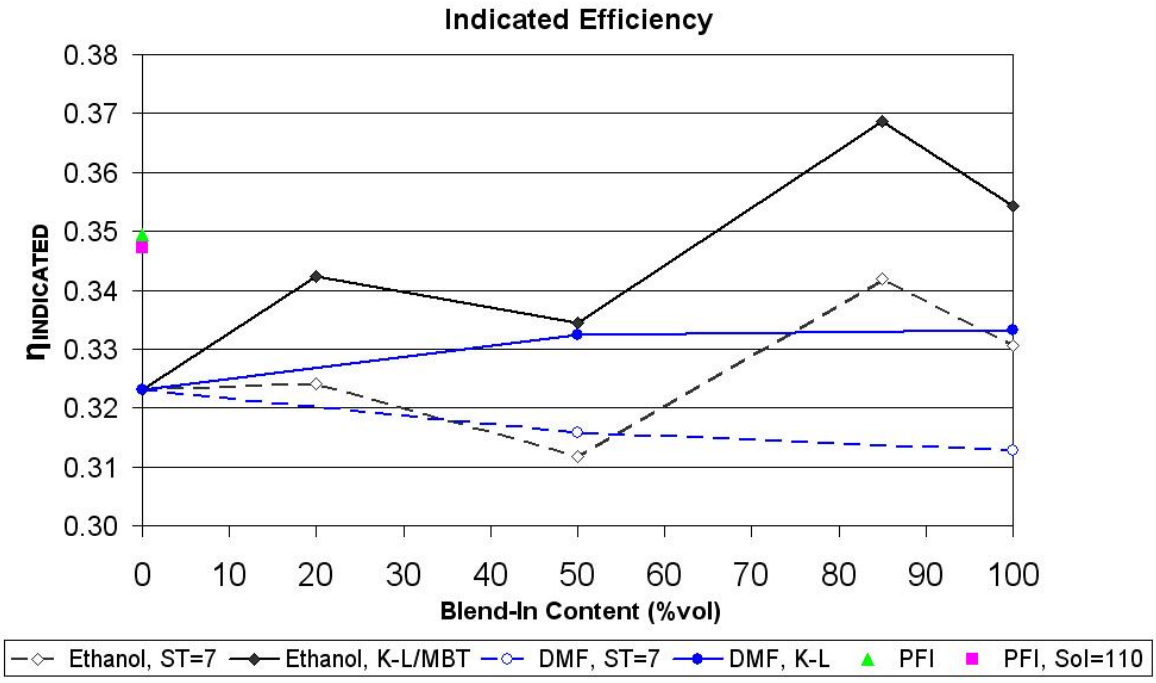

Figure 6.13 Full load SI, Indicated efficiency

6.2 Effect of Split Injection on Bio-Ethanol/Gasoline Blends

For this study a split injection strategy is compared to the standard single injection strategy (SoI=280° $bTDC_{COMB}$). A split injection strategy is chosen to reduce the penetration length of the injected fuel spray plume. This is to reduce the amount of fuel impinged on the piston crown and the cylinder walls, which leads to increased hydrocarbon, carbon monoxide and particulate matter emissions.

The engine set-up and operation is identical to that in Section 6.1 (Table 6.1) including using MBT spark timings. The start of injection timings for the two parts of the split strategy are 280° $bTDC_{COMB}$ and 240° $bTDC_{COMB}$ respectively. These timings are chosen so all of the fuel is

injected while the intake valve is open, but separated sufficiently so the two injections do not overlap (with respect to injector openings). The pulse widths of the two injections are equal in an attempt to produce equal penetration lengths and hence minimise penetration and fuel impingement.

6.2.1 Load

With the engine being operated at a WOT condition the different fuel blends and injection timing (causing changes in efficiency) combinations used lead to differing engine loads being produced. Engine load, presented here as indicated mean effective pressure (IMEP), is shown in Figure 6.14.

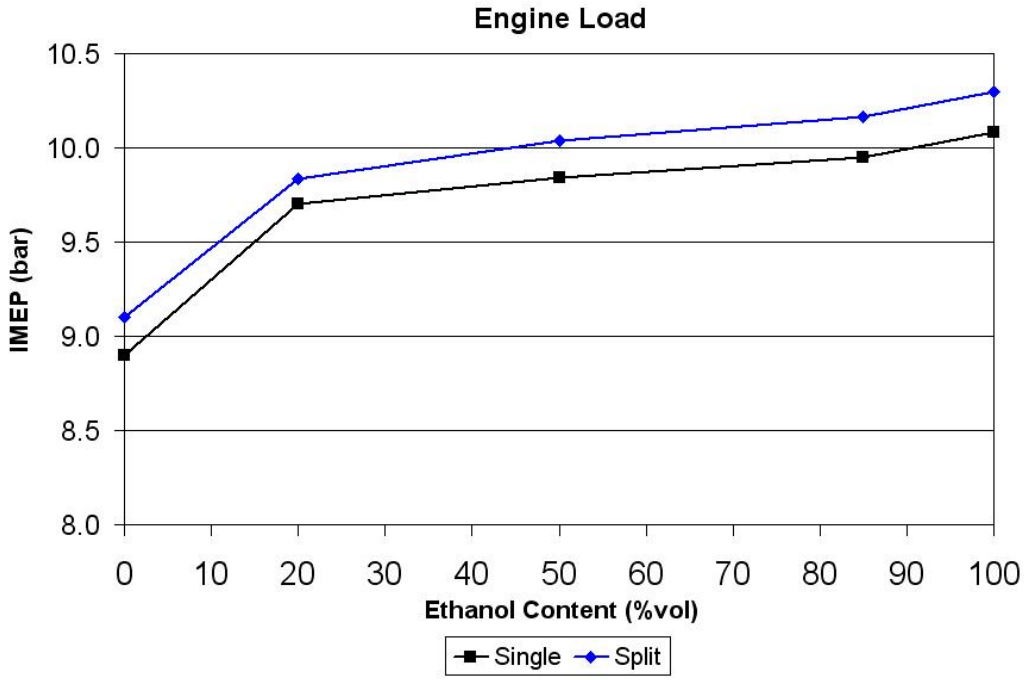

Figure 6.14 Full load split injection SI, Engine load

It can be seen that there is an almost constant 0.2 bar increase in IMEP for the split injection strategy compared to the standard injection. This is attributed to an increase in combustion performance and stability (Section 6.2.2). This increase in load is despite a reduction in volumetric efficiency (Figure 6.15) for the split injection case. This reduction in volumetric efficiency is caused by a shorter time (time between end of second injection and IVC) for charge cooling to lower the in-cylinder pressure and hence for more fresh air to be inducted into the cylinder.

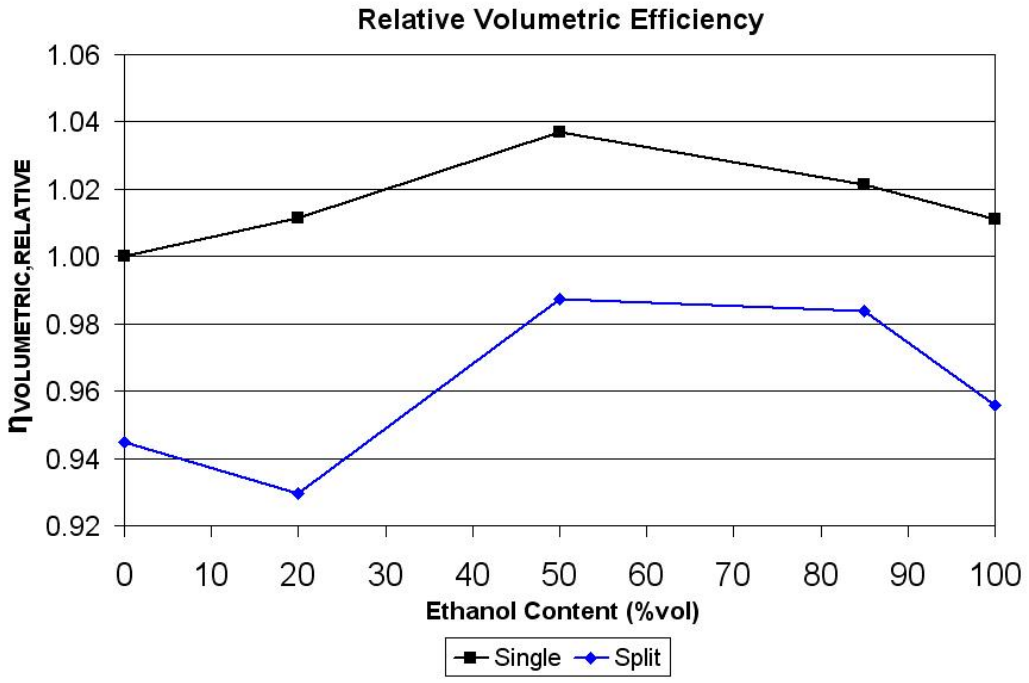

Figure 6.15 Full load split injection SI, Relative volumetric efficiency

6.2.2 Combustion Performance

Ignition delay is presented in Figure 6.16. It can be seen that split injection reduces the ignition delay by a significant amount (~1 – 2 CAD) compared to the standard single injection. For the split injection as the ethanol content is increased up to 50% the ignition delay reduces, but for further ethanol addition the ignition delay increases. The reduction up to 50% is caused by the increase in laminar flame velocity of ethanol. The reduction for greater than 50% ethanol content is caused by a lowering of the in-cylinder temperature caused by the increase in enthalpy of vaporisation (from the addition of ethanol) and that the split injection strategy results in more fuel evaporating after the intake valve has closed (due to the reduced time between the end of injection and intake valve closing) hence lowering the temperature.

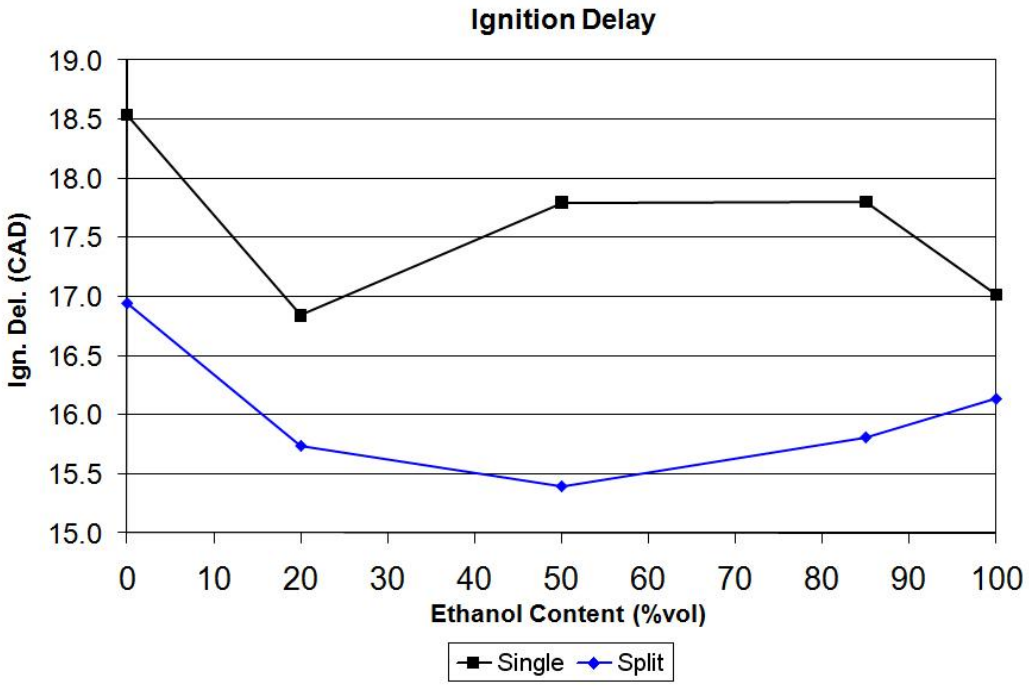

Figure 6.16 Full load split injection SI, Ignition delay

The advancement of the start of combustion (10% MFB) caused by the reduction in ignition delay can be seen in Figure 6.17.

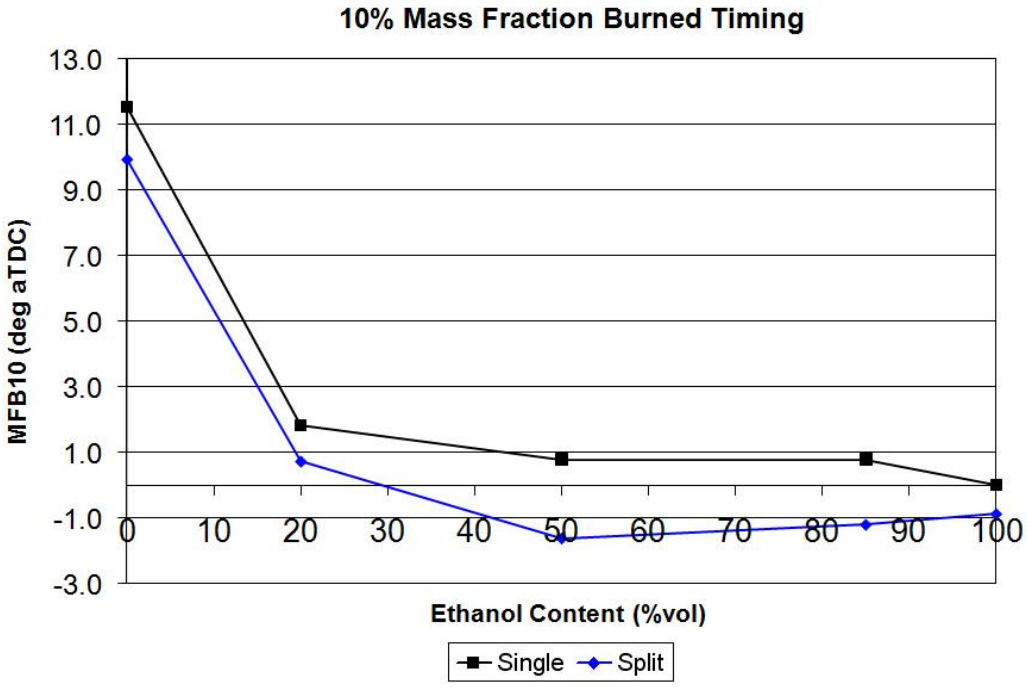

Figure 6.17 Full load split injection SI, 10% mass fraction burned

Split injection leads to faster combustion (presented as 10-90% MFB, Figure 6.18), which is caused by a combination of two effects. The first cause is that the advanced combustion causes more energy to be released when the cylinder is at or near the minimum volume (TDC) which results in a higher in-cylinder temperature, hence promoting combustion. Also the better mixing offered by the split injection (less wall wetting and impingement on the piston crown) results in a more uniform mixture that allows the flame front to travel across the cylinder faster, as lean and overly rich ($\lambda < 0.9$) mixtures have a lower laminar flame velocity [Hara et al (2006)].

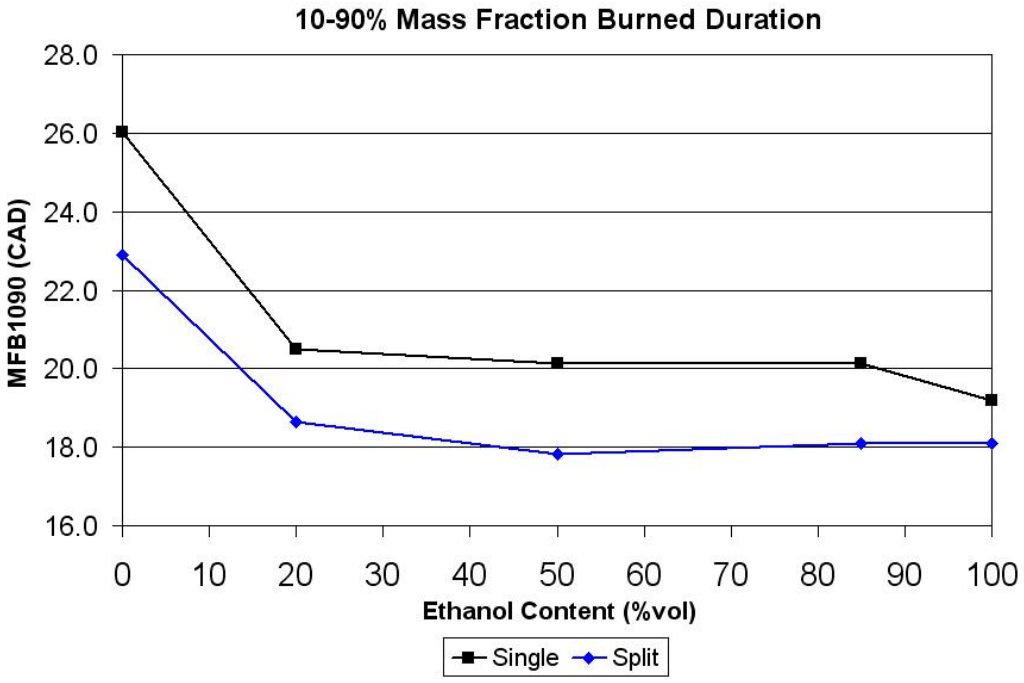

Figure 6.18 Full load split injection SI, Combustion duration

This reduction in combustion duration and increase in mixture uniformity leads to a significant improvement in combustion stability (COV_{IMEP}, Figure 6.19). The split injection provides approximately a factor of two improvement in the coefficient of variation of IMEP for all fuel blends.

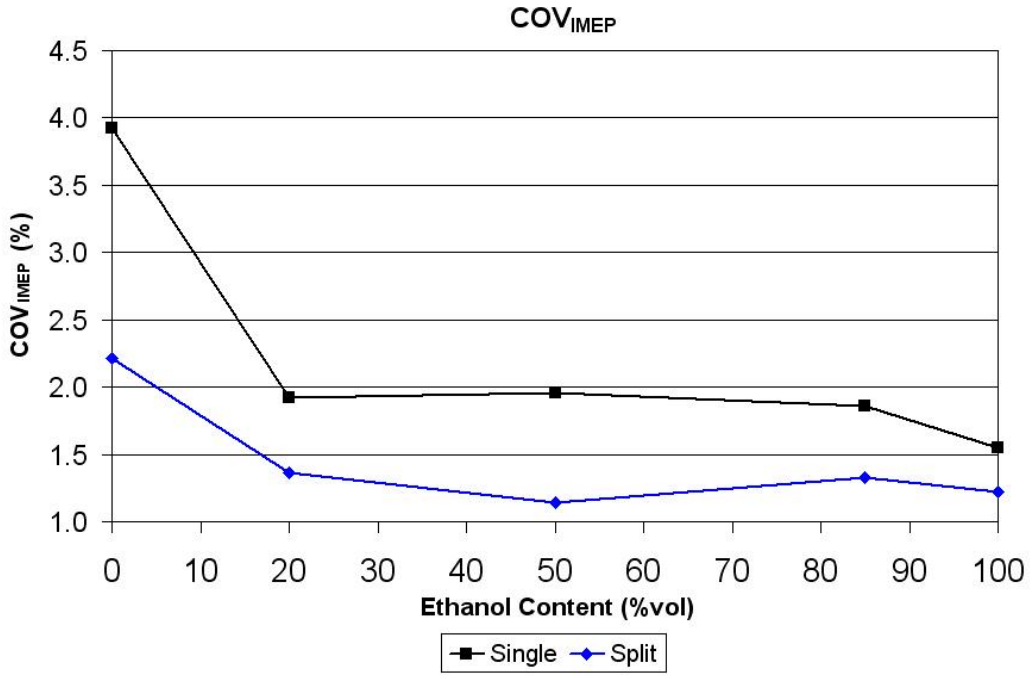

Figure 6.19 Full load split injection SI, Combustion stability

Combustion efficiency is significantly improved by the split injection strategy (Figure 6.20). The cause for this is the reduction in wall wetting and fuel impingement on the piston crown. With a single injection the penetration length of the spray plume is comparable to the stroke of the engine [Price et al (2006)] and hence fuel impingement is likely, especially for the longer injection durations required for increasing ethanol content. It is intended that with the split injection strategy having shorter individual injection pulse widths the cylinder penetration is decreased, reducing and/or eliminating wall wetting and fuel impingement on the piston crown.

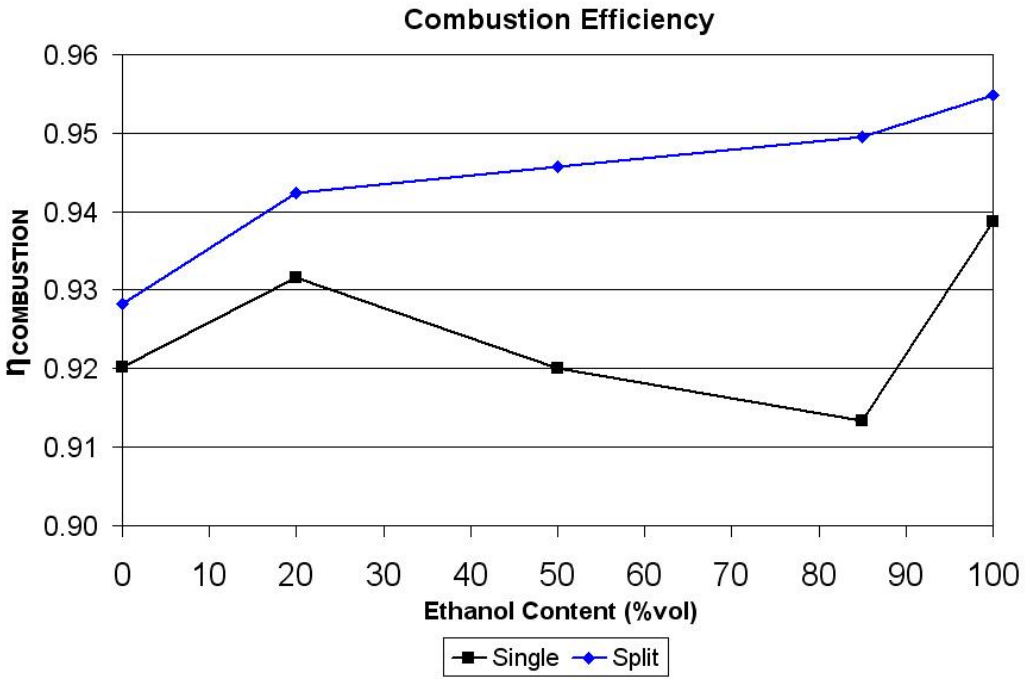

Figure 6.20 Full load split injection SI, Combustion efficiency

The advanced and faster combustion realised by the split injection strategy leads to an increase in peak in-cylinder temperature, this is inferred from the peak in-cylinder pressure presented in Figure 6.21.

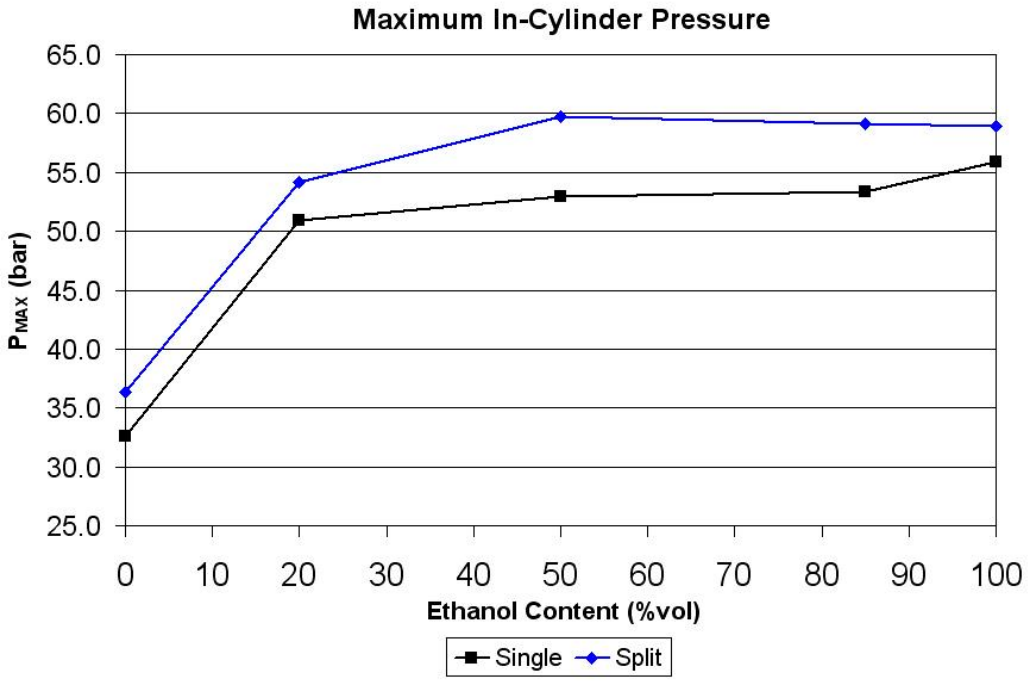

Figure 6.21 Full load split injection SI, Peak in-cylinder pressure

6.2.3 Emissions

The NO_X emissions are presented in Figure 6.22. It can be seen that there is a slight reduction in specific NO_X emissions, but this is caused by the increase in engine load masking an actual increase in NO_X on a by volume basis. This increase is caused by the advanced and more efficient combustion giving rise to an increase in temperature.

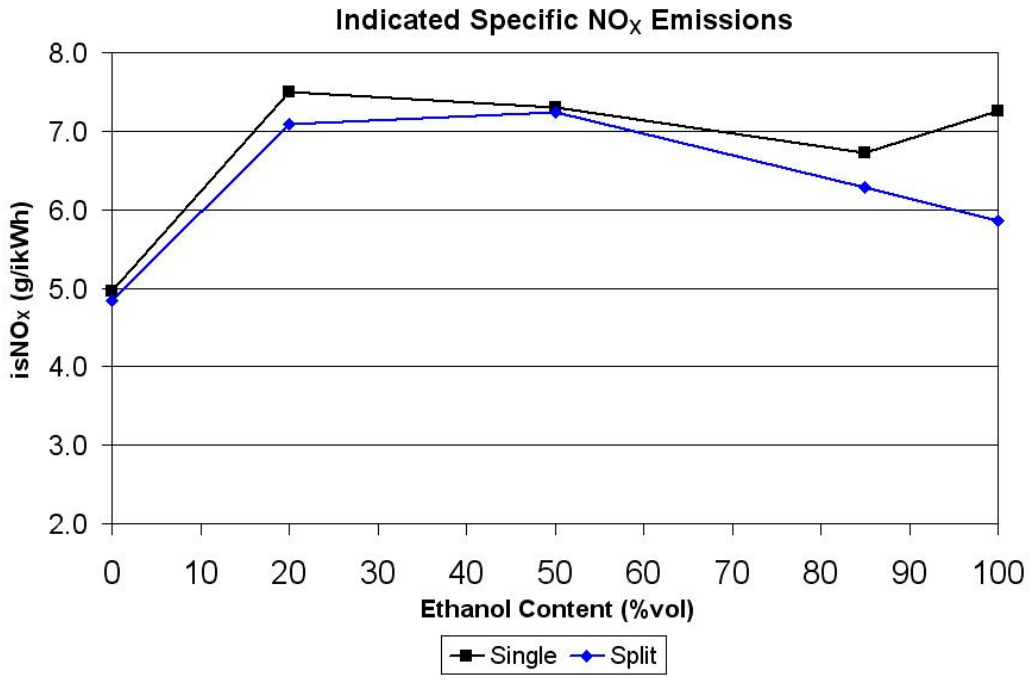

Figure 6.22 Full load split injection SI, Indicated specific NO_X emissions

The improved mixing and reduced fuel impingement resulting from the split injection results in lower hydrocarbon emissions for E20 and higher blends as seen in Figure 6.23. This reduction is real and is observed when the emissions are measured on a volume basis. Standard gasoline shows similar hydrocarbon levels for both injection strategies, with the reduction (for split injection) increasing in magnitude as the ethanol content increases. With the increase in ethanol content the injection duration increases (to account for reduced $AFR_{Stoich.}$) and therefore also the possibility of increased wall wetting and piston impingement, for which the split injection would show a greater advantage.

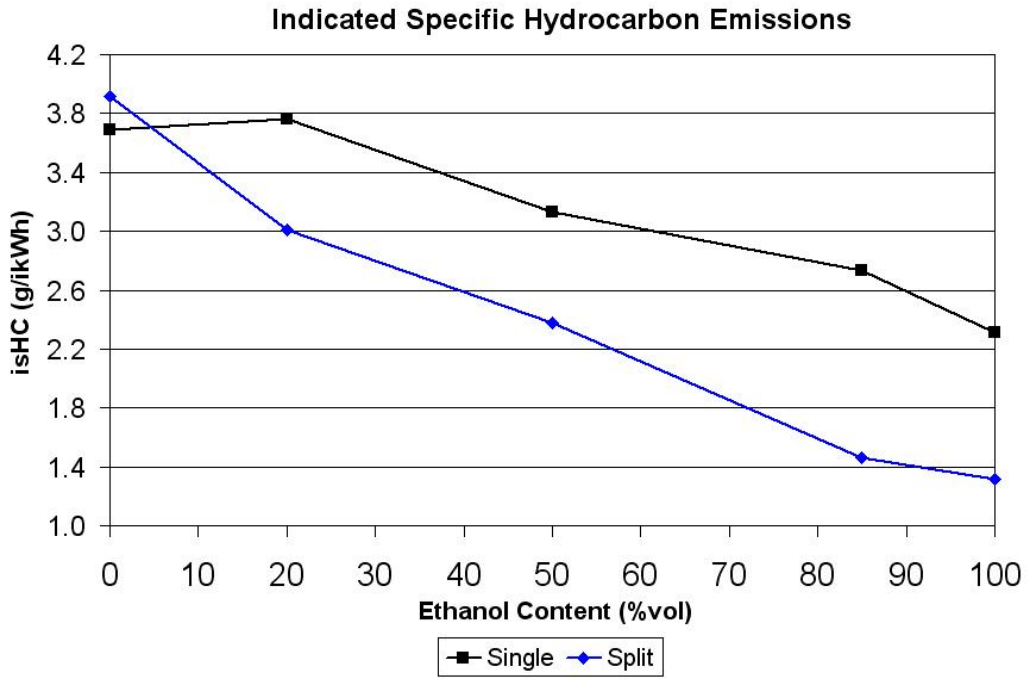

Figure 6.23 Full load split injection SI, Indicated specific hydrocarbon emissions

The split injection strategy provides a considerable reduction in specific carbon monoxide emissions compared to the standard single injection as seen in Figure 6.24. With two injections a greater proportion of the fuel droplets in the cylinder are of a smaller diameter. This is because the droplets around the edge of the spray pattern are of a smaller diameter than those in the main body of the spray. These smaller droplets evaporate more easily and reduce the number of rich spots that produce increased levels of CO emissions.

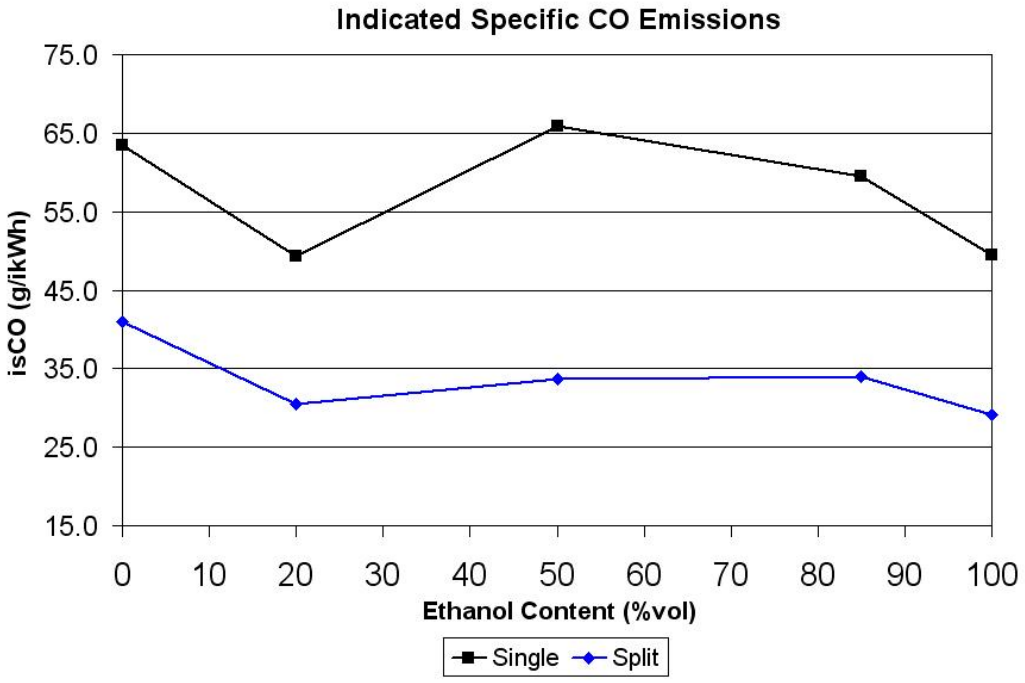

Figure 6.24 Full load split injection SI, Indicated specific carbon monoxide emissions

6.2.4 Efficiency

Indicated efficiency is presented in Figure 6.25. The split injection strategy provides a considerable increase in efficiency of approximately 3 percentage points. This increase is caused by the improvement in combustion efficiency and stability (COV_{IMEP}, Figure 6.19) which is brought about by the reduced fuel impingement/wall wetting offered by the split injection.

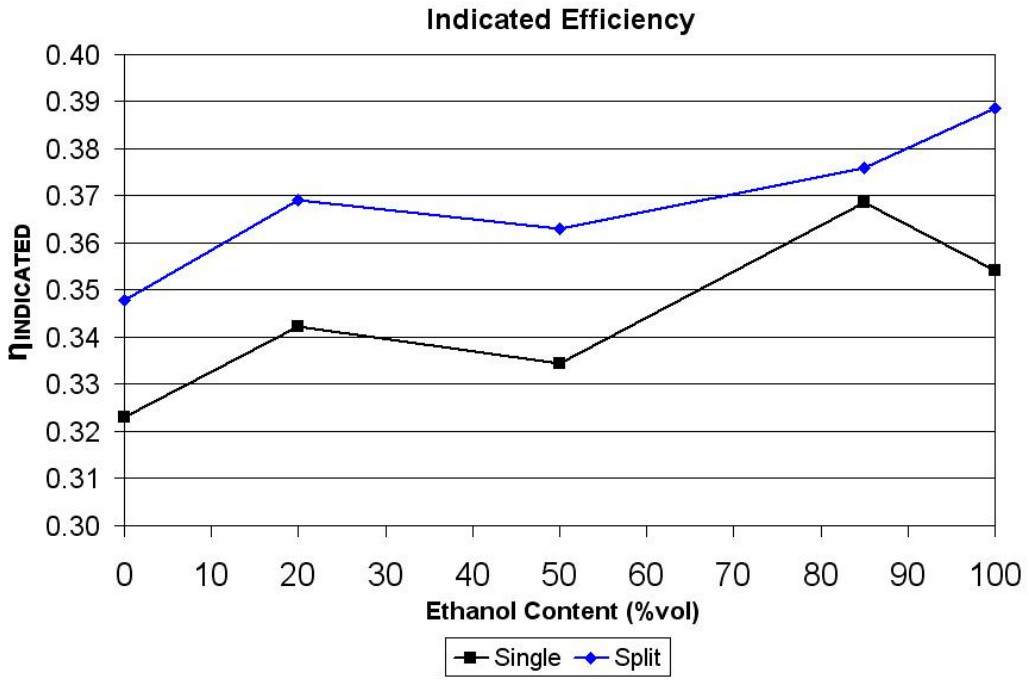

Figure 6.25 Full load split injection SI, Indicated efficiency

6.3 Summary

In this study the addition of both ethanol and DMF shows a reduction in ignition delay and faster combustion. Both fuels show an increase in volumetric efficiency due to charge cooling effects, though ethanol addition generally shows a greater increase than DMF addition due to the more than three times increase in heat of vaporisation for a stoichiometric mixture for ethanol compared to DMF. Most significantly the addition of ethanol and DMF allows the spark timing to be advanced; ethanol blends greater than 20% ethanol can achieve MBT spark timings whilst all of the DMF blends are knock-limited. This advance in spark timings leads to increased load, more stable combustion and increased engine indicated efficiency. At a constant spark timing the addition of ethanol shows a reduction in NO_X emissions due to a lower flame temperature.

However the addition of DMF causes the NO_X emissions to increase and this is thought to be caused by an increase in flame temperature (seen as an increase in exhaust temperature).

When a split injection strategy is employed combustion stability is significantly improved caused by a reduced ignition delay and faster combustion resulting from improved mixing of fuel and inducted air. This improved mixing reduces hydrocarbon and carbon monoxide emissions improving combustion efficiency and overall engine indicated efficiency. The engine load is also increased despite a reduction in volumetric efficiency. The peak in-cylinder temperature is increased with the split injection strategy, resulting in increased NO_X emissions measured on a volumetric basis, but the increase in engine load means the specific (indicated) NO_X emissions are actually reduced.

Likewise the trends in the hydrocarbon emissions with respect to ethanol and to a lesser extent DMF addition need to be considered in conjunction with reduced sensitivity of an FID to detect oxygenated hydrocarbons. The observed reduction in hydrocarbon emissions with increasing ethanol content are most likely to be caused the reduced sensitivity of the FID rather than the improved combustion performance of the fuel blends.

CHAPTER 7

7 The Effect of Bio-Fuels on Direct Injection Spark Ignition (DISI) Particulate Matter Emissions

In this chapter the Particulate Matter (PM) emissions of bio-ethanol/gasoline and 2,5 di-methylfuran/gasoline blends are investigated at two different engine loads, part load (3.4bar IMEP) and full load (wide open throttle) both at 1500 RPM. A thermo-denuder is also used for the ethanol/gasoline blends to investigate the proportion of soluble organic fraction (SOF) and solid carbonaceous elements of the particulate matter emissions.

Particulate matter emissions from first-generation (wall-guided) direct injection spark ignition engines are noticeably higher than those from port injection engines [Hall and Dickens (1999) and Graskow et al (1999)], but with the implementation of second-generation (spray-guided) DI systems the PM emissions are closer to those of a PFI engine as shown by Price et al (2006). The particulate emissions from DISI engines are now a regulated emission. Euro V (2009 onwards) regulations only includes limits for particle mass, but Euro VI (2014 onwards) will also include limits on particulate number. Unlike Diesel engines a significant part of the PM emissions is made up of the soluble organic fraction (SOF) instead of solid carbon particles. Amann and Siegla (1981) report that the SOF contributes to 10-30% of the particulate mass for Diesel PM, while Price et al (2007b) shows that solid carbon accounts for less than 30% of the particulate mass. This increase in PM for DI systems is caused by reduced fuel mixing times (time between fuel injection and spark discharge) and cylinder wall wetting and fuel impinging

onto the piston crown due to the injection penetration lengths being comparable to the engine stroke [Price et al (2006)]. What's more when stratified combustion is used the temperature during the expansion stroke is low and this reduces the amount of post combustion oxidation of the remaining in-cylinder contents [Cole at al (1998)].

The PM emissions are measured with a scanning mobility particle sizer (SMPS) and are measured over the nominal diameter range of 10 – 500nm. For a detailed description of the SMPS operation and setup see Chapter 3, Section 3.2.2. However the work by Abdul-Khalek et al (1999) shows that the number count of particles of less than 50nm in diameter are heavily influenced by the dilution conditions, such as dilution ratio, temperature, relative humidity and residence time. Because the dilution ratio is the only parameter that is fully controlled in these tests the particle counts for particles of sub 50nm diameter have to be viewed with some caution. The SMPS data shown in the following sections is the average of two consecutive measurement runs.

7.1 Part Load Engine Operation

The part load engine condition is defined as 3.4bar IMEP at an engine speed of 1500 RPM. The engine set-up is the same as that for the part load investigations in Chapter 5 and is defined in Table 7.1 below. Three different spark timings are used to investigate the effect of mixing time (time between fuel injection and spark timing) on PM emissions. Three different splash blends of ethanol/gasoline are examined, the blends being 20, 50 and 85%$_{Vol.}$ bio-ethanol in gasoline as well as standard gasoline and pure bio-ethanol. These are designated as Ex, with ‘x’ representing

the percentage by volume of bio-ethanol in the ethanol/gasoline blend. Two different splash blends of 2,5 di-methylfuran/gasoline are examined, these blends are 20 and 50%$_{Vol.}$ 2,5 di-methylfuran in gasoline. These are designated as DMFx, with 'x' representing the percentage by volume of 2,5 di-methylfuran in the ethanol/gasoline blend. Stoichiometric mixtures are used for all tests. To help minimise the effects caused by the day-to-day variations in the atmospheric conditions all of the non-thermo-denuder tests (including DMF blends, Section 7.1.2) were conducted on one day and the entire tests using the thermo-denuder on the following day.

Table 7.1 Engine configuration for part load spark ignition operation

Engine Speed (RPM)	1500
IMEP (bar)	3.4
λ	1.0
IVO (° bTDC$_{GE}$)	16
EVC (° aTDC$_{GE}$)	36
SoI (° bTDC$_{COMB}$)	280
Spark Timing (° bTDC$_{COMB}$)	19, 29, 39

7.1.1 Investigation into the effects of Bio-Ethanol/Gasoline Blends

The particle size distributions for standard gasoline, the ethanol blends and pure ethanol are presented in Figures 7.1 – 7.5. The graph on the left is for total PM emissions and the graph on the right is for the solid carbonaceous particles only, which is obtained by passing the sample through a thermo-denuder before measuring with the SMPS. The figures contain particle distributions for the three spark timings shown in Table 7.1 to see the effects of mixing time on PM emitted. Please note only two spark timings are shown for standard gasoline because for the earliest spark timing (39° $bTDC_{COMB}$) audible knocking was encountered.

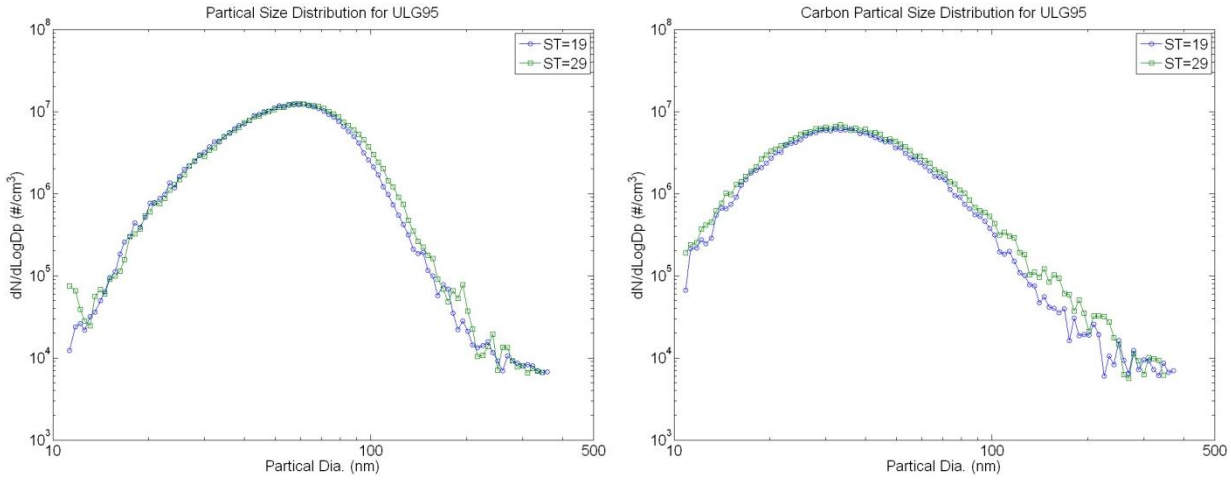

Figure 7.1 Part Load SI, Standard gasoline particle size distributions

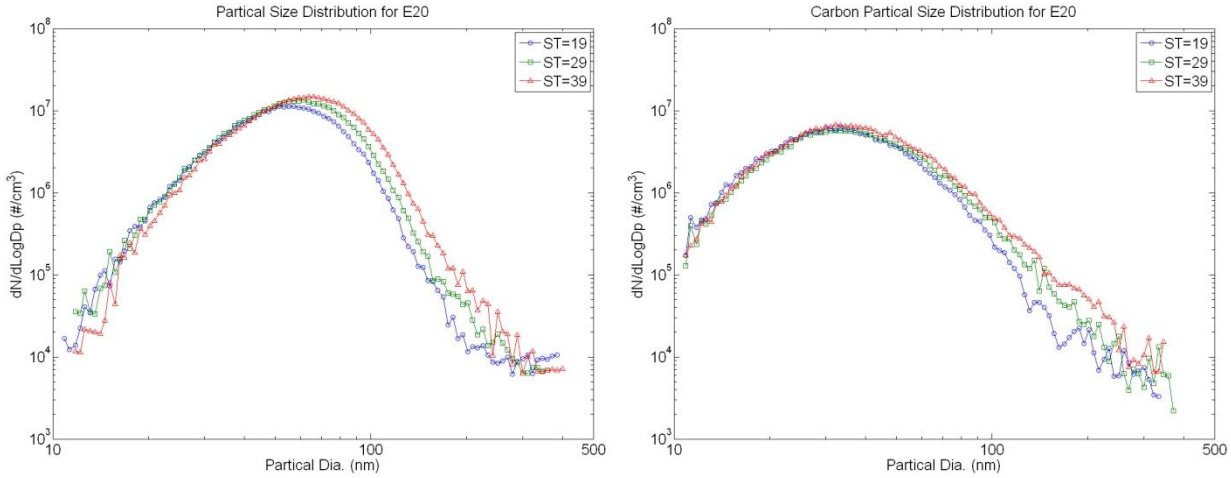

Figure 7.2 Part Load SI, E20 particle size distributions

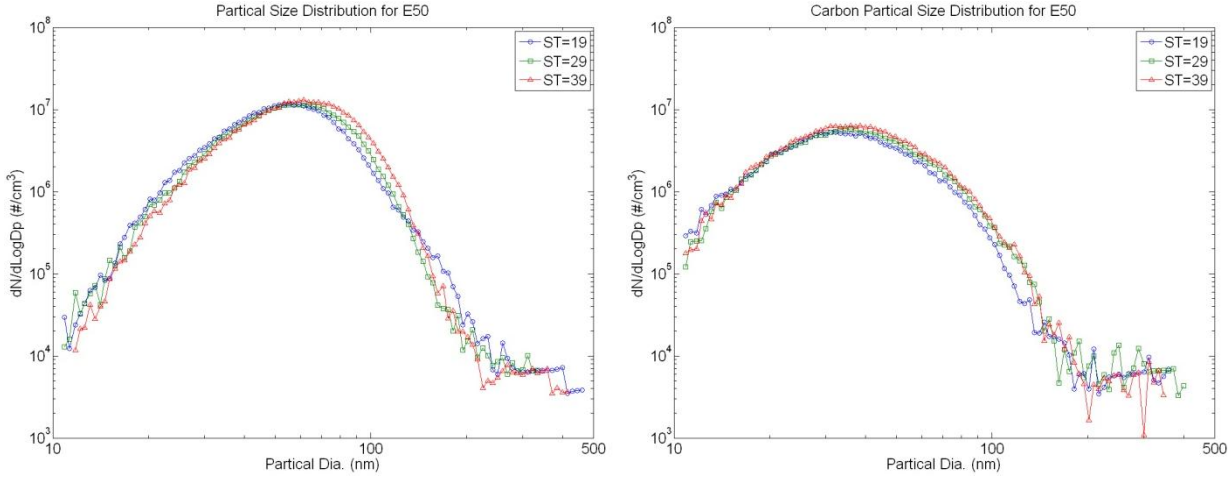

Figure 7.3 Part Load SI, E50 particle size distributions

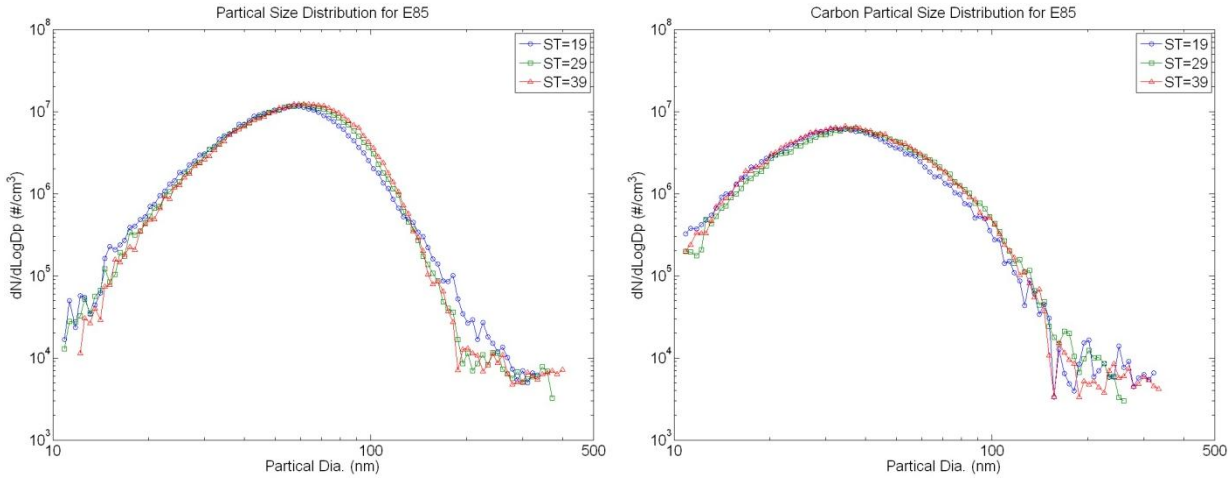

Figure 7.4 Part Load SI, E85 particle size distributions

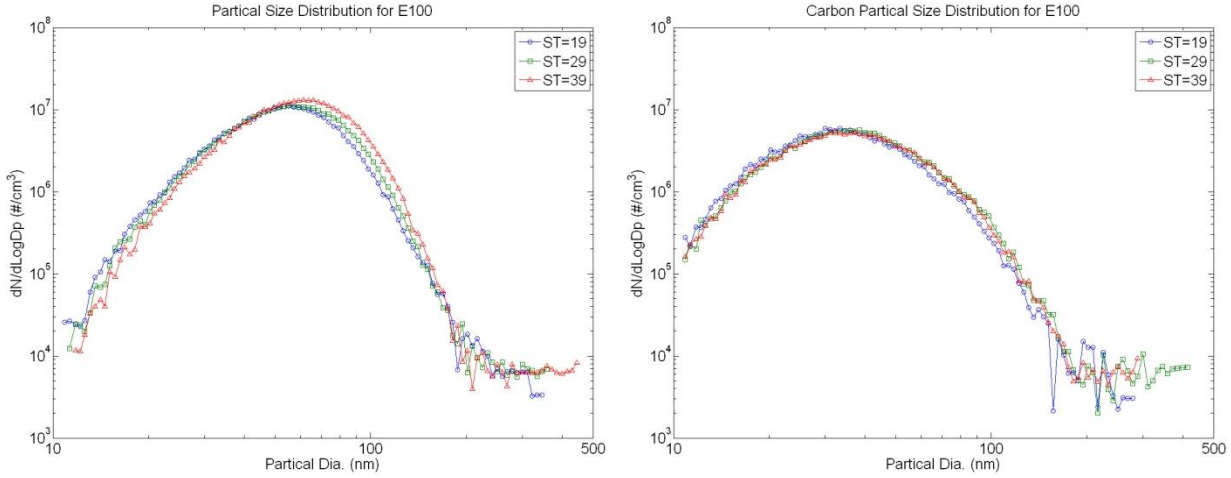

Figure 7.5 Part Load SI, Pure ethanol particle size distributions

It can be seen that the particle distributions are not bi-modal, which is what might be expected as Diesel particle distributions are often bi-modal in shape, but single mode distributions have been found by other authors for spark ignition particulate emissions [Maricq et al (1999) and Price et al (2006)]. It is generally the case that as the spark timing is advanced the accumulation mode (D_P>50nm) increases and this is caused by the combustion of a non-homogeneous mixture caused by the reduction in mixing time available (time between injection and spark discharge).

Ethanol blends of 50% $_{Vol.}$ ethanol and greater are an exception to this generalisation. It can be seen that there is an increase in number count for the larger particles (D_P>150nm) for the most retarded spark timing compared to the other two more advanced timings. This is because a spark timing of 19° $bTDC_{COMB}$ is some distance (CAD) from the MBT timing, and thus required an increased fuelling rate to maintain the same load. This coupled with the lowering of the stoichiometric air-to-fuel ratio (requiring yet another increase in the fuelling rate) is likely to lead to increased amounts of fuel impinging onto the piston crown which has been shown to increase particle size (D_P) and count [Warey et al (2002)]. A further general observation is that as the ethanol blend ratio increases the reduction in accumulation mode PM is accompanied by an increase in nucleation mode (D_P<50nm) PM. This can be attributed to the fact that as the accumulation mode decreases the surface area available for the adsorption of SOF reduces and hence the SOF self nucleates and causes an increase in nucleation mode PM as discussed by Price et al (2007a).

A comparison of the size distributions for all of the tested fuel blends at a spark timing of 29° $bTDC_{COMB}$ is shown in Figure 7.6. Again the left-hand graph shows total PM number count and the right-hand graph shows the number count for the solid carbon particles. Figure 7.7 shows the total number concentration (black lines/left ordinate) and total mass concentration (blue lines/right ordinate). Data for both the total PM (solid lines with circular data points) and solid carbon particles (dotted lines with triangular data points) are presented for the comparison of the proportions of soluble organic fraction and solid carbon particles for the fuel blends investigated.

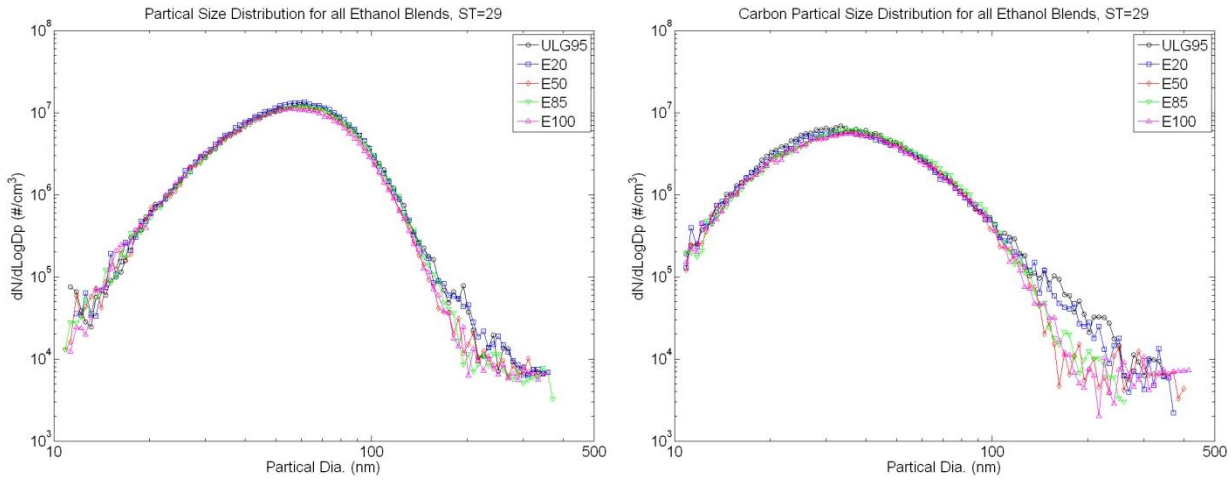

Figure 7.6 Part Load SI, Particle size distributions for all ethanol blends

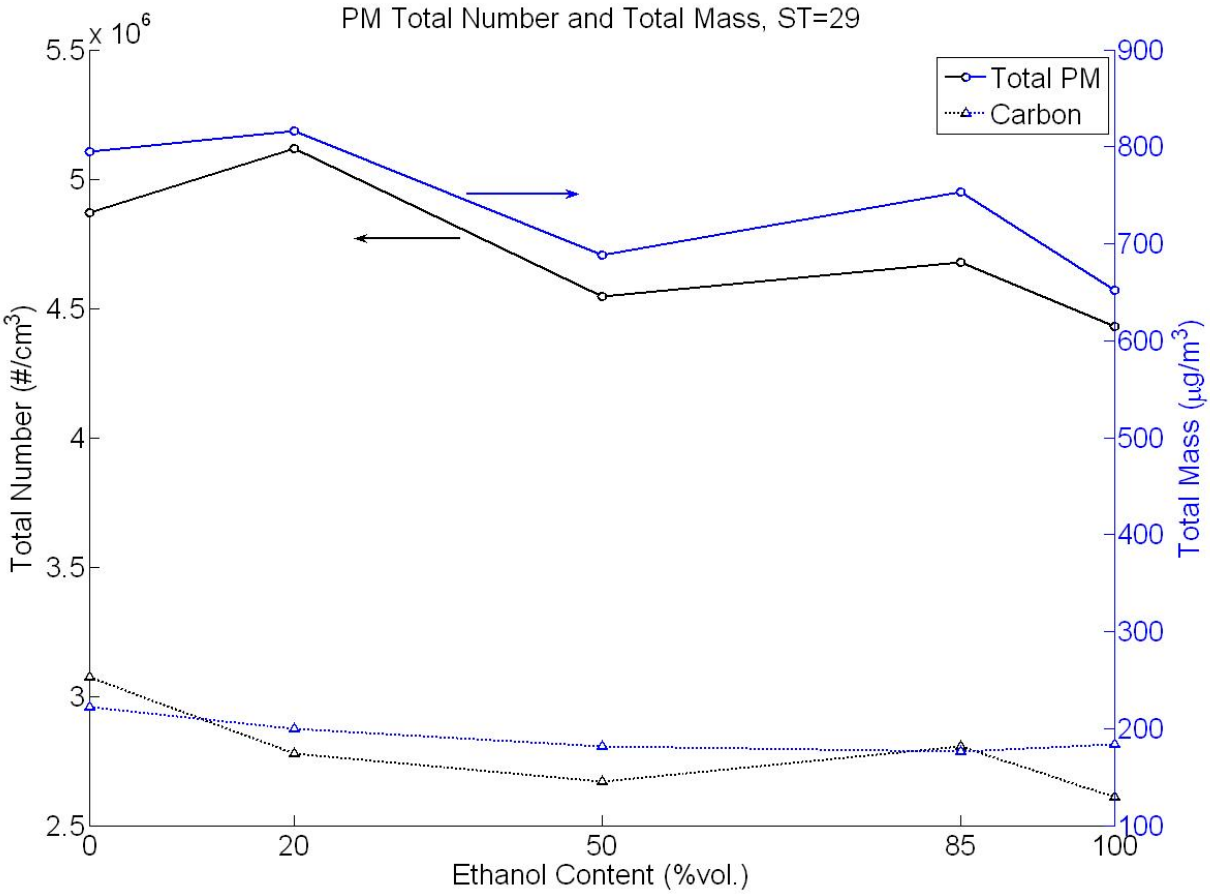

Figure 7.7 Part Load SI, Total number and mass for all ethanol blends

There is very little difference in particle size distributions for all of the fuel blends tested, however the addition of ethanol causes a reduction in the accumulation mode with a noticeable reduction in large particles (D_P of ~120-300 nm) for E50 and above. This difference is even greater when the size distribution for carbon particles is considered, suggesting that this increase is caused by carbon/soot rather than the adsorption of the SOF. This increase for standard gasoline and E20 is likely to be caused by the incomplete evaporation of the heavy fractions found in gasoline causing an increase in the occurrence of the combustion of fuel droplets. The addition of ethanol to gasoline causes a reduction in total number and total mass concentration for both total PM and carbon particles, with this suggesting increased evaporation, mixing and combustion performance.

It can be seen that for all of the fuel blends tested the use of the thermo-denuder results in a reduction in peak number count by around 50%, ~$6x10^6$ particles/cm^3 compared to ~10^7 particles/cm^3. The mean particle size (D_P) is also reduced to ~40 nm from ~59 nm. This reduction in peak number count and mean particle diameter is the reason for the reduction in total mass concentration seen in Figure 7.7 when comparing total PM to carbon particles.

7.1.2 Investigation into the effects of 2,5 Di-methylfuran/Gasoline Blends

The particle size distributions for DMF20 and DMF50 at the three spark timings investigated are presented in Figure 7.8. It can be seen that the response to mixing time is the same as that for the ethanol blends (Section 7.1.1), that is generally there is a reduction in accumulation mode accompanied with an increase in nucleation mode as the mixing time is increased (spark timing is retarded). Once again there is an increase in large particles (D_P> 150 nm) for the spark timing of 19° $bTDC_{COMB}$ that increases with the reduction of gasoline (and $AFR_{Stoich.}$) and is most likely caused by increased fuel impingement onto the piston crown and increased cylinder wall wetting resulting from the increased fuelling rate (necessary to maintain load).

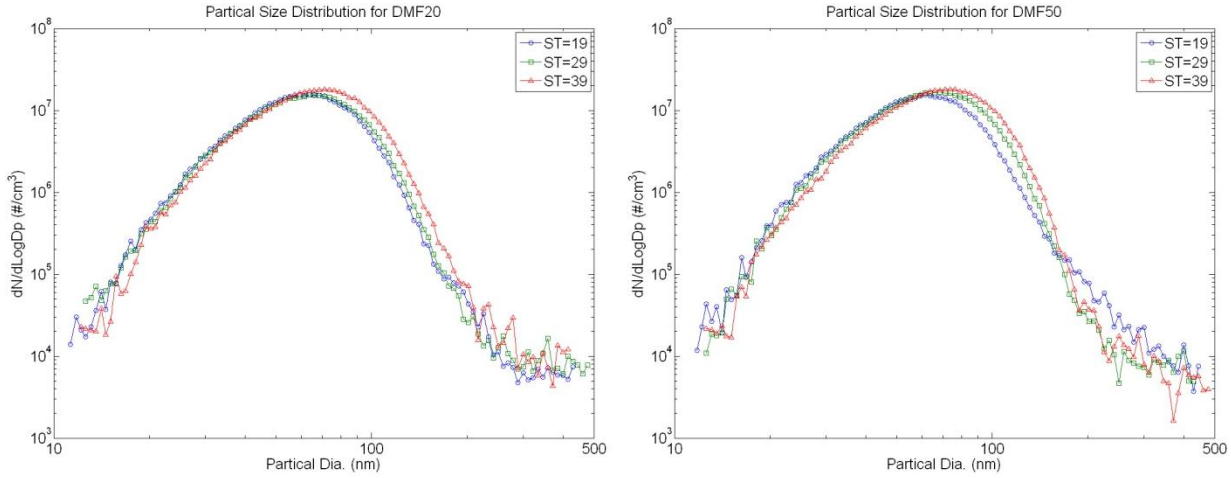

Figure 7.8 Part load SI, DMF20 and DMF50 particle size distributions

When the DMF blends are compared to the equivalent ethanol blends (E20 and E50) at the same spark timing of 29° $bTDC_{COMB}$ in Figure 7.9 it can be seen that there is an increase in number count for particles greater than 50 nm in diameter. This increase in the accumulation mode is accompanied with a slight reduction in the nucleation mode, the increased accumulation mode increases the surface area for any unburned hydrocarbons to adsorb onto and hence reduce the amount of self nucleation. This reduction in nucleation mode and increase in accumulation mode causes a small increase in the mean particle diameter, ~65 nm for the DMF blends compared to ~59 nm for the ethanol blends.

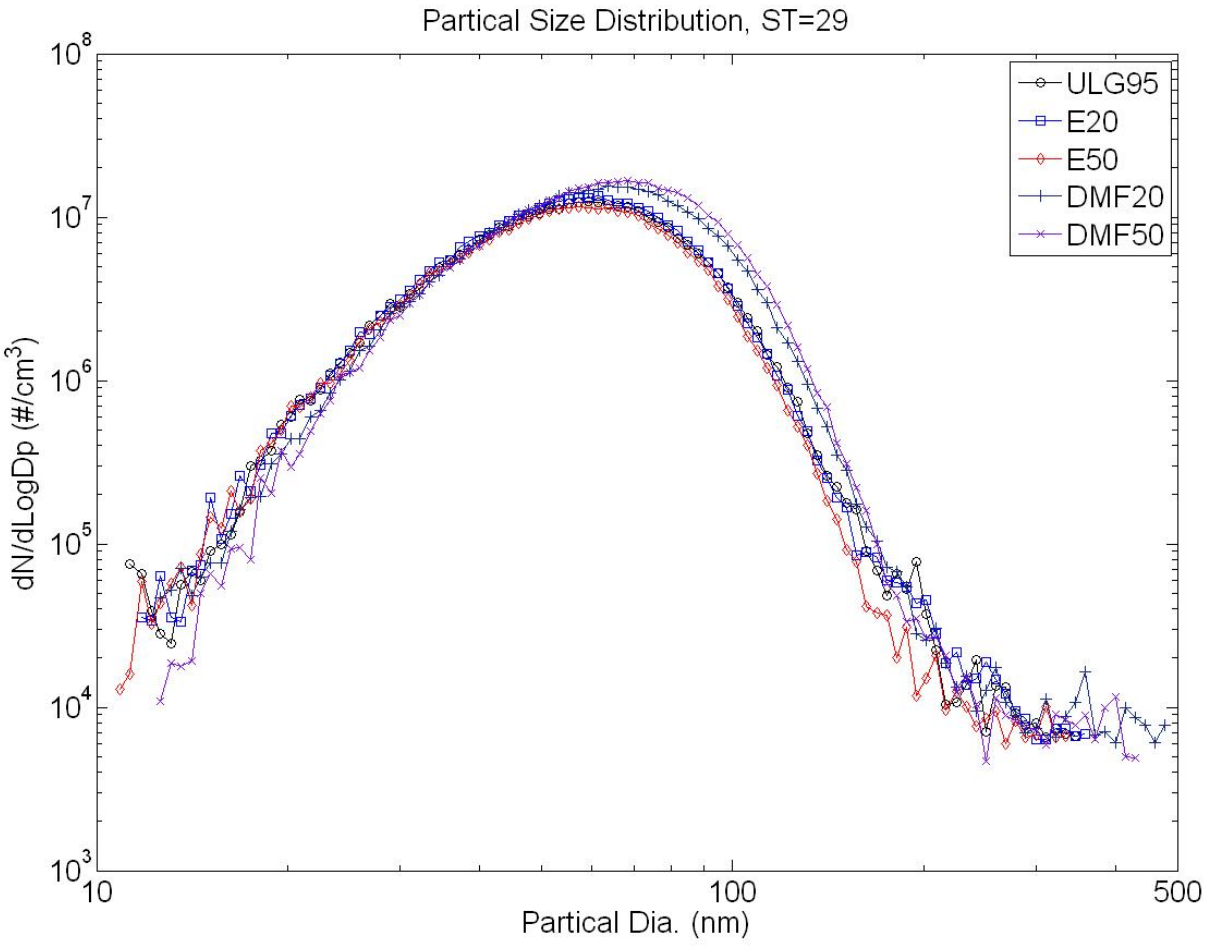

Figure 7.9 Part Load SI, Ethanol and DMF particle size distributions comparison

As seen in Figure 7.10 this increase in the accumulation mode causes an increase in total number (black lines/left ordinate) and total mass (blue lines/right ordinate) concentrations for the DMF blends (dotted lines with triangular data points) compared to standard gasoline and the equivalent ethanol blends (solid lines with circular data points).

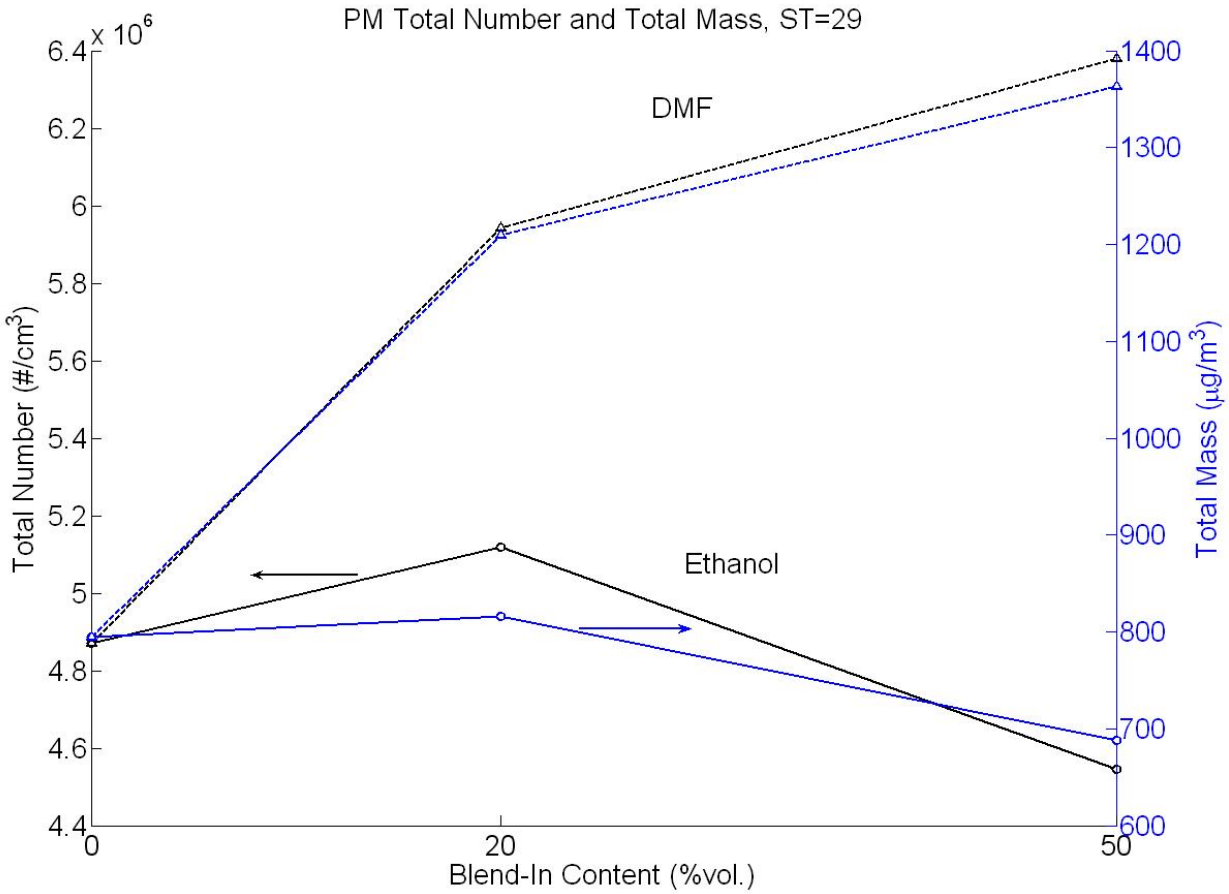

Figure 7.10 Part load SI, Total number and mass for all ethanol and DMF blends

DMF50 shows increases in total number concentration of ~30% and ~40% compared to standard gasoline and E50 respectively. The increases in total mass concentration compared to standard gasoline and E50 are ~70% and ~90% respectively. This increase is contributed to the incomplete combustion of the DMF ring structure, as ring structures are known soot precursors

[Tosaka et al (1989) and Takatori et al (1998)]. This theory is reinforced by the increase in number concentration coming from an increase in larger particles (D_P>50nm) which are most likely to be soot (or SOF adsorbed onto soot), whereas if the increase came from a larger nucleation mode that would suggest an increase in self nucleated volatile organic compounds (VOC). To fully test this theory a thermo-denuder should be used to remove the SOF part of the PM emissions so just the solid carbon/soot particles are measured.

7.2 Full Load Engine Operation

In this sub-section the PM emissions are investigated with the engine being operated at wide open throttle, at an engine speed of 1500 RPM. The engine set-up is the same as that for the full load investigations in Chapter 6 and is defined in Table 7.2 below. Two different spark timings are used, 7° $bTDC_{COMB}$ (MBT timing for standard gasoline, and referred to as retarded timing) and the knock-limited/MBT timing (referred to as advanced timing) for the particular blend tested. The constant spark timing (7° $bTDC_{COMB}$) is used to investigate the differences between the fuel blends at identical operating conditions. This also corresponds to operating an unmodified engine on ethanol blends. The MBT timing is used as this means the engine efficiency is maximised and therefore the most realistic operating condition with respect to automotive applications.

A split injection strategy is chosen to reduce the penetration length of the injected fuel spray plume. This is to reduce the amount of fuel impinged on the piston crown and the cylinder walls, which leads to increased hydrocarbon and particulate matter emissions. The start of injection

timings for the two parts of the split strategy are 280° $bTDC_{COMB}$ and 240° $bTDC_{COMB}$ respectively. These timings are chosen so all of the fuel is injected while the intake valve is open, but separated sufficiently so the two injections do not overlap (with respect to injector openings). The pulse widths of the two injections are equal in an attempt to produce equal penetration lengths and hence minimise penetration and fuel impingement.

Three different splash blends of ethanol/gasoline are examined, the blends being 20, 50 and 85%$_{Vol.}$ bio-ethanol in gasoline as well as standard gasoline and pure bio-ethanol. These are again designated as Ex, with 'x' representing the percentage by volume of bio-ethanol in the ethanol/gasoline blend. Stoichiometric mixtures are used for all tests. To help minimise the effects caused by the day-to-day variations in the atmospheric conditions all of the non-thermo-denuder tests (including split injection, Section 7.2.2) were conducted on one day and the entire tests using the thermo-denuder on the following day.

Table 7.2 Engine configuration for full load spark ignition operation

	Single Injection	**Split Injection**
Engine Speed (RPM)	1500	
IMEP (bar)	WOT	
λ	1.0	
IVO (° $bTDC_{GE}$)	16	
EVC (° $aTDC_{GE}$)	36	
SoI (° $bTDC_{COMB}$)	280	280/240
Spark Timing (° $bTDC_{COMB}$)	7, K-L/MBT	K-L/MBT

7.2.1 Investigation into the effects of Bio-Ethanol/Gasoline Blends

The particle size distributions for all fuel blends investigated at the constant spark timing of 7° $bTDC_{COMB}$ and the knock-limited/MBT spark timings are presented in Figures 7.11 and 7.12 respectively. The graph on the left is for total PM emissions and the graph on the right is for the solid carbonaceous particles only, which is obtained by passing the sample through a thermo-denuder before measuring with the SMPS.

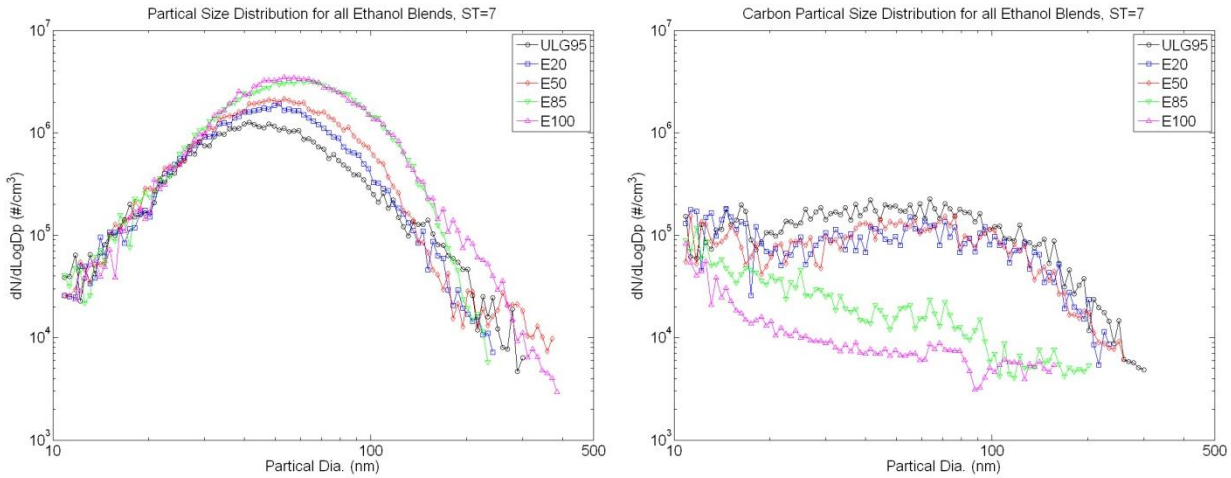

Figure 7.11 Full Load SI, Particle size distributions for all ethanol blends (ST = 7)

It can be seen that for the retarded spark timing (Figure 7.11) as the ethanol content is increased the peak number count (for total PM) increases along with an increase in the mean particle diameter. The peak number concentration increases from ~10^6 particles/cm^3 for standard gasoline to ~$3x10^6$ particles/cm^3 for pure ethanol, with the mean particle diameter increasing from ~53 nm to ~63 nm. This increase is caused by an increase in unburned hydrocarbons that are adsorbing onto existing carbon particles increasing their size and also causing increased levels of particulate coagulation and agglomeration. However this increase in HC emissions was

not seen when the gaseous emissions were measured (Figure 6.11), but as previously discussed in Chapter 5, Section 5.2.2 this discrepancy is caused by the FID's reduced sensitivity towards oxygenated hydrocarbons. Nevertheless when the particulate size distributions are examined for the solid carbon particles it can be seen that there is a significant reduction in particulate numbers, with this reduction increasing as the ethanol content is increased with the distributions for E85 and pure ethanol representing background levels. This increase in HC emissions is caused by the lower combustion temperatures experienced with the retarded spark timing and that the addition of ethanol increase the octane rating of the fuel blend, hence reducing its combustibility.

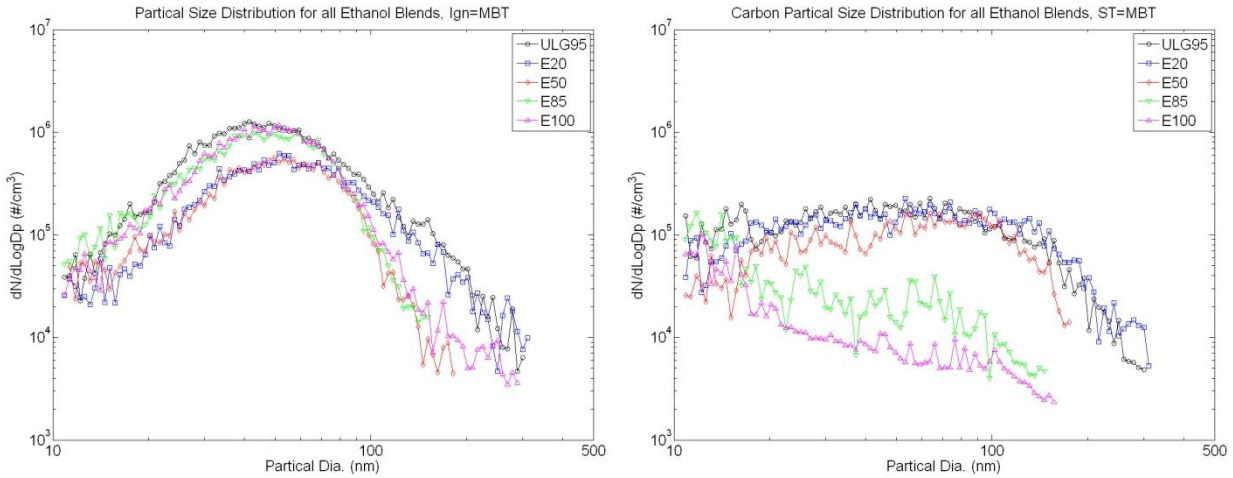

Figure 7.12 Full Load SI, Particle size distributions for all ethanol blends (ST = K-L/MBT)

When the advanced spark timings are used the combustion temperatures are increased and this has a significant effect on the PM emissions as shown in Figure 7.12. E20 shows similar particle counts to those of standard gasoline for particles greater than 100 nm diameter. This is attributed to the heavy fractions of the gasoline that have impinged on the piston crown, not fully evaporating, causing pool fires and significant soot production [Stevens and Steeper (2001)]. There is a reduction in nucleation mode PM for E20 because of the improved mixing and

combustion offered from the addition of ethanol (see Chapter 5). For the higher ethanol blends (E50 and up) there is a significant reduction in number counts for particle diameters greater than 100nm which is attributed to a reduction in heavy fuel fraction impingement on the piston crown. By looking at the carbon particle distributions it can be seen for the E50 and greater ethanol content particles of ~150nm diameter and larger are eliminated (or below detection limits) reinforcing the idea of reduced or eliminated pool fires caused by impinged heavy fuel fractions. E85 and E100 show similar nucleation mode particle number counts (total PM) to standard gasoline and greater counts than those for E20 and E50. This is because of the reduction in carbon particles (and hence adsorption surface area) causing the exhaust stream to become saturated in unburned hydrocarbons, which in turn self nucleate.

Figure 7.13 shows the total number (left graph) and total mass (right graph) concentrations for both total PM and carbon particles for both the advanced (black bars) and retarded (red bars) spark timings.

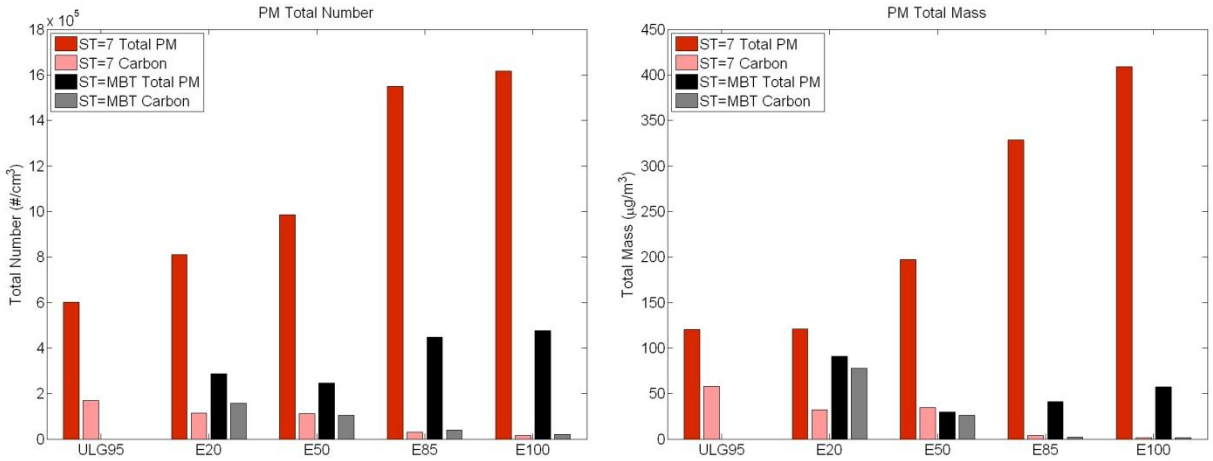

Figure 7.13 Full load SI, Total number and mass for all ethanol blends

Operating the engine with knock-limited/MBT spark timings causes a reduction in the total number and mass concentrations for the total PM (SOF + soot), but little difference is seen for the solid carbon particles alone suggesting the difference seen is caused by increase HC emissions for the retarded spark timings. There is a minimum in both total number and total mass concentrations (for total PM) for E50 which is caused by the balance between the removal of heavy fuel fractions and the increase in fuel injected due to the reduction in stoichiometric air-to-fuel ratio brought about by the addition of ethanol.

7.2.2 Investigation into the effects of Split Injection on Bio-Ethanol/Gasoline Blends

The particle size distributions for all fuel blends investigated with split injection and knock-limited/MBT spark timings are presented in Figure 7.14. The graph on the left is for total PM emissions and the graph on the right is for the solid carbonaceous particles only, which is obtained by passing the sample through a thermo-denuder before measuring it with the SMPS.

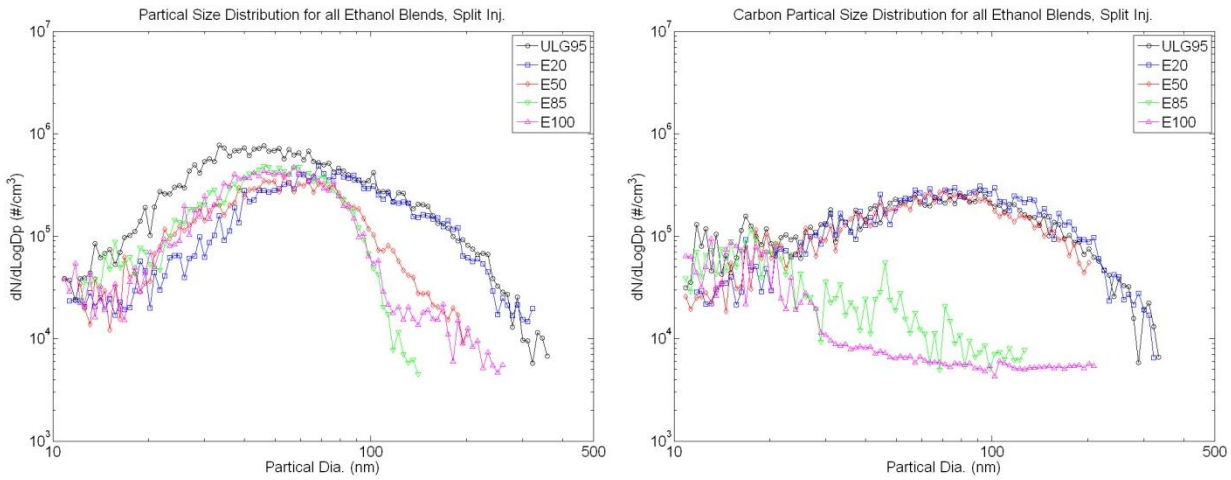

Figure 7.14 Full Load SI, Particle size distributions for all ethanol blends (split injection)

It can be seen that the particle size distributions (both total PM and carbon particles) for the split injection cases are similar in shape to those for the single injection cases, but the mean particle diameters are larger especially for standard gasoline and E20. Figure 7.15 shows the total number (left graph) and total mass (right graph) concentrations for both total PM and carbon particles for the single (black bars) and split (blue bars) injection cases. It can be seen for E85 and pure ethanol split injection reduces the total number and mass concentrations through a reduction in the SOF, as seen by a reduction in total PM whilst maintaining similar carbon particle concentrations. Split injection also provides a reduction in total number concentrations for standard gasoline, E20 and E50, but the total mass concentrations for these three blends actually increase due to the shift in the mean particle diameter. A plausible explanation for this is that although wall wetting/fuel impingement is reduced with the split injection, the two injection plumes interact with each other, causing an increase in the number and/or size of the fuel droplets present in the cylinder prior to combustion and these rich areas increase soot production. Compounding this is that by using split injection the mixing time is effectively reduced. The first half of the fuel injected has the same mixing time as the single injection because the SoI's are identical, however the second injection starts 40 CAD later and hence the mixing time is reduced by this same amount for the second half of the fuel delivered.

The discrepancies in the total mass concentrations for E50 have to be noted. There appears to be an increase in the total mass concentration of the carbon particles compared to total PM for the split injection case. This cannot be true as the thermo-denuder removes the SOF part of the total PM and hence mass should either be constant (if no is SOF present) or reduce. The total number concentration could however increase if agglomerated/coagulated particles are broken up by the

removal of the SOF. There are two possible explanations for this, the first being because the tests with and without the thermo-denuder were conducted on two separate days any changes in the atmospheric conditions could have changed the rate of PM formation, coagulation and agglomeration. The second explanation for this is related to the way the particle size (diameter) is determined. The particles are classified by their electrical-mobility (charge to aerodynamic drag ratio) and the diameter of the particle is given as that of a perfect sphere that has an identical electro-mobility to that of the particle measured. However the particles are very rarely perfectly spherical as seen by the TEM pictures presented by Lee et al (2003) and hence the calculated particle masses are therefore different to the actual particle masses. So if the particle shapes are changed (without mass gain or loss) when they pass through the thermo-denuder their equivalent electrical-mobility diameter and hence mass will be different for the same actual particle mass.

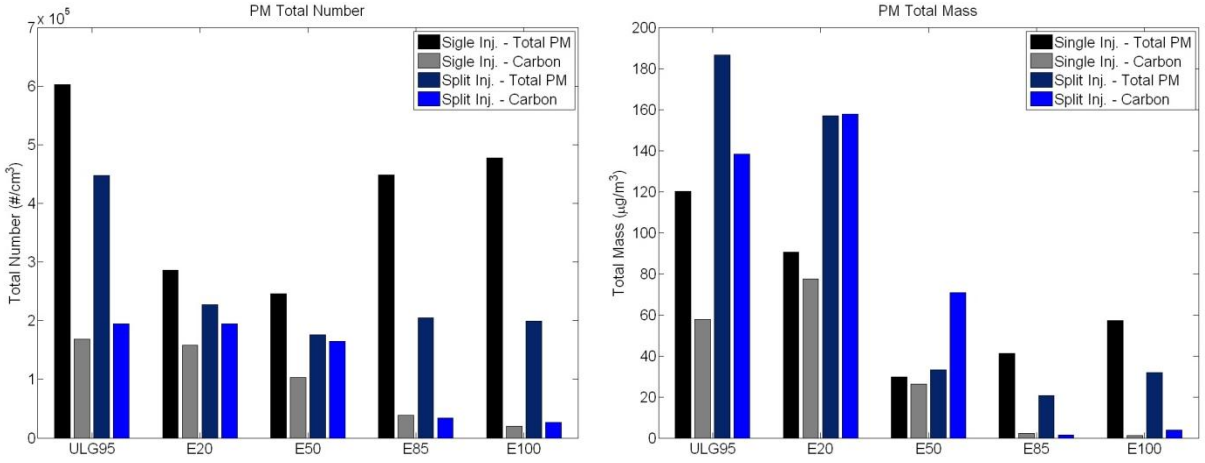

Figure 7.15 Full load SI, Total number and mass for all ethanol blends (split injection)

7.3 Summary

In this chapter the particulate emissions from ethanol/gasoline and 2,5 di-methylfuran/gasoline blends at part load and ethanol/gasoline blends at full, including a split injection strategy have been investigated.

With the engine operating at the part load condition the addition of ethanol shows a reduction in the total number and mass concentrations brought about by a reduction in soot particles caused by the reduction of fuel droplets and rich spots. However the addition of DMF causes an increase in total number and mass which is caused by a suspected increase in soot particles. This increase in soot particles is attributed to the incomplete combustion of the DMF ring structure.

At the full load operating point the addition of ethanol causes an increase in total number and mass concentrations through an increase in nucleation made associated with an increase in unburned hydrocarbon emissions when the standard gasoline spark timing is used. When the spark timing is advanced to the knock-limited/MBT timing the addition of ethanol causes a reduction in total number and mass, with a minimum seen for E50.

The split injection strategy used shows a reduction in PM emissions (both number and mass) for E85 and pure ethanol, but the total mass emissions for the lower ethanol blends and pure gasoline increase because of the suspected interaction of the two spray plumes. A reduction in total number concentration however was seen for all fuel blends when split injection was used.

This study shows that the soluble organic fraction makes up a significant proportion of the PM emissions from a DISI engine at both part and full load. At part load SOF forms around 60% and 70% of the total mass for gasoline and ethanol respectively. For ethanol at wide open throttle (WOT), using MBT spark timings, solid carbon forms less than 10% of the total particulate mass.

CHAPTER 8

8 Conclusions

As presented in the preceding chapters the use of fuel blends, both conventional and bio-derived, have shown potential to reduce emissions and increase efficiency in modern combustion systems. However attention has to be paid to engine calibration to avoid increased levels of particulate matter emissions. The most important findings of this study will be presented in this chapter along with some suggestion for future work.

8.1 Summary of Presented Findings

This thesis contains a wide range of findings on the use of fuel blends in modern combustion systems. These include HCCI combustion of conventional and bio-fuel blends, the use of novel and conventional bio-fuel blends in direct injection spark ignition combustion and the particulate matter emissions of the spark ignited bio-fuel blends. The most important and significant findings and observations are presented in the following sections in the order of the original chapters.

8.1.1 The Effect of Conventional and Bio-Fuel Blends on Gasoline HCCI Combustion and Emissions Performance

The addition of diesel to gasoline has been shown to increase the ignitability of the blend resulting in the increased load-lambda window achievable, The maximum IMEP achievable is increased by a modest 4%, whilst the lowest achievable IMEP is reduced by a significant 19%. The efficiency is increased along with a reduction in engine mechanical loading. The NO_X emissions are reduced by an almost constant 0.1 g/ikWhr. This though is accompanied with an increase in hydrocarbon and soot emissions of 1.5 g/ikWhr and 0.05 FSN respectively. The addition of bio-fuels to gasoline resulted in reduced ignitability resulting in a reduced load-lambda window of 0.25 bar IMEP for the upper load limit along with reduced efficiency. The NO_X emissions are increased by ~70% at high loads (3.5 bar IMEP). There appears to be a fundamental NO_X – HC trade-off for HCCI combustion that is related to in-cylinder temperature and is akin to the NO_X – Soot trade-off seen with conventional compression ignition combustion.

8.1.2 The Effect of Bio-Fuels on Direct Injection Spark Ignition (DISI) Combustion – Part Load

The addition of ethanol to gasoline at part load reduces the ignition delay and combustion duration by 3 CAD and 5 CAD respectively. This faster combustion leads to a 1 percentage point increase in combustion stability (COV_{IMEP}). The NO_X emissions are reduced by upto 0.8 g/ikWhr because of the lower flame temperature of ethanol. The split injection strategy used is only effective up to $30\%_{Vol.}$ ethanol content. Some of the trends seen with increasing ethanol

content are very much non-linear, which is caused by the non-linear change in the blend's vapour pressure with respect to ethanol content. The 2,5 di-methylfuran/gasoline blends show an improvement in combustion efficiency of approximately 0.5 percentage points, linked to the oxygenated nature of the fuel molecule. However the NO_X emissions are increased by 0.5 g/ikWhr for the DMF50 blend, through a suspected increase in flame temperature.

8.1.3 The Effect of Bio-Fuels on Direct Injection Spark Ignition (DISI) Combustion – Full Load

With the engine operating at a wide open throttle condition the addition of ethanol and 2,5 di-methylfuran to gasoline shows an increase (13.5% and 10% respectively) in engine load and efficiency (3 percentage points and 1 percentage point respectively) through the use of MBT or close to MBT spark timings and increased volumetric efficiency. Generally the benefits seen with the addition of DMF are not as great at those seen with the equivalent ethanol blends. At a constant spark timing (MBT timing for standard gasoline) the ethanol blends show a reduction of 1 g/ikWhr in NO_X emissions through reduced flame temperature, whereas the DMF blends show an increase of 2 g/ikWhr through a proposed increased flame temperature. Split injection improved the mixture preparation for the ethanol blends giving rise to a factor of two improvement in combustion stability. Engine load is increased by 0.2 bar IMEP, whilst combustion and indicated efficiency are improved by 1 percentage point and 3 percentage points respectively. A reduction of 0.8 g/ikWhr is seen for the hydrocarbon emissions, with the specific CO emissions being reduced by 40%. Volumetric NO_X emissions are increased, but specific NO_X show a slight reduction because of the accompanied increase in load.

8.1.4 The Effect of Bio-Fuels on Direct Injection Spark Ignition (DISI) Particulate Matter Emissions

With the engine operating at the part load condition the ethanol blends show reduced total number and total mass concentrations brought about by the reduction of fuel droplets and rich spots. E100 shows a reduction of 10% and 17% for total number and total mass concentrations respectively. However the addition of 2,5 di-methylfuran causes an increase in total number and mass concentrations which is attributed to the incomplete combustion of the DMF ring structure. DMF50 has 30% and 70% higher total number and total mass concentrations respectively than standard gasoline. At full load and with the standard gasoline spark timing the addition of ethanol causes a near three times increase in total number and greater than three times increase in total mass concentrations, caused an increase in nucleation made associated with an increase in unburned hydrocarbon emissions. When knock-limited/MBT spark timings are used the addition of ethanol results in a reduction in emitted PM. Maximum reductions of 58% for total number and 67% for total mass are seen for E50. Split injection shows a reduction in PM emissions for the higher ethanol blends, but the total mass emissions for the lower blends and gasoline increase. A reduction in total number concentration however was seen for all fuel blends when split injection was used. It is also shown that the soluble organic fraction makes up a significant proportion of the PM emissions from a DISI engine at both part and full load.

8.2 Suggestions for Future Work

In this thesis the author has presented findings on a range of methods and techniques that are considered to be important and significant for achieving high efficiency, low emission internal combustion engines stipulated by the current and future regulations. However more research is required on many of the presented areas for the technology to become suitable for production.

8.2.1 Dieseline HCCI

The addition of diesel to gasoline has been shown to increase the load window whilst reducing gaseous emissions and increasing efficiency. However an increase in smoke/filter blackening was seen, which needs further investigation to characterise the particulate distribution to assess the total number and total mass concentrations along with the relative proportions of solid carbon and soluble organic fraction. Different diesel fuels should also be considered as Fisher-Tropsch derived fuels have a higher Cetane number and therefore it is likely that lower quantities (blends) would be required, which should show a reduction in the larger particles emitted. Increased injection pressures should be investigated as a means of better fuel atomisation and hence reduced PM levels.

8.2.2 Bio-Fuels HCCI

Due to the ever decreasing oil reserves and increasing concerns towards atmospheric CO_2 levels and global warming the use of bio-derived and renewable fuels will become ever more common as a means of reducing the dependency on crude-derived fuels. More research is required for high blend ratios because it is proposed that this will reduce the load range achievable when

used in direct injection engines. With this being caused by the increased auto-ignition temperatures and enthalpies of vaporisation that is generally associated with these fuels, in particular ethanol.

8.2.3 Exhaust Emissions from Spark Ignited Bio-Fuels

The novel bio-derived fuel, 2,5 di-methylfuran, used in this study has the potential to replace crude-derived gasoline either completely or as a blend-in substitute for means of CO_2 reduction. Nevertheless more research is required on the particulate matter emissions to assess the proportions of solid carbon and soluble organic fraction, to ascertain the most appropriate after-treatment device required for PM reduction. Hydrocarbon speciation techniques should be used to assess the levels and relative toxicity of the individual species found in the exhaust stream as these are likely to be quite different than those from gasoline combustion. Because a Flame Ionisation Detector (FID) has a reduced sensitivity towards oxygenated hydrocarbons, hydrocarbon emissions resulting from oxygenated fuels should be measured by a different technique. On suitable method is to use a Fourier Transform Infrared (FTIR) detector as such a device can successfully measure oxygenated hydrocarbons.

List of References

Abdul-Khalek, I., Kittelson, D., and Brear, F., "The Influence of Dilution Conditions on Diesel Exhaust Particle Size Distribution Measurements". SAE Paper 1999-01-1142. (1999).

Abrantes, R., Assunção, J.V., Pesquero, C. R., Bruns, R.E., and Nóbrega, R.P., "Emission of polycyclic aromatic hydrocarbons from gasohol and ethanol vehicles". Atmospheric Environment 43, 648–654. (2009).

Aceves, S.M., Flowers, D.L., Espinosa-Loza, F., Martinez-Frias, J., Dec, J.E., Sjöberg, M., Dibble, R.W., and Hessel, R.P., "Spatial Analysis of Emissions Sources for HCCI Combustion at Low Loads Using a Multi-Zone Model". SAE Paper 2004-01-1910. (2004).

Adomeit, P., Lang, O., Pischinger, S., Aymanns, R., Graf, M., and Stapf, G., "Analysis of Cyclic Fluctuations of Charge Motion and Mixture Formation in a DISI Engine in Stratified Operation". SAE Paper 2007-01-1412. (2007).

Akira Lijima, and Shoji, H., "A Study on HCCI Combustion Characteristics Using Spectroscopic Techniques", SAE Paper 2007-01-1886. (2007).

Al-Farayedhi, A.A., Al-Dawood, A.M., and Gandhidasan, P., "Effects of Blending Crude Ethanol with Unleaded Gasoline on Exhaust Emissions of SI Engine". SAE Paper 2000-01-2857. (2000)

Alger, T., Hall M., and Matthews, R.D., "Effects of Swirl and Tumble on In-Cylinder Fuel Distribution in a Central Injected DISI Engine". SAE Paper 2000-01-0533. (2000).

Amann, C.A., and Siegla, D.C., "Diesel Particulates—What They Are and Why". Aerosol Science and Technology 1, 73-101. (1981).

Amann, M., Ryan III, T.W., and Kono, N., "HCCI Fuels Evaluations-Gasoline Boiling Range Fuels". SAE Paper 2005-01-3727. (2005).

Angelos, J.P., Andreae, M.M., Green, W.H., Cheng, W.K., Kenney, T., and Xu, Y., "Effects of Variations in Market Gasoline Properties on HCCI Load Limits". SAE Paper 2007-01-1859. (2007).

Aroonsrisopon, T., Foster, D., Morikawa, T., and Iida, M., "Comparison of HCCI Operating Ranges for Combinations of Intake Temperature, Engine Speed and Fuel Composition". SAE Paper 2002-01-1924. (2002).

Baumgarten, H., Bozelie, P., Geiger, J., and Wolters, P., "Vehicle Application of a 4-Cylinder Tumble DISI Engine". SAE Paper 2001-01-0735. (2001).

Bhusnoor, S.S., Babu, M.K.G., and Subrahmanyam, J.P., "Studies on Performance and Exhaust Emissions of a CI Engine Operating on Diesel and Diesel Biodiesel Blends at Different Injection Pressures and Injection Timings". SAE Paper 2007-01-0613. (2007).

Bression, G., Soleri, D., Savy, S., Dehoux, S., Azoulay, D., Hamouda, H. B.-H., Doradoux, L., Guerrassi, N., and Lawrence, N., "A Study of Methods to Lower HC and CO Emissions in Diesel HCCI". SAE Paper 2008-01-0034. (2008).

Bunting, B., "Spark Stabilization of HCCI Combustion". U.S. Department of Energy Advanced Combustion Engine Merit Review (ACE Review). (2004).

Cairns, A., and Blaxill, H., “The Effects of Combined Internal and External Exhaust Gas Recirculation on Gasoline Controlled Auto-Ignition”. SAE Paper 2005-01-0133. (2005).

Cao, L., Zhao, H., Jiang, X., and Kalian, N., “Understanding the influence of valve timings on controlled autoignition combustion in a four-stroke port fuel injection engine”. Journal of Automobile Engineering 219, 807-823. (2005a).

Cao, L., Zhao, H., Jiang, X., and Kalian, N., “Numerical Study of Effects of Fuel Injection Timings on CAI/HCCI Combustion in a Four-Stroke GDI Engine”. SAE Paper 2005-01-0144. (2005b).

Chen, R., and Milovanovic, N., “A computational study into the effect of exhaust gas recycling on homogeneous charge compression ignition combustion in internal combustion engines fuelled with methane”. International Journal of Thermal Sciences 41 805–813. (2002).

Chen, Z., and Mitsuru, K., “Hoe to Put the HCCI Engine to Practical Use: Control the Ignition Timing by Compression Ratio and Increase the Power Output by Supercharge”. SAE Paper 2003-01-1832. (2003).

Cheng W. K., Summers, T., and Collings, N., “The Fast-Response Flame Ionization Detector”. Progress in Energy and Combustion Science 24, 89-124. (1998).

Christensen, M., Hultqvist, A., and Johansson, B., “Demonstrating the Multi Fuel Capability of a Homogeneous Charge Compression Ignition Engine with Variable Compression Ratio”. SAE Paper 1999-01-3679. (1999).

Christensen, M., and Johansson, B., “Supercharged Homogeneous Charge Compression Ignition (HCCI) with Exhaust Gas Recirculation and Pilot Fuel”. SAE Paper 2000-01-1835. (2000).

Cole, R.L., Poola, R.B., and Sekar, R., “Exhaust Emissions of a Vehicle with a Gasoline Direct-Injection Engine”. SAE Paper 982605. (1998).

Crawford, A., Ellis, G., Fraser, N., Steeples, B., and Kollin, K., “Combining High Performance with Euro IV Capability in a Naturally Aspirated Production Engine”. SAE Paper 2002-01-0335. (2002).

Dockery, D. W., Arden Pope, C., Xu, X., Spengler, J. D., Ware, J. H., Fay, M. E., Ferris, B. G., and Speizer, F. E., “An Association between Air Pollution and Mortality in Six U.S. Cities”. The New England Journal of Medicine 329 1753-1759. (1993).

Easley, W.L., Agarwal, A., and Lavoie, G.A., “Modeling of HCCI Combustion and Emissions Using Detailed Chemistry”. SAE Paper 2001-01-1029. (2001).

Ebersole, G.D., and Manning, F.S., “Engine performance and exhaust emissions: methanol versus isooctane”. SAE Paper 720692. (1972).

Elrod, A.C., and Nelson, M.T., “Development of a variable valve timed engine to eliminate the pumping losses associated with throttled operation”. SAE Paper 860537. (1986).

Epping, K., Aceves, S., Bechtold, R., and Dec, J., “The Potential of HCCI Combustion for High Efficiency and Low Emissions”. SAE Paper 2002-01-1923. (2002).

Evans, R.L., Goharian, F., and Hill, P.G., “The performance of a spark-ignition engine fuelled with naturalgas and gasoline”. SAE Paper 840234. (1984).

Fiveland, S.B., Agama, R., Christensen, M., Johansson, B., Hiltner, J., Mauss, F., Assanis, D.N., “Experimental and Simulated Results Detailing The Sensitivity of Natural Gas HCCI Engines to Fuel Composition”. SAE Paper 2001-01-3609. (2001).

Fleming, R.D., and O'Neal, G.B., "Potential for improving the efficiency of a spark ignition engine for natural gas fuel". SAE Paper 852073. (1985).
Gérard, D., Besson, M., Hardy, J.-P., Croguennec, S., Thomine, M., Aoyama, S., and Tomita, M., "HCCI Combustion on a Diesel VCR Engine". SAE Paper 2008-01-1187. (2008).
Gnanam, G., Sobiesiak, A., and Reader, G., "An HCCI Engine Fuelled with Iso-octane and Ethanol". SAE Paper 2006-01-3246. (2006).
Gouli, S., Stournas, S., and Lois, E., "Antiknock Performance of Gasoline Substitutes and their Effects on Gasoline Properties". SAE Paper 981367. (1998).
Graskow, B.R., Kittelson, D.B., Ahmadi, M.R., and Morris, J.E., "Exhaust Particulate Emissions from a Direct Injection Spark Ignition Engine". SAE Paper 1999-01-1145. (1999).
Guohong, T., Zhi, W., Jianxin, W., Shijin, S., and Xinliang, A., "HCCI Combustion Control by Injection Strategy with Negative Valve Overlap in a GDI Engine". SAE Paper 2006-01-0415. (2006).
Hall, D.E., and Dickens, C.J., "Measurement of the Number and Size Distribution of Particles Emitted from a Gasoline Direct Injection Vehicle". SAE Paper 1999-01-3530. (1999).
Han, Z., Uludogan, A., Hampson, G.J., and Reitz, R.D., "Mechanism of Soot and NOx Emission Reduction Using Multiple-Injection in a Diesel Engine". SAE Paper 960633. (1996).
Han, S.B., and Chung, Y.J., "The influence of air-fuel ratio on combustion stability of a gasoline engine at idle". SAE Paper 1999-01-1488. (1999).
Han, D., Han, S.-K., Han, B.-H., and Kim, W.-T., "Development of 2.0L Turbocharged DISI Engine for Downsizing Application". SAE Paper 2007-01-0259. (2007).
Hara, T. and Tanoue, K. 'Laminar Flame Speed of Ethanol, n-Heptane, Iso-Octane Air Mixtures.' SAE Paper No. 2006-05-0409. (2006).
Haraldsson, G., Tunestål, P., Johansson, B., and Hyvönen, J., "HCCI Combustion Phasing in a Multi Cylinder Engine Using Variable Compression Ratio". SAE Paper 2002-01-2858. (2002).
He, B.-Q., Wang, J.-X., Shuai, S.-J., and Yan, X.-G., "Homogeneous Charge Combustion and Emissions of Ethanol Ignited by Pilot Diesel on Diesel Engines". SAE Paper 2004-01-0094. (2004).
He, B.-Q., Xie, H., Zhang, Y., Qin, J., and Zhao, H., "An Experimental Study on HCCI Combustion in a Four-Stroke Gasoline Engine with Reduced Valve Lift Operations". SAE Paper 2005-01-3736. (2005).
Helmantel A., and Denbratt, I., "HCCI Operation of a Passenger Car DI Diesel Engine with an Adjustable Valve Train". SAE Paper 2006-01-0029. (2006).
Honda, T., Kawamoto, M., Katashiba, H., Sumida, M., Fukutomi, N., and Kawajiri, K., "A Study of Mixture Formation and Combustion for Spray Guided DISI". SAE Paper 2004-01-0046. (2004).
Huang, H., Su, W., and Pei, Y., "Experimental and Numerical Study of Diesel HCCI Combustion by Multi-Pulse Injection". SAE Paper 2008-01-0059. (2008).
Hunter Mack, J., Aceves , S.M., and Dibble, R.W., "Demonstrating direct use of wet ethanol in a homogeneous charge compression ignition (HCCI) engine". Energy 34, 782–787. (2009).
Hyvönen, J., Haraldsson, G., and Johansson, B., "Operating Range in a Multi Cylinder HCCI Engine Using Variable Compression Ratio". SAE Paper 2003-01-1829. (2003a).

Hyvönen, J., Haraldsson, G., and Johansson, B., "Supercharging HCCI to Extend the Operating Range in a Multi-Cylinder VCR-HCCI Engine". SAE Paper 2003-01-3214. (2003b).
Ibara, T., Iida, M., and Foster, D.E., "Study on Characteristics of Gasoline Fueled HCCI Using Negative Valve Overlap". SAE Paper 2006-32-0047. (2006).
Iida, M., Aroonsrisopon, T., Hayashi, M., Foster, D., and Martin, J., "The Effect of Intake Air Temperature, Compression Ratio and Coolant Temperature on the Start of Heat Release in an HCCI (Homogeneous Charge Compression Ignition) Engine". SAE Paper 2001-01-1880. (2001).
Jang, J., Yang, K., Yeom, K., Bae, C., Oh, S., and Kang. K., "Improvement of DME HCCI Engine Performance by Fuel Injection Strategies and EGR". SAE Paper 2008-01-1659. (2008).
Jiang, H.-F., Wang, J.-X., Shuai, S.-J., "Visualization and Performance Analysis of Gasoline Homogeneous Charge Induced Ignition by Diesel". SAE Paper 2005-01-0136. (2005).
Johansson, T., Johansson, B., Tunestål. P., and Aulin, H., "HCCI Operating Range in a Turbo-charged Multi Cylinder Engine with VVT and Spray-Guided DI". SAE Paper 2009-01-0494. (2009).
Jun, D., Ishii, K., and Iida, N., "Autoignition and Combustion of Natural Gas in a 4 Stroke HCCI Engine". JSME International Journal, Series B, 46, 60-67. (2003).
Kapus, P.E., Fuerhapter, A., Fuchs H., and Fraidl, G.K., "Ethanol Direct Injection on Turbocharged SI Engines – Potential and Challenges". SAE Paper 2007-01-1408. (2007).
Kar, K., Last, T., Haywood, C. and Raine, R., "Measurements of Vapor Pressures and Enthalpies of Vaporization of Gasoline and Ethanol Blends and Their Effects on Mixture Preparation in an SI Engine". SAE Paper 2008-01-0317. (2008).
Kawano, D., Suzuki, H., Ishii, H., Goto, Y., Odaka, M., Murata, Y., Kusaka, J., and Daisho, Y., "Ignition and Combustion Control of Diesel HCCI". SAE Paper 2005-01-2132. (2005).
Kim, J.M., Kim, Y.T., Lee, J.Y., and Lee, S.Y., "Performance characteristics of hydrogen fuelled engine with the direct injection and spark ignition system". SAE Paper 952498. (1995).
Kim, Y.-J., Lee S.H., and Cho, N.-H., "Effect of Air Motion on Fuel Spray Characteristics in a Gasoline Direct Injection Engine". SAE Paper 1999-01-0177. (1999).
Kim, Y.-J., Kim, K.-B., and Lee, K.-H., "A Study on the Combustion and Emission Characteristics of Diesel Fuel Blended with Ethanol in an HCCI Engine". SAE Paper 2008-32-0026. (2008).
Koga, N., "An Experimental Study on Fuel Behavior during the Cold Start Period of a Direct Injection Spark Ignition Engine". SAE Paper 2001-01-0969. (2001).
Kong, S.-C., Marriott, C.D., Rutland, C.J., and Reitz, R.D., "Experiments and CFD Modeling of Direct Injection Gasoline HCCI Engine Combustion". SAE Paper 2002-01-1925. (2002).
Koopmans, L., and Denbratt, I., "A Four Stroke Camless Engine, Operated in Homogeneous Charge Compression Ignition Mode with Commercial Gasoline". SAE Paper 2001-01-3610. (2001).
Koopmans, L., Ognik, R., and Denbratt, I., "Direct Gasoline Injection in the Negative Valve Overlap of a Homogeneous Charge Compression Ignition Engine". SAE Paper 2003-01-1854. (2003).

Kornhauser, A.A., and Smith, J.L., “A Comparison of Cylinder Heat Transfer Expressions Based on prediction of Gas Spring Hysteresis Loss”. Fluid Flow in Heat Transfer and Reciprocating Machinery, pp. 89-96, ASME 1987.

Lee, K.O., Zhu, J., Ciatti, S., Yozgatligil, A., and Choi, M.Y., “Sizes, Graphitic Structures and Fractal Geometry of Light-Duty Diesel Engine Particulates”. SAE Paper 2003-01-3169. (2003).

Li, J., Matthews, R.D., Stanglmaier, R.H., Roberts, C.E., and Anderson, R.W., “Further Experiments on the Effects of In-Cylinder Wall Wetting on HC Emissions from Direct Injection Gasoline Engines”. SAE Paper 1999-01-3661. (1999).

Li, H., Neill, W.S., Chippior, W., Graham, L., Connolly, T., and Taylor, J.D., “An Experimental Investigation on the Emission Characteristics of HCCI Engine Operation Using N-Heptane”. SAE Paper 2007-01-1854. (2007).

Majer, V., Svoboda, V., and Kehiaian, H.V., “Enthalpies of vaporization of organic compounds”. Oxford : Blackwell Scientific 1985.

Matti Maricq, M., Podsiadlik, D.H., Brehob, D.D., and Haghgooie, M., “Particulate Emissions from a Direct-Injection Spark-Ignition (DISI) Engine”. SAE Paper 1999-01-1530. (1999).

Maurya, R.K., and Agarwal, A.K., “Combustion and Emission Behavior of Ethanol Fuelled Homogeneous Charge Compression Ignition (HCCI) Engine”. SAE Paper 2008-28-0064. (2008).

Mehta, D., Alger, T., Hall, M., Matthews, R., and Ng, H., “Particulate Characterization of a DISI Research Engine using a Nephelometer and In-Cylinder Visualization”. SAE Paper 2001-01-1976. (2001).

Menrad, H., Lee, W., and Bernhardt, W., “Development of a pure methanol fuel car”. SAE Paper 770790. (1977).

Milovanovic, N., Chen, R., and Turner, J., “Influence of variable valve timings on the gas exchange process in a controlled auto-ignition engine”. ”. Journal of Automobile Engineering 218, 567-583. (2004a).

Milovanovic, N., Chen, R., Dowden, R., and Turner, J., “An investigation of using various diesel-type fuels in homogeneous charge compression ignition engines and their effects on operational and controlling issues”. International Journal of Engine Research 5, No. 4, 297-316. (2004b).

Mousdale, D.M., “Biofuels Biotechnology, Chemistry, and Sustainable Development”. 1st Ed. (404 Pages) CRC Press 2008. (2008).

Nabi, M.N., Ogawa, H., and Miyamoto, N. ‘Nature of Fundamental Parameters Related to Engine Combustion for a Wide Range of Oxygenated Fuel.’ SAE Paper 2002-01-2853. (2002).

Nakata, K., Utsumi, S., Ota, A., Kawatake, K., Kawai, Y., and Tsunooka, T., “The Effect of Ethanol Fuel on a Spark Ignition Engine”. SAE Paper 2006-01-3080. (2006).

Narayan, S., and Rajan, S., “Turbulent Temperature Fluctuations in Spark Ignition Engines and Their Effect on NOx Emissions”. SAE Paper 2004-01-0623. (2004).

Negurescu, N., Pana, C., Popa, M.G., and Racovitza, A., “Variable Valve - Control Systems for Spark Ignition Engine”. SAE Paper 2001-01-0671. (2001).

Ng, C.K.W., and Thomson, M.J., "A Computational Study of the Effect of Fuel Reforming, EGR and Initial Temperature on Lean Ethanol HCCI Combustion". SAE Paper 2004-01-0556. (2004).

Noma, K., Iwamoto, Y., Murakami, N., Iida, K., and Nakayama, O., "Optimized Gasoline Direct Injection Engine for the European Market". SAE Paper 980150. (1998).

Nordgren, H., Hultqvist, A., and Johansson, B., "Start of Injection Strategies for HCCI-combustion". SAE Paper 2004-01-2990. (2004).

Noyori, T., "Experimental Study of Smoke Emission on Small-Displacement Spark-Ignition Direct-Injection Engine". SAE Paper 2006-32-0105. (2006).

Oakley, A., Zhao, H., Ladommatos, N., and Ma, T., "Dilution Effects on the Controlled Auto-Ignition (CAI) Combustion of Hydrocarbon and Alcohol Fuels". SAE Paper 2001-01-3606. (2001).

Okamoto, K., Ichikawa, T., Saitoh, K., Oyama, K., Hiraya, K., and Urushihara, T., "Study on relationship between octane number and anti-knock performance in direct injection spark ignition gasoline engine". SAE Paper 2002-08-0327. (2002).

Osborne, R.J., Li, G., Sapsford, S.M., Stokes, J., Lake, T.H., Heikal, M.R., "Evaluation of HCCI for Future Gasoline Powertrains". SAE Paper 2003-01-0750. (2003).

Payri, F., Boada, F., and Macián, V., "Reduction of pumping losses by the use of a variable valve timing system". SAE Paper 844966. (1984).

Peng, Z., Zhao, H., and Ladommatos, N., "Effects of Air/Fuel Ratios and EGR Rates on HCCI Combustion of n-heptane, a Diesel Type Fuel". SAE Paper 2003-01-0747. (2003).

Persson, H., Pfeiffer, R., Hultqvist, A., Johansson, B., and Ström, H., "Cylinder-to-Cylinder and Cycle-to-Cycle Variations at HCCI Operation With Trapped Residuals". SAE Paper 2005-01-0130. (2005).

Pidol, L., Lecointe, B., Pesant L., and Jeuland, N., "Ethanol as a Diesel Base Fuel – Potential in HCCI Mode". SAE Paper 2008-01-2506. (2008).

Piock, W.F., Matsumoto, Y.,. Sikinger, H., and Fraidl, G.K., "The Spray-Guided Concept for the Second Generation of Gasoline DirectInjection". SAE Paper 2004-08-0089. (2004).

Price, P., Stone, R., Collier, T. and Davies, M. "Particulate Matter and Hydrocarbon Emissions Measurements: Comparing First and Second Generation DISI with PFI in Single Cylinder Optical Engines". SAE Paper 2006-01-1263. (2006).

Price, P., Twiney, B., Stone, R., Kar, K., and Walmsley, H., "Particulate and Hydrocarbon Emissions from a Spray Guided Direct Injection Spark Ignition Engine with Oxygenate Fuel Blends". SAE Paper 2007-01-0472. (2007a).

Price, P., Stone, R., OudeNijeweme, D., and Chen, X., "Cold Start Particulate Emissions from a Second Generation DI Gasoline Engine". SAE Paper 2007-01-1931. (2007b).

Risberg, P., Kalghatgi, G., and Angstrom, H-E., "The Influence of EGR on Auto-Ignition Quality of Gasoline-Like Fuels in HCCI Engines", SAE Paper 2004-01-2952. (2004).

Román-Leshkov, Y., Barrett, C.J., Liu, Z.Y. and Dumesic, J.A., "Production of dimethylfuran for liquid fuels from biomass-derived carbohydrates". Nature 447, 982–985. (2007).

Rosati, M.F., and Aleiferis, P.G., "Hydrogen SI and HCCI Combustion in a Direct-Injection Optical Engine". SAE Paper 2009-01-1921. (2009).

Ryan, T.W., Callahan, T.J, and Mehta, D., "HCCI in a Variable Compression Ratio Engine-Effects of Engine Variables", SAE Paper 2004-01-1971. (2004).

Salih, F.M. and Andrews G.E., “The Influence of Gasoline/Ethanol Blends on Emisssions and Fuel Economy”. SAE Paper 922378. (1992).

Sandford, M., Page, G., and Crawford, P., “The All New AJV8”. SAE Paper 2009-01-1090. (2009).

Sandquist, H., and Denbratt, I., “Comparison of homogeneous and stratified charge operation in a direct-injection, sparkignition engine”. SAE Paper 1999-08-0336. (1999).

Sazhina, E.M., Sazhin, S.S., Heikal, M.R., Marooney, C.J., “The Shell autoignition model: applications to gasoline and diesel fuels”. Fuel 78, 389-401. (1999).

Schwarz, C., Schünemann, E., Durst, B., Fischer, J., Witt, A., “Potentials of the Spray-Guided BMW DI Combustion System DI Combustion System”. SAE Paper 2006-01-1265. (2006).

Shen, Y., King, E., Pfahl, U., Krile, R.T., Slone, E., Orban, J.E., and Wright, K., “Fuel Chemistry Impacts on Gasoline HCCI Combustion with Negative Valve Overlap and Direct Injection”. SAE Paper 2007-01-4105. (2007).

Shibata, G., Oyama, K., Urushihara, T., and Nakano, T., “The Effect of Fuel Properties on Low and High Temperature Heat Release and Resulting Performance of an HCCI Engine”. SAE Paper 2004-01-0553. (2004).

Shibata, G., and Urushihara, T., “Auto-Ignition Characteristics of Hydrocarbons and Development of HCCI Fuel Index”. SAE Paper 2007-01-0220. (2007).

Shimotani, K., Oikawa, K., Horada, O., and Kagawa, Y., “Characteristics of gasoline in-cylinder directinjection engine”. SAE Paper 958619. (1995).

Shudo, T., Ono, Y., and Takahashi, T., “Influence of Hydrogen and Carbon Monoxide on HCCI Combustion of Dimethyl Ether”. SAE Paper 2002-01-2828. (20020.

Shudo, T., Futakuchi, T., and Nakajima, Y., “Thermal efficiency analysis in a hydrogen-premixed, spark-ignition engine”. SAE Paper 1999-08-0104. (1999).

Sjöberg, M., Edling, L.-O., Eliassen, T., Magnusson, L., and Angström, H.-E., “GDI HCCI: Effects of Injection Timing and Air and Emissions Formation”. SAE Paper 2002-01-0106. (2002).

Sjöberg, M., and Dec, J.E., “Combined effects of fuel-type and engine speed on intake temperature requirements and completeness of bulk-gas reactions for HCCI combustion”. SAE Paper 2003-01-3173. (2003).

Stanglmaier, R.H., and Roberts, C.E., “Homogeneous Charge Compression Ignition (HCCI): Benefits, Compromises, and Future Engine Applications”. SAE Paper 1999-01-3682. (1999).

Stanglmaier, R.H., Ryan III, T.W., and Souder, J.S., “HCCI Operation of a Dual-Fuel Natural Gas Engine for Improved Fuel Efficiency and Ultra-Low NOx Emissions at Low to Moderate Engine Loads”. SAE Paper 2001-01-1897. (2001).

Stansfield, P.A., Wigley, G., Garner, C.P., Patel, R., Ladommatos, N., Pitcher, G., Turner, J.W.G., Nuglisch, H., Helie, J., “Unthrottled Engine Operation using Variable Valve Actuation: The Impact on the Flow Field, Mixing and Combustion”. SAE Paper 2007-01-1414. (2007).

Steeper, R.R., and De Zilwa, S., “Improving the NO_X-CO_2 Trade-Off of an HCCI Engine Using a Multi-Hole Injector”. SAE Paper 2007-01-0180. (2007).

Stenlåås, O., Christensen, M., Egnell, R., Johansson, B., and Mauss, F., "Hydrogen as Homogeneous Charge Compression Ignition Engine Fuel". SAE Paper 2004-01-1976. (2004).

Stevens, E., and Steeper, R., "Piston Wetting in an Optical DISI Engine: Fuel Films, Pool Fires, and Soot Generation". SAE Paper 2001-01-1203. (2001).

Stone, R., "Introduction to Internal Combustion Engines", 3rd Ed. (659 pages) Macmillan 1999.

Szekely, G.A., and Alkidas, A.C., "Combustion Characteristics of a Spray-Guided Direct-Injection Stratified-Charge Engine with a High-Squish Piston". SAE Paper 2005-01-1937. (2005).

Takatori, Y., Mandokoro, Y., Akihama, K., Nakakita, K., Tsukasaki, Y., Iguchi, S., Yeh, L.I., and Dean, A.M., "Effect of Hydrocarbon Molecular Structure on Diesel Exhaust Emissions Part 2: Effect of Branched and Ring Structures of Paraffins on Benzene and Soot Formation". SAE Paper 982495. (1998).

Taniguchi, S., Yoshida, K. and Tsukasaki, Y., "Feasibility Study of Ethanol Applications to A Direct Injection Gasoline Engine". SAE Paper 2007-01-2037. (2007).

Tosaka, S., Fujiwara, Y., and Murayama, T., "The effect of fuel properties on particulate formation~The effect of molecular structure and carbon number". SAE Paper 891881. (1989).

Turner, J.W.G., Pitcher, G., Burke, P., Garner, C.P., Wigley, G., Stansfield, P., Nuglisch, H., Ladommatos, N., Patel, R., P. Williams, P., "The HOTFIRE Homogeneous GDI and Fully Variable Valve Train Project - An Initial Report". SAE Paper 2006-01-1260. (2006).

Turner, J.W.G., Pearson, R.J., Holland, B., and Peck, R., "Alcohol-Based Fuels in High Performance Engines". SAE Paper 2007-01-0056. (2007).

Uludogan, A., Xin, J., and Reitz, R.D., "Exploring the Use of Multiple Injectors and Split Injection to Reduce DI Diesel Engine Emissions". SAE Paper 962058. (1996).

Urushihara, T., Hiraya, K., Kakuhou, A., and Itoh, T., "Expansion of HCCI Operating Region by the Combination of Direct Fuel Injection, Negative Valve Overlap and Internal Fuel Reformation". SAE Paper 2003-01-0749. (2003).

Verevkin, S.P. and Welle, F.M., "Thermochemical Studies for Determination of the Standard Molar Enthalpies of Formation of Alkyl-Substituted Furans and Some Ethers". Structural Chemistry 9, 215-221. (1998).

Wagner, R.M., Edwards, K.D., Daw, C.S., Green Jr., J.B., and Bunting, B.G., "On the Nature of Cyclic Dispersion in Spark Assisted HCCI Combustion". SAE Paper 2006-01-0418. (2006).

Waldman, J., Nitz, D., Aroonsrisopon. T., Foster, D.E., Iida, M., "Experimental Investigation into the Effects of Direct Fuel Injection During the Negative Valve Overlap Period in an Gasoline Fueled HCCI Engine". SAE Paper 2007-01-0219. (2007).

Wallner, T. and Miers, S.A., "Combustion Behavior of Gasoline and Gasoline/Ethanol Blends in a Modern Direct-Injection 4-Cylinder Engine". SAE Paper 2008-01-0077. (2008).

Wang, Z., Wang, J.-X., Tian, G.-H., Shuai, S.-J., Zhang Z., and Yang, J., "Research on Steady and Transient Performance of an HCCI Engine with Gasoline Direct Injection". SAE Paper 2008-01-1723. (2008).

Wang, Y., Makkapati, S., Jankovic, M., Zubeck, M., and Lee, D., "Control Oriented Model and Dynamometer Testing for a Single-Cylinder, Heated-Air HCCI Engine". SAE Paper 2009-01-1129. (2009).

Warey, A., Huang, Y., Matthews, R., Hall, M., and Ng, H., "Effects of Piston Wetting on Size and Mass of Particulate Matter Emissions in a DISI Engine". SAE Paper 2002-01-1140. (2002).

Weall, A., and Collings, N., "Investigation into Partially Premixed Combustion in a Light-Duty Multi-Cylinder Diesel Engine Fuelled with a Mixture of Gasoline and Diesel". SAE Paper 2007-01-4058. (2007).

West, B.H., López, A.J., Theiss, T.J., Graves, R.L., Storey, J.M., and Lewis, S.A., "Fuel Economy and Emissions of the Ethanol-Optimized Saab 9-5 Biopower". SAE Paper 2007-01-3994. (2007).

Wu, X., Huang, Z., Jin, C., Wang, X., Zheng, B., Zhang, Y. and Wei L., "Measurements of Laminar Burning Velocities and Markstein Lengths of 2,5- Dimethylfuran-Air-Diluent Premixed Flames". Energy & Fuels 23, 4355–4362. (2009).

Wyszynski, L., Stone, R., and Kalghatgi, G., "The Volumetric Efficiency of Direct and Port Injection Gasoline Engines with Different Fuels". SAE Paper 2002-01-0839. (2002).

Xie, H., Wei, Z., He, B., and Zhao, H., "Comparison of HCCI Combustion Respectively Fueled with Gasoline, Ethanol and Methanol through the Trapped Residual Gas Strategy". SAE Paper 2006-01-0635. (2006).

Xu, H.M., Misztal, J., Wyszynski, M. L., Turner, D., Price, P., Stone, R., Wang, J., Shuai, S., and Qiao, J., "HCCI – How Clean Can it be?" Invited presentation, 2007 SAE Intentional HCCI TOPTECH Symposium, 12-14 September 2007, Lund, Sweden.

Yamaoka, S., Kakuya, H., Nakagawa, S., Nogi, T., Shimada, A., and Kihara, Y., "A Study of Controlling the Auto-Ignition and Combustion in a Gasoline HCCI Engine". SAE Paper 2004-01-0942. (2004).

Yang, J., and Anderson, R.W., "Fuel Injection Strategies to Increase Full-Load Torque Output of a Direct-Injection SI Engine". SAE Paper 980495. (1998).

Yang, J., Munoz, R.H., Anderson, R.W., and Lavoie, G.A., "Study of a Stratified-Charge DISI Engine with an Air-Forced Fuel Injection System". SAE Paper 2000-01-2901. (2000).

Yang, J., and Kenney, T., "Some Concepts of DISI Engine for High Fuel Efficiency and Low Emissions". SAE Paper 2002-01-2747. (2002).

Yao, M., Chen, Z., Zheng, Z., Zhang, B., and Xing, Y., "Effect of EGR on HCCI Combustion fuelled with Dimethyl Ether (DME) and Methanol Dual-Fuels". SAE Paper 2005-01-3730. (2005).

Yap, D., Megaritis, A., and Wyszynski,M.L., "An Investigation into Bioethanol Homogeneous Charge Compression Ignition (HCCI) Engine Operation with Residual Gas Trapping". Energy & Fuels 18, 1315-1323. (2004).

Yap, D., Peucheret, S.M., Megaritis, A., Wyszynski, M.L., Xu, H., "Natural gas HCCI engine operation with exhaust gas fuel reforming". International Journal of Hydrogen Energy 31, 587-595. (2006).

Yoshida, K., Shoji, H., and Tanaka, H., "Study on Combustion and Exhaust Gas Emission Characteristics of Lean Gasoline-Air Mixture Ignited by Diesel Fuel Direct Injection". SAE Paper 982482. (1998).

Zhang, Y., He, B.-Q., Xie, H., and Zhao, H., "The Combustion and Emission Characteristics of Ethanol on a Port Fuel Injection HCCI Engine". SAE Paper 2006-01-0631. (2006).

Zhao, H., Peng, Z., Williams, J., and Ladommatos, N., "Understanding the Effects of Recycled Burnt Gases on the Controlled Autoignition (CAI) Combustion in Four-Stroke Gasoline Engines". SAE Paper 2001-01-3607. (2001).

Zhong, S., Wyszynski, M. L., Megaritis, A., Yap, D., and Hongming, X., "Experimental Investigation into HCCI Combustion Using Gasoline and Diesel Blended Fuels". SAE Paper 2005-01-3733. (2005).

Zhong, S., Jin, G., and Wyszynski, M. L., "Promotive Effect of Diesel Fuel on Gasoline HCCI Engine Operated with Negative Valve Overlap (NVO)". SAE Paper 2006-01-0633. (2006).